

Removal of Organic Matter by Classical Biofiltration: Mechanistic Insights Regarding "Biodegradation"

by

Joan Thompson

A thesis

presented to the University of Waterloo

in fulfillment of the

thesis requirement for the degree of

Master of Applied Science

in

Civil Engineering - Water

Waterloo, Ontario, Canada, 2019

©Joan Thompson 2019

Author's Declaration

I hereby declare that I am the sole author of this thesis. This is a true copy of the thesis, including any required final revisions, as accepted by my examiners.

I understand that my thesis may be made electronically available to the public.

Abstract

Pilot-scale biofiltration experiments were conducted at the Region of Waterloo's Mannheim Drinking Water Treatment Plant to inform the scientific and operational understanding of drinking water treatment by biologically-active GAC/sand filtration processes. Three dual-media granular activated carbon (GAC)/sand biofilters and one multi-media GAC-capped anthracite/sand biofilter media configuration were investigated. Both new GAC and GAC that had been biologically active for five years were used. The performance differences between a new, highly adsorptive GAC filter that is undergoing biological acclimation, and a biofilter that is stacked with older, biologically-active GAC media were investigated to increase the mechanistic understanding of natural organic matter (NOM) removal by biofiltration. The performance of a cost-effective, new GAC-capped anthracite/sand biofilter compared to a GAC/sand biofilter also was investigated. Performance was assessed using adenosine tri-phosphate (ATP) concentration associated with attached biomass in the filter media, dissolved organic carbon (DOC), UV-absorbance, and characterization by liquid chromatography-organic carbon detection (LC-OCD) fractionation. The filters were monitored for their performance in headloss accumulation and turbidity removal. Water from the full-scale water treatment plant was coagulated, flocculated, clarified by settling, and then ozonated. It was then directed to the pilot plant filters, which contained the same depth of media, but were operated separately from the full-scale plant. The experiments were conducted from June to September 2018, during warm water conditions (18–27°C).

As expected, the new GAC/sand filter removed substantially more DOC, UV-absorbing compounds, and humic substances than did the biologically-active GAC. There was also a typical pattern of biological acclimation in this filter, as there was high DOC removal, followed by a decline, and then a steady-state period. DOC removal during the steady-state period in the new filter was 25 to 30% on average, which was significantly higher than that in the filter containing media that had been biologically active for five years (13% on average), suggesting that DOC removal might decline over years of service. Interestingly, the new GAC/sand filter did not out-perform the biologically-active GAC/sand filter in biopolymer removal, possibly due to the size (>20 kDa) and shape of these compounds. This observation also suggests that biodegradation of biopolymers (in contrast to other compounds) occurs directly in biologically-active GAC filters, and not necessarily by bioregeneration (freeing up of adsorptive sites). Further, compared to biologically-active GAC/sand, there was no outright disadvantage to running a GAC-capped anthracite/sand biofilter. One month into the experiment, the backwashing procedure was altered to improve filter run times. The increased vigorousness caused the biofilm in the GAC-capped anthracite/sand filter to decrease temporarily, and it also caused a brief decrease in the DOC removal, whereas the GAC/sand biofilter was not affected by the backwashing change.

Overall, it was found that (1) the new GAC filter demonstrated a trend in DOC removal that was expected, with the added finding that the biodegradation or adsorptive capacity declines over a period of several years after acclimation (2) adsorption did not enhance the removal of biopolymers, though they were removed by biofiltration, indicating that biodegradation may occur directly and not necessarily by bioregeneration (adsorption and desorption by biodegradation), and (3) as configured, the GAC/sand biofilter was more effective in removing DOC than the GAC-capped anthracite biofilter.

Acknowledgements

- ❖ I would like to, first and foremost, thank my supervisors, Monica B. Emelko and William (Bill) B. Anderson. You have shown so much patience and support during the rough patches of my thesis. In fact, you have helped me become a more confident individual, both personally and work-wise. It is also such a great opportunity to be able to use the Mannheim pilot plant – the unique perspective I have gained from it will serve me well in my engineering career.
- ❖ I would like to sincerely thank the staff at Mannheim for accommodating me at the pilot plant. And I would like to express a heartfelt thank you to Alex Lee for assisting me all the way through the difficulties I encountered there. I simply could not have done what I did without your help.
- ❖ I would like to thank my readers, Hyung-Sool Lee and James Craig, for taking the time to provide valuable insight, and for being flexible and understanding during the final stretch of my thesis.
- ❖ A very sincere thank you to the technical staff and research associates in the Water STP research group. Maria Mesquita, Philip Schmidt, Mark Sobon, Mark Merlau, and Terry Ridgway. Thank you to Dana Herriman, for helping me with my reimbursements. I would also like to thank Lin Shen, Sigrid Peldszus, and Peter Huck for providing access to the LC-OCD.
- ❖ I consider myself lucky to have had these wonderful PhD and post-doctoral students within arms-reach. Thank you to Jesse Skwaruk, Shoeleh Shams, Alex Chik, and Xiaohui Sun for your mentorship, patience, and willingness to help.
- ❖ Thank you to my many colleagues who provided a constant source of support. This especially includes Tiffany Mah, for the hours upon hours of monotonous lab work you put up with. I would like to give a shout out to Raquel Jara Soto, Benjamin Beelen, Kaitlyn O’Sullivan, Linda Chan, and Tyler Owl-Scott. I am also so grateful for the happy memories I had while spending time with Amy Yang, Thadsha Chandrakumaran, Sabrina Bedjera, Kristina Lee, and Soosan Bahramian,
- ❖ Finally, thank you to my family, Mom and Dad, Valerie, Irene, David, and Mary, and of course, my partner, Ryan. Love and kisses all around.

Table of Contents

<i>Author's Declaration</i>	<i>i</i>
<i>Abstract</i>	<i>ii</i>
<i>Acknowledgements</i>	<i>iii</i>
List of Figures	viii
List of Tables	xvii
<i>List of Abbreviations</i>	<i>xx</i>
1. Introduction	1
1.1. Research Objectives	4
1.2. Research Approach	4
1.3. Thesis Organization	5
2. Literature Review	6
2.1. Biological Filtration – Overview	6
2.2. Biological Filtration – Start-Up	7
2.2.1. Start-Up of New GAC Filters	7
2.2.2. Acclimation Phase – Organic Matter Removal	11
2.2.3. Acclimation Phase – Microbiological Colonization	12
2.2.4. Steady-State Phase – Organic Matter Removal by Biodegradation	13
2.2.5. Removal by Biodegradation: Direct Biodegradation and Bioregeneration	13
2.3. Classical Biological Filtration – Performance Metrics	14
2.3.1. Headloss Accumulation and Turbidity Removal	14
2.3.2. Organic Matter Removal	15
UV ₂₅₄ and SUVA	15
LC-OCD	17
2.4. GAC-Capped Anthracite/sand Filters for Biological NOM Removal	18
2.4.1. NOM Removal during Biological Filtration with GAC and Anthracite Media	19
Biomass Quantity	19
Organic Matter Removal	19
3. Materials and Methods	21

3.1. Research Approach	21
3.2. Region of Waterloo Mannheim Drinking Water Treatment Plant	21
3.2.1. Full-scale WTP Processes – Prior to Pilot-scale Filtration	21
3.2.2. Full-scale WTP Processes – After Connection to Pilot Plant	22
3.3. Pilot Plant	22
3.3.1. Pilot Plant Facility –Media Types	22
3.3.2. Pilot Plant Facility – Filter Media Configurations	24
3.3.3. Pilot Plant Facility – Water and Filter Media Sampling	24
3.3.4. Pilot Plant Equipment and Operation	25
3.4. Backwash and Operation	26
3.4.1. Backwash Protocol	27
3.4.2. Solids Accumulation in the Filters	28
3.4.3. Details on Operating Data Collection	29
Flow	29
Turbidity	29
Headloss	29
Filter run time	29
3.5. Organic Matter Concentration and Characterization	30
3.5.1. DOC	30
3.5.2. UV Absorbance	30
3.5.3. LC-OCD	30
3.6. Microbiological Sampling and Analysis	32
3.7. Statistical Methods	33
3.7.1. Steady-state Filter Performance Analysis Using Linear Regression	33
3.7.2. Paired t-test for comparison	34
4. Results and Discussion	35
4.1. Filter Influent Organic Matter during the Experimental Period	35
4.1.1. Settled, Post-Ozone Water Quality and Prior Treatment Steps	35
4.1.2. Filter Influent DOC	36
4.1.3. Filter Influent UV ₂₅₄ and Organic Matter Fractions	38
4.2. Data Collection Biofiltration Process Performance	39
4.3. Performance of Filter 1 – New GAC	40
4.3.1. Turbidity Removal and Headloss Accumulation	40

4.3.2. DOC	40
4.3.3. UV ₂₅₄ and SUVA	47
4.3.4. Organic Matter (LC-OCD) Fractions	48
4.3.5. ATP Concentration	50
4.4. Performance in Filter 2 – Combination of new and exhausted GAC media	51
4.4.1. Turbidity Removal and Headloss Accumulation	51
4.4.2. DOC	53
4.4.3. UV ₂₅₄ and SUVA	56
4.4.4. Organic Matter (LC-OCD) Fractions	57
4.4.5. ATP Concentration	59
4.5. Performance in Filter 3 – Biologically-active GAC from full-scale plant	60
4.5.1. Turbidity Removal and Headloss Accumulation	60
4.5.2. DOC	62
4.5.3. UV ₂₅₄ and SUVA	69
4.5.4. Organic Matter (LC-OCD) Fractions	70
4.5.5. ATP Concentration	73
4.6. Performance of Filter 4 – Biologically-active, spent GAC cap over new anthracite	74
4.6.1. Turbidity Removal and Headloss Accumulation	74
4.6.2. DOC	75
4.6.3. UV ₂₅₄ and SUVA	78
4.6.4. Organic Carbon (LC-OCD) Fractions	79
4.6.5. ATP Concentration	81
5. Conclusions and Implications	83
References	85
Appendix A – All Raw Data	99
Operational Data	99
Headloss Data	99
Turbidity	101
Run Times	103
Organic Matter Data	105
Dissolved Organic Carbon	105
UV ₂₅₄	109
LC-OCD Data	111
LC-OCD Chromatograms	113

Microbiological Data – ATP Concentration	142
<i>Appendix B – Calculations and Error Determination</i>	144
Backwashing – Estimating Sub-fluidization Velocity	144
Data – Error Evaluation	146
ATP – Necessary Laboratory Adjustment	146
UV Absorbance – Error caused by storage	150
LC-OCD – Error caused by storage	153
<i>Appendix C - Statistical Analysis</i>	155
Equations	155
Linear Regression Equations	155
Paired t-test	155
Testing Assumptions – Normality and Equal Variance	156
Paired t-Tests Histograms – Influent Results	156
Paired t-Test Histograms – Filter 2 Results	158
Paired t-test Histograms – Filter 3 Results	159
Paired t-Test Histograms – Filter 4 Results	161
Linear Regression Residuals – Filter 1 DOC Removal over Experimental Period	165
Linear Regression Residuals – Filter 1 Fractions of DOC Removal over Experimental Period	170
Linear Regression Residuals – Filter 2 DOC Removal Over Experimental Period	172
Linear Regression Residuals – Filter 3 DOC Removal Over Experimental Period	175
Linear Regression Residuals – Filter 3 Fractions of DOC Removal over Experimental Period	179
Linear Regression Residuals – Filter 4 DOC Removal Over Experimental Period	181
<i>Appendix D – Filtration Media Specs</i>	186
Sieve Analysis	186
Wet-Dry Conversion	186
Filtration Media Specification Sheets	187

List of Figures

Figure 1.1: Theoretical representation of the transition from a new GAC filter to a biologically-active one. Reprinted with permission (Dussert and Van Stone, 1994).....	3
Figure 2.1 A scanning electronic micrograph image displays bacterial biofilms on a GAC granule. Reprinted (adapted) with permission from (Weber et al., 1978) Copyright (2019) American Chemical Society.	6
Figure 2.2 Theoretical representations of DOC removal over the operational time of a biologically active filter. Reprinted with permission (2019). Dussert and Van Stone, 1994 (A); Brown et al., 2015 (B); Huck et al., 2000 (C); Korotta-Gamage and Sathasivan, 2017 (D).....	8
Figure 2.3: (A) Typical S-curve of a GAC contactor from the beginning to end of its operational life (Baruth, 2005), (B) the TOC influent and the S-curve shape of the TOC effluent in a new GAC filter becoming biologically active (Moore et al., 2001).....	12
Figure 3.1 Pilot plant schematic with sampling ports and their heights above the base of the filter columns	25
Figure 3.2: Solids masses emerging in Filter 4 (left) and Filter 2 (right) during backwashing on June 29 th , 2018.....	28
Figure 3.3: LC-OCD data output (top) and analysis (i.e. integration to determine peak area) (bottom) (Huber et al., 2011).	31
Figure 4.1: Average daily settled, post-ozone water turbidity and raw water temperature during fluctuation and stable phases of pilot filter operation	36
Figure 4.2: Comparison of DOC at the far port (full-scale ozone effluent redirection point) and Port 1 above the media in each filter, collected during experimental period (n = 21-24,	37
Figure 4.3: Average filter influent organic carbon fraction concentrations at the post-ozone location across the experimental period (mean +/- std. deviation, n=9).....	39
Figure 4.4: Headloss accumulation in Filter 1 during the experimental period	40
Figure 4.5: DOC concentrations in Filter 1 influent and effluent during the whole experimental period (n=23)	41
Figure 4.6: Percentage DOC removal in Filter 1 during the whole experimental period (n=23).....	41
Figure 4.7: Mean DOC concentration across the depth of Filter 1 prior to steady-state DOC removal (June 14 th to July 25 th ; top) and during steady-state removal (Aug 2 nd to Sept 5 th ; bottom) (n=8, and 6, respectively: error bars = +/- std. deviation)	43



Figure 4.8: Mean DOC concentration across the depth of Filter 1 prior to steady-state filter operation (from June 14 th to July 25 th) and after steady-state filter operation (from Aug 2 nd to Sept 5 th) (n=8 and 6, respectively, error bars = +/- std. deviation).	44
Figure 4.9: Fraction of DOC removed in each section of GAC in Filter 1 during the experimental period ( = fraction removed  = least squares linear regression trend line)	46
Figure 4.10: Filter 1 influent and effluent UV ₂₅₄ (left) and SUVA (right) during the experimental period (n = 15 and 13, respectively; \downarrow = minimum value, \uparrow = maximum value observed).....	47
Figure 4.11: Biopolymer concentrations in Filter 1 influent and effluent streams during the experimental period (n=9)	48
Figure 4.12: Humic substances removal in Filter 1 during the experimental period (n=9)	49
Figure 4.13: ATP concentration per g of dry GAC media in Filter 1 during the experimental period.....	50
Figure 4.14: ATP concentration and DOC removal (%) in Filter 1 during the experimental period	51
Figure 4.15: Filter 2 headloss performance trend throughout experimental period	52
Figure 4.16: Filter 2 turbidity performance trend throughout experimental period	52
Figure 4.17: DOC concentrations in Filter 2 influent and effluent during the experimental period (n=17).....	54
Figure 4.18: DOC removal (%) in Filter 2 during the experimental period (n=17)	54
Figure 4.19: Mean DOC concentration across the depth of Filter 2 during steady-state filter operation (from July 18 th to Aug 23 rd) (n = 7 error bars = +/- one standard deviation).....	56
Figure 4.20: Filter 2 influent and effluent UV ₂₅₄ (left) and SUVA (right) during the experimental period (n = 12 and 9, respectively; \downarrow = minimum and \uparrow = maximum value observed)	57
Figure 4.21: Biopolymer concentrations in Filter 2 influent and effluent streams during the experimental period (n = 8)	58
Figure 4.22: Humic substance concentrations in Filter 2 influent and effluent streams during the experimental period (n = 8)	59
Figure 4.23: ATP concentration per g of dry GAC media in Filter 2 during the experimental period.....	60
Figure 4.24: Filter 3 headloss performance trend throughout experimental period	61
Figure 4.25: Headloss accumulation rate for Filters 1 to 3, side by side	62
Figure 4.26: DOC concentrations in Filter 3 influent and effluent during the experimental period (n=20).....	63
Figure 4.27: DOC removal (%) in Filter 3 during the experimental period (n=20)	63
Figure 4.28: Average DOC concentration at each sampling port in Filter 3 during its stable period - June 14 th to Sept 5 th (n=14, error bars = +/- one standard deviation)	65
Figure 4.29: Effluent DOC concentration across the depth of Filters 1 and 3 from Aug 2 nd to Sept 5 th , 2018 (n=6, error bars = +/- one standard deviation, outlier from Filter 3 excluded)	66

Figure 4.30: Average DOC concentration at each sampling depth in Filter 1 (new GAC) and Filter 3 spent GAC), from Aug 2 nd to Sept 5 th (n = 6, error bars = +/- std. deviation, outlier from Filter 3 excluded) ...	66
Figure 4.31: DOC removal across filter depth (day 14 and 35 = before steady-state, day 91 = right before steady-state, day 196 = after steady-state) from (Velten et al., 2011a)	67
Figure 4.32: Fraction of DOC removed in GAC between each sample port in Filter 3 during the experimental period (solid line is fraction of removal, dotted line is a trend line).....	68
Figure 4.33: Filter 3 UV ₂₅₄ (left) and SUVA (right) influent and effluent from June 14 th to Sept 5 th , 2018 (n = 15 and 14, respectively, μ = minimum value, σ = maximum value observed).....	69
Figure 4.34: Biopolymer concentrations in Filter 3 influent and effluent streams during the experimental period (n = 9)	71
Figure 4.35: Humic substances concentrations in Filter 3 influent and effluent streams during the experimental period (n = 9)	71
Figure 4.36: Comparison of LC-OCD components in the effluents of Filter 1 and Filter 3 during the experimental period (n=9, error bars = +/- one standard deviation).....	72
Figure 4.37: ATP concentration per g of dry GAC media in Filter 3 during the experimental period.....	74
Figure 4.38: DOC concentrations in Filter 4 influent and effluent during the experimental period (n=23)	75
Figure 4.39: DOC removal (%) DOC concentrations in Filter 4 during the experimental period (n=23).	76
Figure 4.40: Average DOC concentration at each sampling port in Filter 4. Although there are some non-steady-state periods (Table 4.), the entire period (n=14, error bars = +/- one standard deviation)	78
Figure 4.41: Filter 4 UV (left) and SUVA (right) influent and effluent during the experimental period (n = 16 and 14, respectively, μ = minimum value, σ = maximum value observed).....	79
Figure 4.42: Biopolymer concentrations in Filter 4 influent and effluent streams during the experimental period (n=9)	80
Figure 4.43: Humic Substance concentrations in Filter 4 influent and effluent streams during the experimental period (n = 9)	80
Figure 4.44: ATP concentration per g of dry GAC media in Filter 4 during the experimental period.....	81
Figure A - 1 LC-OCD Data Jul 1 st – F1 PE	113
Figure A - 2 LC-OCD Data Jul 1 st – F2 PE	113
Figure A - 3 LC-OCD Data Jul 1 st – F3 PE	114
Figure A - 4 LC-OCD Data Jul 1 st – F4 PE	114
Figure A - 5 LC-OCD Data Jul 1 st – INF.....	115

Figure A - 6 LC-OCD Data Jul 10 th – F1 PE	115
Figure A - 7 LC-OCD Data Jul 10 th – F2 PE	116
Figure A - 8 LC-OCD Data Jul 10 th – F3 PE – Degradation Day 8	116
Figure A - 9 LC-OCD Data Jul 10 th – F4 PE	117
Figure A - 10 LC-OCD Data Jul 12 th – INF.....	117
Figure A - 11 LC-OCD Data Jul 12 th – F2 PE	118
Figure A - 12 LC-OCD Data Jul 12 th – F3 PE	118
Figure A - 13 LC-OCD Data Jul 12 th – F4 PE	119
Figure A - 14 LC-OCD Data Jul 12 th – F3 PE Degradation Day 16	119
Figure A - 15 LC-OCD Data Jul 12 th – F1 PE	120
Figure A - 16 LC-OCD Data Jul 18 th – INF.....	120
Figure A - 17 LC-OCD Data Jul 18 th – F1 PE	121
Figure A - 18 LC-OCD Data Jul 18 th – F2 PE	121
Figure A - 19 LC-OCD Data Jul 18 th – F3 PE	122
Figure A - 20 LC-OCD Data Jul 18 th – F4 PE	122
Figure A - 21 LC-OCD Data Jul 20 th – INF.....	123
Figure A - 22 LC-OCD Data Jul 20 th – F1 PE	123
Figure A - 23 LC-OCD Data Jul 20 th – F2 PE-2	124
Figure A - 24 LC-OCD Data Jul 20 th – F3 PE	124
Figure A - 25 LC-OCD Data Jul 20 th – F3 PE Degradation Day 20	125
Figure A - 26 LC-OCD Data Jul 20 th – F4 PE	125
Figure A - 27 LC-OCD Data Jul 20 th – F2 PE-2	126
Figure A - 28 LC-OCD Data Jul 27 th – INF.....	126
Figure A - 29 LC-OCD Data Jul 27 th – F1 PE	127
Figure A - 30 LC-OCD Data Jul 27 th – F2 PE	127
Figure A - 31 LC-OCD Data Jul 27 th – F3 PE	128

Figure A - 32 LC-OCD Data Jul 27 th – F4 PE	128
Figure A - 33 LC-OCD Data Jul 27 th – F3 PE Degradation Day 25	129
Figure A - 34 LC-OCD Data Aug 2 nd – INF.....	129
Figure A - 35 LC-OCD Data Aug 2 nd – F1 PE.....	130
Figure A - 36 LC-OCD Data Aug 2 nd – F2 PE.....	130
Figure A - 37 LC-OCD Data Aug 2 nd – F3 PE.....	131
Figure A - 38 LC-OCD Data Aug 2 nd – F4 PE.....	131
Figure A - 39 LC-OCD Data Aug 2 nd – F3 PE Degradation Day 31.....	132
Figure A - 40 LC-OCD Data Aug 14 th – INF	132
Figure A - 41 LC-OCD Data Aug 14 th – F1 PE	133
Figure A - 42 LC-OCD Data Aug 14 th – F2 PE	133
Figure A - 43 LC-OCD Data Aug 14 th – F3 PE	134
Figure A - 44 LC-OCD Data Aug 14 th – F4 PE	134
Figure A - 45 LC-OCD Data Aug 14 th – F3 PE Degradation Day 44	135
Figure A - 46 LC-OCD Data Aug 21 st – INF.....	135
Figure A - 47 LC-OCD Data Aug 21 st – F1 PE	136
Figure A - 48 LC-OCD Data Aug 21 st – F2 PE	136
Figure A - 49 LC-OCD Data Aug 21 st – F3 PE	137
Figure A - 50 LC-OCD Data Aug 21 st – F4 PE	137
Figure A - 51 LC-OCD Data Aug 21 st – F3 PE Degradation Day 52	138
Figure A - 52 LC-OCD Data Sept 2 nd – INF.....	138
Figure A - 53 LC-OCD Data Sept 2 nd – F1 PE	139
Figure A - 54 LC-OCD Data Sept 2 nd – F2 PE	139
Figure A - 55 LC-OCD Data Sept 2 nd – F3 PE	140
Figure A - 56 LC-OCD Data Sept 2 nd – F4 PE	140
Figure A - 57 LC-OCD Data Sept 2 nd – F3 PE Degradation Day 78	141

Figure A - 58: Time of backwashing versus fluidization velocity (Amirtharajah, 1993).....	144
Figure A - 59: Flow chart of steps for experiment that re-creates ATP adsorption in lyse tubes	147
Figure A - 60 ATP Degradation curve in lyse for F1 sample	147
Figure A - 61 ATP Degradation curve in lyse for F2 sample	148
Figure A - 62 ATP Degradation curve in lyse for F3 sample	148
Figure A - 63 ATP Degradation curve in lyse for F4 sample	148
Figure A - 64 ATP Degradation curve in lyse for Control (F1) sample	149
Figure A - 65: Approximations of rate of change in UV absorbance over days that the sample is stored – plotted against the starting UV absorbance of that sample	150
Figure A - 66: UV absorbance in F1 Effluent and correction for the impact of sample storage.....	151
Figure A - 67: UV absorbance in F2 Effluent and correction for the impact of sample storage.....	151
Figure A - 68: UV absorbance in F3 Effluent and correction for the impact of sample storage.....	151
Figure A - 69: UV absorbance in F4 Effluent and correction for the impact of sample storage.....	152
Figure A - 70: Repeated LC-OCD readings over storage of same sample	153
Figure A - 71: Change in LC-OCD concentrations in same sample over its storage	153
Figure A - 72 Histograms for paired t-tests among DOC influent (Post-ozonated influent, and Port 1 from Filter 1, Filter 2, Filter 3 and Filter 4)	156
Figure A - 73: Frequency diagram of differences between pairs for influent biopolymer concentration and Filter 1 effluent biopolymer concentration	157
Figure A - 74: Frequency diagram of differences between pairs for influent humic substance concentration and Filter 1 effluent humic substance concentration	157
Figure A - 75: Frequency diagram of differences between pairs for influent biopolymer concentration and Filter 2 effluent biopolymer concentration	158
Figure A - 76: Frequency diagram of differences between pairs for influent humic substance concentration and Filter 2 effluent humic substance concentration	158
Figure A - 77: Frequency diagram of differences between pairs for influent biopolymer concentration and Filter 3 effluent biopolymer concentration	159

Figure A - 78: Frequency diagram of differences between pairs for the removal of biopolymers in Filter 1 and the removal of biopolymers in Filter 3.....	159
Figure A - 79: Frequency diagram of differences between pairs for influent humic substances concentration and Filter 3 effluent humic substances concentration.....	160
Figure A - 80: Frequency diagram of differences between pairs for the removal of humic substances in Filter 1 and the removal of humic substances in Filter 3.....	160
Figure A - 81: Frequency diagrams of differences between pairs for headloss accumulation in Filter 3 and the headloss accumulation in Filter 4.....	161
Figure A - 82: Frequency diagrams of differences between pairs for the effluent turbidity in Filter 3 and the effluent turbidity in Filter 4.....	161
Figure A - 83: Frequency diagram of differences between pairs for F3 impact on the SUVA of the water and the F4 impact of the SUVA.....	162
Figure A - 84: Frequency diagram of differences between pairs for influent biopolymer concentration and Filter 4 effluent biopolymer concentration.....	163
Figure A - 85: Frequency diagram of differences between pairs for the removal of biopolymers in Filter 3 and the removal of biopolymers in Filter 4.....	163
Figure A - 86: Frequency diagram of differences between pairs for influent humic substances concentration and Filter 4 effluent humic substances concentration.....	164
Figure A - 87: Frequency diagram of differences between pairs for the removal of humic substances in Filter 3 and the removal of humic substances in Filter 4.....	164
Figure A - 88: Linear regression residuals for DOC removal in Filter 1 – Iteration 1.....	165
Figure A - 89: Linear regression residuals for DOC removal in Filter 1 – Iteration 2.....	165
Figure A - 90: Linear regression residuals for DOC removal in Filter 1 – Iteration 3.....	165
Figure A - 91: Linear regression residuals for DOC removal in Filter 1 – Iteration 4.....	166
Figure A - 92: Linear regression residuals for DOC removal in Filter 1 – Iteration 5.....	166
Figure A - 93: Linear regression residuals for DOC removal in Filter 1 – Iteration 6.....	166
Figure A - 94: Linear regression residuals for DOC removal in Filter 1 – Iteration 7.....	167
Figure A - 95: Linear regression residuals for DOC removal in Filter 1 – Iteration 8.....	167

Figure A - 96: Linear regression residuals for DOC removal in Filter 1 – Iteration 9	167
Figure A - 97: Linear regression residuals for DOC removal in Filter 1 – Iteration 10	168
Figure A - 98: Linear regression residuals for DOC removal in Filter 1 – Iteration 11	168
Figure A - 99: Linear regression residuals for DOC removal in Filter 1 – Iteration 12	168
Figure A - 100: Linear regression residuals for DOC removal in Filter 1 – Iteration 13	169
Figure A - 101: Linear regression residuals for DOC removal in Filter 1 – Iteration 14	169
Figure A - 102: Linear regression residuals for fraction of DOC removed between the top to Port 2 in Filter 1– over experimental period	170
Figure A - 103: Linear regression residuals for fraction of DOC removed between Port 2 and Port 3 in Filter 1– over experimental period	170
Figure A - 104: Linear regression residuals for fraction of DOC removed between Port 3 and Port 4 in Filter 1– over experimental period	170
Figure A - 105: Linear regression residuals for fraction of DOC removed between Port 4 and Port 5 in Filter 1– over experimental period	171
Figure A - 106: Linear regression residuals for fraction of DOC removed between Port 5 and Effluent Port in Filter 1– over experimental period	171
Figure A - 107: Linear regression residuals for DOC removal in Filter 2 – Iteration 1	172
Figure A - 108: Linear regression residuals for DOC removal in Filter 2 – Iteration 2	172
Figure A - 109: Linear regression residuals for DOC removal in Filter 2 – Iteration 3	172
Figure A - 110: Linear regression residuals for DOC removal in Filter 2 – Iteration 4	173
Figure A - 111: Linear regression residuals for DOC removal in Filter 2 – Iteration 5	173
Figure A - 112: Linear regression residuals for DOC removal in Filter 2 – Iteration 6	173
Figure A - 113: Linear regression residuals for DOC removal in Filter 2 – Iteration 7	174
Figure A - 114: Linear regression residuals for DOC removal in Filter 2 – Iteration 7	174
Figure A - 115: Linear regression residuals for DOC removal in Filter 3 – Iteration 1	175
Figure A - 116: Linear regression residuals for DOC removal in Filter 3 – Iteration 2	175
Figure A - 117: Linear regression residuals for DOC removal in Filter 3 – Iteration 3	175

Figure A - 118: Linear regression residuals for DOC removal in Filter 3 – Iteration 4	176
Figure A - 119: Linear regression residuals for DOC removal in Filter 3 – Iteration 5	176
Figure A - 120: Linear regression residuals for DOC removal in Filter 3 – Iteration 6	176
Figure A - 121: Linear regression residuals for DOC removal in Filter 3 – Iteration 7	177
Figure A - 122: Linear regression residuals for DOC removal in Filter 3 – Iteration 8	177
Figure A - 123: Linear regression residuals for DOC removal in Filter 3 – Iteration 9	177
Figure A - 124: Linear regression residuals for DOC removal in Filter 3 – Iteration 10	178
Figure A - 125: Linear regression residuals for DOC removal in Filter 3 – Iteration 11	178
Figure A - 126: Linear regression residuals for fraction of DOC removed between the top to Port 2 in Filter 3– over experimental period	179
Figure A - 127: Linear regression residuals for fraction of DOC removed between Port 2 and Port 3 in Filter 3– over experimental period	179
Figure A - 128: Linear regression residuals for fraction of DOC removed between Port 3 and Port 4 in Filter 3– over experimental period	179
Figure A - 129: Linear regression residuals for fraction of DOC removed between Port 4 and Port 5 in Filter 3– over experimental period	180
Figure A - 130: Linear regression residuals for fraction of DOC removed between Port 5 and Effluent Port in Filter 3– over experimental period	180
Figure A - 131: Linear regression residuals for DOC removal in Filter 4 – Iteration 1	181
Figure A - 132: Linear regression residuals for DOC removal in Filter 4 – Iteration 2	181
Figure A - 133: Linear regression residuals for DOC removal in Filter 4 – Iteration 3	181
Figure A - 134: Linear regression residuals for DOC removal in Filter 4 – Iteration 4	182
Figure A - 135: Linear regression residuals for DOC removal in Filter 4 – Iteration 5	182
Figure A - 136: Linear regression residuals for DOC removal in Filter 4 – Iteration 6	182
Figure A - 137: Linear regression residuals for DOC removal in Filter 4 – Iteration 7	183
Figure A - 138: Linear regression residuals for DOC removal in Filter 4 – Iteration 8	183
Figure A - 139: Linear regression residuals for DOC removal in Filter 4 – Iteration 9	183

Figure A - 140: Linear regression residuals for DOC removal in Filter 4 – Iteration 10	184
Figure A - 141: Linear regression residuals for DOC removal in Filter 4 – Iteration 11	184
Figure A - 142: Linear regression residuals for DOC removal in Filter 4 – Iteration 12	184
Figure A - 143: Linear regression residuals for DOC removal in Filter 4 – Iteration 13	185
Figure A - 144: Linear regression residuals for DOC removal in Filter 4 – Iteration 14	185

List of Tables

Table 2.1: BAC filter start-up times to acclimation with new GAC preceded by conventionally-treated ozonated systems.....	10
Table 2.2: LC-OCD fractions and their properties	17
Table 2.3: Biopolymer and humic substance removal by anthracite and GAC biofilters.....	20
Table 3.1: Properties of media used in this study.....	23
Table 3.2: Pilot scale media configurations	23
Table 3.3: Backwash settings used during pilot-scale biofiltration experiments	27
Table 3.4 Media sample rinsing results (ATP concentration in the supernatant after rinsing)	33
Table 3.5: Determining ATP concentration in attached biofilter biomass.....	33
Table 4.1: Paired t-test results between the DOC concentrations at the post ozone sampling location and influent (Port 1) to each of the pilot filters.....	37
Table 4.2: Mean turbidity removal by Filter 1 during the experimental period (n=35)	40
Table 4.3: Linear regression results confirming the period of steady-state DOC removal in Filter 1. This is the period during which filter effluent DOC concentration reached a steady-state, resulting in a slope that was not statistically different than a slope of zero.	42
Table 4.4: Filter 1 port heights and media layers	43
Table 4.5: ATP concentration (mean +/- standard deviation) across the depth of Filter 1 during steady-state operation	51
Table 4.6: Mean turbidity removal by Filter 2 during the experimental period (n=37)	52
Table 4.7: Linear regression results confirming the period of steady-state DOC removal in Filter 2. This is the period during which filter effluent DOC concentration reaches steady-state, resulting in a slope that is not statistically different than a slope of zero.	55
Table 4.8: Filter 2 port heights and media layers	55
Table 4.9: ATP concentration (mean +/- standard deviation) across the depth of Filter 2 during steady-state operation	60

Table 4.10: Mean turbidity removal by Filter 3 during the experimental period (n=34)	61
Table 4.11: Linear regression results confirming the period of steady-state DOC removal in Filter 3. This is the period during which filter effluent DOC concentration reaches steady-state, resulting in a slope that is not statistically different than a slope of zero.....	64
Table 4.12: Filter 3 port heights and media layers	64
Table 4.13: Review of studies that have recorded SUVA changes through BAC filters.....	70
Table 4.14: ATP concentration (mean +/- standard deviation) across the depth of Filter 3 during steady-state operation	74
Table 4.15: Mean turbidity removal by Filter 4 during the experimental period (n=32)	75
Table 4.16: Linear regression results confirming the period of steady-state DOC removal in Filter 4. This is the period during which filter effluent DOC concentration reaches steady-state, resulting in a slope that is not statistically different than a slope of zero.....	77
Table 4.17: Filter 4 port heights and media layers	77
Table 4.18: ATP concentration (mean \pm standard deviation) through Filter 4 during steady-state operation	82
Table 4.19: Fraction of DOC removed in each layer of media within Filter 4	82
Table A - 1: Headloss accumulation rate for each filter (Part 1/2).....	99
Table A - 2: Headloss accumulation rate for each filter (Part 2/2).....	100
Table A - 3: Average effluent turbidity from each filter while it flowed (Part 1/2).....	101
Table A - 4: Average effluent turbidity from each filter while it flowed (Part 1/2).....	102
Table A - 5: Official run times for each filter (Part 1/2).....	103
Table A - 6: Official run times for each filter (Part 2/2).....	104
Table A - 7: DOC data from Filter 1	105
Table A - 8: DOC data from Filter 2	106
Table A - 9: DOC data from Filter 3	107
Table A - 10: DOC data from Filter 4	108
Table A - 11: UV ₂₅₄ influent data summary for all filters.....	109
Table A - 12: UV ₂₅₄ effluent data from all filters.....	110
Table A - 13: NOM Fractions – Post-ozone port	111

Table A - 14: NOM Fractions – Filter 1 Effluent.....	111
Table A - 15: NOM Fractions – Filter 2 Effluent.....	111
Table A - 16: NOM Fractions – Filter 3 Effluent.....	112
Table A - 17: NOM Fractions – Filter 4 Effluent.....	112
Table A - 18: LC-OCD data – Impact of long-term storage of sample	112
Table A - 19: ng ATP per g of dry media for Filter 1	142
Table A - 20: ATP per media for Filter 2	142
Table A - 21: ATP per media for Filter 3	143
Table A - 22: ATP per media for Filter 4	143
Table A - 23: Physical Media Properties	145
Table A - 24: Hydraulic loading rates during low-rate wash (calculated).....	145
Table A - 25: Hydraulic loading rates for air-scour during low-rate wash (from operating filters).....	145
Table A - 26: Sieve analysis results	186
Table A - 27: Wet-dry conversion results.....	186

List of Abbreviations

AOC	Assimilable Organic Carbon
ATP	Adenosine Triphosphate
BAC	Biologically-Active Carbon
BDOC	Biodegradable Dissolved Organic Carbon
DBP	Disinfection By-Product
DOC	Dissolved Organic Carbon
EBCT	Empty Bed Contact Time
EPS	Extracellular Polymeric Substances
Full-scale WTP	Region of Waterloo Mannheim Drinking Water Treatment Plant
GAC	Granular Activated Carbon
HAA	Haloacetic Acid
LC-OCD	Liquid Chromatography-Organic Carbon Detection
LMW	Low Molecular Weight
NOM	Natural Organic Matter
PACl	Polyaluminum Chloride
SCADA	Supervisory Control and Data Acquisition
THAA	Trihaloacetic Acid
THM	Trihalomethane
UF	Ultrafiltration
UV ₂₅₄	Absorbance at a wavelength of 254 nm

1. Introduction

Biological filtration—or the enhancement of filtration by microbiological activity—is a drinking water treatment process that has been extensively studied in recent years. Conventional chemically-assisted filtration in drinking water treatment systems involves the removal of contaminants by physico-chemical mechanisms. In brief, it involves the de-stabilization of particles by chemical coagulants so that they can subsequently attach to collectors during the filtration stage. This requires both particle transport to collector surfaces (via diffusion, interception, sedimentation, inertia, or hydrodynamic action) and subsequent attachment to the filter collector surfaces/media grains (Ryan and Elimelech, 1996). In biological filtration, some of the bacteria that are indigenous to the filter influent water matrix proliferate on the filter medium, and their metabolic activity effectively contributes to contaminant removal (Edzwald, 2011; Kirisits et al., 2019; Urfer et al., 1997).

Biological filtration processes include slow sand filtration and riverbank filtration systems, which have been used for centuries. For these technologies, raw/untreated water enters the filter bed without any pre-treatment or addition of chemicals; most of the contaminant removal occurs within a biofilm that accumulates on the media surface and within the first several centimeters of the filter. These types of filtration processes typically require long residence times, ranging from 2 hours to 10 days (Edzwald, 2011; Zhu et al., 2010), and are constrained as a conventional treatment solution in mature urban areas due to the footprint that they require. Widespread discontinuation of pre-chlorination largely because of disinfection by-product (DBP) concerns (in North America especially), has promoted the use of “classical biofiltration” because of the proliferation of microbiological activity on filtration media and associated enhanced contaminant removal (Kirisits et al., 2019). Biological filtration, which can be aerobic or anaerobic depending on the compounds targeted by the process, can be an effective treatment option for a wide variety of drinking water treatment contaminants, such as nutrients, taste and odour compounds, perchlorates, and heavy metal compounds (Bouwer and Crowe, 1988; Zhu et al., 2010), while still effective in removing particles and pathogens like traditional chemically-assisted filtration processes (Emelko, 2001; Huck et al., 2001, 2002; Emelko et al., 2005; Evans, 2010). Classical biofiltration in otherwise conventional surface water treatment plants is typically focused on natural organic matter (NOM) removal, which improves the biological stability of water, enhances DBP precursor removal, and reduces membrane fouling (Edzwald, 2011).

One of the most extensively studied configurations of classical biological filtration during conventional drinking water treatment is granular activated carbon (GAC) filtration preceded by pre- and post-clarification ozonation. Ozone is a strong oxidant that readily reacts with NOM, breaking it down into

smaller, more biodegradable by-products, including aldehydes, ketones, and carboxylic acids (Amy and Carlson, 1997; Hozalski et al., 1999). Biofilm attached to the filtration media in the downstream GAC contactor subsequently removes many of the biodegradable components of the transformed NOM. GAC is a filtration medium that is engineered to possess micropores (<2 nm) mesopores (2–50 nm) and/or macropores (>50 nm), effectively enhancing each GAC granule with a high adsorptive capacity and augmenting the removal of contaminants (Edzwald, 2011; Sing et al., 1985). Non-adsorptive media, like anthracite and sand, can also support biological activity; however, it has been demonstrated that biologically active GAC filtration achieves better NOM removal under a wider range of operating conditions relative to non-adsorptive media (LeChevallier et al., 1992; McKie et al., 2015; Wang et al., 1995; Kirisitit et al., 2019). While it has been suggested that GAC's irregular surface area protects the microbiological activity from the fluid shear forces of backwashing (Urfer and Huck, 1997), it has also been suggested that GAC adsorbs high levels of NOM, providing accessible substrate to biofilms (Klimenko et al., 2002; Lapidou and Rittmann, 2002; Velten et al., 2011a). The uptake of NOM by attached biofilm effectively regenerates adsorption sites on the GAC media and has been referred to as “bioregeneration” (Rattier et al., 2012; Scholz and Martin, 1997). Recently, it was demonstrated that it is the adsorptive properties of GAC rather than biofilm shielding that lead to enhanced NOM removal by GAC biofiltration (Kirisitit et al., 2019; Spanjers, 2017); however, the exact mechanisms have not been fully elucidated.

Regardless of the mechanism(s) of action, biofiltration on GAC filtration media surfaces can remove a wide spectrum of organic matter, from the larger, more recalcitrant compounds like proteins, polysaccharides, and humics (Gibert, et al. 2013a; Peldszus et al., 2012; Rahman et al., 2014) to smaller, more biodegradable organic matter compounds (LeChevallier et al., 1992; Van der Kooij, 1992). However, steady-state removal of NOM by microbiological activity does not occur immediately. When a GAC filter containing new or regenerated GAC is first put in service during conventional drinking water treatment, the predominant method of NOM removal is adsorption; a significant fraction of NOM can be readily removed during this phase of operation, often up to approximately 80% (Dussert and Van Stone, 1994), depending on the characteristics of the raw water and the operational conditions. Ultimately, the NOM removal rate decreases as the number of adsorption sites is exhausted, and eventually flattens out. Simultaneously, when a new GAC filter or contactor are brought online in absence of pre-oxidation, the adsorptive sites become exhausted with organic matter, and over time, microbial attachment increases and eventually stabilizes. At some point, typically in weeks to months depending on factors such as water temperature, and NOM removal by adsorption and biodegradation reaches an equilibrium and the removal rate stabilizes (Figure 1.1) (Dussert and Tramposch, 1996; Velten et al., 2011a).

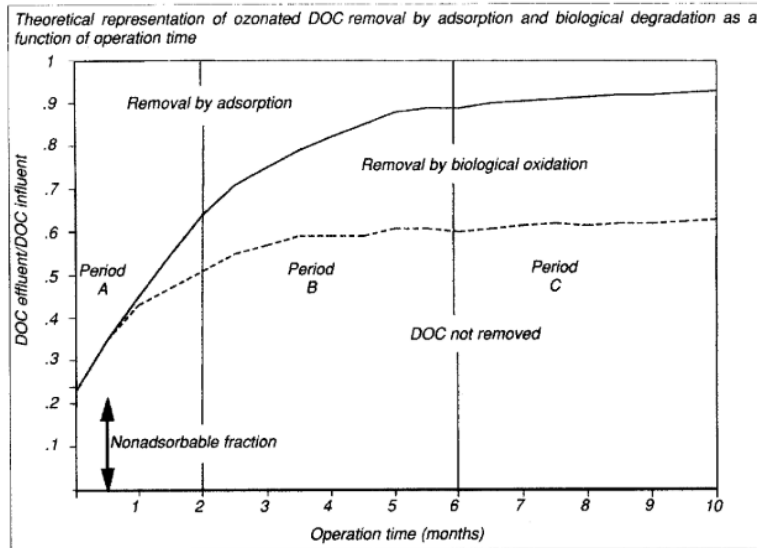


Figure 1.1: Theoretical representation of the transition from a new GAC filter to a biologically-active one. Reprinted with permission (Dussert and Van Stone, 1994).

The stages of biofilter start-up have been well described (Dussert and Van Stone, 1994). For experimentation investigations of treatment process performance and optimization, the period during which a filter is biologically-active and operating at steady-state conditions is of typical focus (see Period C in Figure 1.1). Analogously, the transition from exclusively adsorptive GAC filtration to biologically active GAC filtration, and the associated mechanistic behaviour in these filters, is less well understood. For example, the presence of biological activity can trigger headloss accumulation, or the type of organic matter removed may vary depending on whether adsorption or biodegradation is the dominant removal process.

Importantly, many design and operational questions regarding classical biological filtration during drinking water treatment remain to be answered. For example, studies have provided anecdotal information on biofilters with a GAC cap stacked above a non-adsorptive medium (Andrew de Vera et al., 2019; Ndiongue et al., 2006; Stoddart and Gagnon, 2017), however, these studies have not provided a comparative examination of this filter configuration to all non-adsorptive medium biofilters or dual media GAC over sand filters. Although the operational advantages of GAC media relative to other non-adsorptive media such as anthracite have been widely reported (i.e. more NOM removal by biofiltration, especially at lower water temperatures and improved process resiliency after exposure to disinfectant) (Dussert and Tramposch, 1996; Krasner et al., 1993), the extent to which these advantages are relevant in capped filters is not well understood. Given the common need for utilities to balance target contaminant removal with budgetary constraints (Evans et al., 2010; Moore and Watson, 2007), these design and operational aspects of biological filtration must be investigated further.

1.1. Research Objectives

This research aimed to improve the scientific and operational understanding of drinking water treatment by biologically-active GAC/sand filtration processes. This included studying the relationship between organic matter removal and biomass, determining if the start-up period had an impact on conventional performance metrics, and characterizing the type of organic matter removed. These questions were extended to GAC-capped anthracite filters, as these relationships have not been previously reported in detail. More specifically, the objectives of this research were to:

1. Evaluate the evolution of organic matter removal in a new GAC filter and compare it to that in an established biologically-active GAC filter containing exhausted GAC.
2. Evaluate the types of organic matter that are removed by classical biofiltration.
3. Investigate the potential performance-related advantages or disadvantages of a GAC-capped anthracite-configured biological filters.
4. Characterize NOM removal and traditional aspects of filter operation (headloss accumulation, turbidity removal) among varying filter configurations.

1.2. Research Approach

Pilot-scale experiments were conducted at the Region of Waterloo's Mannheim Drinking Water Treatment Plant in Kitchener, Ontario, Canada (i.e. "the full-scale WTP"), which treats water from the Grand River. The treatment process consists of coagulation, flocculation, sedimentation, ozonation, GAC/sand dual media biofiltration, UV irradiation, followed by free chlorine disinfection. The pilot plant was outfitted with four filters, and was fed with the same ozonated water that entered the full-scale filters.

To document NOM removal in new GAC filters, three of the pilot filters were used to investigate how biofilter performance evolved in (1) new GAC over new sand filter, (2) a biologically-active GAC over new sand filter, and (3) a combination of new and biologically-active GAC, over new sand filter. The biologically-active GAC had been in operation in the full-scale WTP for several years and its adsorptive capacity was exhausted. The new GAC was the same media as in the biologically active GAC filters, but previously unused. These three filter configurations allowed for an in-depth analysis of the operational, and performance differences between filter being started up with fresh versus already acclimated and biologically active media. A fourth filter contained new anthracite over new sand; it enabled comparison to the evolution of biological filter performance with non-adsorptive media. This same filter also was used to investigate biologically-active GAC capping—this was achieved by replacing some of the anthracite with biologically-active GAC during the second phase of experimentation. Traditional aspects of filter performance, including headloss accumulation, turbidity removal, NOM removal (as measured but the

removal of dissolved organic carbon [DOC]), as well as carbon character (measured by LC-OCD), and biomass accumulation were investigated.

1.3. Thesis Organization

A review of relevant literature on biofiltration, including start-up performance, organic matter characterization, and media types, is provided in Chapter 2. Chapter 3 details the experimental procedure, equipment, and analytical methods used for this research. Research results are presented in Chapter 4 and there is extensive discussion in this chapter on the contributions of the research to the body of scientific understanding of classical biological filtration processes and their application for NOM removal during drinking water treatment. Finally, Chapter 5 contains the conclusions that were drawn from this research. The detailed data and background information are presented in several appendices.

2. Literature Review

2.1. Biological Filtration – Overview

In biologically-active filters (biofilters), microorganisms present in the influent water are deposited on filtration media surfaces, where they attach, proliferate, and thrive. These microbes naturally remain attached to the filter media surfaces by biofilm secretion, which allows them to withstand the fluid shear forces of backwashing (Ahmad et al., 1998).

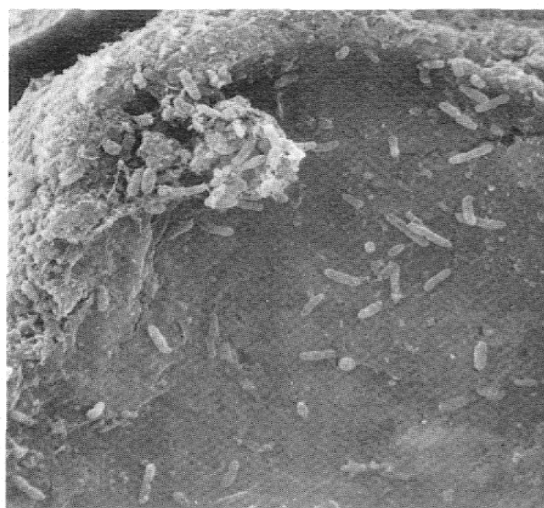


Figure 2.1 A scanning electronic micrograph image displays bacterial biofilms on a GAC granule. Reprinted (adapted) with permission from (Weber et al., 1978) Copyright (2019) American Chemical Society.

The metabolic activity of the microorganisms in biofilters effectively removes contaminants, hence the term ‘biological filtration’. This alternative treatment process is especially prevalent in GAC filters that are preceded by ozonation (without pre-chlorination). In such systems, ozone oxidises and breaks down natural organic matter (NOM) into smaller byproducts that are biodegraded more quickly (Amy and Carlson, 1997; Hozalski et al., 1999). These NOM compounds are a substrate consumed by naturally-occurring microbial populations attached to the GAC medium within the downstream filter bed (Edzwald 2011). GAC media are highly porous media and engineered to remove dissolved drinking water constituents by adsorption. The rough, irregular surface, high surface area, and adsorptive capacity of GAC make its surface an ideal attachment site for microbiological activity (Urfer et al., 1997). The primary treatment goal of a biologically-active carbon (BAC) filter is to remove taste and odour compounds (McDowall et al., 2009), DBP precursors (LeChevallier et al., 1992; Miltner, et al., 1995), membrane foulants (Edzwald, 2011; Van der Hoek et al., 1999), and other substrates that support microbiological proliferation in distribution systems (Van der Kooij 1992; Zhang and Huck 1996). Notably, biologically active filters offer

this contaminant removal capacity while still effective in removing particles and pathogens like traditional chemically-assisted filtration processes (Emelko, 2001; Huck et al., 2001, 2002; Emelko et al., 2005; Evans, 2010; Kirisits et al., 2019). Because of this operational capacity and resilience, biological filtration has been suggested as a key, cost-effective treatment option for climate change adaptation in areas prone to climate change-exacerbated landscape disturbances such as wildfire and hurricanes (Emelko et al., 2011). Moreover, because optimal biofilter performance has been associated with rough media surfaces (Kirisits et al., 2019), it is possible that there particle and pathogen removal performance may be further optimized (Jin et al., 2017;2016;2015a,b). Accordingly, biological filtration processes can play an increasingly important role in many municipal drinking water treatment plants.

2.2. Biological Filtration – Start-Up

The microbial communities that flourish in biological filtration processes are indigenous to the raw water source; thus, it is possible for filters to become biologically active unintentionally, especially in absence of pre-treatment (e.g. chlorination) for prevention of microbiological activity. However, intentional conversion of conventional filters to biologically active operation (by discontinuing or relocating chlorine addition) requires time needed for biofilm establishment. This is frequently referred to as the ‘start-up’ time in biological filtration, and it is an aspect of the technology over which utility operators have little control.

2.2.1. Start-Up of New GAC Filters

When a new GAC filter is put into service with the intention that it will become biologically active, there is a generally expected evolution (or pattern) of dissolved organic carbon (DOC) removal performance. During the first stage, the GAC media are highly adsorptive and remove much if not most of the DOC. As the filter continues to operate, this adsorptive capacity decreases at a decelerated rate, while simultaneously, biological activity begins to develop and stabilize. In the final stage of GAC biofilter start-up, DOC removal stabilizes—it has been suggested that removal then occurs primarily by biodegradation (Dussert and Tramposch, 1996; Dussert and Van Stone, 1994); notably, direct biodegradation, as opposed to bioregeneration (i.e. adsorption followed by biodegradation) has not been demonstrated.

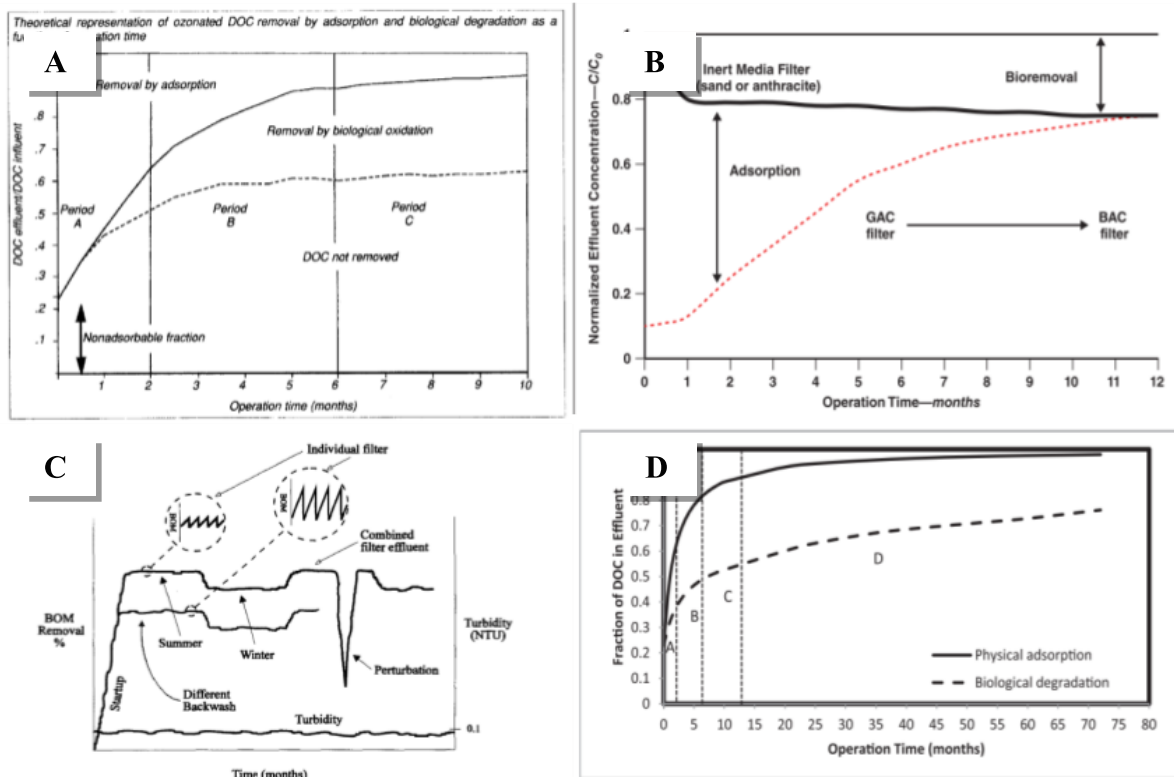


Figure 2.2 Theoretical representations of DOC removal over the operational time of a biologically active filter. Reprinted with permission (2019). Dussert and Van Stone, 1994 (A); Brown et al., 2015 (B); Huck et al., 2000 (C); Korotta-Gamage and Sathasivan, 2017 (D)

Although GAC is widely used for treatment of micro-pollutants because of its adsorptive capacity (Edzwald, 2011), a recent survey of utilities indicates that it is increasingly being used (approximately 30% of the time at present) to enable biological filtration specifically (Schindeman et al., 2012).

Biological activity contributes to the exhaustion of GAC adsorptive sites; however, it also enables utilities to utilize GAC biofiltration to most reliably (relative to other media types) achieve some extent of DOC removal long after the media have been exhausted. Of course, exhausted media still have the capacity to achieve traditional particle filtration goals of conventional filtration processes. It has been hypothesized that BAC filtration processes remove DOC in a synergistic cycle in which organic matter adsorbs to the GAC surface and the biological activity in the vicinity of these sites subsequently removes that DOC by biodegradation, thereby freeing those sites for further adsorption (Azzeh et al. 2015; Gibert, et al. 2013a; Klimenko et al. 2002). Incontrovertible proof of this theory is not currently available, however, and the extent of adsorption or biodegradation that contributes to DOC removal by biofiltration has not been demonstrated. Although it has been speculated that GAC enables more biomass growth than non-adsorptive media (Wang et al., 1995) and accordingly results in more DOC removal than less expensive, non-

adsorptive media (LeChevallier et al., 1992). Several investigations have demonstrated that DOC removal does not necessarily directly correlate with biological proliferation (Emelko et al., 2006; Pharand et al., 2014). Accordingly, classical biofiltration process optimization for maximizing DOC removal during drinking water treatment requires a better understanding of the dynamics and roles of adsorption and direct (i.e. from the bulk suspension as opposed to from the GAC media surface) biodegradation processes.

Many studies have attempted to distinguish between the adsorption and biodegradation phase of biofiltration because the relative dominance of these different mechanisms of contaminant/target compound removal is generally believed to change during these phases of the filter life cycle; thus, in the case of DOC removal, the types of DOC that are most efficiently removed can change. For example, adsorption preferentially removes more aromatic, hydrophobic types of organic matter (Ates et al., 2007; Fu et al., 2017a), whereas biodegradation is more effective at removing more hydrophilic (and more biodegradable) types of organic matter (Hozalski et al., 1995)—the removal of organic matter is discussed in greater detail in Section 2.3.2. Additional operational factors that must be considered when implementing GAC for ultimate biofiltration include the potentially greater release (during the early stages of operation) of heterotrophic bacteria that will exert subsequent oxidant demand, as opposed to well-established BAC filters (Papciak et al., 2016; Servais et al., 1994), and turbidity removal, which may be comparable or even better than that observed using conventional, non-adsorptive anthracite media in some cases (Edzwald, 2011).

In a survey of drinking water professionals, the importance of identifying when a BAC filter reaches steady-state, or in other words, becomes acclimated, was among the most cited concerns and areas of uncertainty (Evans et al., 2010). The general assumption is that the biological activity is stable at the same point as when organic matter removal (typically measured by DOC concentration) reaches steady-state (Dussert and Kovacic, 1996; Dussert and Van Stone, 1994). In recent years, the amount of biomass and/or biological activity in these filters has been frequently evaluated concurrently with DOC removal. Reported process start-up times required to reach acclimation (i.e. steady-state removal of DOC, and biomass concentration or activity) by BAC treatment initiated with new GAC preceded by conventional pre-treatment (coagulation, flocculation, sedimentation) and subsequent ozonation systems are summarized in Table 2.1. From this table it is evident that these two sets of performance parameters do not necessarily stabilize at the same time.

Table 2.1: BAC filter start-up times to acclimation with new GAC preceded by conventionally-treated ozonated systems

Organic matter and type of biomass	Water source	Influent water quality	Empty bed contact time (min)	Temperature (°C)	Time to steady state	Values at steady state	Reference
DOC GAC cell density	Surface and/or ground-water	1.1 to 5.5 mg DOC/L Influent biomass unknown	19	Room Temp.	8 months for DOC 5 months for cell density	33 % DOC removal 0.01 to 0.1 cells per μm^2 of GAC	Gibert et al., 2013a ¹
DOC GAC cell density and ATP-per-cell	Surface water	0.8 to 1.4 mg DOC/L Influent biomass unknown	18	5 to 15	4 months for DOC Unclear for GAC cell density ² 6 weeks for ATP-per-cell	40 – 50% DOC removal 10^7 - 10^8 cells per g ww BAC and $\sim 5 \cdot 10^{-8}$ ATP-per-cell	Lohwacharin et al., 2015
DOC and BDOC Fixed bacterial biomass per GAC	Not specified	1.5 mg DOC/L and 0.4 mg BDOC/L $5 \cdot 10^3$ to 10^4 bacteria/mL	10	9 to 22	3 – 4 months for DOC, BDOC remained roughly stable 3 – 4 months for fixed bacterial biomass ³	$\sim 14\%$ DOC and 50-60% BDOC removal $2.3 \mu\text{g C/cm}^3$ GAC (biomass in carbon)	Servais et al., 1994
DOC O ₂ consumption and CO ₂ release	Surface water	8 – 10 DOC mg/L Influent biomass unknown	40	3 to 21	6 – 7 months for DOC removal O ₂ and CO ₂ did not correlate with DOC	20% DOC removal Varying results	Van Der Aa, et al. 2012; Van Der Aa, et al. 2011
COD _{Mn} Phospholipid biomass	Surface water	2.7 – 4.4 COD _{Mn} mg/L 30 CFU/mL	0.2	7 to 26	~ 2.5 months for COD _{Mn} 4 months for phospholipid biomass	$\sim 45\%$ COD _{Mn} removal 32.5 nmol-P/cm^3 GAC	Liao et al., 2016
DOC Cells per GAC (using ATP)	Not specified	1.5 – 2.0 mg/L DOC Influent biomass unknown	15	> 10	~ 2.5 months for DOC 3 months for cells/GAC	15 – 30% DOC removal $(5.37 \pm 1.10) \cdot 10^7$ cells/g GAC	Fu, et al., 2017a; Fu, et al., 2017b ⁴
<p>1. GAC is not new but regenerated. According to supplier, characteristics should have been similar. 2. GAC cell density was stable from week 1 to week 16 and increased from week 16 to week 28. 3. Slow decrease was apparent in the biomass after stabilizing. 4. Influent water was pre-oxidized and conventionally treated; however, pre-oxidation conditions were not specified.</p>							

The relationship between microbiological proliferation in GAC filters and the removal of organic matter is unclear (Table 2.1), as there are a wide variety of methods for measuring biological activity, or biomass quantity (Evans et al., 2013). Another level of complexity is the variety of ways in which filters are deemed to be biologically active during start-up; in practice, they are most frequently considered biologically active if (1) the media have been extracted from full-scale plant filters that have been operated for at least several years (McKie et al., 2016) or (2) their operation is initiated with new media and they are operated until they contain the same amount of biomass as a reference biological filter (Nemani et al., 2018; Servais et al., 1994). Somewhat recently, the notion of a benchmark quantity of biomass (10^2 to 10^3 ng ATP per cm^3 of GAC or anthracite) that defines whether a filter is biologically active has been proposed (Pharand et al., 2014); however, most studies on this topic were conducted prior to this suggestion. Thus, although there is no unified definition of a fully-acclimated biological filter, the most commonly accepted approach at present is the point at which biological activity and/or organic matter removal reach steady-state. An improved understanding of the relationship between these two parameters is therefore necessary.

2.2.2. Acclimation Phase – Organic Matter Removal

During GAC manufacturing, carbonaceous materials (such as vegetative derivatives, lignite, natural coal, and coke) are heated pyrolytically and activated. The result are granules with a highly porous structure and thus, a large internal surface area that can be as high as 400 to 500 m^2 per gram of media (Weber and Van Vliet, 1980). The final product is a material that is highly suitable for physical adsorption (transport and attachment of adsorbents to the adsorbate due to attractive forces) and chemical adsorption (when the adsorbate reacts with the surface to form a covalent bond or an ionic bond) (Crittenden et al., 2012). Over time, the adsorptive sites of a GAC contactor become exhausted and the GAC requires replacement or regeneration (Edzwald, 2011).

Adsorption is an effective process that has a variety of industrial and treatment applications (air pollution, wastewater). In this context, the influence of adsorption is examined in drinking water filters that involve the treatment of surface water in which DOC is predominantly comprised of NOM. When a new GAC filter is being started up, it typically removes the majority of organic matter (80% – 90%) (Buchanan et al., 2008; Dussert and Van Stone, 1994; Moore et al., 2001). The remaining 10% – 20% fraction of DOC exiting the filter during this period is theorized to be non-adsorptive organic matter (Dussert and Van Stone, 1994; Lohwacharin et al., 2015). Except for this fraction, almost all forms of DOC are removed by adsorption, including the biodegradable fractions of organic matter (Servais et al., 1994). In theory, the concentration of contaminants in the effluent of a GAC contactor follows an S-curve pattern from the beginning to the end of its operational life (see Figure 2.3A). In the first stage, there is 100% removal of the target compound (or very close to it) by the GAC, as there is ample adsorptive capacity within all layers

of the filter. In the second stage, the upper layers of GAC become exhausted, and there is not enough contact time in the GAC filter to contain the entirety of the mass-transfer (i.e. adsorption) zone. In the third stage, breakthrough of the target compound occurs (i.e. the effluent concentration exceeds the targeted effluent concentration) (Baruth, 2005). At this point, the GAC contactor requires replacement or regeneration. In biological filtration, however, DOC removal often continues after the GAC adsorption sites are exhausted. It has been speculated that this occurs either by direct biodegradation from the bulk suspension, by bioregeneration in which the DOC adsorbs on the GAC surface and is subsequently degraded by nearby microorganisms in the biofilm, allowing for further adsorption, or by a combination of these mechanisms.

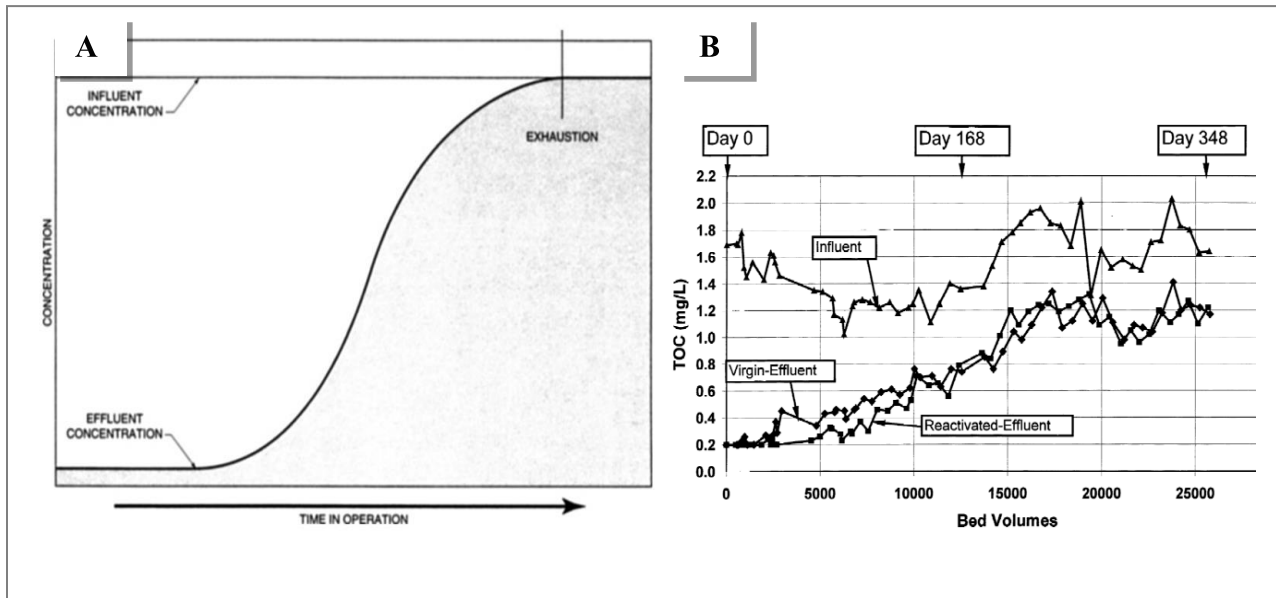


Figure 2.3: (A) Typical S-curve of a GAC contactor from the beginning to end of its operational life (Baruth, 2005), (B) the TOC influent and the S-curve shape of the TOC effluent in a new GAC filter becoming biologically active (Moore et al., 2001)

GAC filter effluent target compound water quality will typically present as an S-curve, like that presented in the conceptual model in Figure 2.3A. This same pattern is also observed in biological GAC filters when they are first put into service, as illustrated in Moore et al. (2001) (Figure 2.3B). Notably, this general trend in biofilter influent and effluent organic matter has been widely observed (DeWaters and DiGiano, 1990; Van Der Aa et al., 2012; Van der Hoek et al., 1999; Velten et al., 2011a; Velten et al., 2007). Thus, although there is rapid microbiological colonization while a new GAC biofilter is becoming exhausted, adsorption is still the dominant mechanism of organic matter removal during the start-up phase.

2.2.3. Acclimation Phase – Microbiological Colonization

During this early phase of biological filtration, relatively few bacterial cells are retained by the GAC media (Papineau et al., 2010; Servais et al., 1994). It is theorized that the microbial cells first come

into contact with the GAC media grains much like any other particles during physico-chemical filtration; that is, as a result of van der Waals attraction, steric interactions, and electrostatic (double layer) interactions (Hermansson, 1999). Once microbial cells do begin to accumulate on the extensive surfaces of GAC collectors, they secrete extra-cellular polymeric substances (EPS) that promote attachment, serve as protective barriers, and mediate the transport of substrate to the biofilm (Sutherland, 2001). EPS can also be hydrolyzed to biomass-associated products and eventually recycled as new substrate (Laspidou and Rittmann, 2002) The active biomass then continues to grow by consuming substrate in its surrounding vicinity and using it to build active biomass and EPS. In an established biofilm, convective flow of the substrate to the inner cell clusters becomes restricted. Diffusion, or the transport of solutes by concentration gradients, is thus the predominant method of solute transport within cell aggregates. Water channels and pores within mature biofilms also provide transport pathways for substrate (Stewart, 2003). Accordingly, because substrate can be transported across mature biofilms (and because biofilms can also be patchy), the adsorptive capacity of filtration media may impact organic matter removal in biologically-active GAC filters, as has been suggested and demonstrated by Spanjers (2017).

2.2.4. Steady-State Phase – Organic Matter Removal by Biodegradation

Eventually during the operation of a biofilter, organic matter removal and microbial biomass will reach an equilibrium—exactly how this happens has been widely theorized. The “diffusion transport resistance” theory relies on mathematical modeling to demonstrate the relationship between bioregeneration and the diffusion of absorbed substrate to the outer surface of a GAC media grain; here, an imbalance between the desorption rate and the concentration of organic matter in the liquid phase cause a decrease in bioregeneration (Speitel and Digiano, 1987). The stabilization of microbiological communities as a result of predation by protozoa also has been suggested (Servais et al., 1994). Diffusion limitation associated with biofilm thickness (i.e. the growth of biofilms until their thickness reaches a critical level beyond which nutrient diffusion across the biofilm cannot occur) also has been proposed (Lazarova and Manem, 1995). Operational conditions such as frequent and consistent backwashing may also impact or “control” biomass growth in biofilters, as a biofilm that is too thick may not only remove NOM less efficiently, but also cause excessive headloss accumulation (Scholz and Martin, 1997). It has been further suggested that bioregeneration efficiency in biologically-active GAC filters may gradually decrease over the long term due to a non-reversible accumulation of inorganic substances and dead cells (Laspidou and Rittmann, 2002; Lohwacharin et al., 2011).

2.2.5. Removal by Biodegradation: Direct Biodegradation and Bioregeneration

Biodegradation is an oxidation process in which the organic matter substrate acts as an electron donor to the electron-accepting biomass (Metcalf and Eddy, 2013). Sometimes, this mediation of electron

transfer between reduced compounds and oxidized compounds can alter inorganic contaminants into forms that are easier to remove during treatment (Brown et al., 2015; Laspidou and Rittmann, 2002). In biological filtration, colloidal solid matter can also become absorbed into porous biofilms (Drury et al., 1993). Primarily, though, biological filtration removes organic matter by uptake and conversion into biofilm (Van der Kooij, 1992).

During classical biofiltration in drinking water treatment with GAC media, the removal of organic matter can continue several years after the GAC has lost most of its adsorptive capacity (Rattier et al., 2012; Scholz and Martin, 1997), either through direct biodegradation from the bulk matrix or as the active biofilm consumes substrate on GAC surfaces, thereby freeing up sites for further adsorption. This latter process is referred to as “bioregeneration”. As diffusion is the dominant substrate transport mechanism within a biofilm (Stewart, 2003), adsorbate can desorb from GAC surfaces during periods of low substrate concentration in the surrounding water matrix, improving accessibility of the substrate to the biofilm and enhancing direct biodegradation; however, if the substrate concentration in the surrounding water matrix is too low, it may hinder biodegradation (Speitel and Digiano, 1987). Dissolved organic matter includes a wide spectrum of molecular configurations (Gjessing et al., 1999) however, and there are likely several potential biodegradation pathways. Another such pathway is the multi-step process of biodegradation of macromolecular structures. Here, the largest macromolecules attach to the outer GAC surface where they can be partially biodegraded by exocellular enzymes. The smaller compounds and biodegradation products can adsorb within the narrower GAC micropores, and once the diffusion gradient shifts, they may desorb, and undergo further biodegradation, continuing the cycle (Korotta-Gamage and Sathasivan, 2017; Simpson, 2008). Substrate remains bioavailable in GAC mesopores (2-50 nm); however, it has been speculated that adsorbates in the microporous sites (< 2 nm) are too strongly attached to desorb and biodegrade (Klimenko et al., 2002). This hypothesis has been supported by at least one investigation in which phenol (a lower-molecular-weight hydrophobic compound) adsorption in the micropores (< 0.7 nm) of activated carbon ultimately made it inaccessible to the exoenzymes necessary to transform it and make it further bioavailable (Martin et al., 2002). Collectively, these investigations demonstrate that the physical structure of the GAC, the adsorption kinetics of the system, and the type of substrate, are collectively important factors affecting biodegradation processes in biofilters.

2.3. Classical Biological Filtration – Performance Metrics

2.3.1. Headloss Accumulation and Turbidity Removal

Headloss accumulation rate, turbidity removal, and filter run time are operational parameters that characterize filtration process performance efficiency—they are relevant to both conventional and biologically chemically-assisted filtration processes. All chemically-assisted filtration processes, including

biofiltration, require regular backwashing to manage headloss accumulation and particle/turbidity breakthrough, though backwashing also may be scheduled in advance for planning/convenience. Backwashing involves reversing water flow so that the filter bed is fluidized, expanding porosity between the collector grains and effectively removing the contaminant particles trapped throughout the depth of the filter (Edzwald, 2011). While it is possible that excessive biofilm growth can exacerbate headloss accumulation in the filters or lead to turbidity breakthrough in these processes (Simpson, 2008), such challenges in the operation of classical biological filtration processes during drinking water treatment (where process influent water is relatively nutrient poor compared to municipal and some industrial wastewater treatment processes) have not been widely reported. To ensure adequate, vigorous backwashing, sub-fluidization water wash has been combined with air scour and referred to as “collapse pulse” backwashing (Amirtharajah, 1993; Amirtharajah et al., 1991). Notably, while this procedure provides a rigorous cleaning of filter beds, it does not have substantively detrimental impacts on biomass or its ability to remove DOC or AOC (Ahmad et al., 1998; Emelko et al., 2006).

2.3.2. Organic Matter Removal

TOC and DOC are bulk parameters that have been used traditionally to quantify organic matter in water. In most natural waters, DOC accounts for greater than 90% of TOC (Thurman, 1986) it also tends to be the most challenging component of natural organic matter for water treatment (Karanfil et al., 2005) because it is a precursor to DBP formation, and also a potential contributor to taste and odour compounds, membrane foulants, and microbial proliferation in distribution systems (Edzwald, 2011). Several methods beyond TOC and DOC exist for characterizing organic matter. These include biodegradable dissolved organic carbon (BDOC), or organic matter that is removed specifically by the oxidation of bacteria (Servais et al., 1989) and assimilable organic carbon (AOC), which is measured by the accrued mass of biofilm development as a direct result of organic matter (Van der Kooij, 1992). These are frequent parameters in biological filtration studies since they have direct implications for the potential for regrowth in the distribution systems (Servais et al., 1989; Van der Kooij, 1992). Fluorescence excitation-emission matrices can be used to identify humic substances, protein-like compounds, and colloidal component of organic matter; however, these methods are still evolving and have limited utility because they are not quantitative (Park and Snyder, 2018; Peiris et al., 2010). UV_{254} , SUVA (specific UV absorbance), and LC-OCD approaches are discussed in detail below.

UV₂₅₄ and SUVA

UV absorbance at a wavelength of 254 nm provides an indication of the quantity of double carbon bonds, and more specifically the aromaticity of organic matter in water. From a practical perspective, UV_{254}

is a useful indicator of larger molecular weight compounds, as they tend to have a higher level of aromaticity (Edzwald, 2011; Shams, 2018).

Specific UV₂₅₄ absorbance (SUVA) is sample UV₂₅₄ normalized to its DOC concentration. Higher SUVA values indicate a higher fraction of aromatic organic matter. SUVA values under 2 L/mg.m are comprised of mostly hydrophilic compounds, and above 4 L/mg.m are mostly hydrophobic, and SUVA values between 2 and 4 L/mg.m are a mixture (Sillanpää, 2014). Notably, SUVA often correlates well with DBP (trihalomethane (THM) and haloacetic acid (HAA)) formation potentials (Fu et al., 2017a; Hua et al., 2015; Susa and Lemus, 2017; Yang et al., 2005).

Carbon double bonds are potential electron donors, so oxidants and disinfectants are quick to chemically react with these compounds (Edzwald and Kaminski, 2009). This theory supports why SUVA is a good predictor of DBP formation potential, however this may not be the case in all circumstances. Nemani et al. (2016) conducted a correlation analysis of the SUVA from biological filtration effluent and the THM₄ and HAA₉ formation potential. Overall, the correlations between these two metrics were poor ($R^2 = 0.33$ and 0.03 , respectively). It was also speculated in that study, however, that the SUVA was very low (between 0.5 and 0.7 L/mg.m) and that the predominance of aliphatic organic matter may have skewed the results of the correlation study. This was also the case in Ates et al. (2007). Overall, a higher SUVA value generally corresponds to increased DBP formation, including THMs, HAAs, THAAs and CFs (Fu et al., 2017a; Hua et al., 2015; Susa and Lemus, 2017; Yang et al., 2005). As with all over-arching theories about NOM, however, there are some limitations. For example, the correlation is not valid for bromo- or bromochloro-DBPs (Yang et al., 2005), also, the relationship between SUVA and DBP can vary significantly depending on the water source or water treatment applied (Ates et al., 2007; Kitis et al., 2004; Tan et al., 2005). Overall, removing DOC quantitatively will reduce DBP formation potential (Selbes et al., 2016), however changes in SUVA are a robust indicator of changes in DBP formation potential.

While new GAC filters preferentially adsorb aromatic compounds (Ates et al., 2007; Kitis et al., 2004), the removal of organic matter by microbiological activity typically does not have an impact on the SUVA of the influent water. This is not surprising, as the microbiological activity targets smaller, more biodegradable components, and UV₂₅₄-absorbing organic matter tends to be larger in size, more aromatic, and less biodegradable (Edzwald, 2011; González et al., 2013). Ozonation typically decreases SUVA; changes in SUVA have not been observed in BAC systems either preceded by ozonation (Selbes et al., 2017; Zhang et al., 2017) or not preceded (Mckie et al., 2019; Zhang et al., 2017). In one case, it was even reported that a BAC system preferentially removed smaller, non-UV absorbing compounds, and therefore caused SUVA to increase (Han et al., 2013).

LC-OCD

Liquid chromatography-organic carbon detection (LC-OCD) is a method that provides information on the different sizes and chemical functions of organic matter, quantifying them on the basis of organic carbon (Huber et al., 2011). Dissolved organic matter is separated into five fractions based on molecular weight and size. The stream is then directed to a thin-film reactor that oxidises the sample and produces corresponding chromatographic peaks. The peaks are integrated to provide information on the quantity of biopolymers, humic substances, building blocks, low molecular weight neutrals and low molecular weight acids (LMW neutrals and LMW acids, respectively) (Huber and Frimmel, 1988). Typical surface water sources are comprised of 2–10% biopolymers, 55–90% humic substances, 10–15% building blocks, 10–15% LMW neutrals, and 2–10% LMW acids (Baghoth et al., 2009; Lautenschlager et al., 2014; Ronteltap et al., 2008). Table 2.2 provides a summary of the current knowledge on what these fractions are and their physical and chemical properties.

Table 2.2: LC-OCD fractions and their properties

LC-OCD fraction	Molecular weight and size	Composition	Properties
Biopolymers	<ul style="list-style-type: none"> • 50,000 – 2·10⁶ Da^a • >> 20,000 Da^b • > 10,000 Da^c 	<ul style="list-style-type: none"> • Polysaccharides, amino acids, proteins^{a,b} 	<ul style="list-style-type: none"> • Hydrophilic, not UV₂₅₄-absorbing^{a,c}
Humic substances	<ul style="list-style-type: none"> • 100 – 100,000 Da^a • 20,000-1,000 Da^b 	<ul style="list-style-type: none"> • Humic substances and fulvic acids^{a,c} 	<ul style="list-style-type: none"> • UV-absorbing^c • Can include both aquagenic, autochthonous compounds and pedogenic, allochthonous compounds^c
Building blocks	<ul style="list-style-type: none"> • 350 – 500 Da^a • 300 – 500 Da^b 	<ul style="list-style-type: none"> • Intermediates to humic substances and LMW acids^{a,c} 	<ul style="list-style-type: none"> • Humic-like substances^c • Cannot be removed by flocculation^c
LMW acids	<ul style="list-style-type: none"> • < 350 Da^a • <<350 Da^b 	<ul style="list-style-type: none"> • Among final degradation products^a 	<ul style="list-style-type: none"> • Highly biodegradable^c
LMW neutrals	<ul style="list-style-type: none"> • < 350 Da^a • <350 Da^b 	<ul style="list-style-type: none"> • Among final degradation products^a • Includes alcohols, aldehydes, ketones and amino acids^{a,c} 	<ul style="list-style-type: none"> • Amphillic^b and hydrophillic^c • Highly biodegradable^c
<p>a. González et al. (2013) – provided size information in g/mol, converted to Da here. b. Kennedy et al. (2005) c. Huber et al. (2011)</p>			

Notably, humic substances and biopolymers are associated with DBP formation (Azzeh et al., 2015; McKie et al., 2015; Wassink et al., 2011) and there is strong evidence that biopolymers contribute to membrane fouling (Peldszus et al., 2012; Rahman et al., 2014; Siembida-Losch et al., 2015; Tian et al.,

2013; Zheng et al., 2009). Biological filtration is generally effective at removing both humic substances (Gibert et al., 2013b; Lautenschlager et al., 2014) and biopolymers (Rahman et al., 2014) from water; however, a variety of factors including filter influent water quality, empty bed contact time (EBCT), and pre-treatment affect performance (Siembida-Losch et al., 2015; Lautenschlager et al., 2014; Rahman et al., 2014). Moreover, it is important to note that multiple types of compounds comprise the LC-OCD fractions of organic matter. For example, in one report, polysaccharides were removed by BAC, but not proteins, although both contribute to the biopolymer fraction (Siembida-Losch et al., 2015).

It is well-known that biological filtration, and especially BAC filtration, is effective for membrane pre-treatment (Peldszus et al., 2012); however, few studies have focused on GAC adsorption as a treatment process for biopolymers and humic substances. Jeong et al. (2016) traced NOM fractions throughout all the treatment processes at a full-scale plant at which chlorination preceded GAC filtration, which was able to remove 44% of biopolymers, 54% of humic substances, and 48% of the LMW neutrals and acids. The building blocks fraction, however, increased by 57%—the authors did suggest a reason for this observation. One possible theory for this is that by chlorinating upstream of the GAC contactors, the larger recalcitrant biopolymers and humic substances were broken down into smaller building blocks. The authors assumed that adsorption was the dominant organic matter removal process within the GAC filters. In another study, a new GAC contactor was operated in parallel with an old, biologically-active GAC filter; there, the biologically-active GAC filter was capable of removing humic- and protein-like substances, whereas the new GAC filter was only capable of removing humic-like substances (Peleato and Andrews, 2015).

2.4. GAC-Capped Anthracite/sand Filters for Biological NOM Removal

Anthracite is a common type of filter media made from coal. Unlike GAC, it is not processed to possess a high adsorptive capacity, and it is less expensive. Dual media anthracite/sand filters are one of the most common filter media configurations. The installation of a GAC as a cap over mono-media or dual-media filters containing anthracite and/or sand offers a cost-effective approach for potentially achieving maximal removal of organic matter with biological filtration without the need to fully invest in more expensive GAC media that also suffers from attrition due to its relative friability over the longer term (Evans, 2010; Evans et al., 2010). In a survey of water treatment plants in Ontario, a sizable fraction (14%) used GAC specifically as a filter cap over anthracite in their treatment process (Moore and Watson, 2007). Although biofiltration performance using anthracite media relative to GAC has been widely compared, relatively little is known about the biofiltration performance of GAC-capped anthracite/sand filters.

While the use of GAC caps during drinking water filtration has been reported; however, these investigations have not focused on organic matter removal specifically. For example, Stoddart and Gagnon (2017) ran GAC-capped anthracite/sand filters in parallel with anthracite/sand filters and focused on pre-

oxidation methods. Ndongue et al. (2006) investigated MIB and geosmin removal by GAC capped filters, and although Andrew et al. (2019) compared GAC-capped anthracite sand to a GAC/sand dual media filter, both filters were fed with HOCl, and the effect of pre-oxidation was also the primary focus of the study. Nonetheless, at the very least, these investigations provide consistent evidence that GAC capped anthracite/sand filters can achieve the traditional filtration performance objective of acceptable turbidity removal, regardless of chlorine addition.

2.4.1. NOM Removal during Biological Filtration with GAC and Anthracite Media

Biomass Quantity

GAC is consistently found to support more biomass than anthracite using a wide spectrum of different biomass quantification methods, even at cold temperatures or when its adsorptive capacity is exhausted (Emelko et al., 2006; LeChevallier et al., 1992). It has been suggested that the rough, irregular surface of GAC media, which is believed to protect bacterial communities against the fluid shear forces during backwashing (Urfer et al., 1997). In one example, GAC and anthracite biofilter performance was compared and biomass quantity was inferred by analyzing ATP biofilm, EPS polysaccharides, and EPS proteins; while the GAC media did not support significantly more ATP biofilm, significantly more EPS proteins and polysaccharides were found on its surface (McKie et al., 2015). GAC has also been found to retain five times more phospholipid biomass than anthracite (~250 versus ~50 nmol lipid-P/g media) (Wang et al., 1995). LeChevallier et al. (1992) examined the biological activity of a GAC/sand filter and a mixed media anthracite/sand/garnet filter and found more heterotrophic bacteria (measured by heterotrophic plate counts; HPC) within the GAC media (3.6×10^8 cfu/g versus 9.7×10^6 cfu/g).

Organic Matter Removal

Organic matter removal by biofiltration was first investigated to identify potential advantages in removing more AOC, or organic matter that directly contributes to regrowth in the distribution systems, than other media (Van der Kooij 1992; LeChevallier et al., 1992). Dussert and Tramposch (1996) studied AOC removal by various biological filtration media and found that (1) GAC removes more AOC than anthracite at lower temperatures, but at temperatures above 12 to 15°C, the removal is comparable, (2) GAC develops biomass sooner, and thus removes AOC sooner, than anthracite, and (3) GAC's high adsorptive capacity during start-up also contributes to AOC removal, unlike non-adsorptive anthracite. Similar observations have been made regarding DOC and TOC removal by biofiltration processes. In some cases, TOC and DOC removals by GAC biofiltration were up to twice as high as those achieved by anthracite media (LeChevallier et al., 1992; McKie et al., 2015; Singh Sidhu et al., 2018). Overall, biologically-active anthracite is capable of removing organic matter (Azzeh et al., 2015; Liu et al., 2001), especially at warm temperatures (Emelko et al., 2006). Curiously, comparative studies between biologically-active anthracite

and GAC have found no effective difference between UV₂₅₄ removal and SUVA change (Selbes et al., 2017; Singh Sidhu et al., 2018; Shuangyi Zhang et al., 2017). Studies that have analysed other carbon fractions have made this topic somewhat more ambiguous. For example, biopolymers and humic substances were removed to varying extents by GAC and anthracite biofilters (Table 2.3).

Table 2.3: Biopolymer and humic substance removal by anthracite and GAC biofilters

Biopolymer removal		Humic substance removal		Source
GAC	Anthracite	GAC	Anthracite	
22% to 25%	-5% to -13% (produced BPs)	0% to 1%	11%	(Singh Sidhu et al., 2018) ¹
17% to 25%	15% to 24%	-2% (produced) to 2% removal	1%	(Azzeh et al., 2015) ²

1. This system preceding the biological filters is a coagulation/flocculation/sedimentation process. The study was conducted during warm water temperatures, between 16 and 23°C.
2. This system differs in that it is direct biofiltration. The ranges of biopolymer and humic substance removal are combined from cold water (5-12°C) and warm water temperatures (17-23°C).
* Both systems had EBCT between 10-11 min.

When compared to anthracite biofilters, GAC biofilters also regularly remove more DBP precursors (DOC), thereby reducing DBP formation potential (Krasner et al., 1993; Wang et al., 1995). In one investigation conducted at warm water conditions (16–23°C), biologically active GAC removed more THM and HAA formation potential (8–17% and 15–24%, respectively), than did anthracite filters (<2% and 5–9%, respectively) (Singh Sidhu et al., 2018). In contrast, Azzeh et al (2015) conducted an experiment in cold water (5–12°C) and warm water conditions (17–25°C), and found no discernable difference between biologically-active GAC and anthracite biofilters in terms of THM and HAA formation-potential removal.

Classical biofiltration is a cost-effective process for removing organic matter to prevent subsequent DBP formation and distribution system regrowth during drinking water treatment. Collectively, the body of available biological filtration research underscores that there is a need to improve the scientific and operational understanding of drinking water treatment by conventional GAC/sand and biologically-active GAC/sand filtration (i.e. classical biofiltration) processes. The amount of GAC required to achieve adequate biofiltration also must be understood, so that the utility of relatively more economical configurations such as GAC caps over non-adsorptive anthracite/sand biofilters can be considered. Accordingly, the relationship between organic matter removal and biomass also must be better understood and the mechanisms that govern it must be better described so that biological filtration can be more efficiently implemented and optimized.

3. Materials and Methods

3.1. Research Approach

A pilot-scale biological filtration investigation was conducted to address the research objectives detailed in Chapter 1. Thus, more tactically, this investigation involved: (1) observing how closely new GAC filters display the trend of transient-to-steady-state organic matter removal, (2) investigating the relationship between steady-state biomass production and organic matter removal, (3) comparing the performance of new GAC filters and new filters started up with established biologically-active media and (4) comparing the performance of a multi-media GAC-capped anthracite/sand filter to a GAC/sand filter to investigate the adequacy of capping for enhanced DOC removal during drinking water treatment. The work was conducted in a pilot plant facility located at the Region of Waterloo's full-scale Mannheim Drinking Water Treatment Plant. The pilot plant was equipped with four filter columns that receive the same influent water as the full-scale filters and have similar operational features, including backwash capacity, valve controls, data collection, etc. The pilot plant filters contained new GAC media, exhausted GAC media from the full-scale WTP, a combination of the two (40% new, 60% old GAC), and new anthracite media with a spent GAC cap. The plant was operated from June 4th to September 5th, 2018. Headloss across the filters and turbidity removal by the filters was evaluated continuously. Grab samples were collected regularly to enable the analysis of DOC (every two to three days), UV₂₅₄ absorbance, biopolymers and humics (by LC-OCD), and biofilm ATP (weekly). The performance of each media configuration is presented and discussed in Chapter 4.

3.2. Region of Waterloo Mannheim Drinking Water Treatment Plant

This research project was conducted at the pilot plant in Region of Waterloo's full-scale Mannheim Drinking Water Treatment Plant. A portion of the full-scale plant filter influent is diverted to the pilot plant facility (Section 3.3), which was operated separately and continuously.

3.2.1. Full-scale WTP Processes – Prior to Pilot-scale Filtration

Water from the Grand River is first stored in reservoirs located at the Hidden Valley Low Lift Station from which it is pumped to the main treatment facility where it undergoes chemically-assisted filtration. When it arrives at the WTP, the flow is separated into two streams that subsequently enter two sides of the treatment plant that are operated in parallel. Poly-aluminum chloride (PACl) is added for coagulation and then flocculated with the aid of a polyelectrolyte (Magnafloc LT22S); the doses were 30 +/- 5 mg/L and 0.22 +/- 0.03 mg/L, respectively during the study period. Following sedimentation, the water is ozonated; the applied dose was 3.1 +/- 0.4 mg O₃/L during the present investigation. The ozone contactor effluents from each of the two treatment trains in the full-scale WTP flow to granular media

filters, but before this, some water is redirected to the pilot plant facility. The ozonated water is the influent to the pilot plant filters; the connection is controlled so that the pilot plant receives either stream of ozonated water, or a mixture of the two. All effluent from the pilot plant was sent to the full-scale WTP waste facility (Region of Waterloo, 2017, 2018).

3.2.2. Full-scale WTP Processes – After Connection to Pilot Plant

Each stream of post-ozonated water was separated further into two streams, entering 4 dual-media biologically-active GAC over sand filters. These full-scale filters had a similar configuration to the pilot plant filters and were thus used as a reference through the experiment. Approximately 1.3 m of FILTRASORB® 816 GAC media (Calgon Carbon Corporation, Pittsburgh, PA), with an effective size (ES) of 1.3 mm to 1.5 mm, is stacked on 0.3 m of silica sand with an ES of 0.45 to 0.55 mm, yielding an overall media depth of 1.6 m. Filtered water is subsequently UV irradiated, chloraminated, and discharged to the distribution system.

3.3. Pilot Plant

The pilot plant consisted of four filters, 4.2 m high, and 20 cm in diameter, and constructed of clear PVC piping. Filter effluent holding tanks are located one floor below, and are connected to a pump that enables backwashing of each filter with its own effluent. The system includes automatic and manual flow valves, headloss meters, and turbidimeters connected to a SCADA system that monitored these parameters every 2 to 5 minutes. For this research project, the pilot plant facility was set up with varying types of media in the filters, which were operated in parallel. The pilot plant was operated as closely as possible to a typical, full-scale water treatment plant, and the performance of the filters was monitored and analysed for the completion of the research objectives.

3.3.1. Pilot Plant Facility –Media Types

To enable direct comparison in performance as a function of the media configuration, the pilot filters were all backwashed using the same protocol (see Section 3.4.1) and all contained a media (either GAC or anthracite) with an effective size of 1.3 to 1.5 mm, over silica sand with an effective size of 0.45 to 0.55 mm. The primary differences in the bulk media are summarized in Table 3.1.

Table 3.1: Properties of media used in this study

Type of media	Past use	Effective size ³	Uniformity coefficient-(UC) ³
New GAC ¹	• New media	1.3 to 1.5 mm	1.4
Spent GAC ¹	• Used in full-scale plant from April 2013 to May 2018	1.3 to 1.5 mm	1.4
Anthracite ²	• New media	1.3 to 1.5 mm	1.4
Silica Sand ²	• New media	0.45 to 0.55 mm	1.5
1. FILTRASORB® 816 GAC by Calgon Carbon Corporation, Pittsburgh, PA. 2. Supplied by Anthrafilter Media & Coal Ltd., Brantford, ON. 3. For additional information and grain size distributions, see Appendix C.			

The origin and prior use of each GAC type is important and was vital to the meeting the research objectives detailed in Chapter 1. The term “spent” GAC refers to GAC that was first used in the full-scale filters starting in April 2013 (after purchase) and was continuously utilized until May 2018, thereby rendering it exhausted. The medium was removed and briefly held in a separate container before being transported into the pilot plant facility. At the time of extraction, the full-scale filter had been in service for approximately 18 h since its last backwash. The new GAC, anthracite, and sand were purchased new from various suppliers (Table 3.1).

The filter media configurations used during the present investigation are provided below (Table 3.2). The bulk medium, composed of various combinations of GAC or anthracite, was 1.0 m in depth situated over 0.3 m of silica sand, providing a total bed depth of 1.3 m. Filters 1 to 3 were dual-media filters, and Filter 4 was a multimedia filter.

Table 3.2: Pilot scale media configurations

Media depth (m)	Filter 1	Filter 2	Filter 3	Filter 4
1.0	New GAC	A mixture of new GAC and spent GAC (ratio 2:3)	Spent GAC	0.2 m of spent GAC laid on top of 0.8 m of new anthracite
0.3	New silica sand	New silica sand	New silica sand	New silica sand

Filters 1 through 3 were configured to provide a deeper understanding of performance differences between new and spent GAC during the filter start up period. Comparison of Filter 4 to Filter 3 informed the performance of a GAC capped anthracite/sand filter relative to a spent GAC/sand filter.

3.3.2. Pilot Plant Facility – Filter Media Configurations

The media were stacked in the filters as per ANSI/AWWA standards B100 and B604 (American Water Works Association et al., 2012). Prior work in the pilot plant involved biologically active filtration (Wong, 2015), so the columns needed to be cleaned and sanitized with sodium hypochlorite to thoroughly remove any bacteria or other microbes that had accumulated on the interior of the columns prior to the present investigation. The new GAC and new anthracite were placed in a separate container and were wetted and rinsed with chloraminated tap water to remove fines. Once all of the media were loaded into the filters, they were backwashed under a reverse hydraulic loading rate of 50 m/h for approximately five minutes to ensure that the fines were removed and the media heights in all of the filters were consistent. It should be noted that this backwashing step briefly exposed all of the GAC media, including the biologically-active media, to chloramines that were present in the water. It likely did not impact the activity of the established biological media because the contact was brief; this lack of impact would be consistent with what has been observed for the full-scale biological filters at the Mannheim WTP, which are regularly backwashed with chlorinated water without any measurable impact on biological filtration performance (Huck et al., 2000). ATP data from the present investigation (first date of experimentation; see Figure 4.13, Figure 4.24, Figure 4.37, and Figure 4.46 in Chapter 4) are consistent with this expectation.

3.3.3. Pilot Plant Facility – Water and Filter Media Sampling

Throughout the experimental period, water and media samples were extracted regularly from ports situated at various depths in the filter media. Figure 3.1 identifies the locations of these ports.

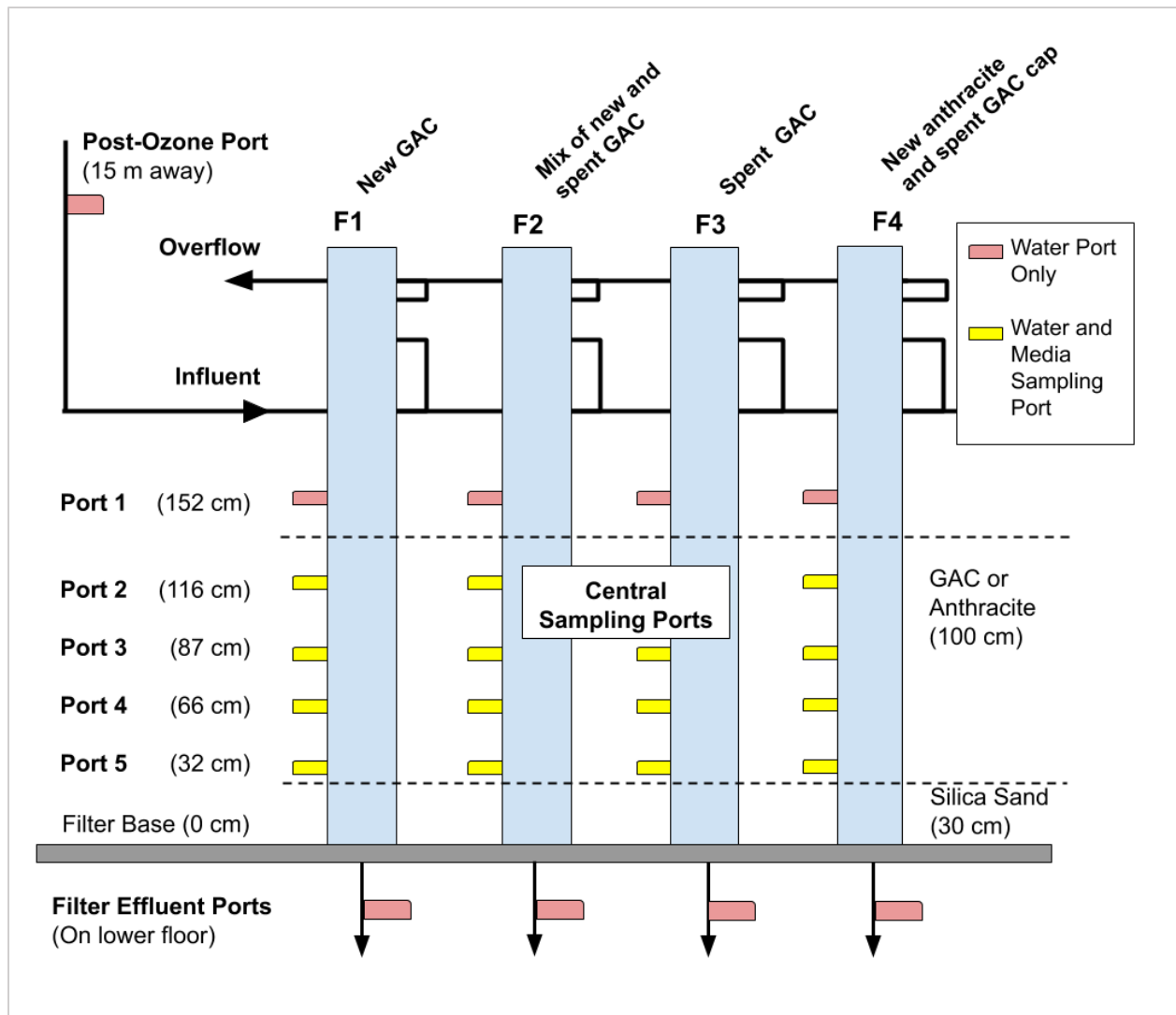


Figure 3.1 Pilot plant schematic with sampling ports and their heights above the base of the filter columns

Filter influent water samples were typically collected from Port 1, located approximately 15 cm above the media surface. They also could be collected at the post-ozone sampling station in the full-scale plant, from which the water must travel through approximately 15 m of piping before reaching the pilot plant. Both water and media could be sampled from the various ports along the depth of the filter columns during operation. Finally, the filter effluent sampling location was located next to the effluent storage tanks, one floor below the pilot plant.

3.3.4. Pilot Plant Equipment and Operation

Headloss, filter effluent turbidity, and effluent flow rate data were collected by an Allen-Bradley supervisory control and data acquisition (SCADA) system (Rockwell Automation, Inc., Milwaukee, WI).

Differential pressure was measured from the base of each filter, to a port approximately 2 m above, using Foxboro IDP10-T differential pressure transmitters (Invensys Foxboro, Foxboro, MA). Filter effluent turbidity was measured using Hach sc100™ 1720E Low Range Turbidimeters (Hach, Loveland, CO).

The pilot filters were operated in constant-head, constant-flow mode using an automated system of effluent control valves. The SCADA system was programmed to control the effluent flow rate using Chemline Q Series electric valve actuators (Chemline Inc., Cranford, NJ). ABB ProcessMaster FEP300 (ABB Inc., Zürich, Switzerland) electromagnetic flow meters reported flow rate data to the SCADA system.

A Porter-Cable Pancake compressor (Pentair, Inc., Arden Hills, MN) was used during the air-scour portion of the backwashing procedure, and the flow rate of the air supply was controlled using a King Instruments 7530 Series acrylic tube flow meter (King Instruments Company, Garden Grove, CA). A Grundfos CRNI vertical multi-stage centrifugal pump (Grundfos Pumps Corp., Bjerringbro, Denmark) was used to backwash the filters.

3.4. Backwash and Operation

The filters were operated at a hydraulic loading rate of 7.6 m/h, which corresponded to an empty bed contact time (EBCT) of 10 minutes. The filters were backwashed approximately every two to three days, however, it should be noted that filter flow rates during the study period frequently declined (sometimes to the point of little or no flow) during the experimental period because of atypical solids accumulation in the filters likely associated with non-ideal pre-treatment at the full-scale plant during the experimental period—the full-scale plant experienced similar challenges in shortened run times during this period, resulting in more frequent backwashing. More frequent filter performance assessment was not possible during the pilot-scale investigation; therefore, this regular back-washing schedule (i.e., every two to three days) was implemented. Most importantly, backwashing occurred with adequate frequency so as to ensure that the filters were always wetted; thus, these periods of declining rate filtration were not expected to substantially impact gross differences in biological filtration performance. It follows that DOC degradation rates could not be reasonably evaluated because of the associated, variable EBCTs in the filters. Evaluation of these rates was not a focus of the present investigation; rather, the focus herein was to identify any key differences in NOM removal, such as differences in the removal of various sized NOM fractions that could help to inform the mechanisms contributing to biofilter performance during the various phases of operation. Operational details are provided in Tables A-1 and A-6.

The pilot filters were in operation from June 4th until September 5th, 2018, with an off-line period from July 13th to the 16th, 2018 to address operational issues. Each filter was backwashed with effluent from

its own dedicated storage tank. The collapsed-pulse backwashing procedure was performed as per Amirtharajah et al. (1991).

3.4.1. Backwash Protocol

Collapsed-pulse backwash consisted of air-scouring the media while undergoing a low-rate up-flow wash, then pausing to wait for the media to settle and any trapped air to dissipate following air shutdown. Next, the media was washed at a sufficiently high rate to achieve 30% bed expansion, followed by slowly decreasing the backwashing rate to achieve media stratification. This backwash procedure was altered slightly after June 29th, 2018 (further discussed in Section 3.4.2). Also, to achieve 30% bed expansion, backwashing procedure was slightly difference among different media configurations (Table 3.3).

The rates of water flow and air flow during this backwash were determined (Appendix B) as per Amirtharajah (1993) and Amirtharajah et al. (1991). Slight modifications to the procedure were then implemented during operation to ensure bed expansion; this was easily done by visual assessment of the filtration media in the clear PVC columns. The hydraulic loading rates, air flow rates, and duration of the backwashing steps are detailed below.

Table 3.3: Backwash settings used during pilot-scale biofiltration experiments

Backwash step	Duration	Loading rate and air flow
Backwash settings from June 4th - June 29th, 2018		
Air scour and low rate wash	6.5 min	Air flow = 54 m ³ /h/m ² HLR = 12.4 m/h (HLR = 14.3 m/h for Filter 4)
Media settling	2 min	-
High rate wash	5 min (or until water exiting is clear)	HLR = 50 m/h
Backwash settings from June 29th - Sept 5th, 2018		
Air scour and low rate wash	6.5 min	Air flow = 54 m ³ /h/m ² HLR = 12.4 m/h (HLR = 14.3 m/h for Filter 4)
Air scour and High rate wash	0.5 - 1 min	Air flow = 54 m ³ /h/m ² HLR = 50 m/h
High rate wash	5 min (or until water exiting is clear)	HLR = 50 m/h
HLR = Hydraulic Loading Rate		

All of the GAC filters were backwashed using the protocol described above. The configuration of Filter 4 included anthracite in addition to a cap layer of GAC. Given the different density of anthracite media, a slightly higher wash rate was required to achieve the same level of bed expansion (see *Air Scour and Low Rate Wash* row in Table 3.3).

3.4.2. Solids Accumulation in the Filters

After the first month of operation, it was found that the backwashing procedure was not sufficient to adequately remove solids (i.e. likely floc carryover from the chemical pre-treatment process as a result of rapid shifts in raw water quality; some biomass also was likely associated with these solids) within the filters. Similar to mudball formation, during these periods it appeared as if the filter media became clumped together in masses that did not completely break up during backwashing. This operational problem has been a hindrance for biological filters both at pilot-scale (Krasner et al., 1993; LeChevallier et al., 1992; Pacini et al., 2005) and full-scale (Evans et al. 2010; USEPA 2013). The solids and biomass caused excessive headloss accumulation and potentially increased the risk of preferential flow pathways. During the first phase of this experiment, some of the filters effectively became clogged almost immediately after the backwashing. On June 29th, 2018, the filters were found to be affected by this issue and underwent additional maintenance after the regular backwashing procedure. This included putting them under a simultaneous air scour and high rate wash for approximately 3 to 5 minutes, at 100 m³/h/m² of air flow and a 50 m/h backwash hydraulic loading rate. Filter 2 underwent another maintenance on August 23rd, 2018.



Figure 3.2: Solids masses emerging in Filter 4 (left) and Filter 2 (right) during backwashing on June 29th, 2018.

After maintenance on June 29th, 2018, the backwash procedure was altered as outlined in Table 3.3. The steps are 1) air-scouring and backwashing at a low-rate, 2) increasing the backwash rate to a high-rate wash 3) shutting off the air scour and continuing high-rate wash for 5 minutes.

3.4.3. Details on Operating Data Collection

Flow

Filter effluent flow rate was measured by electromagnetic flow meters that relayed information every two minutes to the Allen-Bradley supervisory control and data acquisition (SCADA) system.

Turbidity

Filter effluent turbidity was continuously measured using Low Range Turbidimeters. This information was relayed to the SCADA system every two minutes, except for Filter 4 (new anthracite capped with spent GAC), which was precise to every 15 minutes due to a programming error in the local instrument. Additionally, from August 18th to the 23rd, the turbidity meter for Filter 3 (spent GAC) needed to be taken off line for maintenance; thus, turbidity data are not available for this period.

Filter influent turbidity was measured from the post-ozonation stream entering the full-scale filters. This information was also precise to every 2 minutes.

Headloss

Headloss across the pilot filters was measured using differential pressure transmitters – this parameter was measured every 5 minutes.

Filter run time

Following backwashing, the filter influent flow through a filter was resumed at an operational flow rate of 4 L/min. The start of filter run time occurred when the filter effluent turbidity returned to 0.2 NTU after a period of deterioration during ripening. The threshold for the end of a filter run time was when the headloss exceeded 305 cm (the maximum hydraulic head), when the flow rate decreased to below 3 L/min, or when the turbidity exceeded 0.3 NTU for 10 minutes.

As mentioned previously, the filters were operated in constant-flow mode by maintaining a constant water level in the filter columns using an overflow and automated valves that progressively opened to maintain filter effluent flow. Due to full-scale treatment optimization challenges (that affected filter influent water quality) occasional abbreviated filter run times and periods of sub-optimal filtration occurred. Specifically, there were some occasions on which (1) terminal headloss was reached (and flow decreased to outside of the operational criterion of at least 3 L/min), (2) filters did not receive enough influent flow

and water level in the filter column dropped to below the overflow (though never to the point of that the media were not submerged), or (3) turbidity breakthrough occurred. In all of these cases, the filters were backwashed and returned to service and the filter runs were excluded from the present analysis.

3.5. Organic Matter Concentration and Characterization

Water samples were collected from the post-ozone sampling location, port 1 and the filter effluent ports (Figure 3.1) approximately every 2-3 days. The central sampling ports (Figure 3.1) were sampled approximately weekly. Water samples were collected during periods of stable filter operation, approximately 4 to 8 h after the filters were put into service. Sample collection and storage were performed according to Standard Methods 1060 B, which specifies that all glassware should be acid-washed 10% HCl and samples should be stored at 4°C until use; all vials also were pre-rinsed once with the sample matrix before collection (American Water Works Association et al., 2012).

3.5.1. DOC

DOC was analyzed approximately every 3 days in water samples collected from the post-ozone port, port 1, and the effluent sampling ports, and weekly, from the central sampling ports 2 to 5 (Figure 3.1). Samples were collected, stored and analysed according to Standard Methods 5310 C (American Water Works Association et al., 2012). The samples were filtered through 0.45 µm nominal porosity nylon membranes (GVS Filter Technology, Findlay, OH) which were rinsed with organic-free water prior to use. After filtration, the samples were acidified with H₃PO₄ to lower the pH to 2. A Sievers M9 Portable TOC Analyzer (SUEZ Water Technologies & Solutions, Trevese, PA) was used to measure DOC using the UV-persulfate method for analysing organic carbon. The inorganic carbon removal setting on the analyzer was activated.

3.5.2. UV Absorbance

UV₂₅₄ was analyzed approximately every 3 days in water samples collected from the post-ozone port, port 1, and the effluent sampling ports (Figure 3.1). Samples were analysed according to Standard Methods 5910 B (American Water Works Association et al., 2012). As in Section 3.5.1, the water samples were filtered through pre-rinsed 0.45 µm nominal porosity nylon membranes. UV absorbance at a wavelength of 254 nm was measured using a Real Tech UV₂₅₄ Field Meter (PentAir Apopka, FL). As recommended in Standard Method 5910 B, a quartz cuvette was used and was rinsed three times in organic-free water between each sample. Samples were analysed in triplicate.

3.5.3. LC-OCD

Dissolved organic matter in the filter influent and effluent streams was further characterized using liquid chromatography with organic carbon detection (LC-OCD) (Huber et al., 2011). Samples were

collected from the post-ozone port and the filter effluent ports (Figure 3.1) approximately every week; this analysis commenced one month after the filters were first put in to service (July 1, 2018); thus, this analysis focused on the transition from filter start-up to steady-state filtration, as detailed in the research objectives, as opposed to either the filter start-up or steady-state operation period exclusively.

LC-OCD analysis involves passing a water sample through a weak cation exchange column that separates the organic matter based on its molecular size (Huber and Frimmel 1991). Organic matter is typically separated into biopolymers (largest molecular weight, >10 kDa), humic substances, building blocks, low molecular-weight acids, and low molecular-weight neutrals (smallest molecular weight). This analysis occurs in two stages. First, the sample is passed through the instrument, which outputs chromatographic peaks, and then the peaks are integrated to calculate organic matter size fractionation using software and visual interpretation (Figure 3.3).

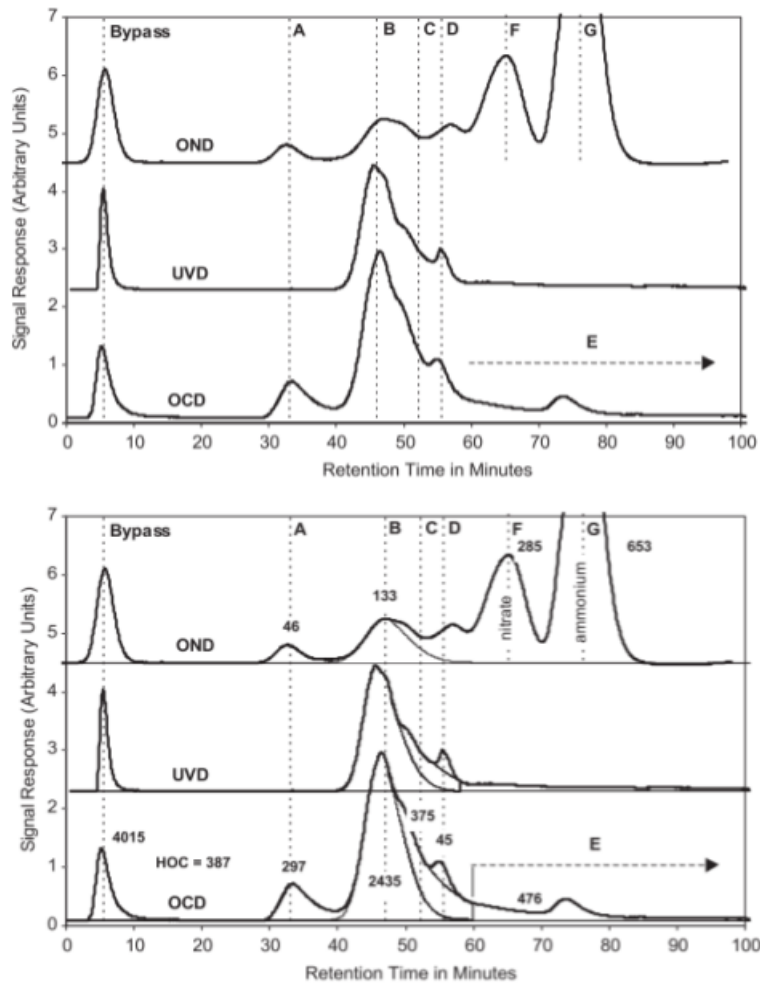


Figure 3.3: LC-OCD data output (top) and analysis (i.e. integration to determine peak area) (bottom) (Huber et al., 2011).

3.6. Microbiological Sampling and Analysis

The amount of active biomass present in the filters was evaluated by quantifying ATP concentration per mass of filter medium. This metric was used because it correlates well with total direct cell counts (Magic-Knezev and van der Kooij, 2004) and serves as a widely accepted indicator of active biofilm quantity in filters (Pharand et al., 2014).

ATP concentration per dry weight of media was determined approximately every 7 to 10 days. Filter media were collected after a filter run had ended and prior to backwashing. The water above the filter was drained prior to collection of the media. Instruments for media collection were sterilized by soaking in ethanol for 2 minutes and rinsed with organic-free water before coming in contact with the filter media. Approximately 5 g of media sample were collected in sterile, 40 mL EPA vials, containing 30 mL of a phosphate buffered saline (PBS) at pH 7.4. Samples were kept in coolers with ice packs and were analysed within 6 h of collection.

ATP concentration was measured using the Deposit & Surface Analysis (DSA) test kit (LuminUltra Technologies Ltd, Fredericton, NB). In brief, cells present in a sample were lysed, causing them to release ATP. Samples were then diluted and Luciferase enzyme was added to cause the ATP molecules to fluoresce. Upon mixing with the enzyme, the samples were immediately analyzed using a luminometer and an established conversion to determine ATP concentration. The manufacture's protocol was altered slightly; it states that once the biomass-covered solid samples are submerged in the lyse, they can be stored for up to one week. In this particular case, our sample medium is GAC covered in biomass, and once they were submerged in lyse, the ATP was released as expected, but the concentration in the supernatant of the lyse solution immediately started to decrease because the ATP was adsorbed onto the GAC. Samples collected on only three occasions (June 20th, June 27th, and July 6th, 2018) were impacted as a result and required a correction. This is discussed in Appendix B.

When biologically-active granular media are physically removed from the filter column, the bacteria present in the sample include cells that are attached (sessile) to the GAC and suspended, water-borne cells. To evaluate biofilter performance, it was intended that only the microbial activity of attached cells be measured; accordingly, a simple rinse step was introduced to avoid including suspended bacteria in the analysis of biomass attached to the filter media. An investigation was undertaken to evaluate the effect of rinsing. It involved the analysis of approximately 5 g of wet, biologically-active GAC in a 50 mL glass beaker, which were swirled gently 3 times after the addition 100 mL of ultra-pure water. ATP concentration in the supernatant from each rinse was analysed immediately using the Quench-Gone™ Aqueous Test Kit (LuminUltra Technologies Ltd, Fredericton, NB).

Table 3.4 Media sample rinsing results (ATP concentration in the supernatant after rinsing)

Effluent from Rinse 1	82 pg ATP/mL
Effluent from Rinse 2	14 pg ATP/mL
Effluent from Rinse 3	7 pg ATP/mL

In general, the first wash appeared to remove most of the suspended bacteria from the sample. However, it must be noted that the use of ultra-pure water instead of a phosphate buffered saline may have lysed some of the attached biofilm bacteria. Thus, the protocol was modified such that PBS at pH 7.4 was used to wash the media samples. The final media washing protocol is presented in Table 3.5.

Table 3.5: Determining ATP concentration in attached biofilter biomass

Phase of Microbiological Testing	Details
Media extraction	Collect 5 g of media from filters using a sterilized metal spatula. Placed in sterilized EPA vial containing 30 mL of PBS at pH 7.4. Stored on ice in coolers until analysis.
Media rinsing	Upon return to lab after media collection, immediately, gently invert sample vials 5 times. Slowly decant PBS supernatant to waste and weigh GAC.
Lab-bench ATP test	Add 1.00 g of wet media into the lyse solution, dilute it, combine 100 μ L of this solution to 100 μ L of Luciferase. Immediately analyze the sample using a luminometer.
Conversion to ATP concentration	Convert RLU reading to ATP concentration using following formula: $\frac{\text{ng ATP}}{\text{g dry} \cdot \text{media}} = \frac{\text{RLU}_{\text{Calibration}}}{\text{RLU}_{\text{Media Sample}}} \cdot \frac{50 \text{ ATP (ng)}}{\text{wet mass (g)}} \cdot \frac{\text{wet weight (g)}}{\text{dry weight (g)}}$

To determine the ATP concentration per mass of dry media, the ratio of wet weight to dry weight was calculated. This was done by simply extracting 1 kg of wet GAC and wet anthracite, weighing them, and reweighing them following air-drying. This was completed once prior to each experiment.

3.7. Statistical Methods

3.7.1. Steady-state Filter Performance Analysis Using Linear Regression

There is no universal indicator of when a biological filter has reached the end of its acclimation phase. As mentioned in Section 2.2.1, it is widely assumed that steady-state filter performance is achieved when the removal of biodegradable organic matter reaches steady-state. This approach was used here to determine when the pilot filters were acclimated and operating at steady-state.

Least squares linear regression analysis was used to determine the best fit line ($Y_i = \beta_0 + \beta_1 X_i + \varepsilon_i$) to the DOC removal data analyzed for each filter run. Specifically, the period of steady-state DOC removal in the filter was confirmed by calculating the best fit line to subsets of ten consecutive data points, (a minimum sample size of ten is considered acceptable for a simple linear regression (Harell et al., 1984)) starting from the beginning of the experiment (June 14th to July 27th, 2018) and proceeding in a stepwise manner with an increment of one sampling occasion until reaching the end of the study period (July 27 to September 5, 2018). Analysis of the significance of slope of that line was then used to confirm and establish the onset of steady-state filtration. The period of steady-state DOC removal was defined as the period during which filter effluent DOC concentration reaches steady-state, resulting in a slope that is not statistically different than a slope of zero. Variations of this approach have been used before to determine whether or not experimental data display transient or steady-state behaviour (Di Prima et al., 2018).

IBM® SPSS Statistics® Version 25.0 was used to conduct each linear regression. A parameter estimates analysis was conducted for each calculated linear model. It included a test of whether the slope (β_1) significantly contributed to the model (i.e. whether the slope was significantly different from zero). The 5% significance level ($\alpha=0.05$) was used. Thus, if $p > 0.05$ for β_1 , the slope of the linear regression model was not considered significant and it was concluded that the filter was operating at steady-state.

Notably, a linear regression model is appropriate if the data meet the following assumptions: (1) a linear model is appropriate for the relationship being described (as opposed to a non-linear model), 2) each observation (X_i) of the independent variable is measured without error, 3) the errors associated with the dependent variable (Y) are normally distributed, and 4) the variance is roughly equal along the regression line. The validity of these assumptions was confirmed using residuals plots (Appendix A). Data that presented any of these issues were log-transformed (base 10 and e) or square-root transformed, and analysed again, as recommended by Gotelli and Ellison (2013). For linear regression equations, see Appendix B.

3.7.2. Paired t-test for comparison

A paired-samples t-test was conducted to compare the performance data (organic matter removal etc.) between filters throughout the experimental period. Two-tailed tests were conducted using a 5% significance level ($\alpha=0.05$). The assumptions of a paired t-test are that (1) the differences between the matched pairs follows a roughly normal distribution and (2) that the variance between the two data sets is approximately equal. These assumptions were tested by visually inspecting the histograms for the differences between the matched pairs, as recommended by Gotelli and Ellison (2013) and McDonald (2014). The histograms need to display a severe deviation from normality for the assumption to be violated. All paired t-tests were conducted using IBM® SPSS Statistics® Version 25.0, and the assumptions tests and paired t-test equations are presented in Appendix B.

4. Results and Discussion

From June 4th to September 5th, 2018, four pilot plant filters at the Region of Waterloo Mannheim drinking water treatment plant were operated. Three were dual-media GAC over sand, all of which contained the same grain-size distribution and types of media, however, biological activity varied among them. The fourth was a multi-media filter with a GAC cap over anthracite and sand. Throughout the experimental period, traditional performance (headloss accumulation, turbidity removal), organic matter removal and character (DOC, UV₂₅₄, LC-OCD) and biomass accumulation (ATP concentration per gram of media) were analyzed.

4.1. Filter Influent Organic Matter during the Experimental Period

The influent water entering the pilot plant was surface water from the Grand River that had been pumped to the full-scale Mannheim WTP where it was coagulated with PACl, flocculated with a polyelectrolyte flocculant aid (floc aid), clarified and ozonated. The full-scale plant experienced some treatment challenges during the experimental period; therefore, it was necessary to evaluate the associated shifts in water quality that occurred (Section 4.1.1). The DOC, UV₂₅₄ and LC-OCD data (Section 4.1.2-4.1.3) are the best available indicators of pilot filter influent water quality because they were measured at the pilot plant while the filters were running, from a port just above the granular media. The other performance indicators were filter effluent turbidity and headloss (see Sections 4.3.2, 4.4.2, 4.5.2, and 4.6.2). Because of operational challenges at the full-scale plant and associated impacts on pilot plant operation, the collection of DOC, UV₂₅₄, and LC-OCD data could not commence until June 14th, 2018, even though the filters were first put in service on June 4th, 2018. Biofilm ATP was collected throughout the experimental period, however, because of the need to confirm biofilm development and filter acclimation, even if impacted by operational and pre-treatment challenges.

4.1.1. Settled, Post-Ozone Water Quality and Prior Treatment Steps

Raw water temperature at the entry point of the full-scale WTP (24 h averages) and settled, post-zone (i.e. filter influent) turbidity are presented in Figure 4.1. There were some relatively rapid changes in settled, post-zone water quality from approximately June 4th, 2018 to July 9th, 2018, with raw water temperature fluctuating between 18 and 27°C, and turbidity ranging from 1 to 7 NTU within a span of a few days—these fluctuations were even more pronounced over the course of each day and challenged both the pilot- and full-scale filters. PACl, floc aid, and applied ozone doses in the full-scale plant had to be adjusted regularly—the ranges of applied doses are also presented in Figure 4.1.

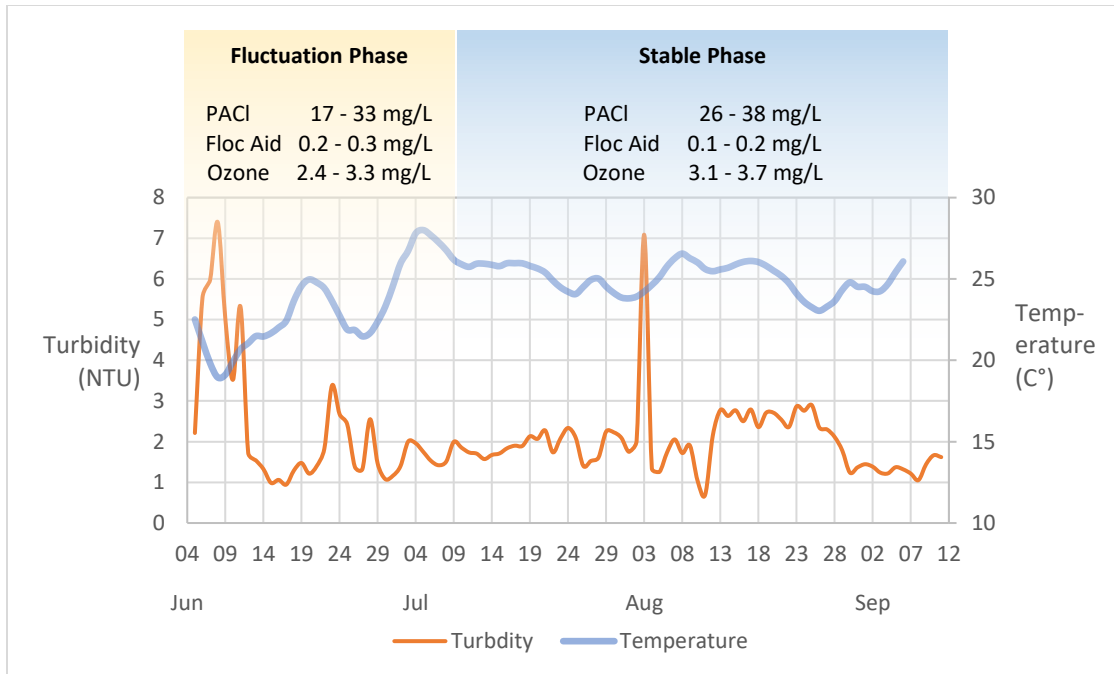


Figure 4.1: Average daily settled, post-ozone water turbidity and raw water temperature during fluctuation and stable phases of pilot filter operation

For discussion and analysis purposes, the influent water quality conditions over the experimental period were divided into two phases: the “fluctuating phase” before approximately July 9th, 2018, and the “stable phase” after July 9th, 2018, when the raw water quality stabilized, except for a single turbidity spike on August 3rd, 2018. The PACl, floc aid, and ozone dosage requirements also stabilized with raw water quality. As discussed in Section 3.4.2, the sub-optimal chemical pre-treatment that occurred during this period appeared to result in some solids/floc carryover from the sedimentation tank to the filters during these challenges periods; fortunately, these operational challenges were overcome using a more vigorous, collapse-pulsing backwash protocol (as described in Section 3.4.1).

4.1.2. Filter Influent DOC

The DOC concentration entering the pilot plant remained relatively steady, averaging 4.1 +/- 0.3 mg/L (mean +/- standard deviation) (Figure 4.2). As mentioned in Section 3.3.3, filter influent DOC concentration was characterized using water that could be collected from five possible locations: the post-ozone sampling station that is farthest away from the filter media surface, separated by approximately 15 m of piping from the pilot plant, and the four ports (Port 1) that are located directly above the media in each of the pilot filters.

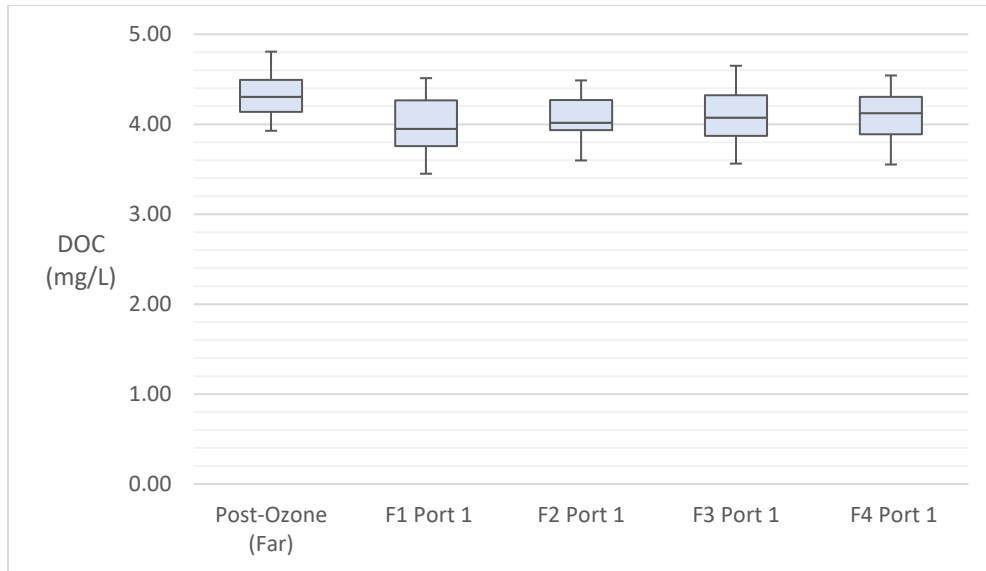


Figure 4.2: Comparison of DOC at the far port (full-scale ozone effluent redirection point) and Port 1 above the media in each filter, collected during experimental period (n = 21-24, μ = minimum value, τ = maximum value observed)

The DOC concentration measured at the sample port 15 m away from the plant averaged at 4.3 +/- 0.3 mg/L while that from the sample ports, averaged across each filter and over each experimental date, were 4.1 +/- 0.3 mg/L DOC (mean +/- standard deviation). The DOC concentrations at all of the sampling locations was analysed statistically (student's paired t-test, $\alpha = 0.05$, n = 17 to 24, depending on the specific location) and it was found that the influent from the post ozone sampling location approximately 15 m away from the filters was significantly different from those measured at each of the sample ports on the filter columns Table 4.1). In contrast, the DOC concentrations in the filter influent samples collected from directly above the media (Port 1) were not significantly from one another, except in the case of Filters 1 and 4 (i.e., new and spent GAC, respectively).

Table 4.1: Paired t-test results between the DOC concentrations at the post ozone sampling location and influent (Port 1) to each of the pilot filters.

	Post-Ozone	F1 Port 1	F2 Port 1	F3 Port 1	F4 Port 1
Post-Ozone	-	p < 0.0005	p = 0.001	p < 0.0005	p = 0.003
F1 Port 1	-	-	p = 0.397	p = 0.297	p = 0.044
F2 Port 1	-	-	-	p = 0.771	p = 0.407
F3 Port 1	-	-	-	-	p = 0.639
F4 Port 1	-	-	-	-	-

See Appendix C for histograms that demonstrate the assumptions of the paired t-test were met.

It is not clear why the DOC concentration 15 m upstream of the pilot plant was consistently slightly higher than that in the water just above the media in each filter. Given that the water was not pre-chlorinated prior to filtration, it is likely that some biodegradation in the 15 m of piping and/or in the water column above the filters, thereby resulting in some removal of DOC between these locations. Regardless, this difference was inconsequential in determining DOC removal by the biofilters because the samples collected from Port 1 just above the media and the effluent of each filter were used in this determination (and not the post-ozone DOC). Specifically, DOC removal during each filter run was calculated by subtracting the filter effluent DOC concentration in each filter from that in the influent concentration. Some natural variation in influent DOC concentration across the study filters would be expected; thus, the filter influent concentration on each date was calculated as the arithmetic mean of the samples collected from the Port 1 on each of the four filters. DOC concentrations were not included in removal calculations if the port in the sample location was broken, or if there appeared to be new GAC media were stuck inside the port.

4.1.3. Filter Influent UV₂₅₄ and Organic Matter Fractions

Filter influent UV₂₅₄ absorbance was calculated using the same approach as that used to determine the filter influent DOC concentrations (i.e. an average across all four filters was calculated). On average, the filter influent UV₂₅₄ over the duration of this investigation was 0.048 +/- 0.006 cm⁻¹. Accordingly, the mean filter influent SUVA was 1.2 +/- 0.1 L/mg.m⁻¹ (mean +/- standard deviation). This level of aromatic DOC in water entering filters was typical of natural surface water sources that had undergone conventional chemical pre-treatment (i.e. coagulation, flocculation, and sedimentation) followed by ozonation (Baghoth et al., 2009; Velten et al., 2011b; Zhang et al., 2017).

Filter influent organic carbon fraction concentrations evaluated by LC-OCD in samples collected at the post-ozone location were generally consistent with those that would be expected in natural surface waters containing both pedogenic, allochthonous compounds that originate from small rivers influenced by land runoff, and more aquagenic, autochthonous compounds, found in large water bodies, that are produced *in-situ* by microbial activity (Huber et al., 2011). They were also consistent with values previously reported after ozonation at the Mannheim WTP (Shams, 2017). Overall, the distributions of biopolymers, humic substances, building blocks, LMW neutrals and LMW acids was typical of what would be expected in surface water, with humic substances dominating the composition of the DOC (Figure 4.3).

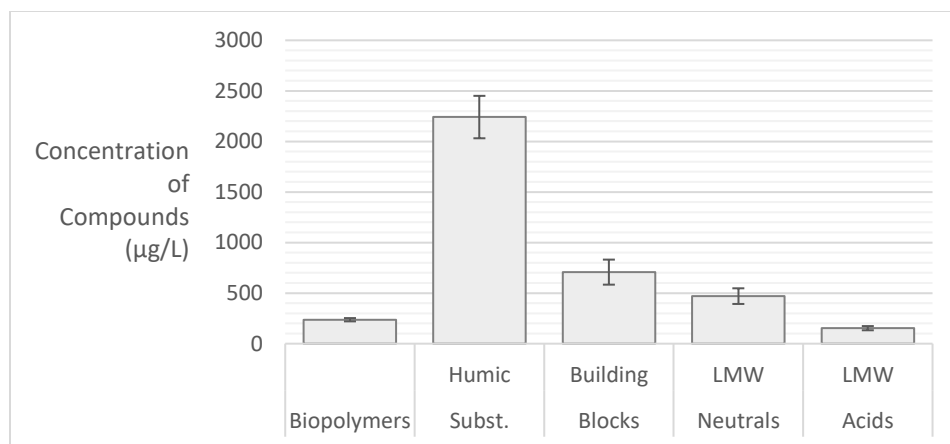


Figure 4.3: Average filter influent organic carbon fraction concentrations at the post-ozone location across the experimental period (mean +/- std. deviation, n=9)

4.2. Data Collection Biofiltration Process Performance

The removal of organic matter by each of the individual filters during the experimental period from June 4th to September 5th, 2018 (i.e. day 1 to day 93 of operation) is discussed here. The filters were backwashed approximately every 2 days during the experimental period (Section 3.4). In practice, filters would normally be backwashed prior to reaching the end of their run but on occasion during this research the filters were prematurely in need of backwashing resulting in the filters reaching end of run before backwashing. Turbidity removal was calculated as the difference between the full-scale filter influent turbidity (recorded by the plant's SCADA system) and the filter effluent turbidity values collected for each pilot filter and recorded by the SCADA system. Headloss accumulation rates exceeding 0.5 m/hour were omitted (as determined by the upper quartile range $Outlier = Q_3 + 1.5 * IQR$) as these unusually high rates were likely caused by floc carryover in the filter influent during non-optimal periods of pre-treatment in the full-scale plant.

For organic matter quantification and characterisation, DOC, UV_{254} , SUVA and LC-OCD are presented. It should be noted that the DOC and UV_{254} readings can be interpreted more easily because there is substantially more data (n = 14 to 20); in contrast, only 8 to 10 samples per filter could be analysed using LC-OCD. Although the LC-OCD results differentiate the organic matter into five fractions, the fractions of main interest are the larger, more recalcitrant humic substances and biopolymers, since these have been linked to DBP formation potential and membrane reversible and irreversible fouling (Zheng et al., 2009).

4.3. Performance of Filter 1 – New GAC

4.3.1. Turbidity Removal and Headloss Accumulation

Overall, Filter 1 achieved excellent turbidity removal, as the average filter run produced effluent less than 0.1 NTU (Table 4.2). Specifically, the filter effluent turbidity was 0.008 +/- 0.007 NTU (mean +/- standard deviation) during the experimental period. Filter cycles were generally terminated because of headloss accumulation in this filter in which turbidity breakthroughs above 0.3 NTU did not occur. The headloss accumulation rate in Filter 1 was 0.20 +/- 0.10 m/h (mean +/- standard deviation) during the experimental period. Notably, headloss accumulation in this filter varied somewhat during the experimental period (Figure 4.4), even considering extreme values above 0.5 m/h were removed.

Table 4.2: Mean turbidity removal by Filter 1 (new GAC) during the experimental period (n=35)

	Influent entering filter (NTU)	Filter effluent (NTU)	% Removal
Mean	0.93	0.09	88%
Std. deviation	0.44	0.01	6%

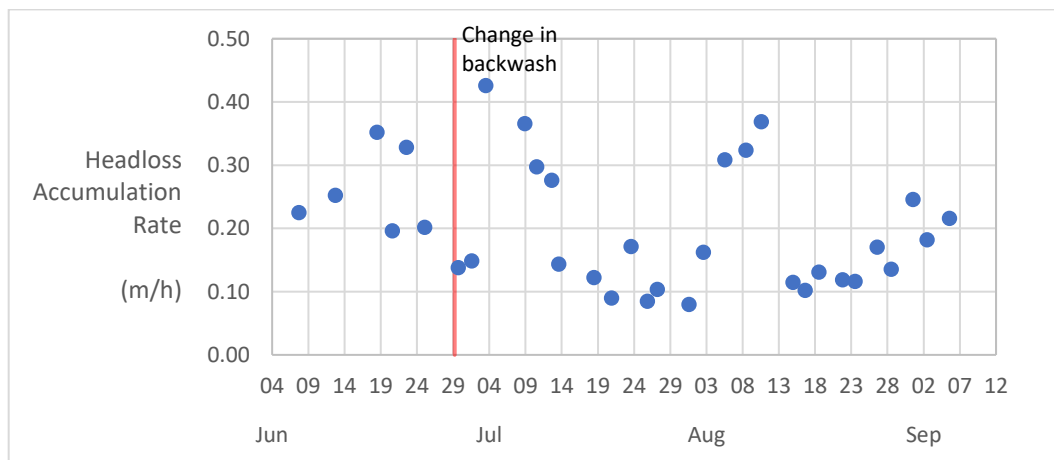


Figure 4.4: Headloss accumulation in Filter 1 (new GAC) during the experimental period

4.3.2. DOC

The effluent DOC concentration in Filter 1 was 2.3 +/- 0.8 DOC mg/L (mean +/- standard deviation) over the experimental period (Figure 4.5). DOC removal dropped from 85% to 50% in the first two weeks of the experiment (June 14th to June 30th, 2018) as the media became exhausted. It continued to

decrease until it reached steady-state (~25% removal) after approximately 2 months of operation (August 1st to September 5th, 2018).

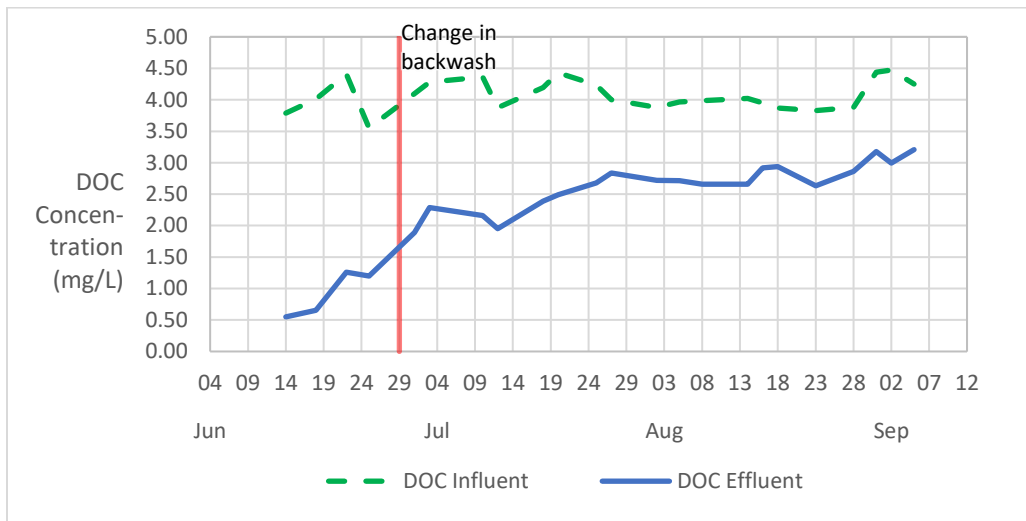


Figure 4.5: DOC concentrations in Filter 1 (new GAC) influent and effluent during the whole experimental period (n=23)

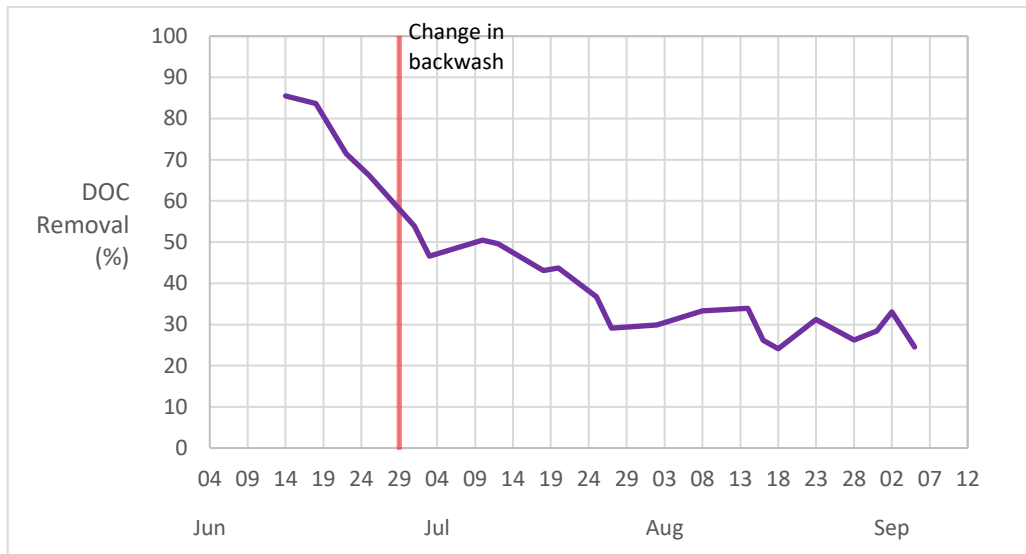


Figure 4.6: Percentage DOC removal in Filter 1 (new GAC) during the whole experimental period (n=23)

The period of steady-state DOC removal in the filter was confirmed by analyzing the slopes of the best fit lines (Table 4.3) determined for consecutive subsets of 10 data points by least squares linear regression (Section 3.7.1).

Table 4.3: Linear regression results confirming the period of steady-state DOC removal in Filter 1. This is the period during which filter effluent DOC concentration reached a steady-state, resulting in a slope that was not statistically different than a slope of zero.

Data included	Statistical significance of slope [†]
June 14 th to July 10 th	p < 0.0005
June 18 th to July 25 th	p < 0.0005
June 22 nd to July 27 th	p < 0.0005
June 25 th to Aug 2 nd	p < 0.0005
July 1 st to Aug 5 th	p < 0.0005
July 3 rd to Aug 8 th	p = 0.001
Jul 10 th to Aug 14 th	p = 0.002
Jul 12 th to Aug 16 th	p = 0.003
July 18 th to Aug 18 th	p = 0.005
July 20 th to Aug 23 rd	p = 0.041
July 25th to Aug 28th	p = 0.106
July 27th to Aug 31st	p = 0.316
Aug 2nd to Sept 2nd	p = 0.570
Aug 5th to Sept 5th	p = 0.259
† For every linear regression analysis ($Y_i = \beta_0 + \beta_1 X_i + \varepsilon_i$) units Y and X are in % removal and days since start of experiment, respectively.	

DOC removal fluctuated during the experimental period, as would be expected, because it included both initial filter (with fresh GAC media) and steady-state operation (after the GAC media were exhausted). Accordingly, performance analysis required consideration. Critically, the linear regression analysis described above (Table 4.3) enabled clear differentiation between the two operational periods. The filter performance data were divided into two stages: the initial operational period (June 4th to July 25th, 2018) and steady-state operational period (July 25th to Sept 5th, 2018).

Although the GAC in Filter 1 appeared to have exhausted much of its adsorptive capacity, it still removed 25% to 30% of the influent DOC concentration in the last month of the study period. This performance was well within the range of what has been reported elsewhere where new GAC filters were put in operation in conventional treatment plants with ozonation. For example, Krasner et al. (1993) reported an initial TOC removal of 33% after a new GAC filter had operated for one day, decreasing to 10-20% after 3 days. This relatively quick exhaustion was attributed to the filter's low EBCT of 1.4 minutes (vs x minutes in this case). Another investigation with a new GAC filter operated at an EBCT of 19 minutes reported DOC removals of 60-95% during the first 2 months of operation, with subsequent DOC removals at an average of 33% for the subsequent 8 to 12 months after presumed exhaustion (Gibert et al., 2013b). For reference purposes, Table 4.4 provides information the media configuration above each port.

Table 4.4: Filter 1 (new GAC) port heights and media layers

Port #	Height above the base	Layer of media above specified port
Port 2	116 cm	12 cm of new GAC media
Port 3	87 cm	29 cm of new GAC media
Port 4	66 cm	21 cm of new GAC media
Port 5	32 cm	34 cm of new GAC media
Effluent Port	Located on floor below	2 cm of new GAC media, 30 cm of silica sand followed by ~30 m of piping

The DOC concentration across the depth of the filters was measured approximately weekly (Figure 4.7). It is presented in two stages, before and during steady-state operational conditions.

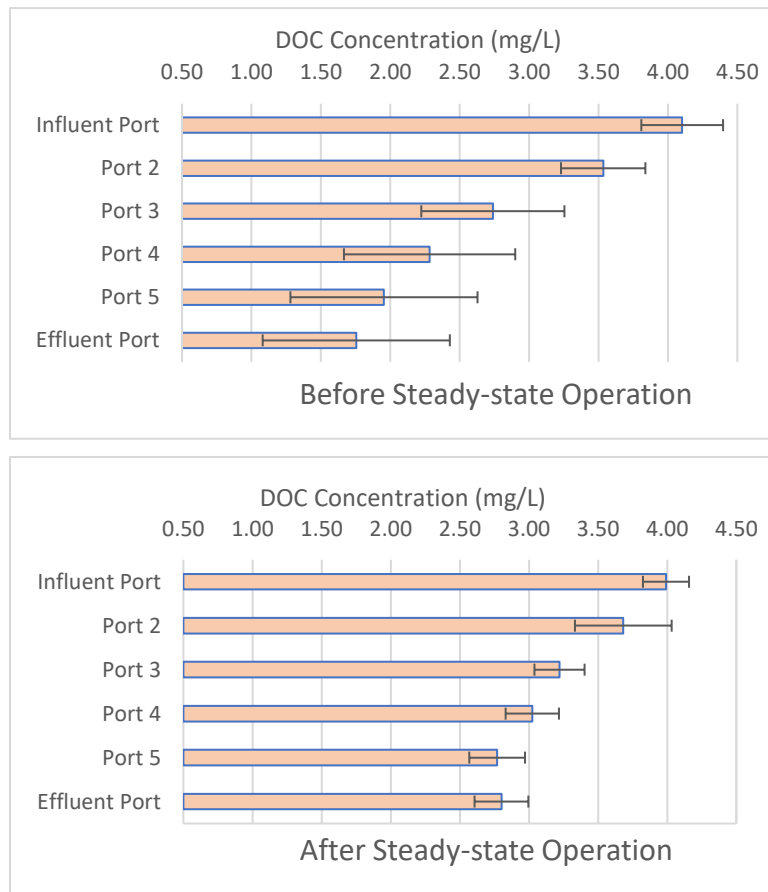


Figure 4.7: Mean DOC concentration across the depth of Filter 1 (new GAC) prior to steady-state DOC removal (June 14th to July 25th; top) and during steady-state removal (Aug 2nd to Sept 5th; bottom) (n=8, and 6, respectively; error bars = +/- std. deviation)

The DOC concentrations across the depth of Filter 1 were exactly as expected. The higher DOC concentration in the effluent of Port 2 shows that the top 12 cm of GAC had lost more of its adsorptive capacity than the lower layers of the filter. Also, the effluent DOC concentration at Ports 3, 4 and 5 changed appreciably between the two periods of operation; in contrast, the DOC concentration at Port 2 did not change very much (specifically, it increased from ~3.6 mg/L to ~3.7 mg/L on average). GAC filters are expected to lose their adsorptive capacity in the layers of media that are first exposed to the influent stream. As the first layers become exhausted, the subsequent layers are exposed to steadily higher concentrations of organic matter (Edzwald, 2011). Thus, there is a pattern of the upper depths of GAC media adsorbing and removing higher quantities of DOC than the lower layers. This was observed both before steady-state and after steady-state conditions in Filter 1 (Figure 4.8). This suggests that the lower layers of GAC were not yet exhausted (as would be expected if the adsorption zone extended beyond the depth of the filter), but the layers at Port 2 and above had lost most of their adsorptive capacity (Edzwald, 2011; Metcalf and Eddy, 2013). In a biologically active filter, this type of performance could also be associated with initial exhaustion of adsorptive activity that was not (rapidly enough) re-enabled by biological activity through bioregeneration at the onset of the steady-state operational period. During the steady-state operation period, continued DOC removal is enabled by biodegradation; specifically, via direct biodegradation from the bulk matrix or bioregeneration (as discussed in Section 4.5.4).

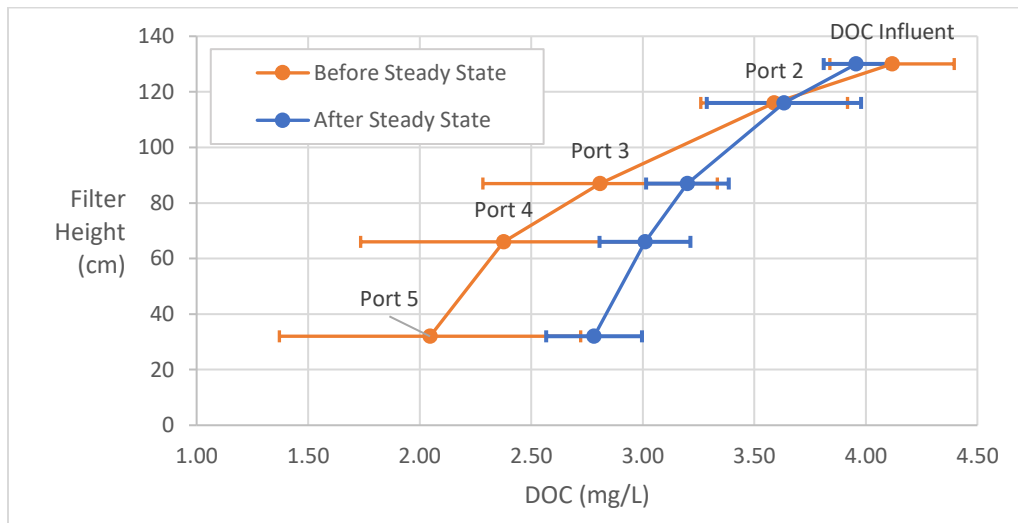


Figure 4.8: Mean DOC concentration across the depth of Filter 1 (new GAC) prior to steady-state filter operation (from June 14th to July 25th) and after steady-state filter operation (from Aug 2nd to Sept 5th) (n=8 and 6, respectively, error bars = +/- std. deviation).

DOC removal across the depth of Filter 1 was examined to evaluate how each layer of GAC contributed to overall DOC removal on any given sampling date and over the duration of the experimental period (Figure 4.9).

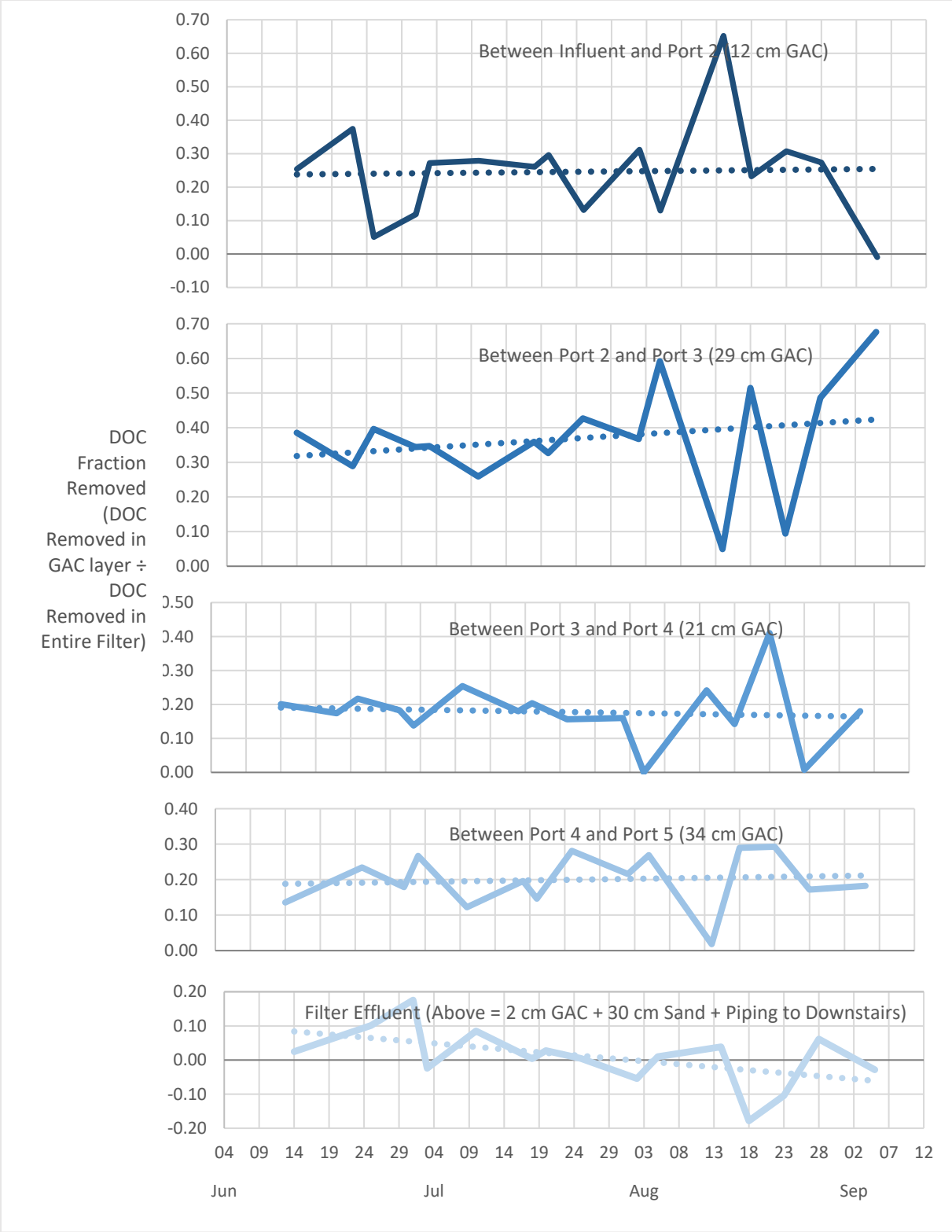


Figure 4.9: Fraction of DOC removed in each section of GAC in Filter 1 (new GAC) during the experimental period (— = fraction removed ••• = least squares linear regression trend line)

The analysis of DOC removal in each of the layers of the filter (for example; fraction removed = $[\text{DOC}_{\text{Port 3}} - \text{DOC}_{\text{Port 4}}] / [\text{DOC}_{\text{Influent}} - \text{DOC}_{\text{Effluent}}]$) generally indicated that steady-state removal of DOC predominantly occurred in the upper layers of the filter, but also began to progress to the lower layers of the filter (i.e. positive slope (albeit not significant with $p=0.447$) observed above Port 3 (Figure 4.9). This observation is generally consistent with previous investigations that have indicated that the majority of DOC biodegradation during drinking water treatment with exhausted GAC biofilters occurs in the upper layers of the media, but also extends to deeper layers, including the sand layer (Emelko et al., 2006; Gibert, et al., 2013a). This analysis suggests a longer-term establishment of biological activity across the depth of the biofilter that may have extended beyond the duration of the experimental period of this investigation. A longer-term analysis would be very useful in informing biofilm development and biological activity in biofilters across the longer term of operation; however, it was beyond the scope of the present investigation.

4.3.3. UV₂₅₄ and SUVA

UV₂₅₄ reduction in Filter 1 was 52 +/- 22% (n = 15) during the experimental period; this was generally consistent with DOC removal, which was 43 +/- 18% (n = 23) during this period. The adsorptive capacity of Filter 1 had an impact on SUVA ($p = 0.009$), which decreased by a mean of 16 +/- 17% (n = 13) over the experimental period. The filter influent SUVA also decreased, from 1.2–1.5 L/m.mg, to ~1.1 L/m.mg as the period of stable filter operation started (see Section 4.1.1), and the DOC concentration remained constant (Figure 4.5). Accordingly, a higher fraction of lower-weight, biodegradable, organic matter entered the filter during this period.

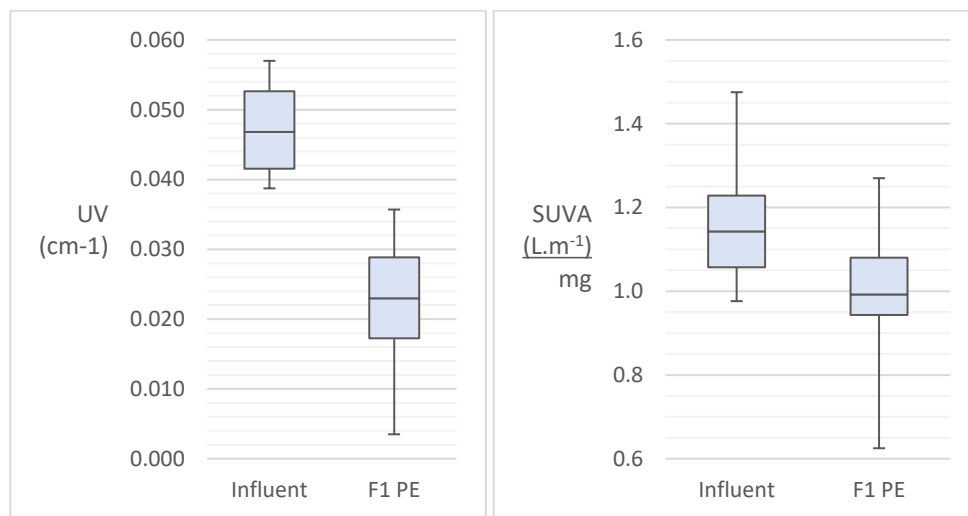


Figure 4.10: Filter 1 (new GAC) influent and effluent UV₂₅₄ (left) and SUVA (right) during the experimental period (n = 15 and 13, respectively; \blacktriangle = minimum value, \blacktriangledown = maximum value observed)

4.3.4. Organic Matter (LC-OCD) Fractions

Filter 1 influent and effluent biopolymer concentrations during the experimental period are presented in Figure 4.11. The biopolymer concentration in the influent stream ($237 \pm 16 \mu\text{g/L}$); was significantly different ($p = 0.005$) than that in the effluent stream ($203 \pm 12 \mu\text{g/L}$; mean \pm standard deviation), moreover, this relationship did not appear to vary substantially throughout the experiment.

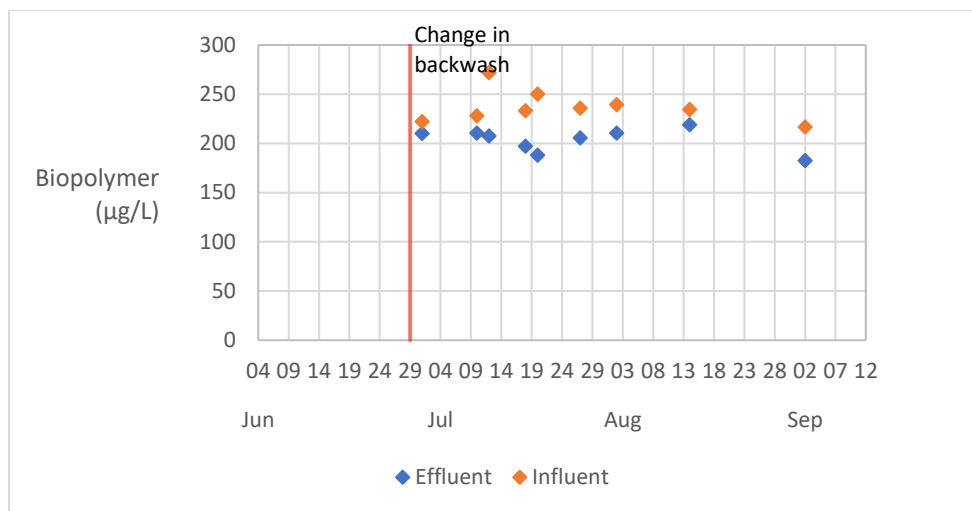


Figure 4.11: Biopolymer concentrations in Filter 1 (new GAC) influent and effluent streams during the experimental period (n=9)

Biopolymer removal in Filter 1 did not correlate with DOC removal (Figure 4.6). Critically, the first five samples analyzed were collected prior to steady-state filtration conditions during which the filter still exhibited substantial adsorptive capacity; it was only the last four samples that were collected after the GAC in Filter 1 had been exhausted. Nonetheless, the removal of biopolymers did not vary substantially during these two periods, averaging at 15% and 12%, respectively. It should be noted that there were too few points to conduct an unpaired t-test and compare a difference in means between the non-steady-state ($n = 5$) and the steady-state ($n = 4$) phases of filter operation. These data demonstrate that biopolymer removal was not significantly impacted by GAC adsorptive capacity. It should be further noted that the concentration of the biopolymer fraction of the organic matter was relatively low and only ranged from 180 to 280 $\mu\text{g/L}$ during the experimental period. Rahman et al. (2014) found that at biopolymer concentrations below 0.2 mg/L, the biopolymer removal was significantly correlated with the influent concentration in biologically-active filters; the present investigation may help to better understand those observations, which are consistent with the data reported herein. Specifically, the lack of enhanced biopolymer removal by new, highly adsorptive GAC was likely due the relatively large size of biopolymer macromolecules, which would

limit their access to the internal pore structure of GAC media. Given that biopolymers do not adsorb to GAC (Velten et al., 2011b), their removal at comparable levels by the new/adsorptive and exhausted GAC media in Filter 1 investigated herein suggests that (a) the media were biologically active throughout most of the experimental period and (b) the mechanism of biopolymer removal by biofiltration (i.e. “biodegradation”) is direct biodegradation rather than bioregeneration (see Section 4.3.5 for biological activity). Thus, biopolymer removal by biofiltration would be expected to correlate with filter influent biopolymer concentration, as observed by Rahman et al. (2014). The data reported herein further build on the mechanistic work of Spanjers (2017), who demonstrated that the adsorptive capacity of filtration media (not the roughness and associated surface area) substantially enhanced the removal of organic matter by biofiltration and further speculated that biofilters may be able to partially attenuate spikes of organic matter through biological action alone (i.e. direct biodegradation). While other mechanisms such as bioregeneration may be associated with the removal of other fractions of organic matter during classical biofiltration with GAC filtration media during drinking water treatment, the present investigation provided evidence of direct biodegradation, which was likely responsible for biopolymer removal in the pilot filters.

In contrast to biopolymer removal, the removal of humic substances by biofiltration with new, highly adsorptive GAC media was generally similar to DOC removal (Figure 4.6). A high level of humic substance removal was achieved by the filter prior to exhaustion (i.e. from July 1st to July 20th, 2018); it decreased after the adsorptive capacity of the filter was exhausted (i.e. July 27th to Sept 2nd, 2018). The removal in these two phases averaged at 45% and 29%, respectively. Overall, the filter influent concentration of humic substances (2,241 +/- 210 µg/L) was significantly different ($p < 0.0005$) from the effluent concentration (1,393 +/- 229 µg/L) (mean +/- standard deviation).

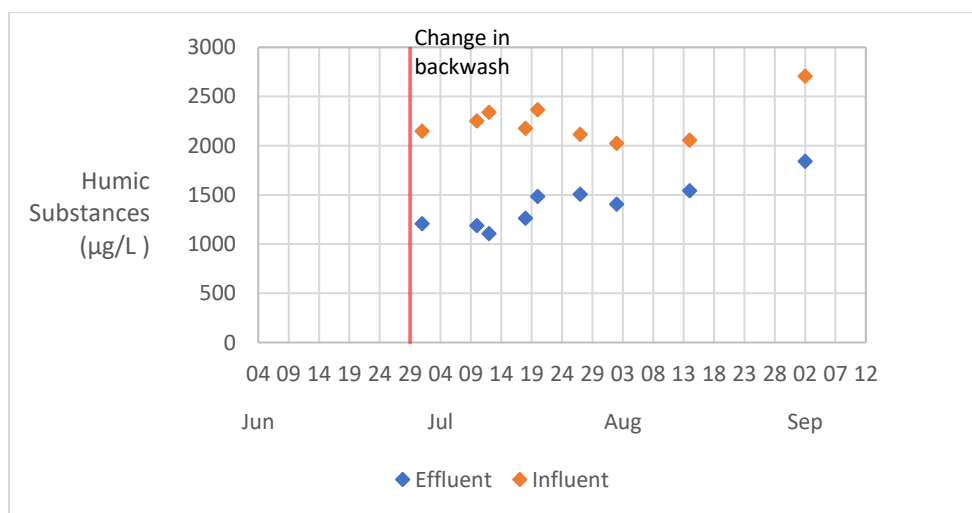


Figure 4.12: Humic substances removal in Filter 1 (new GAC) during the experimental period (n=9)

Although not discussed extensively here, the removal of each of the building blocks, low-molecular-weight neutrals, and low-molecular-weight acids fractions of organic matter in Filter 1 was also significant ($p < 0.0005$). These data are available in Appendix A.

4.3.5. ATP Concentration

ATP concentrations associated with biomass attached to the filtration media were collected from Ports 2 to 5 (see Figure 3.1) on several occasions during the experimental period. In Filter 1, the concentration of ATP steadily increased during the initial period of filter operation (from June 4th to approximately July 23rd, 2018) and then did not change considerably during the steady-state period of biofilter operation (Figure 4.13). The average ATP concentration across the depth of Filter 1 during steady-state operation is presented in Table 4.5; it was generally consistent across the depth of the filter during steady-state operation (Figure 4.13; Table 4.5). It is possible that the stabilization in ATP concentration that was observed was related to the presence of more biodegradable compounds (SUVA; Section 4.3.3) in the filter influent; unfortunately, a detailed assessment of this relationship was beyond the scope of the present investigation. Notably, the ATP concentration and DOC removal in Filter 1 stabilized at approximately the same time (Figure 4.14), suggesting GAC exhaustion (Velten et al. 2007; Velten et al. 2011a) in late July, as discussed above (Section 4.2). Thus, the organic matter removal performance of Filter 1 was consistent with the conceptual model described by Dussert and Van Stone (1994), despite the raw water quality fluctuations and associated pre-treatment challenges that occurred during the initial phase of filter operation (see Section 4.1.1). Specifically, after the start up of a new GAC biofilter, adsorptive capacity dominated organic matter removal during the initial phase of operation and biological activity enabled continued removal of organic matter after the adsorptive capacity of the GAC medium was essentially exhausted.

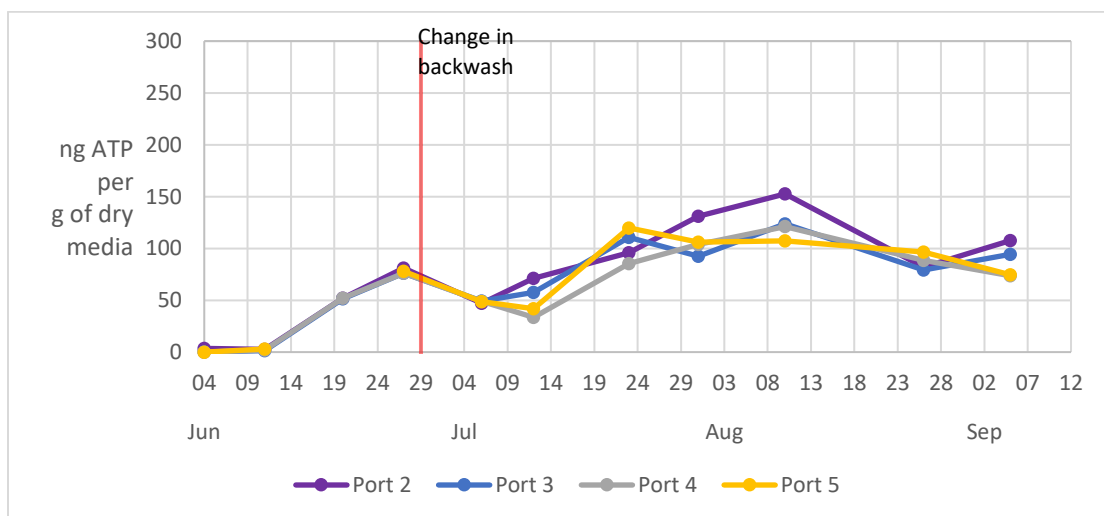


Figure 4.13: ATP concentration per g of dry GAC media in Filter 1 (new GAC) during the experimental period

Table 4.5: ATP concentration (mean +/- standard deviation) across the depth of Filter 1 (new GAC) during steady-state operation

Port	ATP Concentration
Port 2	114 +/- 28 ng ATP/g dry GAC
Port 3	100 +/- 17 ng ATP/g dry GAC
Port 4	95 +/- 18 ng ATP/g dry GAC
Port 5	101 +/- 17 ng ATP/g dry GAC

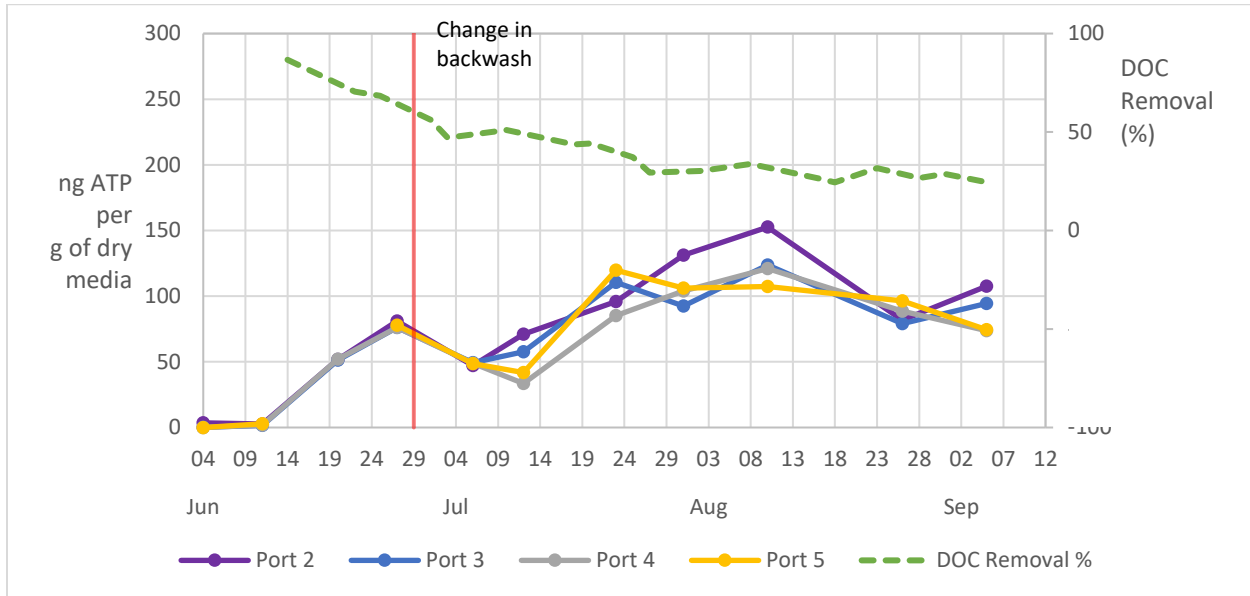


Figure 4.14: ATP concentration and DOC removal (%) in Filter 1 (new GAC) during the experimental period

4.4. Performance in Filter 2 – Combination of new and exhausted GAC media

4.4.1. Turbidity Removal and Headloss Accumulation

Filter 2 contained 60% exhausted GAC from an operating full-scale filter and 40% new GAC. Overall, Filter 2 achieved acceptable turbidity removal, as the average filter run produced effluent less than 0.3 NTU (Table 4.7). Specifically, the filter effluent turbidity was 0.21 +/- 0.11 NTU (mean +/- standard deviation) during the experimental period. The relatively high filter effluent turbidities that were observed in the Filter 2 effluent could not be attributed to any specific factor, an instrumentation error is unlikely as the turbidimeters were tested and calibrated prior to experimentation. Filter cycles were generally terminated because of headloss accumulation in this filter (31 of 39 filter runs); turbidity breakthroughs above 0.3 NTU occurred six times. The headloss accumulation rate in Filter 2 was 0.19 +/- 0.12 m/h (mean +/- standard deviation) during the experimental period (Figure 4.16).

Table 4.6: Mean turbidity removal by Filter 2 (combination of new and spent GAC) during the experimental period (n=37)

	Influent entering filter (NTU)	Filter effluent (NTU)	Percentage removal (%)
Mean	0.954	0.209	73
Std. deviation	0.443	0.107	26

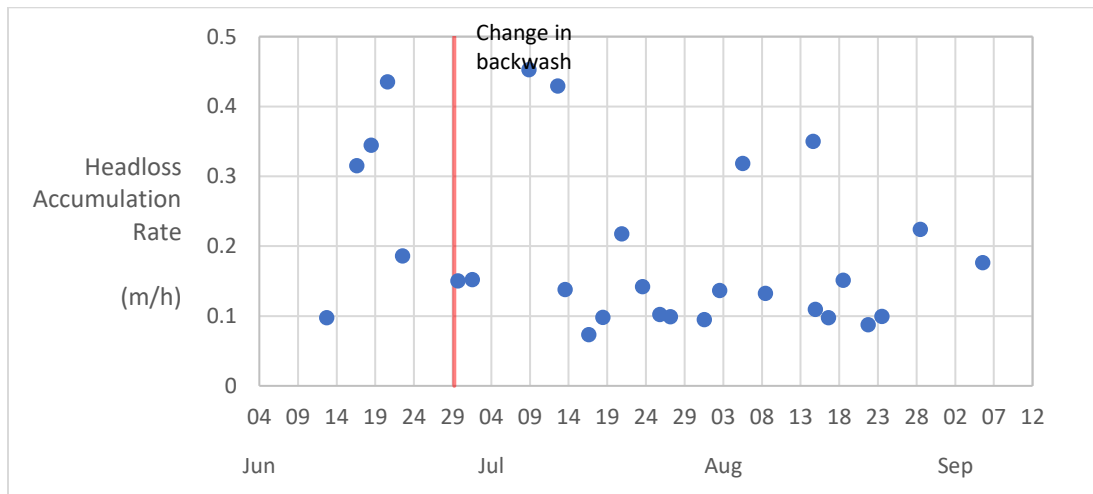


Figure 4.15: Filter 2 (combination of new and spent GAC) headloss performance trend throughout experimental period

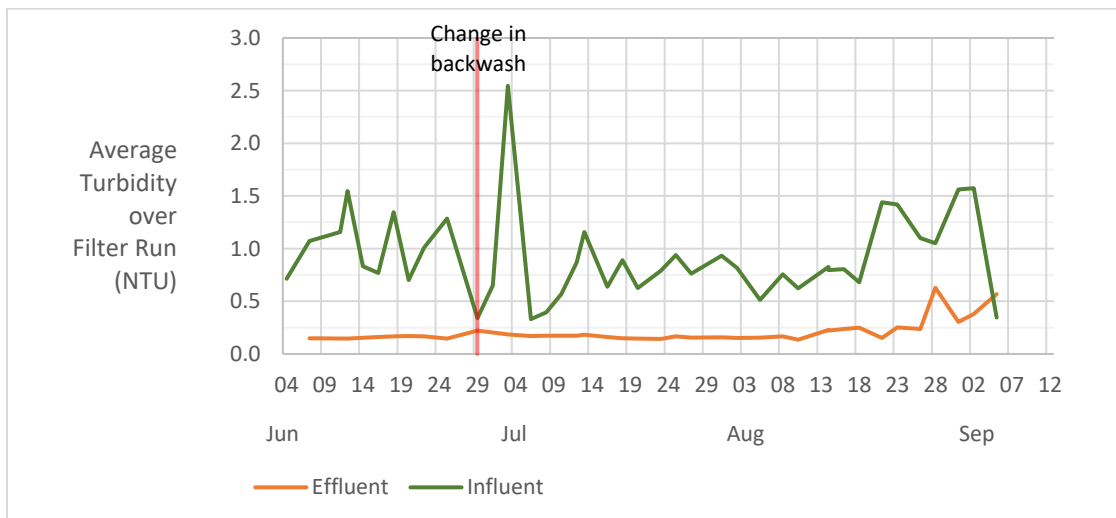


Figure 4.16: Filter 2 (combination of new and spent GAC) turbidity performance trend throughout experimental period

Given the pre-treatment challenges that occurred in the full-scale water treatment plant that provided settled, ozonated water to the pilot filters, it is possible that solids carryover and deposition in some of the lines may have contributed to the observed breakthrough events. For example, the dislodging of solids in the tubing between the filter effluent sampling locations and the turbidimeter may have been attributable for the turbidity spike that occurred during the last filter run (Sept 5th; Figure 4.16), during which the average filter effluent turbidity (0.57 NTU) exceeded the average filter influent turbidity (0.35 NTU) while other water quality parameters such as DOC (see Section 4.4.2 below) did not substantially fluctuate. As turbidity breakthrough is a sign that preferential pathways are forming through which water and particles can pass through the filter, these conditions would also be expected to result in increased DOC passage through the filter. Accordingly, the possibility of an instrumentation error rather than true filter breakthrough on this occasion was possible.

4.4.2. DOC

The effluent DOC concentration in Filter 2 averaged 3.1 +/- 0.4 DOC mg/L (mean +/- standard deviation) over the experimental period (n=17; Figure 4.17). DOC removal ranged from 50 to 85% during the start of the experiment (June 14th to June 30th, 2018) when the media were adsorptive (Figure 4.18). As the media became exhausted, DOC removal decreased and reached steady-state (~25% removal), after approximately 2 months of operation (August 1st to September 5th, 2018). Although Filter 2 did not contain as much new GAC as Filter 1 (40% versus 100%); DOC removal still followed a trend similar to that observed in Filter 1. Although, the sample collected on August 23rd, 2018 indicated unusually low DOC removal (5%), DOC removal generally returned to (or near to) steady-state immediately thereafter; specifically, DOC removal was 19%, 20%, and 12% on the August 28th, September 2nd, and September 5th sampling occasions, respectively.

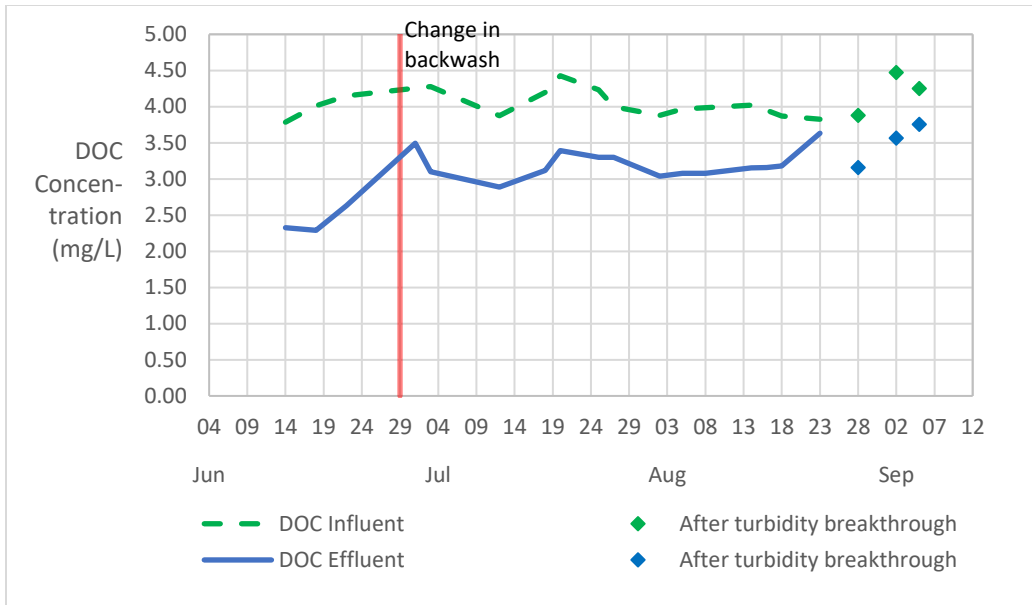


Figure 4.17: DOC concentrations in Filter 2 (combination of new and spent GAC) influent and effluent during the experimental period (n=17)

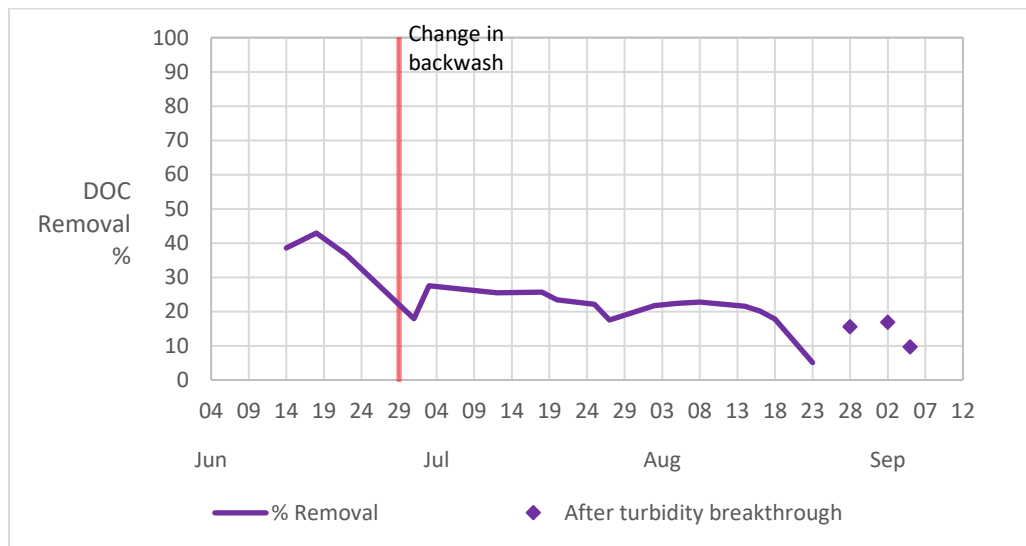


Figure 4.18: DOC removal (%) in Filter 2 (combination of new and spent GAC) during the experimental period (n=17)

The period of steady-state DOC removal in the filter also was evaluated by analyzing the slopes of the best fit lines determined for consecutive subsets of 10 data points by least squares linear regression (Section 3.7.1). Using this approach, Filter 2 generally achieved steady DOC removal after approximately 2 months time, although there was a bit of fluctuation during the period from July 12 to August 14 (Table 4.8). These findings are generally consistent with the DOC data, which indicated that between

approximately July 3rd and July 25th, Filter 2 reached a steady-state DOC removal of ~25%, which was generally comparable to that observed in Filter 1 during steady-state operation. Given that the adsorptive capacity was being utilized during the first few months of operation, this general convergence in the DOC removal performance of Filters 1 and 2 is not surprising.

Table 4.7: Linear regression results confirming the period of steady-state DOC removal in Filter 2 (combination of new and spent GAC). This is the period during which filter effluent DOC concentration reaches steady-state, resulting in a slope that is not statistically different than a slope of zero.

Data included	Statistical significance of slope [†]
June 14 th to July 27 th	p = 0.003
June 18 th Aug 2 nd	p = 0.012
July 1st to Aug 5th	p = 0.064
Jul 3rd to Aug 8th	p = 0.570
Jul 12 th to Aug 14 th	p = 0.041
Jul 18th to Aug 16th	p = 0.119
Jul 20th to Aug 18th	p = 0.107
Jul 25th to Aug 23rd	p = 0.079
† For every linear regression analysis ($Y_i = \beta_0 + \beta_1 X_i + \varepsilon_i$) units Y and X are in % removal and days since start of experiment, respectively.	

For reference purposes, Table 4.8 below provides the depth of the GAC layer that is above each port along the vertical length of Filter 2.

Table 4.8: Filter 2 (combination of new and spent GAC) port heights and media layers

Port #	Height above filter base	Depth of media above port
Port 2	116 cm	12 cm of GAC mixture (2:3, new GAC: full-scale GAC)
Port 3	87 cm	29 cm of GAC mixture
Port 4	66 cm	21 cm of GAC mixture
Port 5	32 cm	34 cm of GAC mixture
Effluent port	Located on floor below	2 cm of GAC mixture, 30 cm of silica sand And ~30 m of piping

As with Filter 1, the DOC concentration across the vertical depth of Filter 2 was examined during steady-state filter operation (data points were excluded if they were collected during the turbidity

breakthrough). Notably, the filter effluent DOC concentration was substantially higher than the filter influent concentration on two occasions—these occasions are indicated as outliers in Figure 4.19. While the outlier in Port 4 cannot be attributed to a specific event, the outlier in Port 2 was observed on August 23rd, 2018, a date on which other DOC anomalies were observed in other filters as well. Thus, it is possible that there may have been a sample handling issue on that date or an operational disturbance (e.g. hydraulic surge) that caused sloughing in all of the filters; sloughing was likely as it also would explain the relatively poor turbidity removal that also occurred in Filter 2 on August 23rd (see Section 4.4.1).

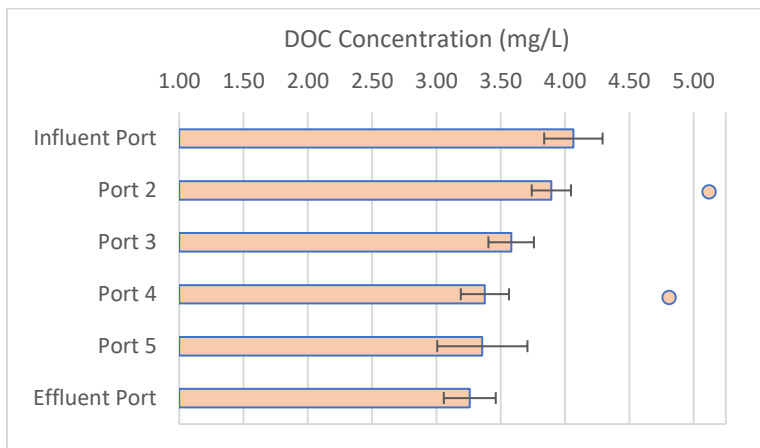


Figure 4.19: Mean DOC concentration across the depth of Filter 2 (combination of new and spent GAC) during steady-state filter operation (from July 18th to Aug 23rd) (n = 7 error bars = +/- one standard deviation).

4.4.3. UV₂₅₄ and SUVA

UV₂₅₄ removal in Filter 2 averaged 40 +/- 22% (n = 12) during the experimental period. The adsorptive capacity of Filter 2 had an impact on SUVA, as it decreased by an average of 8 +/- 11% (n = 9) over the experimental period, however this difference in the SUVA influent and effluent was subtle from a statistical standpoint (p=0.049). The finding that Filter 2 caused a decrease in SUVA confirms that adsorption preferentially removes aromatic compounds.

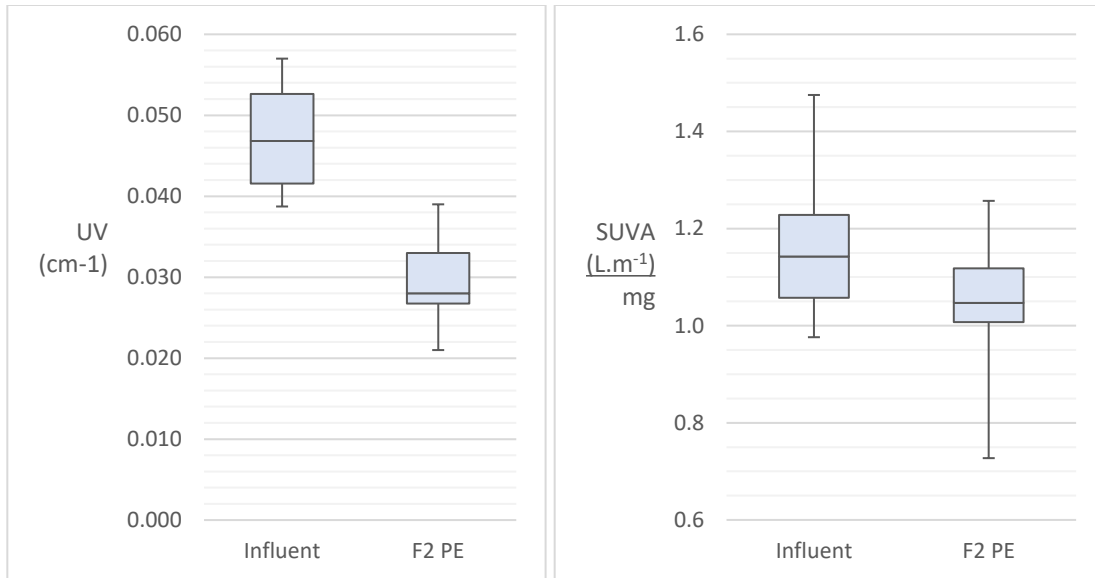


Figure 4.20: Filter 2 (combination of new and spent GAC) influent and effluent UV₂₅₄ (left) and SUVA (right) during the experimental period (n = 12 and 9, respectively; \blacktriangle = minimum and \blacktriangledown = maximum value observed)

4.4.4. Organic Matter (LC-OCD) Fractions

The Filter 2 influent and effluent biopolymer concentrations during the experimental period are presented in Figure 4.21. The biopolymer concentration in the effluent stream (201 +/- 24 $\mu\text{g/L}$; mean +/- standard deviation), was significantly different ($p = 0.001$) than that in the influent stream (237 +/- 16 $\mu\text{g/L}$); like in Filter 1, this relationship did not appear to vary substantially over the course of the experimental period. Similar to Filter 1, these data demonstrate that biopolymer removal was not significantly impacted by GAC adsorptive capacity and also suggest direct biodegradation of biopolymers by BAC filtration rather than adsorption and subsequent bioregeneration.

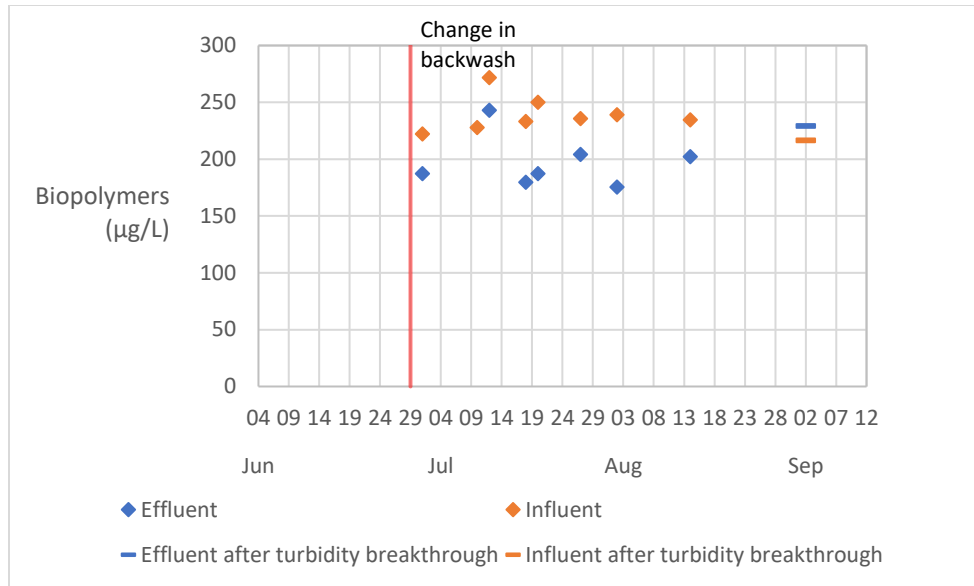


Figure 4.21: Biopolymer concentrations in Filter 2 (combination of new and spent GAC) influent (n=9) and effluent (n=8) streams during the experimental period

Humic substances also were removed by Filter 2 (Figure 4.22). Overall, the average filter influent concentration of humic substances (2,241 +/- 210 µg/L) was significantly different (p =0.001) from the effluent concentration (1,669 +/- 190 µg/L) (mean +/- standard deviation). Although it was possible to observe how the removals of biopolymers and humic substances were affected as the GAC media became exhausted over the experimental period in Filter 1, this was not possible for Filter 2 because it had lost most of its adsorptive capacity before the first samples were collected for LC-OCD analysis. Notably, there was no measurable difference in biopolymer removal between Filters 1 and 2 over the experimental period; they averaged 14% and 18%, respectively. In contrast, there was an appreciable difference in humic substances removal: Filter 1 averaged 38% and Filter 2 averaged 23%. Thus, these observations substantiate the finding that unlike humic substances, biopolymer removal by BAC filtration is not affected by the adsorptive capacity of GAC.

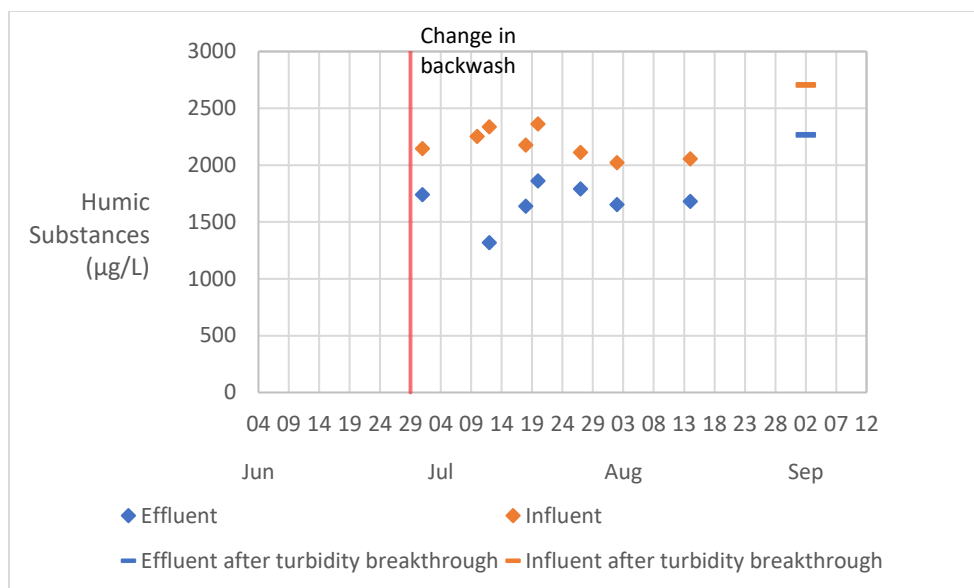


Figure 4.22: Humic substance concentrations in Filter 2 (combination of new and spent GAC) influent and effluent streams during the experimental period (n = 8)

The single biopolymer data point after the turbidity breakthrough on September 2nd, 2018, further substantiates the theory that sloughing may have occurred after maintenance of the filter on August 23rd, 2018. By dry-weight, biopolymers can make up as much as 95% of the total microbial mass (Bitton et al., 2002); thus, this is the LC-OCD fraction that is most attributed to microbiologically-sourced proteins, polysaccharides, and lipids. Accordingly, a higher concentration of biopolymers in the filter effluent than in the influent could suggest a release of microbes from the filter.

Although not discussed extensively here, the removal of each the building blocks, low-molecular-weight neutrals and low-molecular-weight acids fractions of organic matter in Filter 2 was also significant ($p = 0.001, 0.028, 0.003$, respectively). These data are available in Appendix A.

4.4.5. ATP Concentration

As was the case for Filter 1, ATP concentrations associated with biomass attached to the filtration media were collected from Ports 2 to 5 on Filter 2 (see Figure 3.1) on several occasions during the experimental period. In Filter 2, the ATP concentration across the depth of the filter steadily increased from June 4th to July 23rd, 2018, though it briefly decreased after the change in backwash and stabilized thereafter.

The average ATP concentration across the depth of Filter 2 during steady-state operation is presented in Table 4.9. It decreased slightly across the depth of the filter during this period (Figure 4.23); however, this difference likely was not statistically significant. Thus, biomass development in Filter 2 was

generally consistent with that observed in Filter 1, though slightly higher. This observation is consistent with some of the GAC media in Filter 2 already being biological active during start up; moreover, it suggests that possibility of more biomass/ATP development in Filter 1 over the longer term. Of course, natural variability between filters may also account for the slight difference in steady-state ATP concentration observed between Filters 1 and 2.

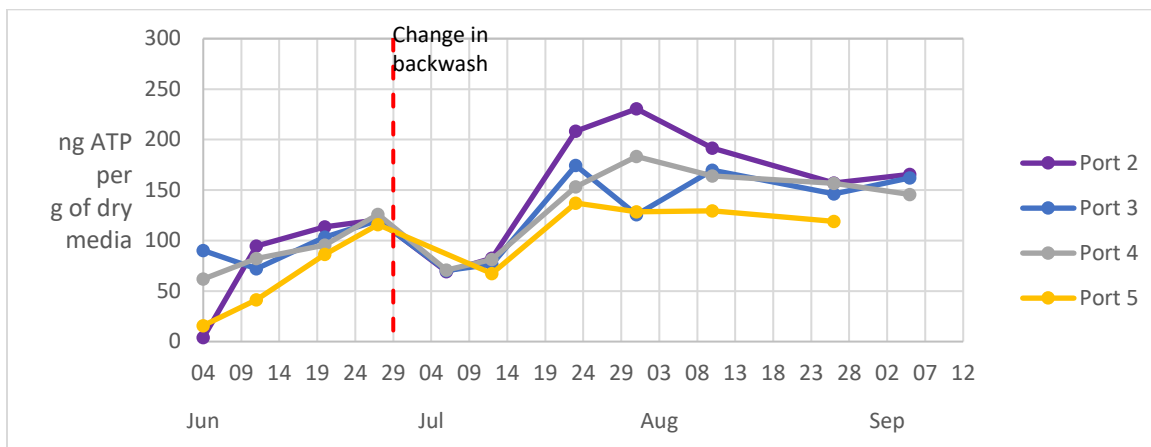


Figure 4.23: ATP concentration per g of dry GAC media in Filter 2 (combination of new and spent GAC) during the experimental period

Table 4.9: ATP concentration (mean +/- standard deviation) across the depth of Filter 2 (combination of new and spent GAC) during steady-state operation

Port	ATP concentration
Port 2	191 +/- 30 ng ATP/g dry GAC
Port 3	156 +/- 20 ng ATP/g dry GAC
Port 4	161 +/- 14 ng ATP/g dry GAC
Port 5	128 +/- 7 ng ATP/g dry GAC

4.5. Performance in Filter 3 – Biologically-active GAC from full-scale plant

4.5.1. Turbidity Removal and Headloss Accumulation

Overall, Filter 3 achieved very good turbidity removal, as the average filter run produced effluent of ~0.1 NTU (Table 4.11). Specifically, the filter effluent turbidity was 0.12 +/- 0.02 NTU (mean +/- standard deviation) during the experimental period. Filter cycles were generally terminated because of headloss accumulation in this filter in which turbidity breakthroughs above 0.3 NTU did not occur. The average head loss accumulation rate in Filter 3 was 0.14 m/h +/- 0.08 m/h (n = 32) (Figure 4.24), whereas

in Filters 1 and 2, it was 0.20 +/- 0.10 m/h (n =33) and 0.19 +/- 0.12 m/h (n =28), respectively (mean +/- standard deviation). This difference in headloss performance is also strikingly apparent in Figure 4.25. From this perspective, it appears as if the headloss accumulation in Filter 3 was more consistent than in Filters 1 and 2.

Table 4.10: Mean turbidity removal by Filter 3 (spent GAC) during the experimental period (n=34)

	Influent entering filter (NTU)	Filter effluent (NTU)	% Removal
Mean	0.91	0.12	83%
Std. Deviation	0.47	0.02	9%

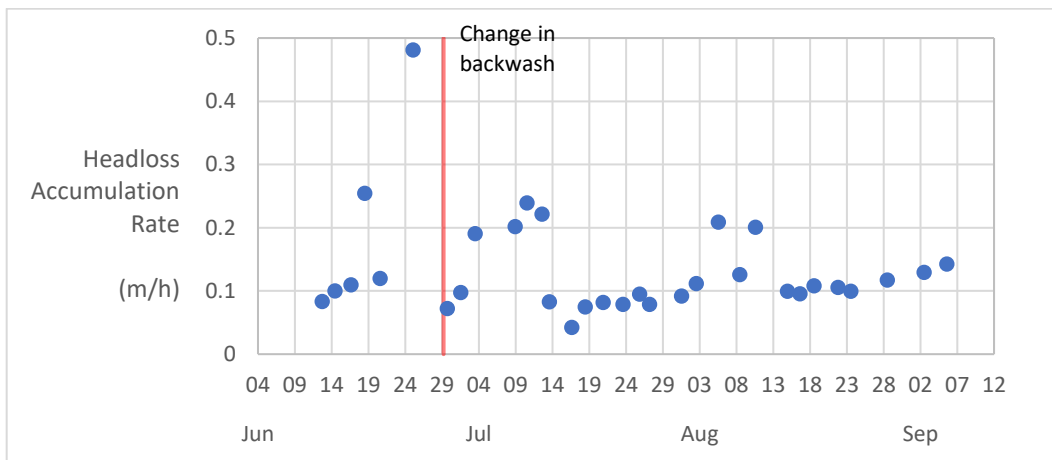


Figure 4.24: Filter 3 (spent GAC) headloss performance trend throughout experimental period

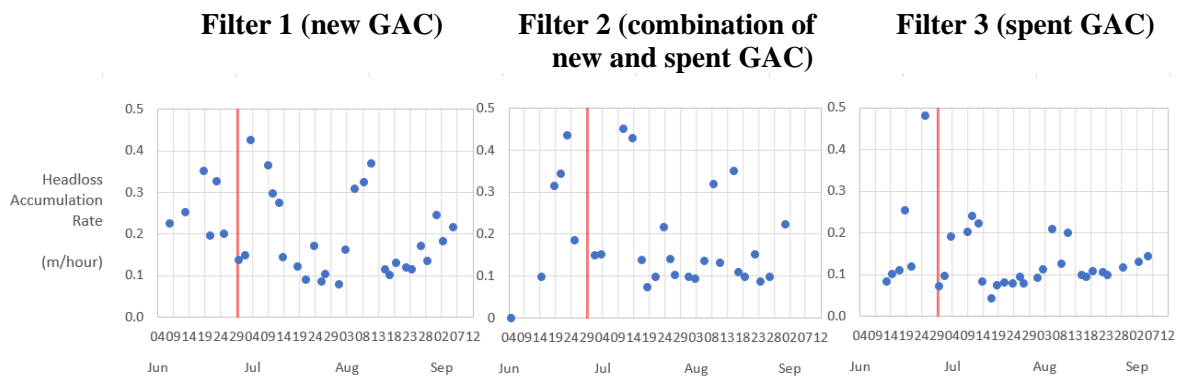


Figure 4.25: Headloss accumulation rate in Filters 1 to 3 (new GAC, combination of new and spent GAC, and spent GAC)

It is unclear why the headloss accumulation is higher in Filter 1 and 2 than Filter 3. ANSI/AWWA standards B100 and B604 (American Water Works Association et al., 2012) recommend washing out GAC fines when new GAC is stacked in a filter. It is possible that the new GAC was not adequately washed before being placed in Filter 1 and Filter 2, and the presence of fines caused high headloss accumulation.

4.5.2. DOC

The effluent DOC concentration in Filter 3 was 3.6 +/- 0.2 DOC mg/L (mean +/- standard deviation) over the experimental period (Figure 4.26). DOC removal during the first 10 days of filter operation could not be measured because of operational challenges. Thereafter, DOC removal by the biologically-active media consistently ranged from 6 to 22%, with an average removal of 12% (Figure 4.27). Notably, a previous investigation conducted at the same pilot plant with the same media and backwash protocol reported an overall average DOC removal rate of 15% (Wong, 2015). The only main operational difference was that in this previous experiment, the filter run times were longer (Region of Waterloo, 2018; Wong, 2015) because solids carryover from pre-treatment processes prior to filtration did not occur. A GAC filter that had been in operation for 5 years removed DOC at 13%, and a GAC filter with 3 years of operation removed DOC at 15%. If this difference was significant it would suggest that the biological activity on filters degrade over the long term (Lohwacharin et al., 2011)—this is hypothesized to be a result of the long-term accumulation of inert biomass compounds and organic matter in biofilters as they mature (Korotta-Gamage and Sathasivan, 2017; Lapidou and Rittmann, 2002). This theory would

also explain why the steady-state removal in Filter 1, after 3 months of acclimation, is higher than Filter 3, which underwent 5 years of acclimation.

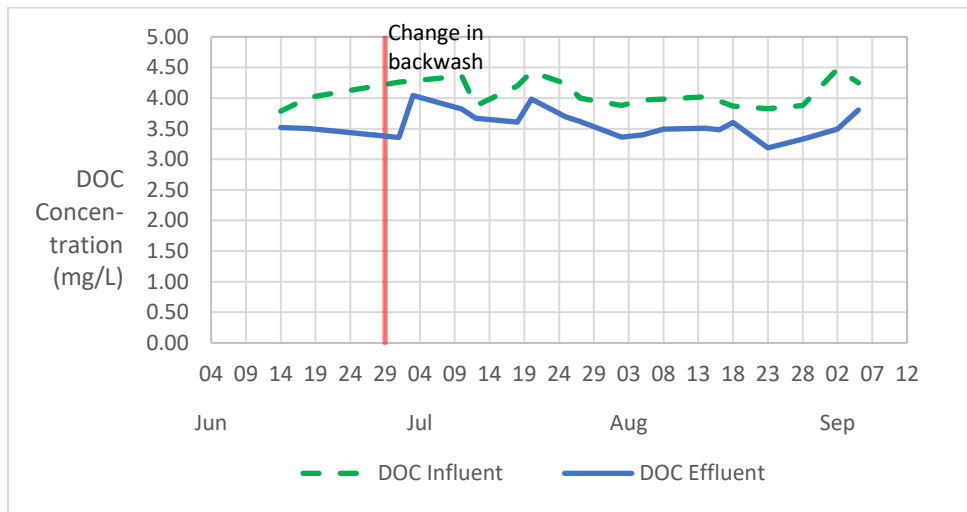


Figure 4.26: DOC concentrations in Filter 3 (spent GAC) influent and effluent during the experimental period (n=20)

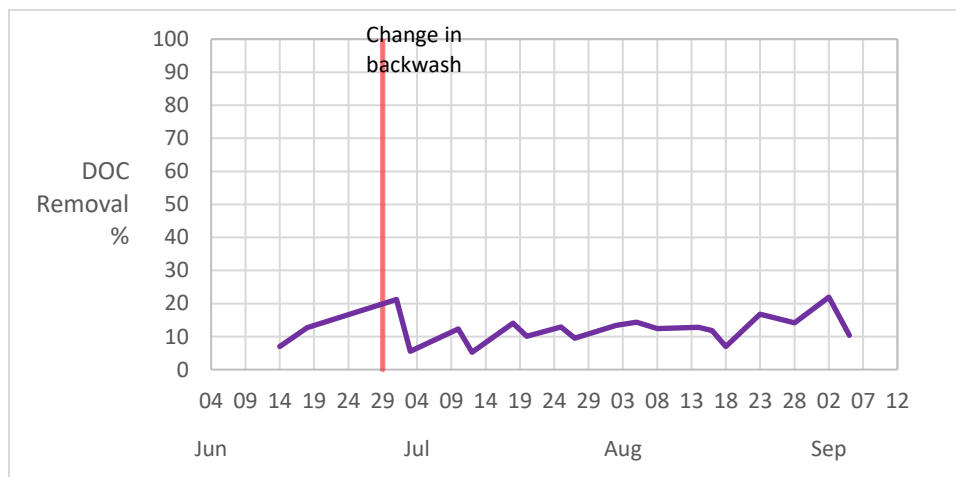


Figure 4.27: DOC removal (%) in Filter 3 (spent GAC) during the experimental period (n=20)

The period of steady-state DOC removal in the filter was confirmed by analyzing the slopes of the best fit lines determined for consecutive subsets of 10 data points by least squares linear regression (Section 3.7.1). DOC removal by Filter 3 was as steady-state (Figure 4.27; Table 4.11) throughout the experimental period, as would be expected given that the media in the filter were obtained from a full-scale filter that had been in operation for several years.

Table 4.11: Linear regression results confirming the period of steady-state DOC removal in Filter 3 (spent GAC). This is the period during which filter effluent DOC concentration reaches steady-state, resulting in a slope that is not statistically different than a slope of zero.

Data included	Statistical significance of slope [†]
June 14 th to July 27 th 1	p = 0.838
June 18 th Aug 2 nd 1	p = 0.909
July 1 st to Aug 5 th	p = 0.698
Jul 3 rd to Aug 8 th	p = 0.060
Jul 3 rd to Aug 14 th	p = 0.170
Jul 10 th to Aug 16 th	p = 0.115
Jul 12 th to Aug 18 th	p = 0.525
Jul 18 th to Aug 23 rd	p = 0.436
Jul 20 th to Aug 28 th	p = 0.478
Jul 25 th to Sept 2 nd	p = 0.064
Jul 27 th to Sept 5 th	p = 0.469

† For every linear regression analysis ($Y_i = \beta_0 + \beta_1 X_i + \varepsilon_i$) units Y and X are in % removal and days since start of experiment, respectively.
 1. Data needed to be square-root transformed so it better fit the assumption of homogeneity of variance and normal distribution.

The DOC concentration in Filter 3 was measured across the depth of the filter. The port locations and thickness of media layers are outlined in Table 4.12.

Table 4.12: Filter 3 (spent GAC) port heights and media layers

Port #	Height above filter base	Layer of media above port
Port 2	116 cm	12 cm of full-scale GAC
Port 3	87 cm	29 cm of full-scale GAC
Port 4	66 cm	21 cm of full-scale GAC
Port 5	32 cm	34 cm of full-scale GAC
Effluent Port	Located on floor below	2 cm of full-scale GAC media, 30 cm of silica sand And ~30 m of piping

The DOC concentration at each sampling port in Filter 3 during steady-state operation, which included the entire sampling period (June 4th to Sept 5th, 2018) is presented in Figure 4.28. On August 23rd, 2018, there was an unusually high DOC concentration measured at Port 2. However, DOC anomalies also occurred in Filters 2 and 4 on this date, so it may have been that either there was a sample handling issue

or there was an operational disturbance (e.g. hydraulic surge, air entrapment, etc.) that caused solids sloughing in all of the filters. Other than on this one occasion, the effluent DOC concentrations across the depth of Filter 3 followed a stable and predictable pattern. Specifically, the DOC concentration in Filter 3 steadily decreased across its depth; this is similar to what was observed in Filter 1; however, less DOC was removed by Filter 3, as would be expected given that Filter 1 contained fresh, highly adsorptive GAC upon startup. The effluent DOC across the depth of Filters 1 and 3 is compared in Figure 4.29. The substantially lower effluent DOC concentrations in Filter 1 (especially in the lower ports closer to the bottom of the filter bed) relative to Filter 3 provide substantial evidence to suggest that Filter 1 still had some adsorptive capacity, relative to the exhausted GAC media in Filter 3.

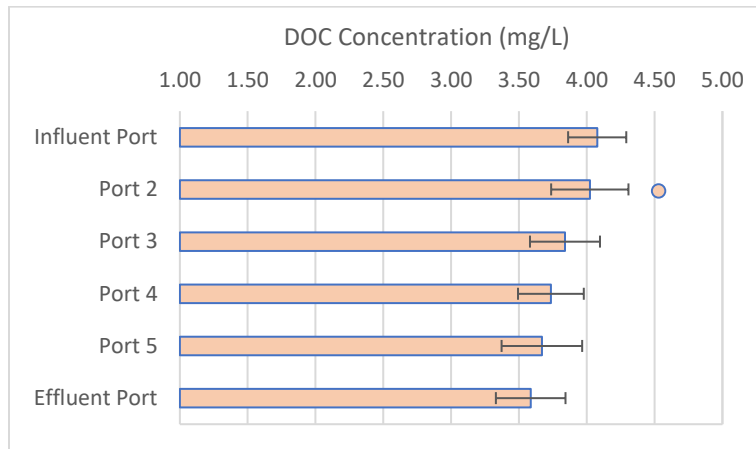


Figure 4.28: Average DOC concentration at each sampling port in Filter 3 (spent GAC) during its stable period - June 14th to Sept 5th (n=14, error bars = +/- one standard deviation)

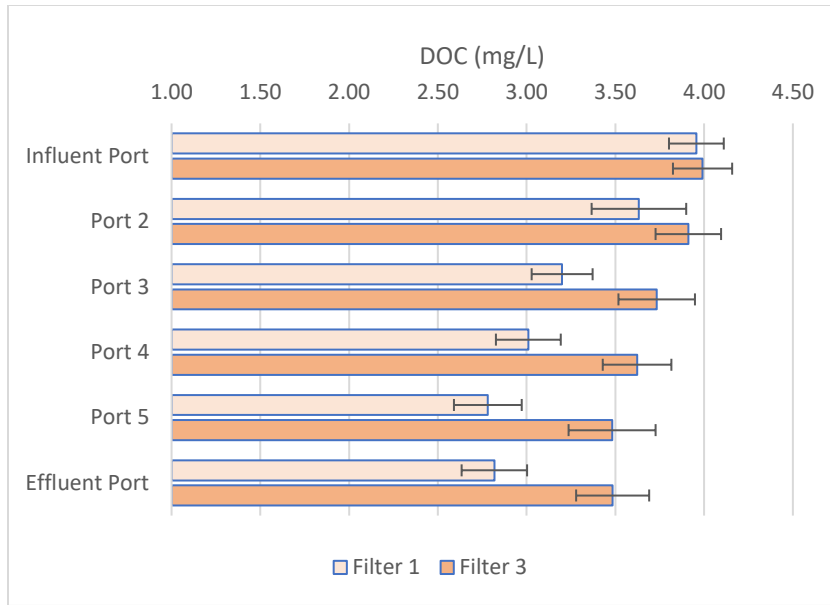


Figure 4.29: Effluent DOC concentration across the depth of Filters 1 and 3 (new and spent GAC, respectively) from August 2nd to September 5th, 2018 (n=6, error bars = +/- one standard deviation, outlier from Filter 3 excluded)

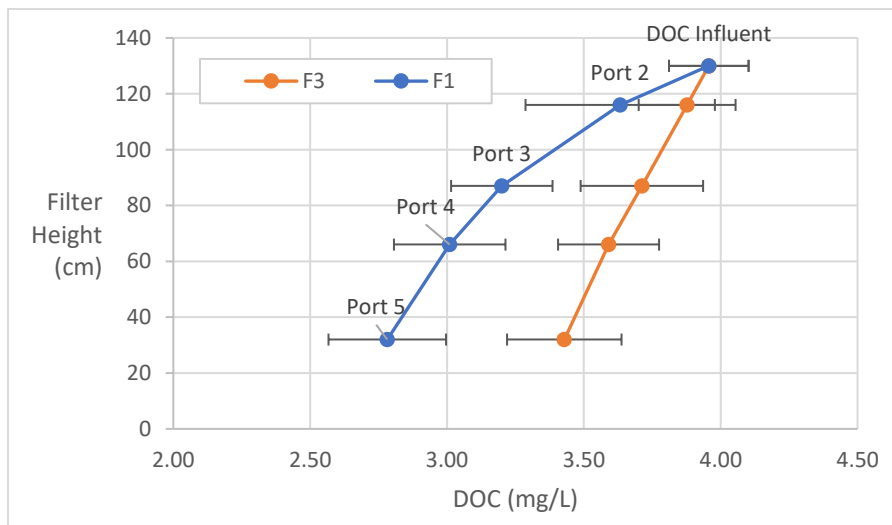


Figure 4.30: Average DOC concentration at each sampling depth in Filters 1 and Filter 3 (new and spent GAC, respectively), from August 2nd to September 5th (n = 6, error bars = +/- std. deviation, outlier from Filter 3 excluded)

Another interesting observation was that the pattern of DOC removal across the depths of Filter 1 and Filter 3 appeared different, even though they are compared after Filter 1 is at steady-state conditions

(Figure 4.31). Unlike Filter 1, the DOC removal by each section of media in Filter 3 was roughly proportional to the depth of that media. This observation similar to another report in which DOC removal across the depth of a filter was compared before and after a filter reached steady-state; in that investigation, periods of GAC exhaustion demonstrated more linear trends in DOC removal across the depth of the filters relative to periods in which adsorption was a primary removal mechanism (Figure 4.31; Velten et al., 2011a).

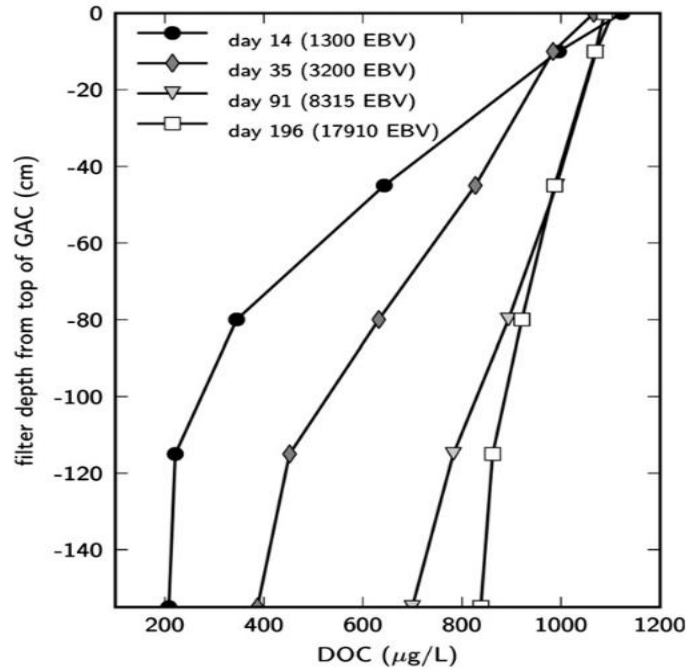


Figure 4.31: DOC removal across filter depth (day 14 and 35 = before steady-state, day 91 = right before steady-state, day 196 = after steady-state) from (Velten et al., 2011a)

As was the case in Filter 1 (Figure 4.9), DOC removal across the depth of Filter 3 (Figure 4.32) was examined to evaluate how each layer of GAC contributed to overall DOC removal on any given sampling date and over the duration of the experimental period.

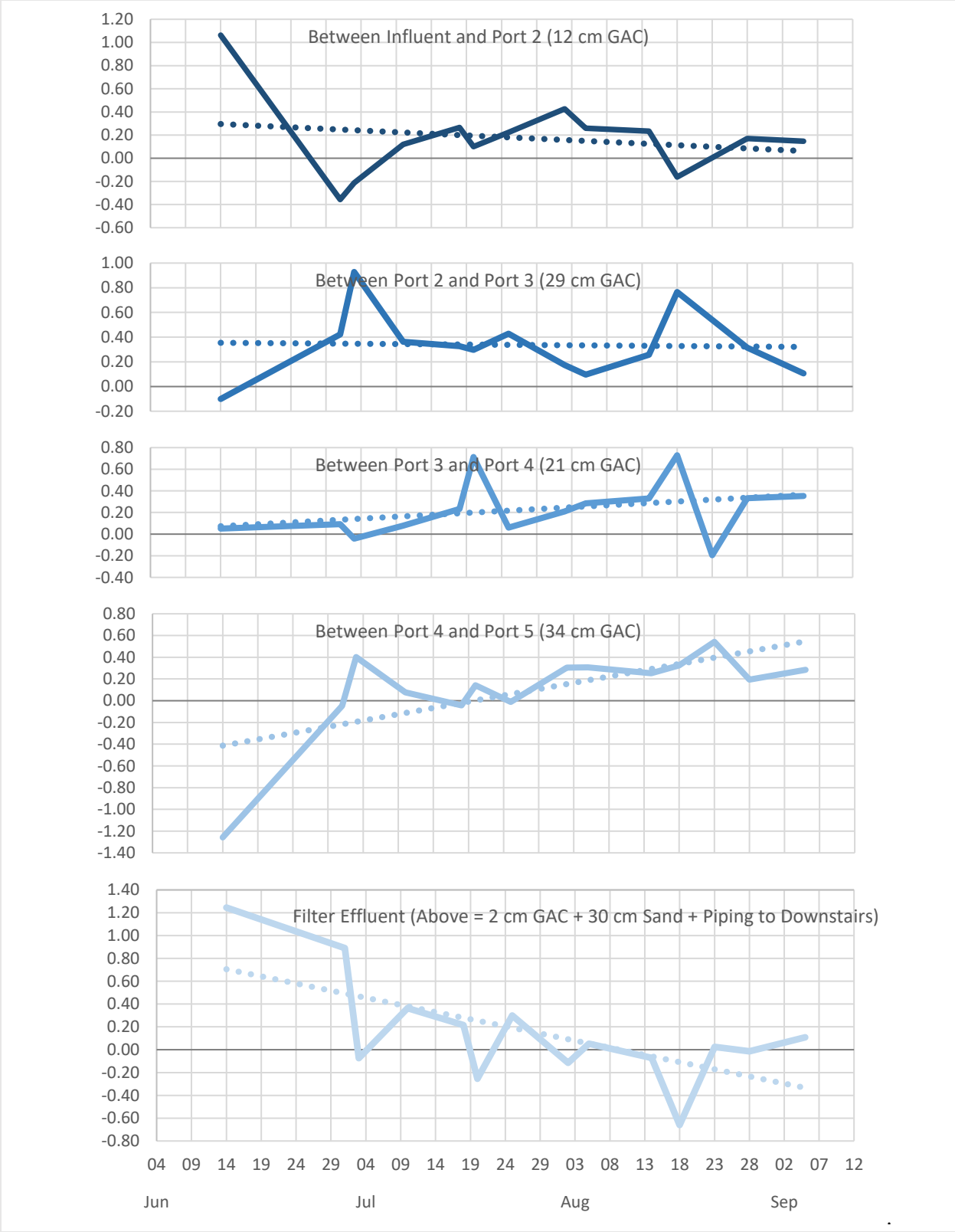


Figure 4.32: Fraction of DOC removed in GAC between each sample port in Filter 3 (spent GAC) during the experimental period (solid line = fraction of removal, dotted line = trend line)

The analysis DOC removal across the layers of the filter (for example; fraction removed = $[\text{DOC}_{\text{Port 3}} - \text{DOC}_{\text{Port 4}}] / [\text{DOC}_{\text{Influent}} - \text{DOC}_{\text{Effluent}}]$) generally indicated that the steady-state fraction of DOC removed was neither increasing nor decreasing in the upper layers of Filter 3. The fraction of DOC removed by the media layer at Port 5 appeared to be increasing ($p = 0.010$); it appeared to be decreasing at the filter effluent port ($p = 0.012$; Figure 4.32). The cause for these differences is unknown; however, they may be associated with establishing biological activity in the sand media, which were not biologically active when Filter 3 was started up, unlike the GAC media, which could be harvested from a full-scale biologically active filter. Extracting biologically active filtration media from the bottom of a full-scale filter would not be feasible because of media depth and mixing that would occur when attempting to remove the media from the filter.

4.5.3. UV₂₅₄ and SUVA

Average UV₂₅₄ reduction in Filter 3 was 13 +/- 8% ($n = 15$) during the experimental period; this was generally consistent with DOC removal, which was 12 +/- 4% ($n = 20$) during this period (Figure 4.33). On average, Filter 3 decreased the SUVA by 1 +/- 10%, and overall, did not significantly remove aromatic compounds.

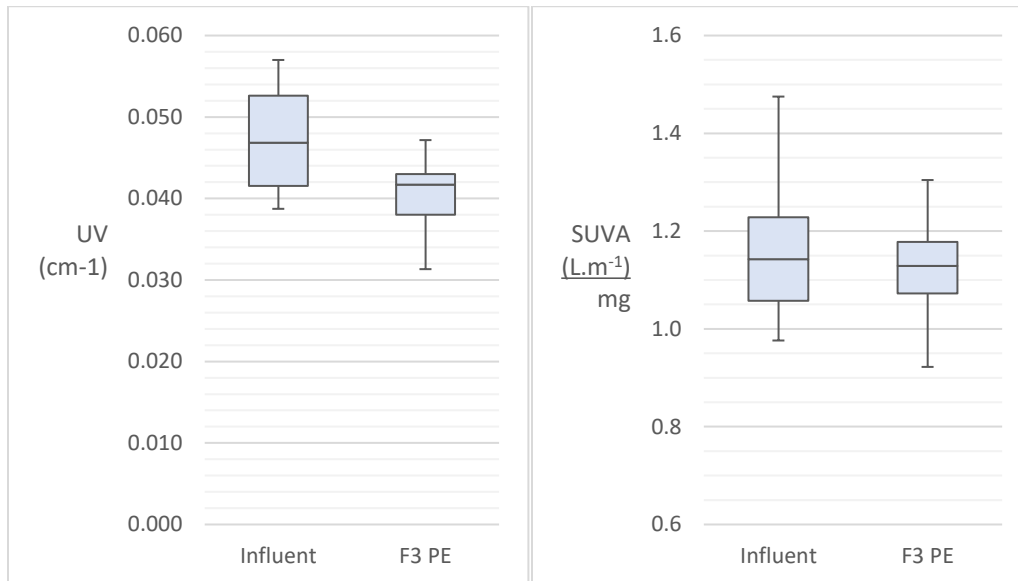


Figure 4.33: Filter 3 (spent GAC) UV₂₅₄ (left) and SUVA (right) influent and effluent from June 14th to September 5th, 2018 ($n = 15$ and 14 , respectively, \blacktriangle = minimum value, \blacktriangledown = maximum value observed)

It is well established at this point that Filter 1 had remaining adsorptive capacity (see Section 4.5.3). Therefore, from the SUVA data in Filters 1, 2 and 3, it can be seen that SUVA was most affected by GAC

adsorption, and less affected by biodegradation. It is clear that Filter 1 removes substantially more humic substances than Filter 3 (see Section 4.5.5), and humic substances tend to contain more aromatic carbon double bonds. The higher removal of humic substances is at the core of a high DOC removal since, in natural waters, humic substances contribute to 60 to 80% of the natural organic matter (Huber et al., 2011). From this perspective, a higher quantity of DOC removed overall might mean that SUVA is also reduced. To explore this theory, several biological filtration studies were reviewed, and their respective DOC and SUVA results were assessed (Table 4.14). Overall, a clear relationship between DOC removal and SUVA reduction was not evident. Regardless, it would generally be expected that some components that contribute to a higher SUVA would be removed by adsorption.

Table 4.13: Review of studies that have recorded SUVA changes through BAC filters

DOC Influent and Effluent (mg/L)	DOC Removal (%)	SUVA Influent and Effluent (L/mg/m-1)	SUVA Reduction	Notes	Source ^a
Not clear	3 – 10	1.6 1.4	No reduction	Despite change in SUVA (1.4 to 1.6) no decrease occurred	(Zhang et al., 2017)
1.48 mg/L 1.09 mg/L	26	1.36 1.08	21 %	Bench-scale biofilters. Included winter months	(Fu et al., 2017b)
~5.5 mg/L ~3.0 mg/L	45	1.7 1.5	13%	Same distribution of LC-OCD compounds in influent and effluent	(Baghoth et al., 2009)
2.09 mg/L 1.35 mg/L	35	1.96 2.07	- 6 %	SUVA increased in this study	(Han et al., 2013)

a. Study criteria: biologically-active carbon filters operated at temperatures of at least 10°C.

4.5.4. Organic Matter (LC-OCD) Fractions

The biopolymer concentration (Figure 4.35) in the effluent stream (199 +/- 15 µg/L; mean +/- standard deviation), was significantly different (p = 0.001) than that in the influent stream (238 +/- 17 µg/L); moreover, like in Filters 1 and 2, this relationship did not appear to vary substantially over the course of the experimental period.

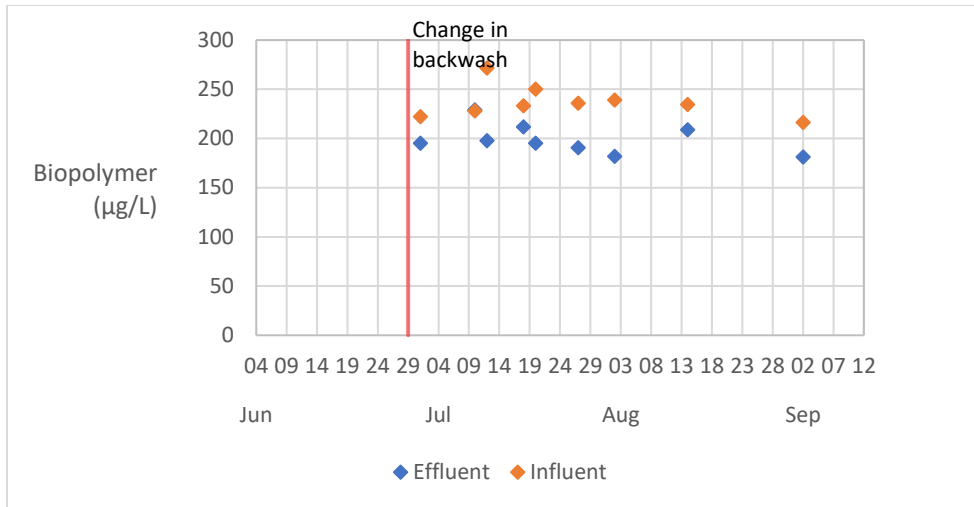


Figure 4.34: Biopolymer concentrations in Filter 3 (spent GAC) influent and effluent streams during the experimental period (n = 9)

The humic substances concentration (Figure 4.35) in the Filter 3 effluent (1,953 µg/L +/- 188 µg/L) was significantly less than the influent concentration (2,241 +/- 210 µg/L) (p = 0.001). Filter 3 removed 16% of biopolymers and 13% of humic substances during the experimental period, on average.

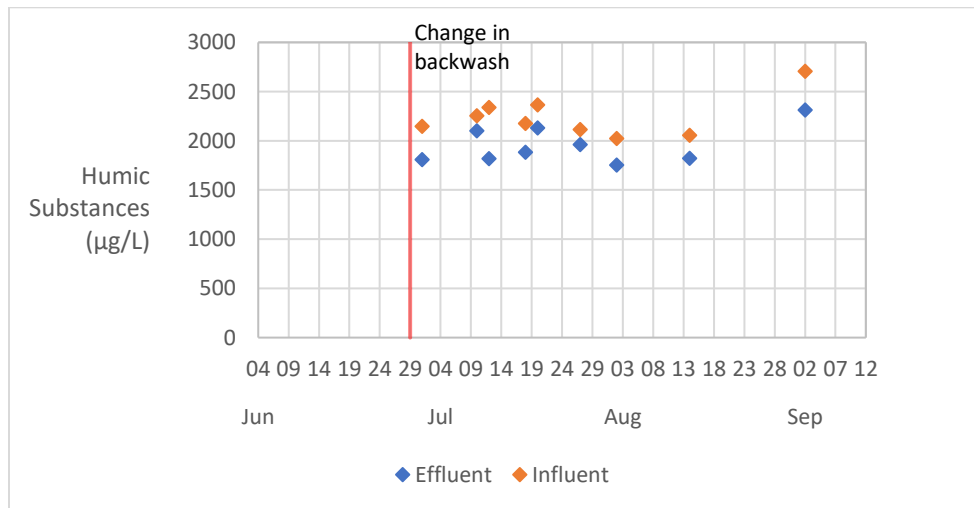


Figure 4.35: Humic substances concentrations in Filter 3 (spent GAC) influent and effluent streams during the experimental period (n = 9)

As expected, more DOC was removed in Filter 1 (new GAC) than Filter 3 (spent GAC), presumably due to more adsorptive capacity, even though DOC removal had reached steady-state in Filter 1. SUVA decreased in Filter 1 as adsorptive capacity was increasingly exhausted, while it remained essentially unchanged in Filter 3. One possible theory for this is that humic substances comprise most of the organic matter, and there are strong links between humics and aromaticity (Huber et al., 2011). Filter 1 was capable of removing more DOC, and therefore, removed more of the dominant organic matter fraction, humics, which decreased the SUVA fraction.

The adsorption capacity in Filter 1 made it capable of removing humic substances, building blocks, LMW neutrals and LMW acids – at a higher rate than in Filter 3 (Figure 4.36). The most prominent theory to explain this is that the size and shape of biopolymers (hydrophilic, > 10 kDa) isn't amenable to the adsorptive sites of GAC (Velten et al., 2011b). This finding has strong implications for water treatment research for membrane pre-treatment.

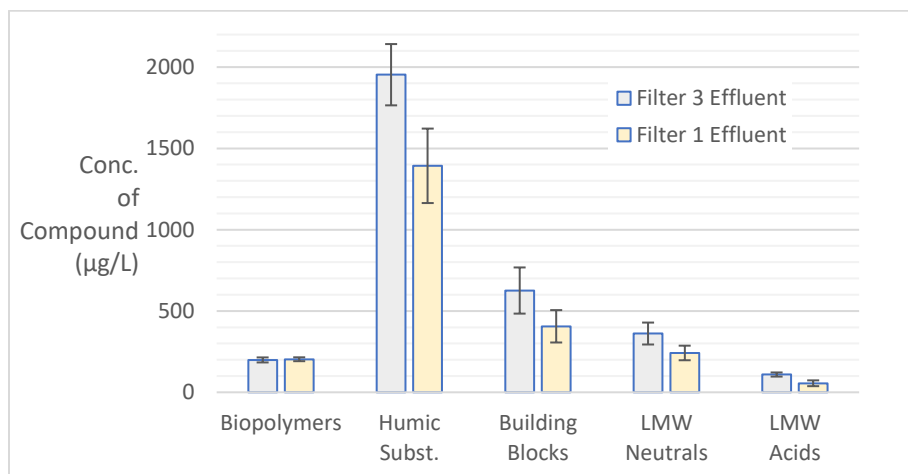


Figure 4.36: Comparison of LC-OCD components in the effluents of Filter 1 and Filter 3 (new and spent GAC, respectively) during the experimental period (n=9, error bars = +/- one standard deviation)

Overall, biofiltration processes are capable of removing biopolymers (Baghoth et al., 2009; Hallé et al., 2009), however the precise role of biodegradation in this process is unclear. For example, although increasing the retention time within a filter (i.e. an increase in EBCT) can frequently enable more biodegradation, increased EBCT does not necessarily improve biopolymer removal during biological filtration (Hijnen et al., 2018; Nemani et al., 2016; Siembida-Losch et al., 2015). Similarly, higher temperatures also can enhance biodegradation and have been associated with improved biopolymer removal

in biofilters (Pharand et al., 2015), however, higher temperatures may also result in higher biopolymer concentrations in filter influents (Rahman et al., 2014). In this experiment, Filter 3 had been in operation much longer and with a higher concentration of ATP than Filter 1 (see Section 4.5.6), yet there were no significant differences in biopolymer removal between Filters 1 and 3 ($p = 0.535$); this observation that biomass concentration does not correlate with activity has been widely reported (Emelko et al., 2006; Pharand et al., 2014).

Again, the biopolymer removal in Filter 1 is essentially the same as the biopolymer removal in Filter 3, which supports that biopolymers are not significantly affected by physical adsorption. Only two known studies that have explored the relationship between biopolymer removal and physical adsorption by new GAC could be located. One study compared two new types of GAC media—where one had a higher total pore volume and BET surface area than the other, yet the biopolymer removal was negligible for both filters. This was despite the fact that both GAC filters removed other NOM fractions, and the filter with the higher porosity removed more NOM overall (Velten et al., 2011b). Contrarily, another experiment with new GAC was successful in removing biopolymers near the start of operation (Gibert et al., 2013b). Both of these experiments even had similar biopolymer concentrations in the influent of the filters ($\sim 70 \mu\text{g/L}$). For reference, the BET surface area of the carbon used in Filter 1 of this experiment was likely $1,050 \text{ m}^2/\text{g}$ (Edzwald, 2011), within the same range as the GAC in the other studies ($790 \text{ m}^2/\text{g}$, $1,050 \text{ m}^2/\text{g}$, $1,060 \text{ m}^2/\text{g}$, $1,300 \text{ m}^2/\text{g}$ etc.). The results from this study would support the hypothesis stated in Velten et al. (2011b), that most of the biopolymer materials are too large ($>10 \text{ kDa}$) to be adsorbed in GAC micropores and mesopores, which range in size between 0 and 2 nm (Edzwald, 2011).

Given that biopolymers do not adsorb to GAC (Velten et al., 2011b), their removal at comparable levels by the new (Filter 1) and long-exhausted (Filter 3) GAC media investigated herein demonstrates that (a) both the new and exhausted GAC biofilters in the present investigation were biologically active at least one month after filter start up and (b) the mechanism of biopolymer removal by biofiltration (i.e. “biodegradation”) was direct biodegradation rather than another mechanisms such as bioregeneration.

4.5.5. ATP Concentration

ATP concentrations associated with biomass attached to the filtration media were collected from Ports 2 to 5 (see Figure 3.1) on several occasions during the experimental period (Figure 4.37 and Table 4.15).

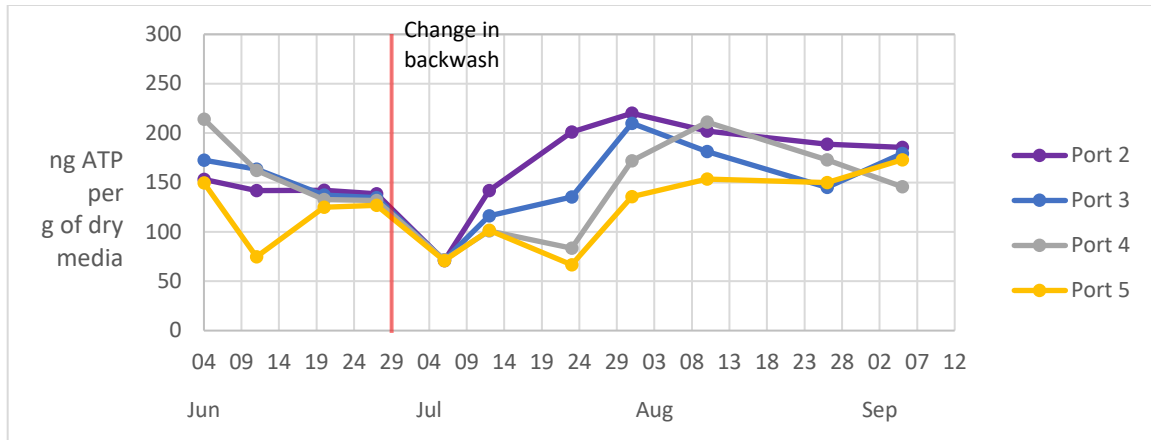


Figure 4.37: ATP concentration per g of dry GAC media in Filter 3 (spent GAC) during the experimental period

As mentioned previously, the change in backwash that occurred on June 29th, 2018, effectively removed a lot of the active biomass attached to the GAC. It is worth noting that the first ATP concentration measured on June 4th was shortly after the media were removed from the full-scale, biologically-active filters, and before the first pilot-scale backwash. It is interesting, therefore, to note that the media in Filter 3 returned to its original level of biological activity immediately after the change in backwash. These data speak to the stability and resilience of biological filters temporarily exposed to different, potentially stressful operational conditions.

Table 4.15: ATP concentration (mean +/- standard deviation) across the depth of Filter 3 (spent GAC) during steady-state operation

Port	ATP Concentration
Port 2	199 +/- 16 ng ATP/g dry GAC
Port 3	179 +/- 27 ng ATP/g dry GAC
Port 4	175 +/- 27 ng ATP/g dry GAC
Port 5	153 +/- 15 ng ATP/g dry GAC

4.6. Performance of Filter 4 – Biologically-active, spent GAC cap over new anthracite

4.6.1. Turbidity Removal and Headloss Accumulation

Overall, Filter 4 achieved very good turbidity removal, as the average filter run produced effluent of ~0.1 NTU (Table 4.16). Specifically, the filter effluent turbidity was 0.099 +/- 0.010 NTU (mean +/- standard deviation) during the experimental period. Filter cycles were generally terminated because of

headloss accumulation in this filter (28 of 31 runs) in which turbidity breakthrough above 0.3 NTU only occurred twice. The headloss accumulation rate in Filter 4 was 0.12 +/- 0.06 m/h (mean +/- standard deviation) during the experimental period.

Table 4.14: Mean turbidity removal by Filter 4 (biologically active, spent GAC cap over new anthracite) during the experimental period (n=32)

	Influent Entering Filter (NTU)	Filter Effluent (NTU)	% Removal
Mean	0.860	0.099	87
Std. Deviation	0.361	0.010	7

4.6.2. DOC

The average effluent DOC concentration in Filter 4 was 3.5 +/- 0.3 DOC mg/L (mean +/- standard deviation) (Figure 4.38). From the first measurement that was taken after 10 days of operation, Filter 4 performed relatively well in terms of organic removal, averaging at 8%. Filter 4 reached steady-state performance after approximately 50 days of operation (Figure 4.39; Table 4.16) this was within reported peak organic matter removal and steady-state biomass accumulation in new anthracite filters (Stoddart and Gagnon, 2015; Wert et al., 2008). Filter 4’s successful performance is either because biological activity began to accumulate on the media within the first week (see Figure 4.44), removing DOC early on by biological degradation, or the top layer of biologically-active GAC removed a larger-than-proportional fraction of DOC.

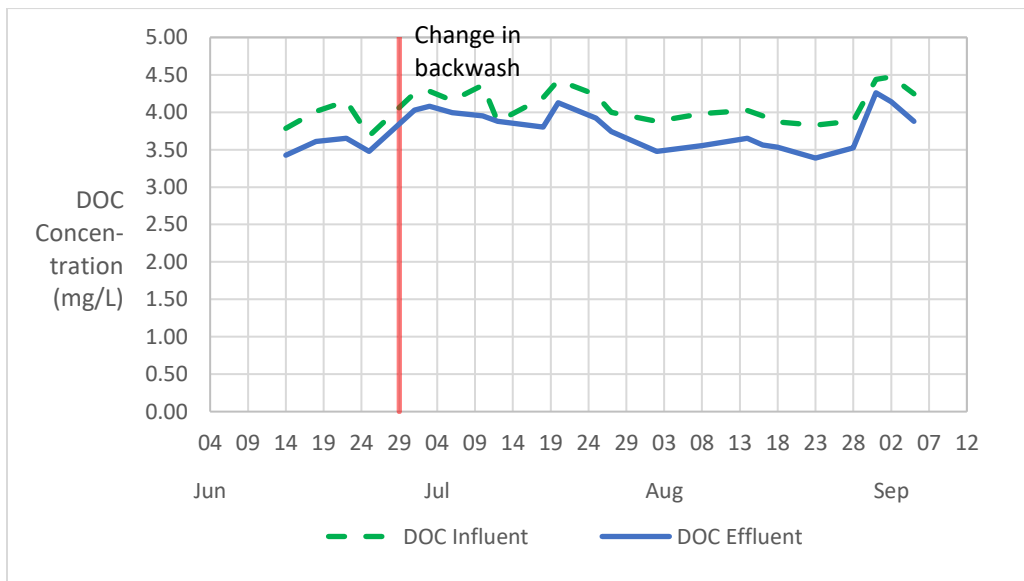


Figure 4.38: DOC concentrations in Filter 4 (biologically active, spent GAC cap over new anthracite) influent and effluent during the experimental period (n=23)

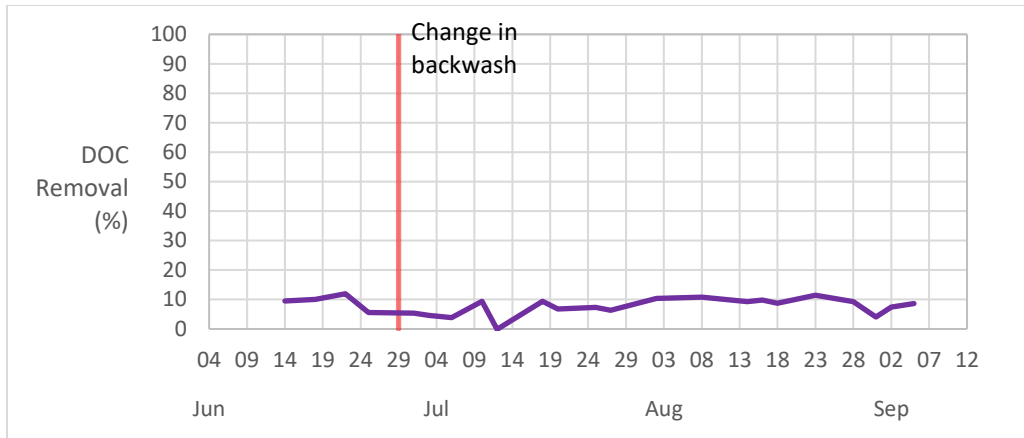


Figure 4.39: DOC removal (%) DOC concentrations in Filter 4 (biologically active, spent GAC cap over new anthracite) during the experimental period (n=23)

The pattern of DOC removal in Filter 4 is stable overall. Except for the abnormality on July 12th, 2018, the rate of removal ranges from 4 to 12%, and averages 8%. However, by visual observation, there is a gentle increase in DOC removal after the new backwashing method is employed (Figure 4.39). What likely happened to produce these results is that; there was a higher total biomass in the beginning of the experiment, causing more DOC removal by biodegradation, then this biomass was effectively removed by the change in backwash on June 29th, 2018, and the new biomass slowly accumulated and, finally, the biomass stabilized during the last month of experimentation.

A linear regression analysis was done on 10 consecutive data points for the percent DOC removal in Filter 4. The results are shown in Table 4.16 and they confirm what can be visually observed in Figure 4.40, that there is a gentle positive slope occurring after the backwashing procedure changed.

Table 4.15: Linear regression results confirming the period of steady-state DOC removal in Filter 4 (biologically active, spent GAC cap over new anthracite). This is the period during which filter effluent DOC concentration reaches steady-state, resulting in a slope that is not statistically different than a slope of zero

Data Included	Statistical Significance of Slope [†]
June 14 th to July 18 th	p = 0.199
June 18 th July 20 th	p = 0.349
June 22 nd to July 25 th 1	p = 0.761
June 25 th to July 27 th	p = 0.475
July 1 st to Aug 2 nd	p = 0.144
Jul 3 rd to Aug 8 th	p = 0.056
Jul 6 th to Aug 14 th	p = 0.067
Jul 10 th to Aug 16 th	p = 0.089
Jul 12 th to Aug 18 th	p = 0.027
Jul 18 th to Aug 23 rd	p = 0.041
Jul 20 th to Aug 28 th	p = 0.038
Jul 25 th to Aug 31 st 1	p = 0.927
Jul 27 th to Sept 2 nd	p = 0.497
Aug 2 nd to Sept 5 th	p = 0.084

† For every linear regression analysis ($Y_i = \beta_0 + \beta_1 X_i + \varepsilon_i$) units Y and X are in % removal and days since start of experiment, respectively.
 1. Data needed to be square-root transformed so it better fit the assumption of homogeneity of variance and normal distribution.

For reference purposes, Table 4.17 below provides information on what layers of media exist above each port.

Table 4.16: Filter 4 (biologically active, spent GAC cap over new anthracite)port heights and media layers

Port #	Height above the base	Layer of media above port
Port 2	116 cm	12 cm of full-scale GAC
Port 3	87 cm	8 cm of full-scale GAC 21 cm of new anthracite
Port 4	66 cm	21 cm of new anthracite
Port 5	32 cm	34 cm of new anthracite
Effluent Port	Located on floor below	2 cm of new anthracite 30 cm of silica sand And ~30 m of piping

It should be noted that the GAC is only assumed to be at the top of the filter due to its lighter particle density, however, there is likely to have been some inter-mixing between the anthracite and GAC.

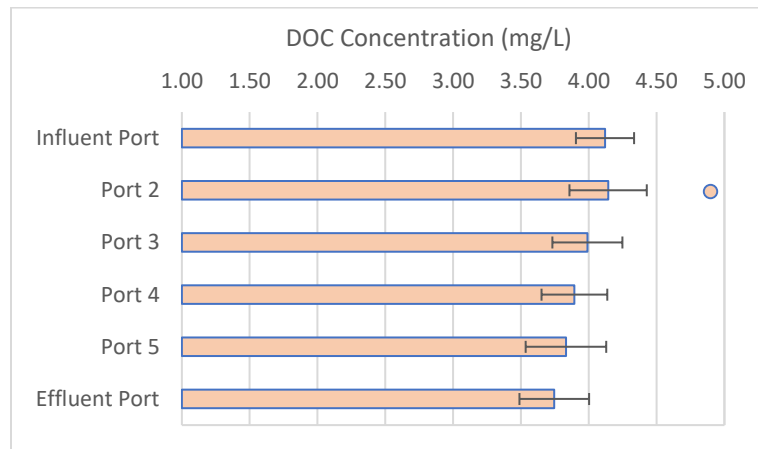


Figure 4.40: Average DOC concentration at each sampling port in Filter 4 (biologically active, spent GAC cap over new anthracite). Although there are some non-steady-state periods (Table 4.), the entire period (n=14, error bars = +/- one standard deviation)

There is one outlier that occurred on August 23rd, 2018, in Port 2. As mentioned earlier in Section 4.5.3, unusually high DOC concentrations in the depth of the filter also occurred in Filters 2 and 3 on August 23rd, so it is likely to be an operational anomaly and is excluded from the data.

Overall, Figure 4.41 shows that DOC removal by biodegradation occurred throughout the depth of Filter 4, as it did with Filter 3 (Figure 4.29) although biodegradation does successfully occur within a few months of start-up, DOC removal in the GAC-capped anthracite-sand filter did average at 8% versus 12% in the GAC-sand filter.

4.6.3. UV₂₅₄ and SUVA

On average, Filter 4 reduced UV₂₅₄ by 5 +/- 5% (n = 16) (Figure 4.42) similarly, Filter 4 removed DOC by 8 +/- 3% (n = 23). This UV₂₅₄ removal was low, yet significant (p=0.002). Filter 4 did not have an impact on SUVA, in fact, SUVA increased by 2 +/- 6% (n = 14) albeit not at a significant level (p=0.192).

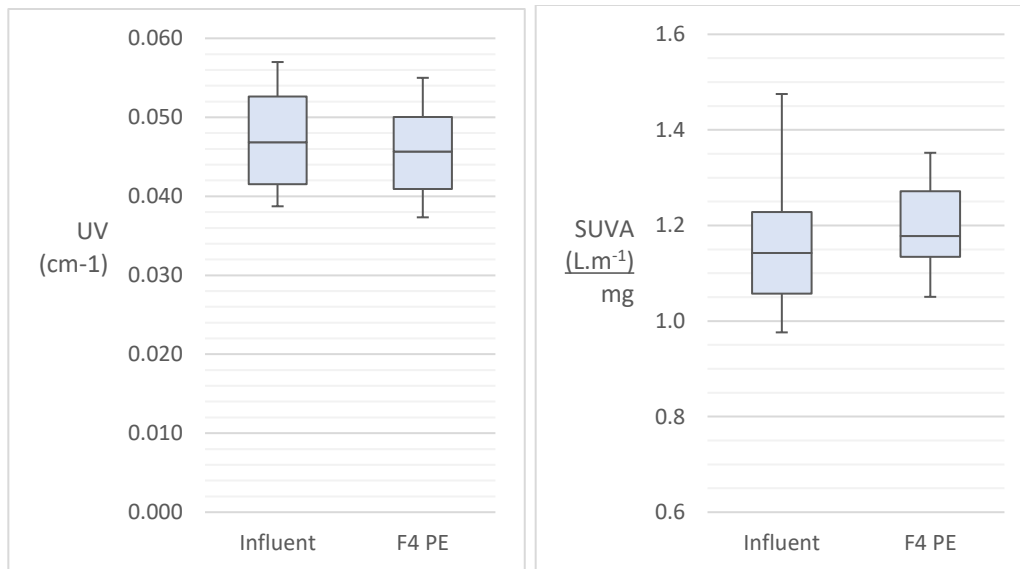


Figure 4.41: Filter 4 (biologically active, spent GAC cap over new anthracite) UV (left) and SUVA (right) influent and effluent during the experimental period (n = 16 and 14, respectively, \blacktriangle = minimum value, \blacktriangledown = maximum value observed)

These results are conducive to another study with an anthracite/sand filter with a GAC cap – which also did not see any change on the SUVA of the influent and effluent (Stoddart and Gagnon, 2017). SUVA is reportedly not affected by biodegradation (Basu and Huck, 2004). There was a statistically significant difference ($p = 0.037$) between Filter 3’s impact on the influent SUVA (decrease by 1%) and Filter 4’s impact on the influent SUVA (increase by 2%), however, from an operational perspective, Filter 3 does not have any advantage over Filter 4 in terms of removing more aromatic, recalcitrant compounds.

4.6.4. Organic Carbon (LC-OCD) Fractions

There is some variability in the biopolymer removal rate in Filter 4 (Figure 4.43), however, a paired t-test still found that there is a statistically significant difference ($p = 0.002$) between the influent ($238 \pm 17 \mu\text{g/L}$) and effluent (206 ± 26) biopolymer concentration, showing that Filter 4 was capable of removing biopolymers.

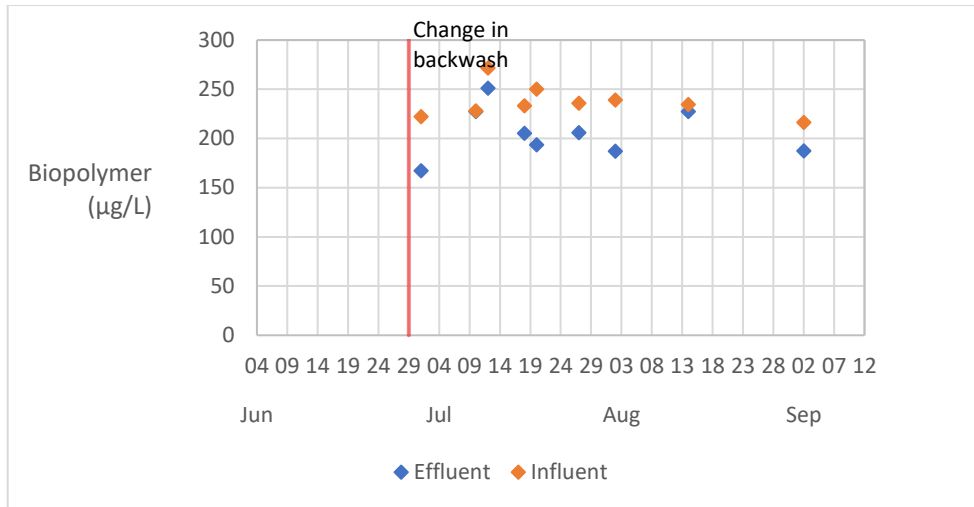


Figure 4.42: Biopolymer concentrations in Filter 4 (biologically active, spent GAC cap over new anthracite) influent and effluent streams during the experimental period (n=9)

Statistically, Filter 4 was also capable of removing humic substance compounds ($p = 0.001$). The influent averaged at $2,241 \pm 210 \mu\text{g/L}$ and the effluent at $2,046 \pm 213 \mu\text{g/L}$ (Figure 4.44).

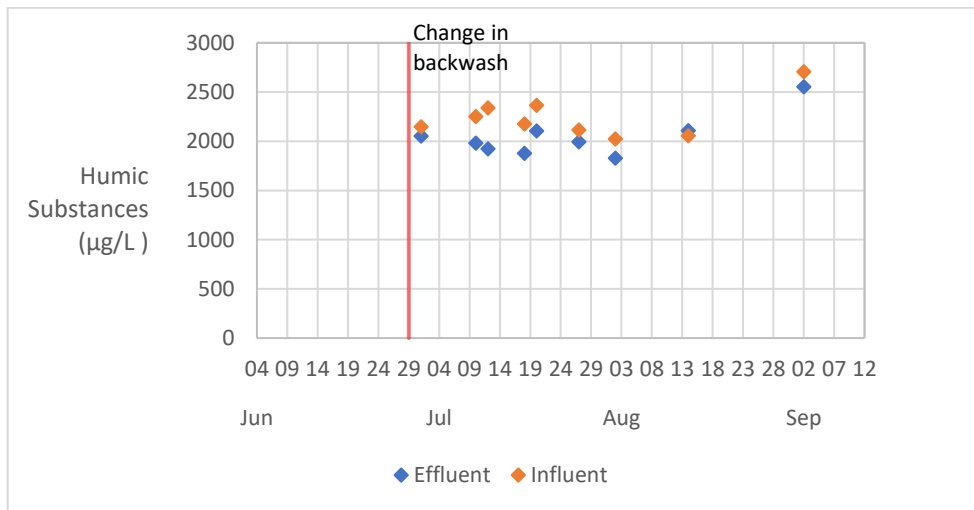


Figure 4.43: Humic Substance concentrations in Filter 4 (biologically active, spent GAC cap over new anthracite) influent and effluent streams during the experimental period (n = 9)

Filter 4 removed biopolymers and humic substances at a rate of 13% and 9%, respectively.

No studies were found that provide information on biopolymer and humic substance removal for GAC-capped anthracite/sand filters – so studies with anthracite/sand filters were reviewed for comparison

purposes. Overall, biopolymer removal by anthracite biofiltration continues to be complex. Two separate studies were reviewed that had roughly the same system configuration, which was surface water sent to a roughing filter to minimize the impact of low water quality events, then directed to an anthracite/sand biofilter. In one system, the biopolymer influent ranged between 50 and 250 $\mu\text{g/L}$ and the biopolymer removal ranged between 10% and 35% and averaged 21% (Rahman et al., 2014). In the other system, the biopolymer influent ranged between 90 and 530 $\mu\text{g/L}$, and the biopolymer removal rate was 40 to 90% (Hallé et al., 2009). Overall, the removal rate of biopolymers by Filter 4 in this experiment is reasonable.

There is no significant difference between the biopolymer and humic substance removal rate of Filter 4 and Filter 3 ($p = 0.421$, and $p = 0.082$, respectively) – which shows that there is no added benefit of using GAC instead of anthracite for the purpose of removing irreversible membrane foulants. The humic substance removal rate of Filter 4 mirrored its DOC removal rate, as was the case in Filters 1, 2 and 3.

4.6.5. ATP Concentration

ATP concentrations associated with biomass attached to the filtration media was collected from Ports 2 to 5 (see Figure 3.1) in Filter 4.

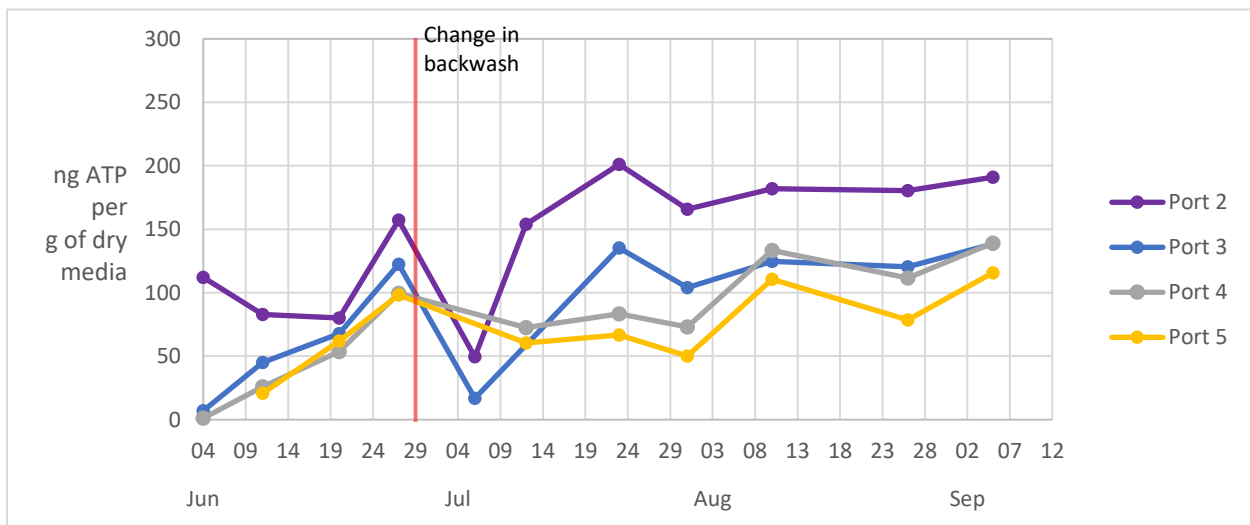


Figure 4.44: ATP concentration per g of dry GAC media in Filter 4 (biologically active, spent GAC cap over new anthracite) during the experimental period

The biological activity in Port 2 reflects the top layer of GAC, and samples from Port 3, 4 and 5 are directly under the new anthracite. This is demonstrated plainly at the start of the experiment, with the high ATP concentration in Port 2 and minimal ATP concentration in Ports 3, 4 and 5 (Figure 4.45). Filter 4 behaves similarly to Filter 1, 2 and 3 in that the biomass quantity dips after the backwash maintenance on June 29th, 2018, then rises and stabilizes after July 23rd, 2018. Shortly after the backwashing maintenance,

the DOC removal rate decreased for a brief period (Figure 4.40), which is presumably due to this decrease in biomass quantity – this stresses the need to consider the impact on organic removal if a GAC-capped anthracite/sand filter requires a higher-energy backwashing procedure.

It is also worth noting that the amount of biomass in the GAC layer (Port 2) is higher throughout the experiment than the other layers. This confirms a common finding among biological filtration studies – that GAC can support more biomass than anthracite (Stoddart and Gagnon, 2017; Wang et al., 1995).

Table 4.17: ATP concentration (mean ± standard deviation) through Filter 4 (biologically active, spent GAC cap over new anthracite) during steady-state operation

Port	n	ATP concentration
Port 2	5	184 +/- 13 ng ATP/g dry GAC
Port 3	5	125 +/- 14 ng ATP/g dry GAC
Port 4	5	108 +/- 29 ng ATP/g dry GAC
Port 5	5	84 +/- 28 ng ATP/g dry GAC

The GAC layer within Filter 4 is a considerable contribution to the DOC removal throughout the depth of Filter 4, (Table 4.19).

Table 4.18: Fraction of DOC removed in each layer of media within Filter 4 (biologically active, spent GAC cap over new anthracite)

Layer and media configuration	Fraction of DOC removed through GAC layer in Filter 4
12 cm of full-scale GAC	-0.07 ^a
8 cm of full-scale GAC 21 cm of new anthracite	0.43 ^a
21 cm of new anthracite	0.26
34 cm of new anthracite	0.16
2 cm of new anthracite 30 cm of silica sand and ~30 m of piping	0.26
a. Calculations do not contain the single outlier presented in Section 4.6.3., when included, these layers are -0.24 and 0.56, respectively.	

In the first 12 cm of the GAC layer, DOC is released (-7%), and then removed substantially in the following 29 cm layer of combined GAC and anthracite (43%). This demonstrates that although a higher quantity of biomass was measured Port 2, biological activity and thus biodegradation occurred throughout the depth of the filter, as found by Velten et al., (2011a).

5. Conclusions and Implications

This research was focused on advancing the scientific and operational understanding of drinking water treatment by varying select configurations of GAC/sand and biologically-active GAC/sand filtration (i.e. classical biofiltration), including the utility of relatively more economical configurations such as GAC caps over non-adsorptive anthracite/sand biofilters. Pilot-scale biofiltration experiments were conducted to evaluate biomass development and the removal of organic matter. Filter 1 contained 1 m of new GAC, Filter 2 contained new and spent GAC (40% and 60%, respectively), Filter 3 contained spent GAC (5 years of acclimation), and Filter 4 contained 0.2 m of spent GAC over 0.8 m of new anthracite. The main conclusions from this work are:

1. New, highly adsorptive GAC media operated to encourage biological activity (i.e., without pre-chlorination) (a) generally removed more organic matter (DOC, humic substances, building blocks, LMW neutrals and LMW acids) than exhausted biologically-active GAC, b) demonstrated a trend of decreasing to eventual steady-state DOC removal, with evidence to show that subtle declines in performance could potentially continue to occur for several years after start-up, and c) preferentially removed aromatic compounds, as would be expected based on the extensive available literature.
2. The removal of biopolymers, which are associated with membrane fouling, was comparable between the new and exhausted GAC media in the biofilters. The lack of enhanced biopolymer removal by new, highly adsorptive GAC was likely due the relatively large size of biopolymer macromolecules, which would limit their access to the internal pore structure of GAC media.
 - Given that biopolymers do not adsorb to GAC (Velten et al., 2011b), their removal at comparable levels by the new and exhausted GAC biofilters investigated herein suggests that (a) both the new and exhausted GAC biofilters in the present investigation were biologically active after one month of start-up and (b) the mechanism of biopolymer removal by biofiltration (i.e. “biodegradation”) is direct biodegradation rather than bioregeneration. This novel mechanistic finding has important implications for biofiltration process design because it demonstrates that biopolymer removal is limited by biological activity rather than available adsorptive sites. It also resolves the mechanistic work of Spanjers (2017) by demonstrating that, in addition to other mechanisms, direct biodegradation occurs in classical biofiltration with GAC filtration media during drinking water treatment.

3. GAC caps over anthracite/sand filtration media may offer an economical alternative to GAC/sand biofilters for organic matter removal. Although less DOC was removed by the GAC-capped anthracite/sand filter when compared to the biologically-active GAC/sand biofilter (even during warm-water conditions), the two types of filters achieved comparable levels of SUVA, humic substances, and biopolymer removal. It should also be noted that the quantity of biomass in GAC-capped anthracite/sand filter appeared to be more affected by changes in backwashing conditions than the biologically-active GAC/sand filter.
4. Several operational factors such as filter influent water quality, hydraulic loading rate, and EBCT as well as design parameters such as the depth of the GAC cap will affect the traditional and organic matter removal performance of GAC capped biofilters. The data presented herein suggest that a more rigorous investigation of these factors and their implications to GAC capped biofilter performance is warranted.

References

- Ahmad, R., Amirtharajah, A., Al-Shawwa, A., & Huck, P. M. (1998). Effects of backwashing on biological filters. *Journal of the American Water Works Association*, 90(12), 62–73.
- American Water Works Association, American Public Health Association, & Water Environment Federation. (2012). *Standard Methods for the Examination of Water and Wastewater*. (E. Rice, R. Baird, A. Eaton, & L. Clesceri, Eds.) (22nd ed.). Washington, DC: American Public Health Association.
- Amirtharajah, A. (1993). Optimum backwashing of filters with air scour: A review. *Water Science and Technology*, 27(10), 195–211.
- Amirtharajah, A., McNelly, N., Page, G., & McLeod, J. (1991). *Optimum backwash of dual media filters and granular activated carbon filter-adsorbers with air scour*. Denver, CO.
- Amy, G., & Carlson, K. (1997). The formation of filter-removable biodegradable organic matter during ozonation. *Ozone: Science & Engineering*, 19(2), 179–199. Retrieved from <http://www.informaworld.com/10.1080/01919519708547314>
- Andrew de Vera, G., Lauderdale, C., Alito, C. L., Hooper, J., & Wert, E. C. (2019). Using upstream oxidants to minimize surface biofouling and improve hydraulic performance in GAC biofilters. *Water Research*, 148, 526–534. <https://doi.org/10.1016/j.watres.2018.10.085>
- Ates, N., Kitis, M., & Yetis, U. (2007). Formation of chlorination by-products in waters with low SUVA — correlations with SUVA and differential UV spectroscopy. *Water Research*, 41, 4139–4148. <https://doi.org/10.1016/j.watres.2007.05.042>
- AWWA, & ANSI. (2002). *AWWA Standards*. Denver, CO.
- Azzeh, J., Taylor-edmonds, L., & Andrews, R. C. (2015). Engineered biofiltration for ultrafiltration fouling mitigation and disinfection by-product precursor control. *Water Science & Technology: Water Supply*, 15(1), 124–133. <https://doi.org/10.2166/ws.2014.091>
- Baghouth, S. A., Dignum, M., Grefte, A., Kroesbergen, J., & Amy, G. L. (2009). Characterization of NOM in a drinking water treatment process train with no disinfectant residual. *Water Science and Technology: Water Supply*, 9(4), 379–386. <https://doi.org/10.2166/ws.2009.569>
- Baruth, E. E. (2005). *Water Treatment Plant Design - AWWA and ASCE* (Fourth). New York, NY: McGraw-Hill.

- Basu, O. D., & Huck, P. M. (2004). Integrated biofilter-immersed membrane system for the treatment of humic waters. *Water Research*, 38(3), 655–662. <https://doi.org/10.1016/j.watres.2003.10.043>
- Bitton, G., Bailey, J., Kepos, P., Kroschwitz, J. I., Thomas, S., Chu, K., ... Murrell, S. (2002). *Encyclopedia of Environmental Microbiology* (Vol. 1–6). John Wiley & Sons, Inc. <https://doi.org/10.1007/978-1-62703-712-9>
- Bouwer, E. J., & Crowe, P. B. (1988). Biological Processes in Drinking Water Treatment. *Journal - American Water Works Association*, 80(9), 82–93.
- Brown, J., Summers, R. S., Le Chevallier, M., Collins, H., Roberson, J. A., Hubbs, S., & Dickenson, E. (2015). Biological drinking water treatment? Naturally. *Journal - American Water Works Association*, 107(12), 20–30. <https://doi.org/10.5942/jawwa.2015.107.0183>
- Buchanan, W., Roddick, F., & Porter, N. (2008). Removal of VUV pre-treated natural organic matter by biologically activated carbon columns. *Water Research*, 42(13), 3335–3342. <https://doi.org/10.1016/j.watres.2008.04.014>
- Crittenden, J. C., Trussell, R. R., Hand, D. W., Howe, K. j., Tchobanoglous, G., & Borchardt, J. H. (2012). *MWH's Water Treatment Principles and Design* (3rd ed.). Hoboken, NJ: John Wiley & Sons, Inc.
- DeWaters, J. E., & DiGiano, F. A. (1990). The influence of ozonated natural organic matter on the biodegradation of a micropollutant in a GAC Bed. *Journal of the American Water Works Association*, 82(8), 69–75. <https://doi.org/10.1002/j.1551-8833.1990.tb07011.x>
- Di Prima, S., Lassabatere, L., Rodrigo-Comino, J., Marrosu, R., Pulido, M., Angulo-Jaramillo, R., ... Pirastru, M. (2018). Comparing transient and steady-state analysis of single-ring infiltrometer data for an abandoned field affected by fire in Eastern Spain. *Water (Switzerland)*, 10(4). <https://doi.org/10.3390/w10040514>
- Drury, W. J., Characklis, W. G., & Stewart, P. S. (1993). Interactions of 1 µm latex particles with *Pseudomonas aeruginosa* biofilms. *Water Research*, 27(7), 1119–1126.
- Dussert, B. W., & Kovacic, S. L. (1996). Impact of drinking water preozonation on granular activated carbon quality and performance. *Ozone : Science & Engineering : The Journal of the International Ozone Association*.
- Dussert, B. W., & Tramposch, W. G. (1996). Impact of support media on the biological treatment of ozonated drinking water. *Ozone: Science & Engineering: The Journal of the International Ozone Association*, 19(2), 97–108.

- Dussert, B. W., & Van Stone, G. R. (1994). The biological activated carbon process for water purification. *Water Engineering & Management*, 141(12), 22. Retrieved from <http://www.wwdmag.com/desalination/biological-activated-carbon-process-water-purification>
- Edzwald. (2011). *Water Quality and Treatment: A Handbook on Drinking Water - AWWA* (Sixth). McGraw-Hill.
- Edzwald, B. J. K., & Kaminski, G. S. (2009). A practical method for water plants to select coagulant dosing. *Journal NEWWA*, 123(March), 15–31.
- Emelko, M. B. (2001). *Removal of Cryptosporidium parvum by granular media filtration*. Ph.D. Thesis, University of Waterloo, Waterloo, Ontario, Canada.
- Emelko, M. B., Huck, P. M., & Coffey, B. M. (2005). A review of *Cryptosporidium* removal by filtration. *Journal of the American Water Works Association*, 97:12:101-115. <https://doi.org/10.1002/j.1551-8833.2005.tb07544.x>
- Emelko, M. B., Huck, P. M., Coffey, B. M., & Smith, E. F. (2006). Effects of media, backwash, and temperature on full-scale biological filtration. *Journal of the American Water Works Association*, 98:12:61–73. <https://doi.org/10.1002/j.1551-8833.2006.tb07824.x>
- Emelko, M. B., Silins, U., Bladon, K. D., & Stone, M. (2011). Implications of land disturbance on drinking water treatability in a changing climate: Demonstrating the need for "source water supply and protection" strategies. *Water Research*, 45:2:461-472. <https://doi.org/10.1016/j.watres.2010.08.051>
- Evans, P. (2010). Nature works biological treatment methods yield high-quality water. *Opflow*, 36(7), 12–15.
- Evans, P. J., Opitz, E. M., Daniel, P. a., & Schulz, C. R. (2010). *Biological Drinking Water Treatment Perceptions and Actual Experiences in North America*. Denver, CO.
- Evans, P. J., Smith, J. L., Lechevallier, M. W., Schneider, O. D., Weinrich, L. a., & Jjemba, P. K. (2013). *Biological Filtration Monitoring and Control Toolbox: Guidance Manual*.
- Fu, J., Lee, W.-N., Coleman, C., Meyer, M., Carter, J., Nowack, K., & Huang, C.-H. (2017). Pilot investigation of two-stage biofiltration for removal of natural organic matter in drinking water treatment. *Chemosphere*, 166, 311–322. <https://doi.org/10.1016/j.chemosphere.2016.09.101>
- Fu, J., Lee, W. N., Coleman, C., Nowack, K., Carter, J., & Huang, C. H. (2017). Removal of disinfection byproduct (DBP) precursors in water by two-stage biofiltration treatment. *Water Research*, 123, 224–235. <https://doi.org/10.1016/j.watres.2017.06.073>

- Gibert, O., Lefèvre, B., Fernández, M., Bernat, X., Paraira, M., Calderer, M., ... Martínez-Llado, X. (2013). Characterising biofilm development on granular activated carbon used for drinking water production. *Water Research*, 47(3), 1101–1110. <https://doi.org/DOI.10.1016/j.watres.2012.11.026>
- Gibert, O., Lefèvre, B., Fernández, M., Bernat, X., Paraira, M., & Pons, M. (2013). Fractionation and removal of dissolved organic carbon in a full-scale granular activated carbon filter used for drinking water production. *Water Research*, 47, 2821–2829. <https://doi.org/10.1016/j.watres.2013.02.028>
- Gjessing, E. T., Egeberg, P. K., & Hakedal, J. (1999). Natural organic matter in drinking water -- The “NOM-typing project” background and basic characteristics of original water samples and NOM isolates. *Environment International*, 25(2–3), 145–159. Retrieved from <http://www.sciencedirect.com/science/article/B6V7X-3WVB89J-2/2/376594e41d23c57ebeafece2127948bd>
- González, O., Justo, A., Bacardit, J., Ferrero, E., Malfeito, J. J., & Sans, C. (2013). Characterization and fate of effluent organic matter treated with UV/H₂O₂ and ozonation. *Chemical Engineering Journal*, 226, 402–408. <https://doi.org/10.1016/j.cej.2013.04.066>
- Gotelli, N. J., & Ellison, A. M. (2013). *A Primer of Ecological Statistics* (2nd ed.). Sunderland, MA: Sinauer Associates, Inc.
- Hallé, C., Huck, P. M., Peldszus, S., Haberkamp, J., & Jekel, M. (2009). Assessing the performance of biological filtration as pretreatment to low pressure membranes for drinking water. *Environmental Science and Technology*, 43(10), 3878–3884. <https://doi.org/10.1021/es803615g>
- Han, L., Liu, W., Chen, M., Zhang, M., Liu, S., Sun, R., & Fei, X. (2013). Comparison of NOM removal and microbial properties in up-flow/down-flow BAC filter. *Water Research*, 47(14), 4861–4868. <https://doi.org/10.1016/j.watres.2013.05.022>
- Harell, F. E., Lee, K. L., Califf, R. M., Pryor, D. B., & Rosati, R. A. (1984). Regression modelling strategies for improved prognostic prediction. *Statistics in Medicine*, 3, 143–152. <https://doi.org/doi:10.1002/sim.4780090503>.
- Hermansson, M. (1999). The DLVO theory in microbial adhesion. *Colloids and Surfaces*, 14, 105–119.
- Hijnen, W. A. M., Schurer, R., Bahlman, J. A., Ketelaars, H. A. M., Italiaander, R., van der Wal, A., & van der Wielen, P. W. J. J. (2018). Slowly biodegradable organic compounds impact the biostability of non-chlorinated drinking water produced from surface water. *Water Research*, 129, 240–251. <https://doi.org/10.1016/j.watres.2017.10.068>

- Hozalski, R., Bouwer, E., & Goel, S. (1999). Removal of natural organic matter (NOM) from drinking water supplies by ozone-biofiltration. *Water Science and Technology*. [https://doi.org/10.1016/S0273-1223\(99\)00652-6](https://doi.org/10.1016/S0273-1223(99)00652-6)
- Hozalski, R. M., Goel, S., & Bouwer, E. J. (1995). TOC removal in biological filters. *Journal / American Water Works Association*, 87(12), 40–54.
- Hua, G., Reckhow, D. A., & Abusallout, I. (2015). Correlation between SUVA and DBP formation during chlorination and chloramination of NOM fractions from different sources. *Chemosphere*, 130, 82–89. <https://doi.org/10.1016/j.chemosphere.2015.03.039>
- Huber, S., Balz, A., Abert, M., & Pronk, W. (2011). Characterisation of aquatic humic and non-humic matter with size-exclusion chromatography - organic carbon detection - organic nitrogen detection (LC-OCD-OND). *Water Research*, 45(2), 879–885. <https://doi.org/10.1016/j.watres.2010.09.023>
- Huber, S., & Frimmel, F. (1991). Flow injection analysis of organic and inorganic carbon in the low-ppb range. *Analytical Chemistry*, 63(19), 2122–2130. <https://doi.org/10.1021/ac00019a011>
- Huber, S., & Frimmel, F. H. (1988). A liquid chromatographic system with multi-detection for the direct analysis of hydrophilic organic compounds in natural waters, 91(Iii), 198–200.
- Huck, P. M., Coffey, B. M., Amirtharajah, A., & Bouwer, E. J. (2000). *Optimizing Filtration in Biological Filters*. American Water Works Association Research Foundation, Denver, CO.
- Huck, P. M., Coffey, B. M., Anderson W. B., Emelko, M. B., Maurizio D. D., Slawson, R. M., Douglas I. P., Jasim, S. Y., & O'Melia, C. R. (2002). Using turbidity and particle counts to monitor *Cryptosporidium* removals by filters. *Water Science & Technology: Water Supply*, 2:3:65-71. <https://doi.org/10.2166/ws.2002.0086>
- Huck, P. M., Emelko, M. B., Coffey, B. M., Maurizio, D. D., & O'Melia, C. R. (2001). *Filter Operation Effects on Pathogen Passage*. American Water Works Association Research Foundation, Denver, CO.
- Jeong, S., Nguyen, T. V., Vigneswaran, S., Kandasamy, J., & Dharmabalan, D. (2016). Removal of natural organic matter at the Gunbower water treatment plant. *Desalination and Water Treatment*, 57, 0. <https://doi.org/10.1080/19443994.2015.1029006>
- Jin C., Glawdel, T., Ren, C. L., & Emelko, M. B. (2015a). Non-linear, non-monotonic effect of nano-scale roughness on particle deposition in absence of an energy barrier: Experiments and modeling. *Scientific Reports*, 5, 17747:1-14. <https://doi.org/10.1038/srep17747>

- Jin C., Normani, S., & Emelko, M. B. (2015b). Surface roughness impacts on granular media filtration at favorable conditions: Experiments and modeling. *Environmental Science & Technology*, 49:13:7879-7888. <https://doi.org/10.1021/acs.est.5b01998>
- Jin C., Ren, C. L., & Emelko, M. B. (2016). Concurrent modeling of hydrodynamics and interaction forces improves particle deposition predictions. *Environmental Science & Technology*, 50:8:4401-4412. <https://doi.org/10.1021/acs.est.6b00218>
- Jin C., Zhao, W., Normani, S., Zhao, P., & Emelko, M. B. (2017). Synergies of media surface roughness and ionic strength on particle deposition during filtration. *Water Research*, 114:286-295. <https://doi.org/10.1016/j.watres.2017.02.010>
- Karanfil, T., Erdogan, I., & Schlautman, M. (2005). *The role of filtration in DOC, UV-254 and SUVA-254 determinations*. Denver, CO.
- Kennedy, M. D., Chun, H. K., Quintanilla Yangali, V. A., Heijman, B. G. J., & Schippers, J. C. (2005). Natural organic matter (NOM) fouling of ultrafiltration membranes: Fractionation of NOM in surface water and characterisation by LC-OCD. *Desalination*, 178(1-3 SPEC. ISS.), 73–83. <https://doi.org/10.1016/j.desal.2005.02.004>
- Kirisits, M. J., Emelko, M. B., & Pinto, A. J. (2019). Applying biotechnology for drinking water biofiltration : advancing science and practice. *Current Opinion in Biotechnology*, 57(June), 197–204.
- Kitis, M., Karanfil, T., & Kilduff, J. E. (2004). The Reactivity of Dissolved Organic Matter for Disinfection By-Product Formation. *Turkish Journal of Engineering and Environmental Science*, 28, 167–179.
- Klimenko, N., Winther-nielsen, M., & Smolin, S. (2002). Role of the physico-chemical factors in the purification process of water from surface-active matter by biosorption. *Water Research*, 36, 5132–5140.
- Korotta-Gamage, S. M., & Sathasivan, A. (2017). A review: Potential and challenges of biologically activated carbon to remove natural organic matter in drinking water purification process. *Chemosphere*, 167, 120–138. <https://doi.org/10.1016/j.chemosphere.2016.09.097>
- Krasner, S. W., Sclimenti, M. J., & Coffey, B. M. (1993). Testing biologically active filters for removing aldehydes formed during ozonation. *Journal / American Water Works Association*, 85(5), 62–71. <https://doi.org/10.1002/j.1551-8833.1993.tb05987.x>
- Laspidou, C. S., & Rittmann, B. E. (2002). A unified theory for extracellular polymeric substances, soluble microbial products , and active and inert biomass. *Water Research*, 36, 2711–2720.

- Lautenschlager, K., Hwang, C., Ling, F., Liu, W. T., Boon, N., Köster, O., ... Hammes, F. (2014). Abundance and composition of indigenous bacterial communities in a multi-step biofiltration-based drinking water treatment plant. *Water Research*, 62, 40–52. <https://doi.org/10.1016/j.watres.2014.05.035>
- Lazarova, V., & Manem, J. (1995). Biofilm characterization and activity analysis in water and wastewater treatment. *Water Research*, 29(10), 2227–2245.
- LeChevallier, M. W., Becker, W. C., & Lee, R. G. (1992). AOC reduction by biologically active filtration. *Water Science Journal*, 84(April), 113–142.
- Liao, X., Chen, C., Wang, Z., Wan, R., Chang, C. H., Zhang, X., & Xie, S. (2013). Changes of biomass and bacterial communities in biological activated carbon filters for drinking water treatment. *Process Biochemistry*, 48(2), 312–316. <https://doi.org/10.1016/j.procbio.2012.12.016>
- Liao, X., Zou, R., Chen, C., Yuan, B., Zhou, Z., Ma, H., & Zhang, X. (2016). Biomass development in GAC columns receiving influents with different levels of nutrients. *Water Science and Technology: Water Supply*, 16(4), 1024–1032. <https://doi.org/10.2166/ws.2016.016>
- Liu, X., Huck, P. M., & Slawson, R. (2001). Factors affecting drinking water biofiltration. *American Water Works Association*, 93(12), 16.
- Lohwacharin, J., Phetrak, A., Takizawa, S., Kanisawa, Y., & Okabe, S. (2015). Bacterial growth during the start-up period of pilot-scale biological activated carbon filters: Effects of residual ozone and chlorine and backwash intervals. *Process Biochemistry*, 50(10), 1640–1647. <https://doi.org/10.1016/j.procbio.2015.06.012>
- Lohwacharin, J., Yang, Y., Watanabe, N., Phetrak, A., Sakai, H., Murakami, M., ... Takizawa, S. (2011). Characterization of DOM removal by full-scale biological activated carbon (BAC) filters having different ages. In *IWA Specialty Conference on Natural Organic Matter*. Costa Mesa, CA.
- Magic-Knezev, A., & van der Kooij, D. (2004). Optimisation and significance of ATP analysis for measuring active biomass in granular activated carbon filters used in water treatment. *Water Research*, 38(18), 3971–3979. <https://doi.org/10.1016/j.watres.2004.06.017>
- Martin, M. J., Artola, A., Balaguer, M. D., & Rigola, M. (2002). Enhancement of the activated sludge process by activated carbon produced from surplus biological sludge. *Biotechnology Letters*, 24, 163–168.
- McDonald, J. H. (2014). *Handbook of Biological Statistics* (3rd ed.). Baltimore, MA: Sparky House

Publishing.

- McDowall, B., Hoefel, D., Newcombe, G., Saint, C. P., & Ho, L. (2009). Enhancing the biofiltration of geosmin by seeding sand filter columns with a consortium of geosmin-degrading bacteria. *Water Research*, *43*(2), 433–440. <https://doi.org/10.1016/j.watres.2008.10.044>
- McKie, M. J., Andrews, S. A., & Andrews, R. C. (2016). Conventional drinking water treatment and direct biofiltration for the removal of pharmaceuticals and artificial sweeteners: A pilot-scale approach. *Science of the Total Environment*, *544*, 10–17. <https://doi.org/10.1016/j.scitotenv.2015.11.145>
- McKie, M. J., Taylor-Edmonds, L., Andrews, S. A., & Andrews, R. C. (2015). Engineered biofiltration for the removal of disinfection by-product precursors and genotoxicity. *Water Research*, *81*, 196–207. <https://doi.org/10.1016/j.watres.2015.05.034>
- Mckie, M. J., Ziv-el, M. C., Taylor-edmonds, L., Andrews, R. C., & Kirisits, M. J. (2019). Biofilter scaling procedures for organics removal: A potential alternative to piloting. *Water Research*, *151*, 87–97. <https://doi.org/10.1016/j.watres.2018.12.006>
- Metcalf, & Eddy (Eds.). (2013). *Wastewater Engineering: Treatment and Resource Recovery* (5th ed.). McGraw-Hill.
- Miltner, R. J., Summers, R. S., & Wang, J. Z. (1995). Biofiltration performance: part 2, effect of backwashing. *Journal / American Water Works Association*, *87*(12), 64–70.
- Moore, B. C., Cannon, F. S., Westrick, J. A., Metz, D. H., Shrive, C. A., DeMarco, J., & Hartman, D. J. (2001). Changes in GAC pore structure during full-scale water treatment at Cincinnati: A comparison between virgin and thermally reactivated GAC. *Carbon*, *39*(6), 789–807. [https://doi.org/10.1016/S0008-6223\(00\)00097-X](https://doi.org/10.1016/S0008-6223(00)00097-X)
- Moore, L. F., & Watson, S. B. (2007). The Ontario Water Works Consortium: a functional model of source water management and understanding. *Water Science & Technology*, *55*(5), 195–201. <https://doi.org/10.2166/wst.2007.179>
- Ndiongue, S., Anderson, W. B., Tadwalkar, A., Rudnickas, J., Lin, M., & Huck, P. M. (2006). Using Pilot-Scale Investigations to Estimate the Remaining Geosmin and Using Pilot-Scale Investigations to Estimate the Remaining Geosmin and MIB Removal Capacity of Full-Scale GAC-Capped Drinking Water Filters. *Water Quality Research Journal Canada*, *41*(3), 296–306. <https://doi.org/10.2166/wqrj.2006.033>
- Nemani, V. A., Mckie, M. J., Taylor-edmonds, L., & Andrews, R. C. (2018). Impact of biofilter operation

- on microbial community structure and performance. *Journal of Water Process Engineering*, 24(February), 35–41. <https://doi.org/10.1016/j.jwpe.2018.05.009>
- Nemani, V. A., Taylor-Edmonds, L., Peleato, N. M., & Andrews, R. C. (2016). Impact of operational parameters on biofiltration performance: organic carbon removal and effluent. *Water Science & Technology: Water Supply*, 16(6), 1683–1692. <https://doi.org/10.2166/ws.2016.093>
- Pacini, V. A., Ingallinella, A. M., & Sanguinetti, G. (2005). Removal of iron and manganese using biological roughing up flow filtration technology. *Water Research*, 39(18), 4463–4475. <https://doi.org/10.1016/j.watres.2005.08.027>
- Papciak, D., Kaleta, J., Puskarewicz, A., & Tchórzewska-Cieślak, B. (2016). The Use of Biofiltration Process To Remove Organic Matter From Groundwater. *Journal of Ecological Engineering*, 17(3), 119–124. <https://doi.org/10.12911/22998993/63481>
- Papineau, I., Tufenkji, N., Servais, P., & Barbeau, B. (2010). Impact of media aging on granular filtration performance for the removal of *Cryptosporidium*. *Water Quality Technology Conference and Exposition 2010*, (May), 603–611. [https://doi.org/10.1061/\(ASCE\)EE.1943-7870.0000672](https://doi.org/10.1061/(ASCE)EE.1943-7870.0000672).
- Park, M., & Snyder, S. A. (2018). Sample handling and data processing for fluorescent excitation- emission matrix (EEM) of dissolved organic matter (DOM). *Chemosphere*, 193, 530–537. <https://doi.org/10.1016/j.chemosphere.2017.11.069>
- Peiris, R. H., Halle, C., Budman, H., Moresoli, C., Peldszus, S., Huck, P. M., & Legge, R. L. (2010). Identifying fouling events in a membrane-based drinking water treatment process using principal component analysis of fluorescence excitation-emission matrices. *Water Research*, 44(1), 185–194. <https://doi.org/10.1016/j.watres.2009.09.036>
- Peldszus, S., Benecke, J., Jekel, M., & Huck, P. M. (2012). Direct biofiltration pretreatment for fouling control of ultrafiltration membranes. *Journal - American Water Works Association*, 104(7), 45–46. <https://doi.org/10.5942/jawwa.2012.104.0093>
- Peleato, N. M., & Andrews, R. C. (2015). Contributions of spatial, temporal, and treatment impacts on natural organic matter character using fluorescence- based measures. *Water Science & Technology*, 15(3), 589–598. <https://doi.org/10.2166/ws.2015.013>
- Peleato, N. M., Sidhu, B. S., Legge, R. L., & Andrews, R. C. (2017). Investigation of ozone and peroxone impacts on natural organic matter character and biofiltration performance using fluorescence spectroscopy. *Chemosphere*, 172, 225–233. <https://doi.org/10.1016/j.chemosphere.2016.12.118>

- Pharand, L., Van Dyke, M. I., Anderson, W. B., & Huck, P. M. (2014). Assessment of biomass in drinking water Biofilters by Adenosine triphosphate. *Journal - American Water Works Association*, 106(10), E433–E444. <https://doi.org/10.5942/jawwa.2014.106.0107>
- Pharand, L., Van Dyke, M. I., Anderson, W. B., Yohannes, Y., & Huck, P. M. (2015). Full-scale ozone – biofiltration: seasonally related effects on nom removal. *Journal - American Water Works Association*, (August), 425–435.
- Rahman, I., Ndiongue, S., Jin, X., Van Dyke, M. I., Anderson, W. B., & Huck, P. M. (2014). Fouling of low-pressure membranes during drinking water treatment: Effect of NOM components and biofiltration pretreatment. *Water Science and Technology: Water Supply*, 14(3), 453–460. <https://doi.org/10.2166/ws.2013.221>
- Rattier, M., Reungoat, J., & Gernjak, W. (2012). *Organic Micropollutant Removal by Biological Activated Carbon Filtration: A Review Urban Water Security Research Alliance Technical Report No . 53. Urban Water Security Research Alliance Technical Report*. [https://doi.org/10.1002/1618-2863\(20021008\)2:10<317::AID-ELSC317>3.0.CO;2-M](https://doi.org/10.1002/1618-2863(20021008)2:10<317::AID-ELSC317>3.0.CO;2-M)
- Region of Waterloo. (2017). *Drinking-Water Systems Regulation O. Reg. 170/03 - Annual Report*. Retrieved from <https://www.regionofwaterloo.ca/en/living-here/resources/Documents/water/reports/2017WaterQualityReport.pdf>
- Region of Waterloo. (2018). (*No Title*). Personal Communication.
- Ronteltap, M., Baghoth, S. A., Maeng, S. K., Rodri, S. G. S., Sharma, S., Kennedy, M., & Amy, G. L. (2008). An urban water cycle perspective of natural organic matter (NOM): NOM in drinking water, wastewater effluent, storm water , and seawater. *Water Science & Technology: Water Supply*, 8(6), 701–707. <https://doi.org/10.2166/ws.2008.146>
- Schindeman, L., Strathmann, T., Metz, D., Isabel, R. S., & Cummings, J. (2012). Evaluating GAC Filters for Control of DBP Precursors and Trace Organic Contaminants, 121.
- Scholz, M., & Martin, R. J. (1997). Ecological equilibrium on biological activated carbon. *Water Research*, 31(12), 2959–2968. [https://doi.org/10.1016/S0043-1354\(97\)00155-3](https://doi.org/10.1016/S0043-1354(97)00155-3)
- Selbes, M., Amburgey, J., Peeler, C., Alansari, A., & Karanfil, T. (2016). Evaluation of seasonal performance of conventional and phosphate-amended biofilters. *Journal - American Water Works Association*, 108(10), E523–E532. <https://doi.org/10.5942/jawwa.2016.108.0151>
- Selbes, M., Brown, J., Lauderdale, C., & Karanfil, T. (2017). Removal of selected C- and N-DBP precursors

- in biologically active filters. *Journal - American Water Works Association*, 109(3), E73–E84.
<https://doi.org/10.5942/jawwa.2017.109.0014>
- Servais, P., Anzil, A., & Ventresque, C. (1989). Simple method for determination of biodegradable dissolved organic carbon in water. *Applied and Environmental Microbiology*, 55(NOVEMBER 1989), 2732–2734. <https://doi.org/0099-2240/89/102732-03>
- Servais, P., Billen, G., & Bouillot, P. (1994). Biological colonization of granular activated carbon filters in drinking water treatment. *Journal of Environmental Engineering and Science*, 120(4), 888–899.
- Shams, S. (2018). *Wildfire and Forest Harvesting Effects on Natural Organic Matter: Implications to Drinking Water Treatability*. University of Waterloo.
- Siembida-Losch, B., Anderson, W. B., Wang, M., Bonsteel, J., & Huck, P. M. (2015). Effect of ozone on biopolymers in biofiltration and ultrafiltration processes. *Water Research*, 70, 224–234.
<https://doi.org/10.1016/j.watres.2014.11.047>
- Sillanpää, M. (2014). *Natural Organic Matter in Water*. Butterworth-Heinemann.
- Simpson, D. R. (2008). Biofilm processes in biologically active carbon water purification. *Water Research*, 42(12), 2839–2848. <https://doi.org/10.1016/j.watres.2008.02.025>
- Sing, K. S. W., Everett, D. H., Haul, R. A. W., Moscou, L., Pierotti, R. A., Rouquerol, J., & Siemienewska, T. (1985). Reporting physisorption data for gas/solid systems with special reference to the determination of surface area and porosity. *Pure and Applied Chemistry*, 57(4), 603–619.
- Singh Sidhu, B., Taylor-Edmonds, L., McKie, M. J., & Andrews, R. C. (2018). Pre-oxidation strategies for biofiltration performance improvement. *Journal of Water Process Engineering*, 26(September), 116–123. <https://doi.org/10.1016/j.jwpe.2018.09.007>
- Spanjers, M. G. (2017). *Biologically Active Filtration Media Properties: Practical and Mechanistic Implications*. University of Waterloo.
- Speitel, G. E., & Digiano, F. A. (1987). The bioregeneration of gac used to treat micropollutants. *Journal - AWWA*, 79(January), 64–73. <https://doi.org/10.1002/j.1551-8833.1987.tb02785.x>
- Stewart, P. S. (2003). Diffusion in Biofilms. *Journal of Bacteriology*, 185(5), 1485–1491.
<https://doi.org/10.1128/JB.185.5.1485>
- Stoddart, A. K., & Gagnon, G. A. (2015). Full-scale prechlorine removal: Impact on filter performance and water quality. *Journal - American Water Works Association*, 107(12), E638–E647.

<https://doi.org/10.5942/jawwa.2015.107.0180>

- Stoddart, A. K., & Gagnon, G. A. (2017). Water quality and filter performance of nutrient-, oxidant- and media-enhanced drinking water biofilters. *Environmental Science: Water Research and Technology*, 3(3), 520–533. <https://doi.org/10.1039/c6ew00293e>
- Susa, M. R., & Lemus, M. F. P. (2017). Exopolymeric substances from drinking water biofilms : Dynamics of production and relation with disinfection by products, 116, 304–315. <https://doi.org/10.1016/j.watres.2017.03.036>
- Sutherland, I. W. (2001). Exopolysaccharides in biofilms, flocs and related structures. *Water Science & Technology*, 43(6), 77–86.
- Tan, Y., Kildu, J. E., Kitis, M., & Karanfil, T. (2005). Dissolved organic matter removal and disinfection byproduct formation control using ion exchange. *Desalination*, 176, 189–200. <https://doi.org/10.1016/j.desal.2004.10.019>
- Thurman, E. M. (1986). *Organic geochemistry of natural waters* (1st ed.). The Netherlands: Dordrecht : M. Nijhoff.
- Tian, J. yu, Ernst, M., Cui, F., & Jekel, M. (2013). Correlations of relevant membrane foulants with UF membrane fouling in different waters. *Water Research*, 47(3), 1218–1228. <https://doi.org/10.1016/j.watres.2012.11.043>
- Urfer, D., & Huck, P. M. (1997). Effects of hydrogen peroxide residuals on biologically active filters. *Ozone Science & Engineering*, 19, 371386.
- Urfer, D., Huck, P. M., Booth, S. D. J., & Coffey, B. M. (1997). Biological filtration for BOM and particle removal: a critical review. *Journal - AWWA*, 89(12), 83–98.
- USEPA. (2013). A Monitoring and Control Toolbox for Biological Filtration. *Water Research Foundation*, 321.
- Van Der Aa, L. T. J., Kolpa, R. J., Rietveld, L. C., & Van Dijk, J. C. (2012). Improved removal of pesticides in biological granular activated carbon filters by pre-oxidation of natural organic matter. *Journal of Water Supply: Research and Technology - AQUA*, 61(3), 153–163. <https://doi.org/10.2166/aqua.2012.031>
- Van Der Aa, L. T. J., Rietveld, L. C., & Van der Kooij, D. (2011). Effects of ozonation and temperature on the biodegradation of natural organic matter in biological granular activated carbon filters. *Drinking*

Water Engineering and Science, 4, 25–35. <https://doi.org/10.5194/dwes-4-25-2011>

- Van der Hoek, J. P., Hofman, J. A. M. H., & Graveland, A. (1999). The use of BAC filtration for the removal of NOM and organic micropollutants from water. *Water Science & Technology*, 40(9), 257–264.
- Van der Kooij, Dirk. (1992). Assimilable carbon as an indicator of bacterial regrowth. *American Water Works Association*, 84(2), 57–65.
- Velten, S., Boller, M., Köster, O., Helbing, J., Weilenmann, H. U., & Hammes, F. (2011). Development of biomass in a drinking water granular active carbon (GAC) filter. *Water Research*, 45(19), 6347–6354. <https://doi.org/10.1016/j.watres.2011.09.017>
- Velten, S., Hammes, F., Boller, M., & Egli, T. (2007). Rapid and direct estimation of active biomass on granular activated carbon through adenosine tri-phosphate (ATP) determination. *Water Research*, 41(9), 1973–1983. <https://doi.org/10.1016/j.watres.2007.01.021>
- Velten, S., Knappe, D. R. U., Traber, J., & Kaiser, H. (2011). Characterization of natural organic matter adsorption in granular activated carbon adsorbers. *Water Research*, 45, 3951–3959. <https://doi.org/10.1016/j.watres.2011.04.047>
- Wang, J. Z., Summers, R. S., & Miltner, R. J. (1995). Biofiltration performance: part 1, relationship to biomass. *Journal / American Water Works Association*, 87(12), 55–63.
- Wassink, J. K., Andrews, R. C., Peiris, R. H., & Legge, R. L. (2011). Evaluation of fluorescence excitation-emission and LC-OCD as methods of detecting removal of NOM and DBP precursors by enhanced coagulation. *Water Science and Technology: Water Supply*, 11(5), 621–630. <https://doi.org/10.2166/ws.2011.101>
- Weber, W. J., Pirbazari, M., & Melson, G. L. (1978). Biological growth on activated carbon: an investigation by scanning electron microscopy. *Environmental Science and Technology*, 12(7), 817–819. <https://doi.org/10.1021/es60143a005>
- Weber, W. J., & Van Vliet, B. M. (1980). *Activated carbon adsorption of organics from the aqueous phase*. (I. J. Suffet & M.J., Eds.) (Vol. 1). Ann Arbor: McGuire (Eds.).
- Wert, E. C., Neemann, J. J., Rexing, D. J., & Zegers, R. E. (2008). Biofiltration for removal of BOM and residual ammonia following control of bromate formation. *Water Research*, 42(1–2), 372–378.
- Wong, A. W. T. (2015). *Investigating the Enhancement of Biological Filtration with Capping Material*

Designs and Nutrient Amendments. University of Waterloo.

- Yang, X., Ñ, C. S., & Huang, J. (2005). DBP formation in breakpoint chlorination of wastewater, *39*, 4755–4767. <https://doi.org/10.1016/j.watres.2005.08.033>
- Zhang, Shuangyi, Gitungo, S. W., Axe, L., Raczko, R. F., & Dyksen, J. E. (2017). Biologically active filters - An advanced water treatment process for contaminants of emerging concern. *Water Research*, *114*, 31–41. <https://doi.org/10.1016/j.watres.2017.02.014>
- Zhang, Shulin, & Huck, P. M. (1996). Removal of AOC in Biological Water Treatment Processes: A Kinetic Modeling Approach. *Water Research Foundation*, *1354(95)*, 1195–1207.
- Zheng, X., Ernst, M., & Jekel, M. (2009). Identification and quantification of major organic foulants in treated domestic wastewater affecting filterability in dead-end ultrafiltration. *Water Research*, *43(1)*, 238–244. <https://doi.org/10.1016/j.watres.2008.10.011>
- Zhu, I. X., Getting, T., & Bruce, D. (2010). Review of biologically active filters in drinking water applications. *Journal - American Water Works Association*, *102(December)*, 67–77.

Appendix A – All Raw Data

Operational Data

Headloss Data

Table A - 1: Headloss accumulation rate for each filter (Part 1/2)

Head Loss Accumulation Rate (m/h)				
Start of Filter Run Time	F1	F2	F3	F4
2018-06-04 15:28	0.93	0.65	0.11	0.10
2018-06-07 16:15	0.22	0.53	0.09	0.04
2018-06-08 10:13	6.00	6.00	3.27	3.15
2018-06-11 17:21	0.10	0.04	0.08	0.09
2018-06-12 17:26	0.25	0.10	0.08	0.07
2018-06-14 10:40	0.21	0.13	0.10	0.09
2018-06-16 15:30	0.24	0.32	0.11	0.10
2018-06-18 11:27	0.35	0.34	0.25	0.33
2018-06-20 14:13	0.20	0.44	0.12	0.19
2018-06-22 13:17	0.33	0.19	0.87	0.12
2018-06-25 1:44	0.20	0.95	0.48	0.08
2018-06-27 21:42	2.71	1.31	1.28	6.55
2018-06-29 17:09	0.14	0.15	0.07	0.09
2018-07-01 13:16	0.15	0.15	0.10	0.09
2018-07-03 12:20	0.43	0.73	0.19	0.15
2018-07-06 16:28	4.48	3.23	1.18	0.24
2018-07-08 21:45	0.37	0.45	0.20	0.12
2018-07-10 13:09	0.30	0.63	0.24	0.11
2018-07-12 14:20	0.28	0.43	0.22	0.14
2018-07-13 13:56	0.14	0.14	0.08	0.05
2018-07-16 14:42	0.05	0.07	0.04	0.05
2018-07-18 10:41	0.12	0.10	0.07	0.07
Formatting Legend				
<u>Reason for end of filter run time</u>				
X.XX	Head loss exceeded target of 305 cm, or...			
X.XX	Flow rate fell below 3 L/min (target is 4 L/min)			
X.XX	Turbidity exceeded 0.3 NTU for more than 10 min			
X.XX	End because shut off and backwashed			
<u>Other considerations</u>				
X.XX	Run time affected by loss of influent			
X.XX	Excluded outlier			
NR	Could not collect data			

Table A - 2: Headloss accumulation rate for each filter (Part 2/2)

Head Loss Accumulation Rate (m/h)				
Start of Filter Run Time	F1	F2	F3	F4
2018-07-20 21:07	0.09	0.22	0.08	0.09
2018-07-23 13:50	0.17	0.14	0.08	0.18
2018-07-25 19:44	0.08	0.10	0.10	0.06
2018-07-27 4:33	0.10	0.10	0.08	0.06
2018-07-31 13:15	0.08	0.09	0.09	0.07
2018-08-02 13:08	0.16	0.14	0.11	0.10
2018-08-05 12:44	0.31	0.32	0.21	0.27
2018-08-08 11:00	0.32	0.13	0.13	0.16
2018-08-10 13:29	0.37	0.60	0.20	0.12
2018-08-14 14:54	1.52	0.35	13.14	4.29
2018-08-14 22:12	0.11	0.11	0.10	0.09
2018-08-16 15:07	0.10	0.10	0.10	0.07
2018-08-18 12:41	0.13	0.15	0.11	0.10
2018-08-21 18:36	0.12	0.09	0.11	0.10
2018-08-23 12:54	0.12	0.10	0.10	0.10
2018-08-26 13:35	0.17	12.13	1.98	0.08
2018-08-28 11:51	0.14	0.22	0.12	0.11
2018-08-31 11:57	0.25	2.02	4.97	0.08
2018-09-02 11:36	0.18	1.85	0.13	0.23
2018-09-05 13:44	0.22	0.18	0.14	0.10

Formatting Legend	
<u>Reason for end of filter run time</u>	
X.XX	Head loss had exceeded 305 cm, or...
X.XX	Flow rate fell below 3 L/min (target is 4 L/min)
X.XX	Turbidity exceeded 0.3 NTU for more than 10 min
X.XX	End because shut off and backwashed
<u>Other considerations</u>	
X.XX	Run time affected by loss of influent
X.XX	Excluded outlier
NR	Could not collect data

Turbidity

Table A - 3: Average effluent turbidity from each filter while it flowed (Part 1/2)

Average Effluent (NTU)				
Start of Filter Run Time	F1	F2	F3	F4
2018-06-04 15:28	0.065	0.245	0.159	0.153
2018-06-07 16:15	0.075	0.197	0.140	0.091
2018-06-08 10:13	NR	NR	0.131	0.087
2018-06-11 17:21	0.112	0.135	0.147	0.113
2018-06-12 17:26	0.089	0.146	0.132	0.080
2018-06-14 10:40	0.080	0.156	0.138	0.084
2018-06-16 15:30	0.078	0.159	0.143	0.088
2018-06-18 11:27	0.079	0.168	0.147	0.124
2018-06-20 14:13	0.084	0.168	0.150	0.103
2018-06-22 13:17	0.083	0.166	0.152	0.098
2018-06-25 1:44	0.082	0.144	0.143	0.090
2018-06-27 21:42	NR	NR	NR	NR
2018-06-29 17:09	0.093	0.222	0.146	0.110
2018-07-01 13:16	0.087	0.205	0.144	0.110
2018-07-03 12:20	0.092	0.186	0.145	0.119
2018-07-06 16:28	0.105	0.171	0.142	0.110
2018-07-08 21:45	0.112	0.173	0.114	0.114
2018-07-10 13:09	0.089	0.173	0.121	0.101
2018-07-12 14:20	0.088	0.173	0.118	0.108
2018-07-13 13:56	0.089	0.181	0.122	0.102
2018-07-16 14:42	0.095	0.160	0.108	0.100
2018-07-18 10:41	0.085	0.149	0.105	0.098
Formatting Legend				
<u>Reason for end of filter run time</u>				
X.XXX	Head loss had exceeded 305 cm, or...			
X.XXX	Flow rate fell below 3 L/min (target is 4 L/min)			
X.XXX	Turbidity exceeded 0.3 NTU for more than 10 min			
X.XXX	End because shut off and backwashed			
<u>Other considerations</u>				
X.XXX	Run time affected by loss of influent			
NR	Could not collect data			

Table A - 4: Average effluent turbidity from each filter while it flowed (Part 1/2)

Average Effluent (NTU)				
Start of Filter Run Time	F1	F2	F3	F4
2018-07-20 21:07	0.088	0.145	0.107	0.101
2018-07-23 13:50	0.087	0.143	0.106	0.098
2018-07-25 19:44	0.087	0.167	0.101	0.095
2018-07-27 4:33	0.086	0.153	0.100	0.097
2018-07-31 13:15	0.092	0.158	0.101	0.091
2018-08-02 13:08	0.088	0.153	0.104	0.088
2018-08-05 12:44	0.091	0.156	0.107	NR
2018-08-08 11:00	0.092	0.167	0.107	0.096
2018-08-10 13:29	0.089	0.135	0.109	0.094
2018-08-14 14:54	0.089	0.228	NR	0.105
2018-08-14 22:12	0.083	0.221	0.143	0.092
2018-08-16 15:07	0.083	0.238	0.174	0.097
2018-08-18 12:41	0.081	0.250	NR	0.086
2018-08-21 18:36	0.082	0.153	NR	0.100
2018-08-23 12:54	0.093	0.253	0.131	0.100
2018-08-26 13:35	0.083	0.238	0.132	0.089
2018-08-28 11:51	0.083	0.628	0.093	0.089
2018-08-31 11:57	0.091	0.304	0.136	0.101
2018-09-02 11:36	0.091	0.380	0.102	0.100
2018-09-05 13:44	0.086	0.567	0.095	0.093
Formatting Legend				
<u>Reason for end of filter run time</u>				
X.XXX	Head loss had exceeded 305 cm, or...			
X.XXX	Flow rate fell below 3 L/min (target is 4 L/min)			
X.XXX	Turbidity exceeded 0.3 NTU for more than 10 min			
X.XXX	End because shut off and backwashed			
<u>Other considerations</u>				
X.XXX	Run time affected by loss of influent			
NR	Could not collect data			

Run Times

Table A - 5: Official run times for each filter (Part 1/2)

Run Times				
Start of Filter Run Time	F1	F2	F3	F4
2018-06-04 15:28	1:22	0:00	8:22	1:28
2018-06-07 16:15	13:02	2:00	8:26	3:24
2018-06-08 10:43	0:00	0:00	15:22	11:22
2018-06-11 17:21	9:08	12:36	12:58	23:12
2018-06-12 17:26	9:24	26:32	38:15	34:55
2018-06-14 10:40	16:38	24:24	26:30	32:44
2018-06-16 15:30	15:23	11:42	21:53	20:20
2018-06-18 11:27	6:52	6:58	7:08	6:46
2018-06-20 14:13	16:03	8:53	22:20	14:55
2018-06-22 13:17	13:22	16:47	3:06	24:29
2018-06-25 1:44	20:20	1:24	5:59	21:32
2018-06-27 21:42	0:00	0:00	0:00	0:00
2018-06-29 17:09	27:17	26:10	37:36	33:01
2018-07-01 13:16	21:20	18:36	27:58	33:45
2018-07-03 12:20	14:05	4:54	12:36	14:46
2018-07-06 16:28	0:23	0:48	1:25	4:56
2018-07-08 21:45	7:59	6:24	14:13	23:32
2018-07-10 13:09	12:50	4:10	13:23	26:08
2018-07-12 14:20	7:13	6:48	7:07	6:52
2018-07-13 13:56	2:16	2:16	2:02	1:40
2018-07-16 14:42	36:38	31:42	42:38	42:30
2018-07-18 10:41	25:02	24:52	38:01	28:44
Formatting Legend				
<u>Reason for end of filter run time</u>				
X:XX	Head loss had exceeded 305 cm, or...			
X:XX	Flow rate fell below 3 L/min (target is 4 L/min)			
X:XX	Turbidity exceeded 0.3 NTU for more than 10 min			
X:XX	End because shut off and backwashed			
<u>Other considerations</u>				
X:XX	Run time affected by loss of influent			
NR	Could not collect data			

Table A - 6: Official run times for each filter (Part 2/2)

Run Times				
Start of Filter Run Time	F1	F2	F3	F4
2018-07-20 21:07	27:21	25:51	30:36	26:47
2018-07-23 13:50	25:18	24:19	34:19	3:54
2018-07-25 19:44	30:52	29:40	31:08	22:32
2018-07-27 4:33	31:32	34:14	38:06	35:04
2018-07-31 13:15	28:14	25:01	35:27	35:47
2018-08-02 13:08	21:22	24:54	26:32	33:32
2018-08-05 12:44	10:46	8:20	17:04	9:00
2018-08-08 11:00	10:08	24:16	22:08	20:24
2018-08-10 13:29	10:52	6:36	17:51	23:57
2018-08-14 14:54	5:36	5:34	0:00	0:52
2018-08-14 22:12	30:26	29:42	30:10	35:46
2018-08-16 15:07	23:28	27:24	20:24	11:36
2018-08-18 12:41	19:00	8:42	18:18	21:58
2018-08-21 18:36	27:40	20:36	28:32	31:22
2018-08-23 12:54	23:58	3:34	29:32	28:29
2018-08-26 13:35	24:32	0:04	1:56	37:44
2018-08-28 11:51	26:21	4:26	25:42	31:48
2018-08-31 11:57	18:16	0:00	0:23	35:29
2018-09-02 11:36	6:12	0:00	6:06	10:09
2018-09-05 13:44	24:18	0:00	24:44	33:08
Formatting Legend				
<u>Reason for end of filter run time</u>				
X:XX	Head loss had exceeded 305 cm, or...			
X:XX	Flow rate fell below 3 L/min (target is 4 L/min)			
X:XX	Turbidity exceeded 0.3 NTU for more than 10 min			
X:XX	End because shut off and backwashed			
<u>Other considerations</u>				
×:XX	Run time affected by loss of influent			
NR	Could not collect data			

Organic Matter Data

Dissolved Organic Carbon

Table A - 7: DOC data from Filter 1

Date	Day*	Post-Ozone**	Port 1 (Inf)	Avg Influent***	Port 2	Port 3	Port 4	Port 5	Effluent
14-Jun-18	10	NR	3.45	3.79	2.96	1.72	1.07	0.63	0.55
18-Jun-18	14	4.61	3.76	4.01	NR	NR	NR	NR	0.66
22-Jun-18	18	NR	4.15	4.41	3.23	2.32	1.77	NR	1.26
25-Jun-18	21	NR	3.68	3.55	3.43	2.50	1.99	1.44	1.20
1-Jul-18	27	4.32	4.26	4.10	3.84	3.08	2.67	2.28	1.89
3-Jul-18	29	NR	4.49	4.28	3.74	3.05	2.77	2.24	2.29
10-Jul-18	36	4.34	4.27	4.36	3.75	3.18	2.62	2.35	2.16
12-Jul-18	38	4.42	4.19	3.88	NR	NR	NR	NR	1.95
18-Jul-18	44	4.34	4.31	4.20	3.72	3.08	2.75	2.40	2.39
20-Jul-18	46	4.81	4.31	4.43	3.86	3.22	2.83	2.55	2.49
25-Jul-18	51	4.60	4.23	4.23	4.03	3.37	3.12	2.69	2.68
27-Jul-18	53	4.29	4.26	4.00	NR	NR	NR	NR	2.84
2-Aug-18	59	3.99	3.76	3.88	3.52	3.09	2.91	2.66	2.72
5-Aug-18	62	4.16	3.95	3.97	3.81	3.06	3.06	2.73	2.71
8-Aug-18	65	4.14	3.90	3.98	NR	NR	NR	NR	2.66
14-Aug-18	71	4.03	3.68	4.02	3.13	3.07	2.74	2.71	2.66
16-Aug-18	73	4.17	3.95	3.95	NR	NR	NR	NR	2.92
18-Aug-18	75	4.01	3.81	3.87	3.65	3.17	3.04	2.77	2.94
23-Aug-18	80	3.93	3.63	3.83	3.46	3.35	2.86	2.51	2.63
28-Aug-18	85	4.14	3.80	3.88	3.60	3.11	3.10	2.93	2.86
31-Aug-18	88	4.66	4.51	4.44	NR	NR	NR	NR	3.18
2-Sep-18	90	4.52	4.40	4.47	NR	NR	NR	2.68	3.00
5-Sep-18	93	4.50	NR	4.25	4.26	3.56	3.37	3.18	3.21

* Days from when the filter first started running
 ** DOC data is in mg/L
 *** Average Influent is average of port 1 across all filters in experiment
 NR – Could not collect data

Table A - 8: DOC data from Filter 2

Date	Day*	Post-Ozone**	Port 1 (Inf)	Avg Influent***	Port 2	Port 3	Port 4	Port 5	Effluent
14-Jun-18	10	NR	4.25	3.79	3.03	3.12	NR	2.38	2.33
18-Jun-18	14	4.61	3.86	4.01	NR	NR	NR	NR	2.29
22-Jun-18	18	NR	3.77	4.15	3.47	3.27	NR	3.00	2.63
1-Jul-18	27	4.32	4.36	4.26	3.95	3.87	NR	3.82	3.49
3-Jul-18	29	NR	3.95	4.28	NR	NR	NR	NR	3.10
12-Jul-18	38	4.42	3.08	3.88	NR	NR	NR	NR	2.89
18-Jul-18	44	4.34	3.99	4.20	3.90	3.66	3.51	3.25	3.12
20-Jul-18	46	4.81	4.39	4.43	4.11	3.73	4.81	3.40	3.39
25-Jul-18	51	4.60	4.29	4.23	3.96	3.69	3.65	3.52	3.30
27-Jul-18	53	4.29	4.16	4.00	NR	NR	NR	NR	3.30
2-Aug-18	59	3.99	3.97	3.88	3.73	3.42	3.31	3.13	3.04
5-Aug-18	62	4.16	4.07	3.97	NR	NR	NR	NR	3.08
8-Aug-18	65	4.14	3.95	3.98	NR	NR	NR	NR	3.08
14-Aug-18	71	4.03	4.11	4.02	3.77	3.75	3.37	4.03	3.16
16-Aug-18	73	4.17	4.02	3.95	NR	NR	NR	NR	3.16
18-Aug-18	75	4.01	3.97	3.87	NR	3.56	3.32	3.23	3.18
23-Aug-18	80	3.93	3.60	3.83	5.12	3.27	3.10	2.94	3.63

* Days from when the filter first started running
 ** DOC data is in mg/L
 *** Average Influent is average of port 1 across all filters in experiment
 NR – Could not collect data

Table A - 9: DOC data from Filter 3

Date	Day*	Post-Ozone**	Port 1 (Inf)	Avg Influent***	Port 2	Port 3	Port 4	Port 5	Effluent
14-Jun-18	10	NR	3.64	3.79	3.50	3.53	3.52	3.85	3.52
18-Jun-18	14	4.61	4.32	4.01	NR	NR	NR	NR	3.50
1-Jul-18	27	4.32	4.38	4.26	4.36	4.05	3.98	4.02	3.36
3-Jul-18	29	NR	4.11	4.28	4.33	4.11	4.12	4.03	4.04
10-Jul-18	36	4.34	4.34	4.36	4.30	4.10	4.06	4.02	3.82
12-Jul-18	38	4.42	4.05	3.88	NR	NR	NR	NR	3.67
18-Jul-18	44	4.34	4.22	4.20	4.04	3.85	3.71	3.74	3.61
20-Jul-18	46	4.81	4.45	4.43	4.38	4.25	3.93	3.87	3.98
25-Jul-18	51	4.60	4.16	4.23	4.11	3.88	3.85	3.85	3.69
27-Jul-18	53	4.29	3.56	4.00	NR	NR	NR	NR	3.62
2-Aug-18	59	3.99	3.84	3.88	3.66	3.57	3.46	3.30	3.36
5-Aug-18	62	4.16	4.09	3.97	3.82	3.77	3.60	3.43	3.40
8-Aug-18	65	4.14	3.87	3.98	NR	NR	NR	NR	3.49
14-Aug-18	71	4.03	4.06	4.02	3.90	3.77	3.60	3.47	3.51
16-Aug-18	73	4.17	3.86	3.95	NR	NR	NR	NR	3.48
18-Aug-18	75	4.01	3.87	3.87	3.91	3.71	3.51	3.42	3.60
23-Aug-18	80	3.93	3.92	3.83	4.53	3.43	3.55	3.20	3.19
28-Aug-18	85	4.14	3.89	3.88	3.79	3.61	3.43	3.32	3.33
2-Sep-18	90	4.52	4.56	4.47	NR	NR	NR	NR	3.49
5-Sep-18	93	4.50	NR	4.25	4.19	4.14	3.98	3.86	3.81

* Days from when the filter first started running
 ** DOC data is in mg/L
 *** Average Influent is average of port 1 across all filters in experiment
 NR – Could not collect data

Table A - 10: DOC data from Filter 4

Date	Day*	Post-Ozone**	Port 1 (Inf)	Avg Influent***	Port 2	Port 3	Port 4	Port 5	Effluent
14-Jun-18	10	NR	3.80	3.79	3.58	3.61	3.68	3.65	3.43
18-Jun-18	14	4.61	4.07	4.01	NR	NR	NR	NR	3.61
22-Jun-18	18	NR	3.94	4.15	4.30	3.91	3.84	3.81	3.65
25-Jun-18	21	NR	3.55	3.68	3.97	3.80	3.89	3.64	3.48
1-Jul-18	27	4.32	4.24	4.26	4.44	3.95	4.20	4.29	4.03
3-Jul-18	29	NR	4.54	4.28	4.49	4.43	4.17	4.14	4.08
6-Jul-18	32	4.31	4.20	4.16	NR	NR	NR	NR	4.00
10-Jul-18	36	4.34	4.46	4.36	4.35	4.30	4.09	4.03	3.95
12-Jul-18	38	4.42	4.12	3.88	NR	NR	NR	NR	3.88
18-Jul-18	44	4.34	4.27	4.20	4.12	4.07	3.95	3.87	3.80
20-Jul-18	46	4.81	4.54	4.43	4.38	4.26	4.17	4.22	4.13
25-Jul-18	51	4.60	4.38	4.23	4.31	4.21	4.07	3.86	3.92
27-Jul-18	53	4.29	4.30	4.00	NR	NR	NR	NR	3.74
2-Aug-18	59	3.99	3.85	3.88	3.87	3.70	3.58	3.64	3.48
8-Aug-18	65	4.14	4.05	3.98	NR	NR	NR	NR	3.55
14-Aug-18	71	4.03	4.13	4.02	3.99	3.90	3.77	3.71	3.65
16-Aug-18	73	4.17	3.86	3.95	NR	NR	NR	NR	3.56
18-Aug-18	75	4.01	3.91	3.87	3.91	3.81	3.81	3.80	3.53
23-Aug-18	80	3.93	4.28	3.83	4.90	3.86	3.58	3.47	3.39
28-Aug-18	85	4.14	3.90	3.88	3.86	3.68	3.62	3.21	3.52
31-Aug-18	88	4.66	4.33	4.44	NR	NR	NR	NR	4.26
2-Sep-18	90	4.52	4.38	4.47	NR	NR	NR	NR	4.14
5-Sep-18	93	4.50	NR	4.25	4.27	4.16	4.00	3.98	3.88

* Days from when the filter first started running
 ** DOC data is in mg/L
 *** Average Influent is average of port 1 across all filters in experiment
 NR – Could not collect data

UV₂₅₄

Table A - 11: UV₂₅₄ influent data summary for all filters

Date	Day*	Post-Ozone	F1 Port 1	F2 Port 1	F3 Port 1	F4 Port 1	Avg Inf ¹
14-Jun-18	10	NR	0.054	0.073	0.049	0.047	0.056
18-Jun-18	14	0.070	0.038	0.040	0.057	0.053	0.048
01-Jul-18	27	NR	0.054	0.055	0.055	0.055	0.055
03-Jul-18	29	NR	NR	0.056	0.058	0.056	0.057
06-Jul-18	32	0.051	0.053	0.052	0.053	0.052	0.052
10-Jul-18	36	0.050	0.042	0.048	0.046	0.048	0.046
12-Jul-18	38	0.047	0.037	0.035	0.041	0.049	0.041
18-Jul-18	44	0.046	0.045	0.044	0.044	0.047	0.045
05-Aug-18	62	0.040	0.035	0.039	0.040	0.040	0.039
08-Aug-18	65	0.041	0.041	0.041	0.042	0.041	0.041
16-Aug-18	73	0.042	0.043	0.042	0.041	0.041	0.042
18-Aug-18	75	0.042	0.040	0.043	0.042	0.042	0.041
28-Aug-18	85	0.044	0.045	0.045	0.045	0.046	0.045
02-Sep-18	90	0.056	0.053	0.053	0.052	0.051	0.053
05-Sep-18	93	0.048	NR	NR	NR	NR	NR

* Days from when the filter first started running
 UV data is in cm⁻¹
 NR – Could not collect data
 1 - Average of F1 Port 1, F2 Port 1, F3 Port 1 and F4 Port 1

Table A - 12: UV₂₅₄ effluent data from all filters

Date	Day*	F1 Effluent	F2 Effluent	F3 Effluent	F4 Effluent
14-Jun-18	10	0.004	0.028	0.042	0.046
18-Jun-18	14	0.007	0.025	0.046	0.047
01-Jul-18	27	0.024	NR	0.042	0.051
03-Jul-18	29	0.023	0.039	0.043	0.055
06-Jul-18	32	0.010	0.028	0.047	0.051
10-Jul-18	36	0.014	0.027	0.043	0.046
12-Jul-18	38	0.021	0.021	0.036	0.041
18-Jul-18	44	0.023	0.033	0.040	0.043
05-Aug-18	62	0.021	0.027	0.031	0.038
08-Aug-18	65	0.025	0.031	0.037	0.037
16-Aug-18	73	0.029	0.035	0.038	0.041
18-Aug-18	75	0.029	0.033	0.042	0.042
28-Aug-18	85	NR	NR	0.038	0.040
02-Sep-18	90	0.033	NR	0.042	0.052
05-Sep-18	93	0.035	NR	0.045	0.046
* Days from when the filter first started running UV data is in cm ⁻¹ NR – Could not collect data					

LC-OCD Data

Table A - 13: NOM Fractions – Post-ozone port

Date	Biopolymers	Humic Substances	Building Blocks	LMW Neutrals	LMW Acids
01-Jul	222	2147	778	525	136
10-Jul	228	2251	666	369	158
12-Jul	272	2338	579	413	145
18-Jul	233	2176	752	550	164
20-Jul	250	2363	804	542	121
27-Jul	236	2113	859	421	133
02-Aug	239	2022	713	383	180
14-Aug	235	2055	759	461	178
02-Sep	216	2706	457	569	165
*All compounds measured in µg/L					

Table A - 14: NOM Fractions – Filter 1 Effluent

Date	Biopolymers	Humic Substances	Building Blocks	LMW Neutrals	LMW Acids
01-Jul	210	1206	285	213	29
10-Jul	210	1188	296	337	37
12-Jul	207	1106	340	190	39
18-Jul	197	1262	444	210	48
20-Jul	188	1481	468	267	55
27-Jul	206	1505	525	219	67
02-Aug	210	1404	494	235	77
14-Aug	219	1542	503	277	72
02-Sep	182	1840	298	229	75
*All compounds measured in µg/L					

Table A - 15: NOM Fractions – Filter 2 Effluent

Date	Biopolymers	Humic Substances	Building Blocks	LMW Neutrals	LMW Acids
01-Jul	187	1739	521	539	74
10-Jul	NR	NR	NR	NR	NR
12-Jul	243	1318	427	213	64
18-Jul	180	1639	630	309	88
20-Jul	187	1861	633	299	91
27-Jul	204	1792	652	370	91
02-Aug	175	1654	620	290	102
14-Aug	202	1681	695	846	82
02-Sep	229	2267	315	480	115
*All compounds measured in µg/L					

Table A - 16: NOM Fractions – Filter 3 Effluent

Date	Biopolymers	Humic Substances	Building Blocks	LMW Neutrals	LMW Acids
01-Jul	195	1806	591	251	78
10-Jul	229	2100	548	488	114
12-Jul	198	1818	703	354	117
18-Jul	212	1882	598	359	112
20-Jul	195	2129	771	352	122
27-Jul	191	1961	715	434	109
02-Aug	182	1750	677	319	112
14-Aug	209	1822	728	363	115
02-Sep	181	2311	301	333	104

*All compounds measured in µg/L

Table A - 17: NOM Fractions – Filter 4 Effluent

Date	Biopolymers	Humic Substances	Building Blocks	LMW Neutrals	LMW Acids
01-Jul	167	2053	638	465	112
10-Jul	227	1979	729	353	121
12-Jul	251	1920	717	360	116
18-Jul	205	1877	741	580	126
20-Jul	193	2105	829	573	124
27-Jul	206	1992	709	402	117
02-Aug	187	1828	630	340	122
14-Aug	227	2105	534	339	125
02-Sep	187	2553	406	420	136

*All compounds measured in µg/L

Table A - 18: NOM Fractions – Impact of long-term storage of sample

Date	Day of Storage	Biopolymers	Humic Substances	Building Blocks	LMW Neutrals	LMW Acids
10-Jul	0	- sample was taken				
18-Jul	8	229	2100	548	488	114
26-Jul	16	212	1962	700	333	109
30-Jul	20	217	1922	751	292	105
04-Aug	25	208	2028	645	355	112
10-Aug	31	217	1973	715	312	115
23-Aug	44	230	1899	777	325	104
26-Sep	78	256	2273	327	298	115

*All compounds measured in µg/L

LC-OCD Chromatograms

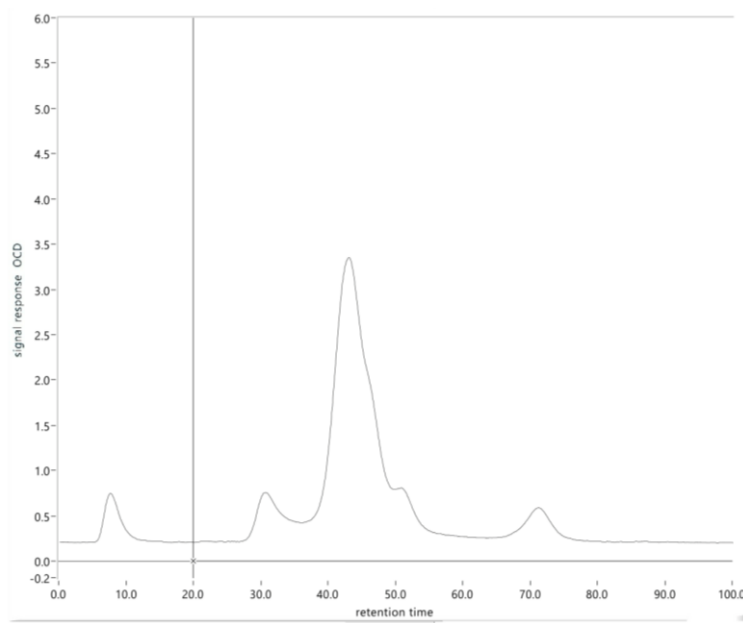


Figure A - 1 LC-OCD Data Jul 1st – F1 PE

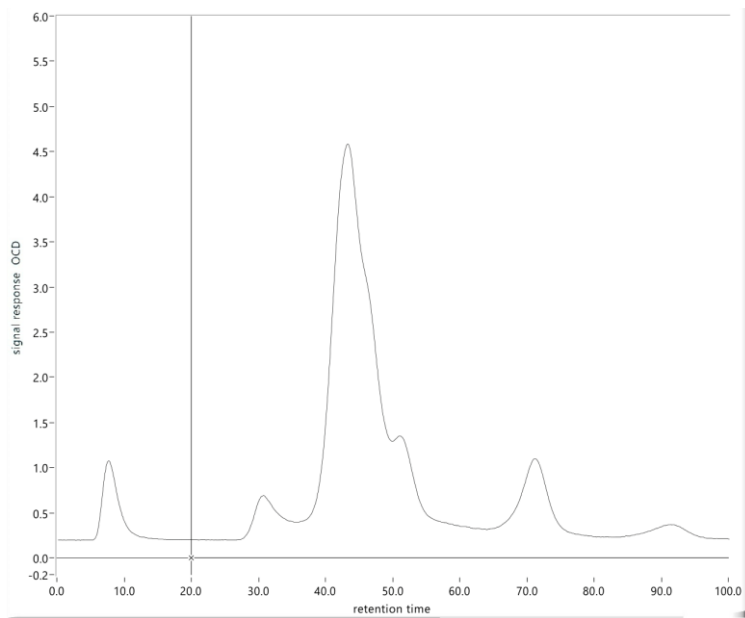


Figure A - 2 LC-OCD Data Jul 1st – F2 PE

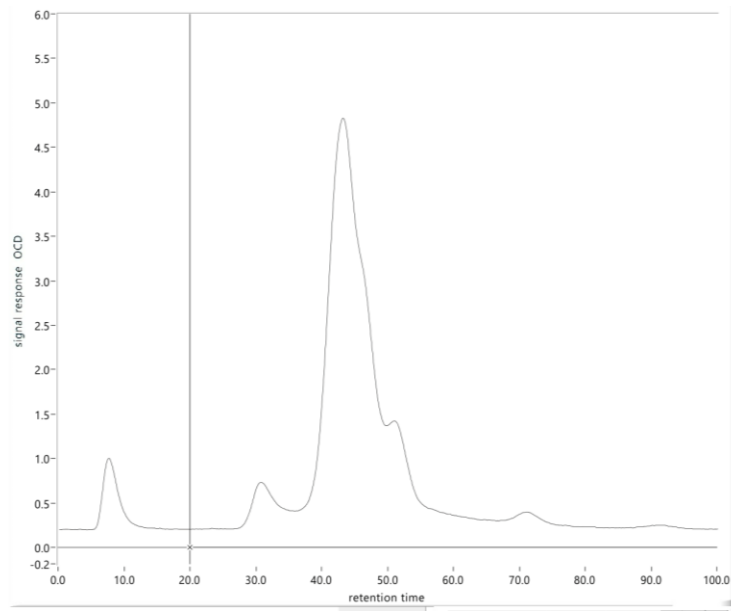


Figure A - 3 LC-OCD Data Jul 1st – F3 PE

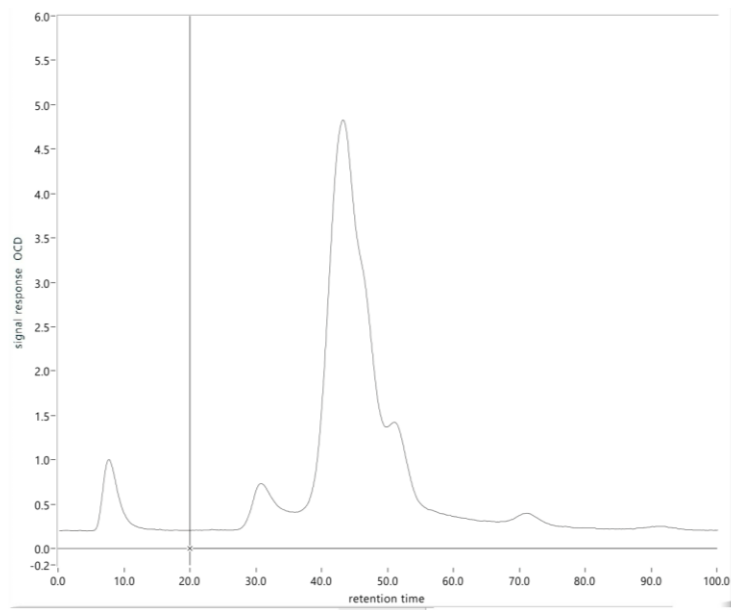


Figure A - 4 LC-OCD Data Jul 1st – F4 PE

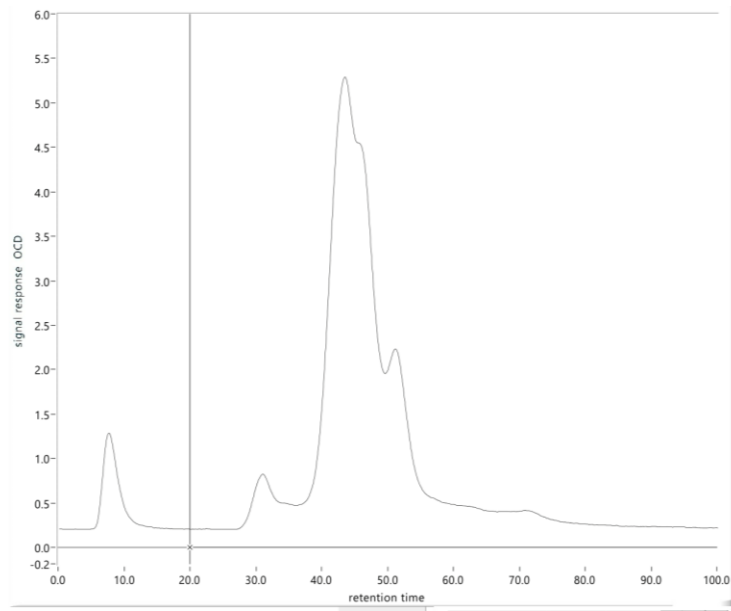


Figure A - 5 LC-OCD Data Jul 1st – INF

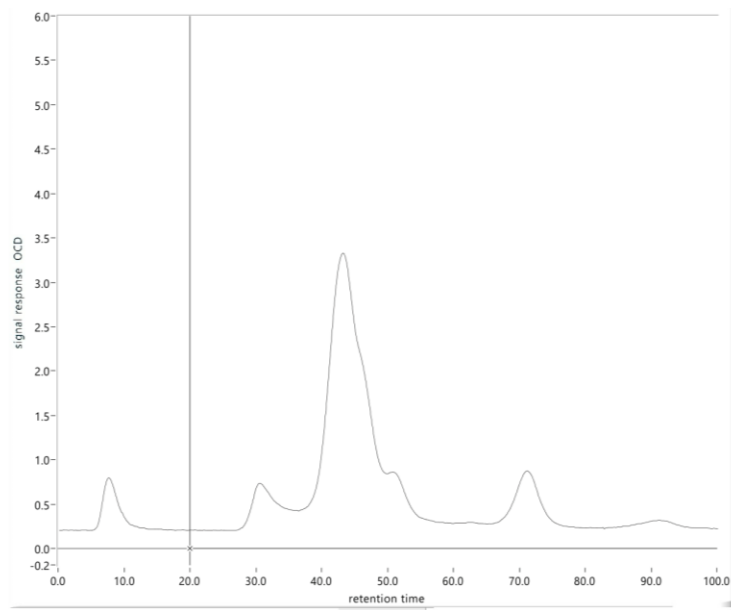


Figure A - 6 LC-OCD Data Jul 10th – F1 PE

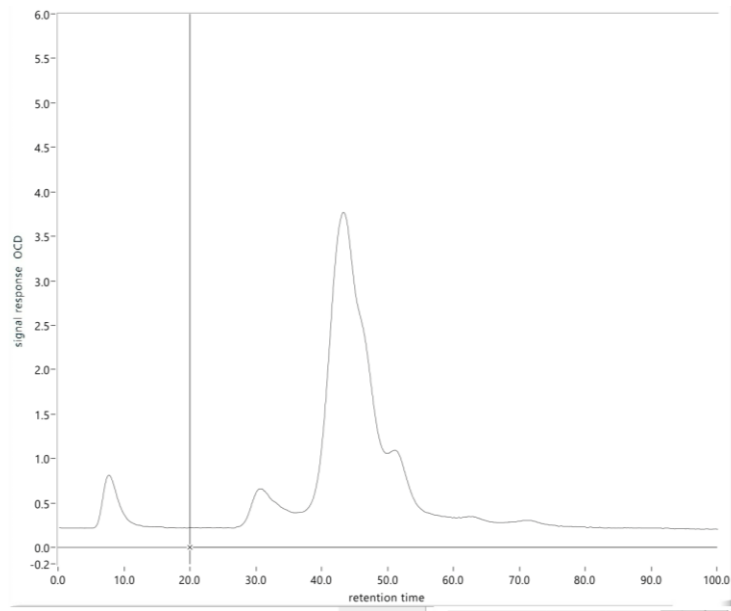


Figure A - 7 LC-OCD Data Jul 10th – F2 PE

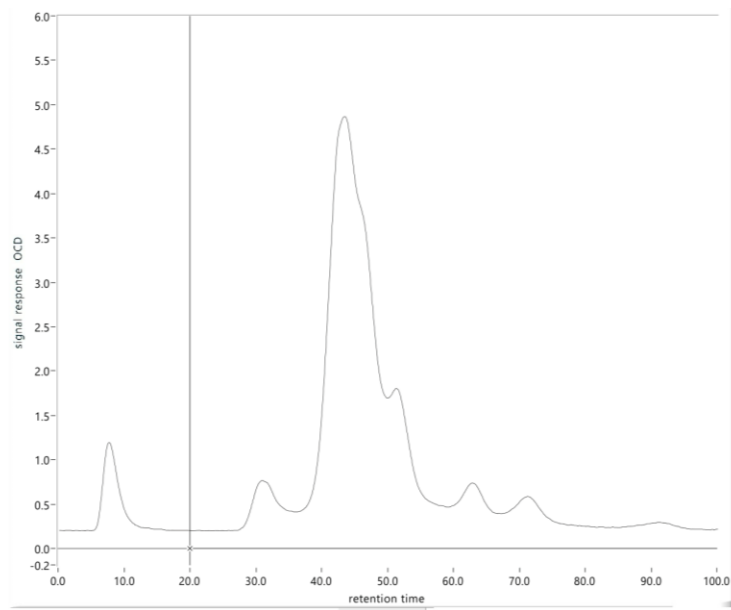


Figure A - 8 LC-OCD Data Jul 10th – F3 PE – Degradation Day 8

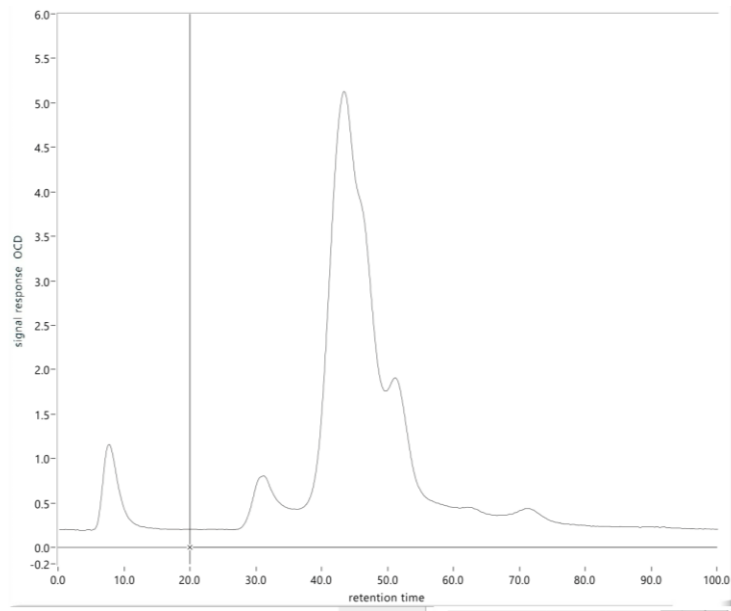


Figure A - 9 LC-OCD Data Jul 10th – F4 PE

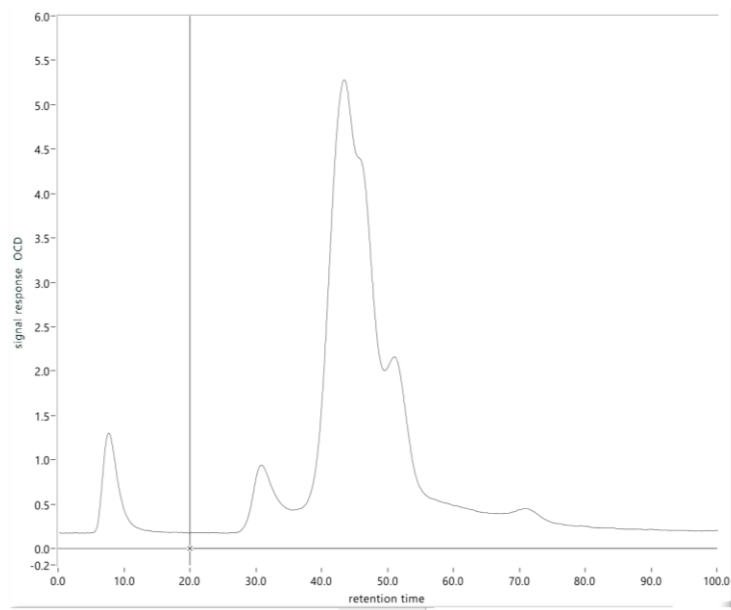


Figure A - 10 LC-OCD Data Jul 12th – INF

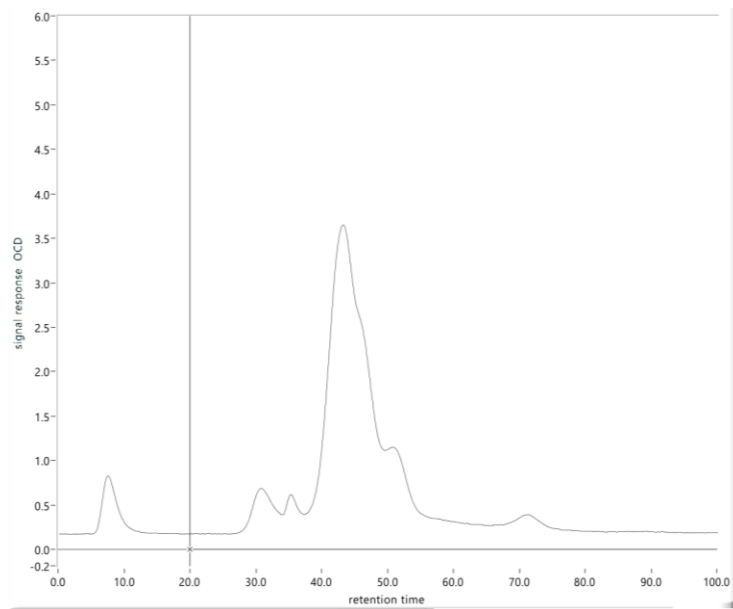


Figure A - 11 LC-OCD Data Jul 12th – F2 PE

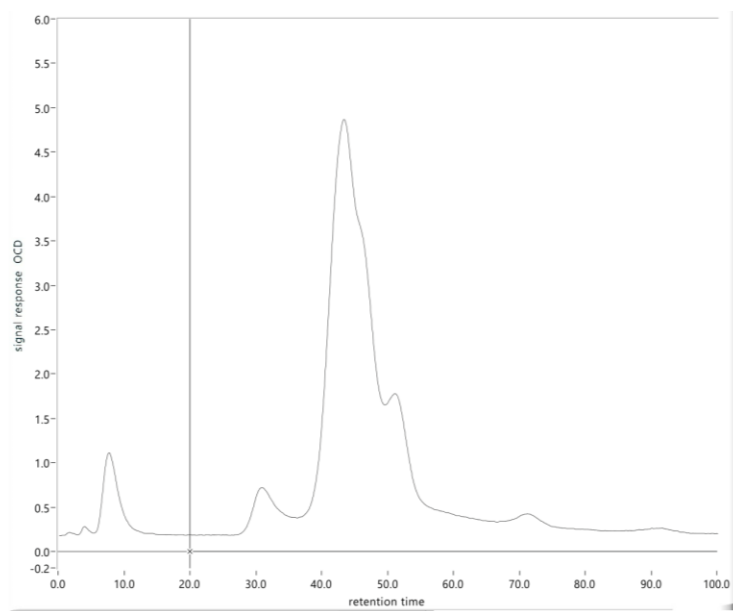


Figure A - 12 LC-OCD Data Jul 12th – F3 PE

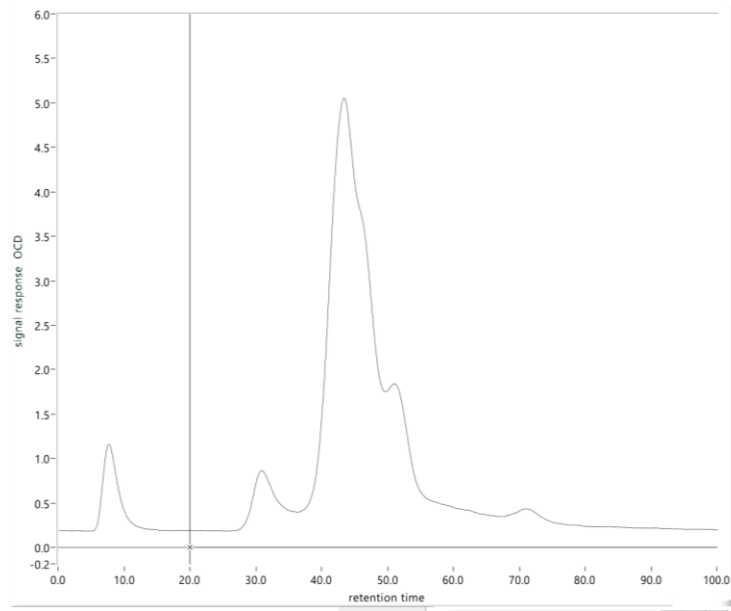


Figure A - 13 LC-OCD Data Jul 12th – F4 PE

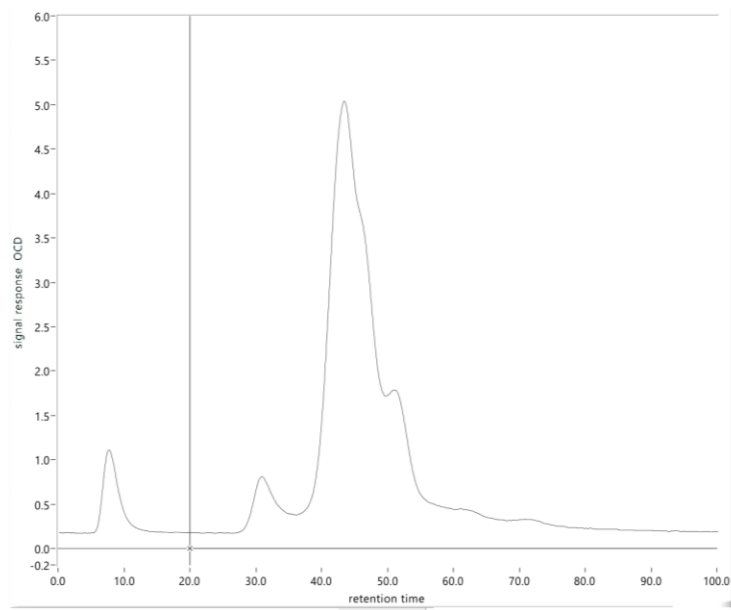


Figure A - 14 LC-OCD Data Jul 12th – F3 PE Degradation Day 16

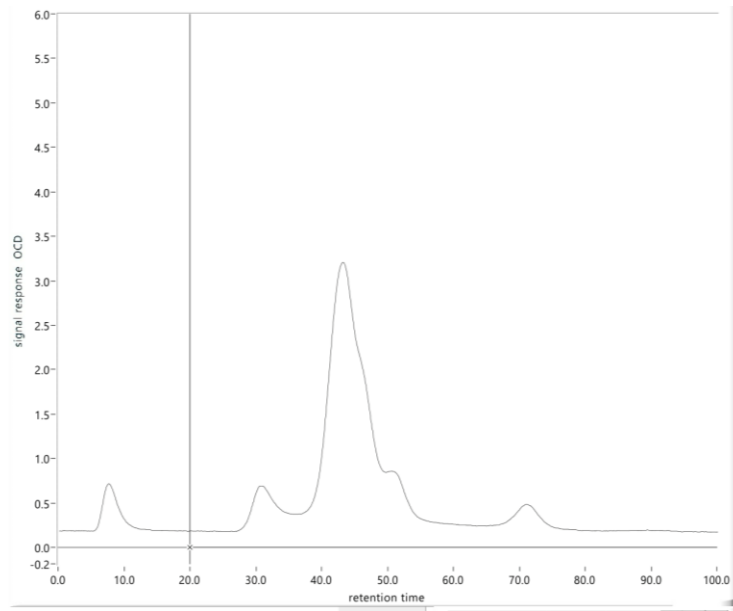


Figure A - 15 LC-OCD Data Jul 12th – F1 PE

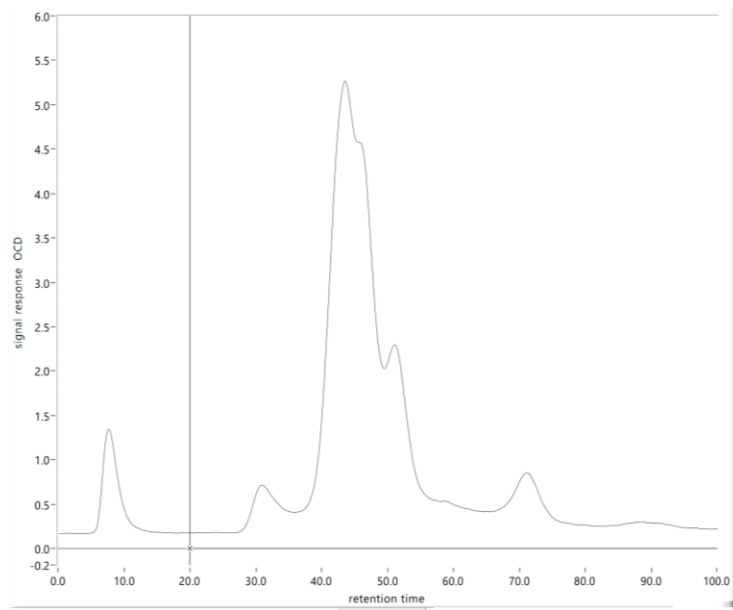


Figure A - 16 LC-OCD Data Jul 18th – INF

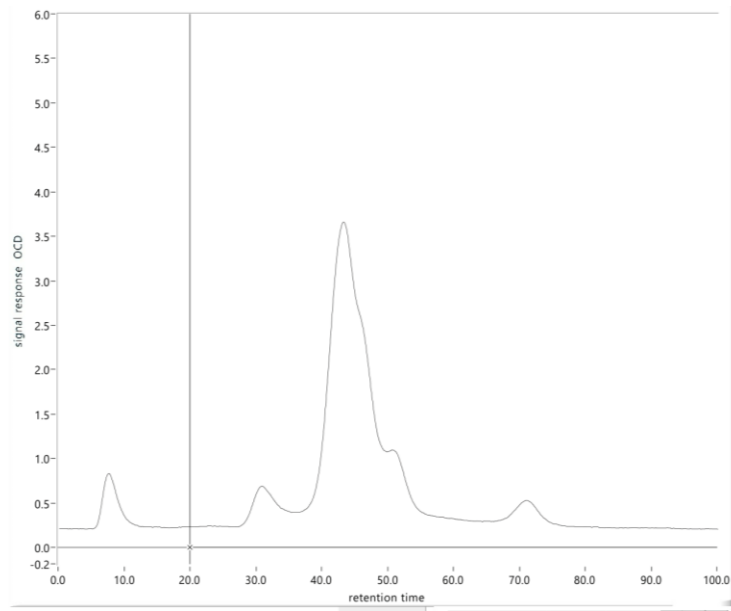


Figure A - 17 LC-OCD Data Jul 18th – F1 PE

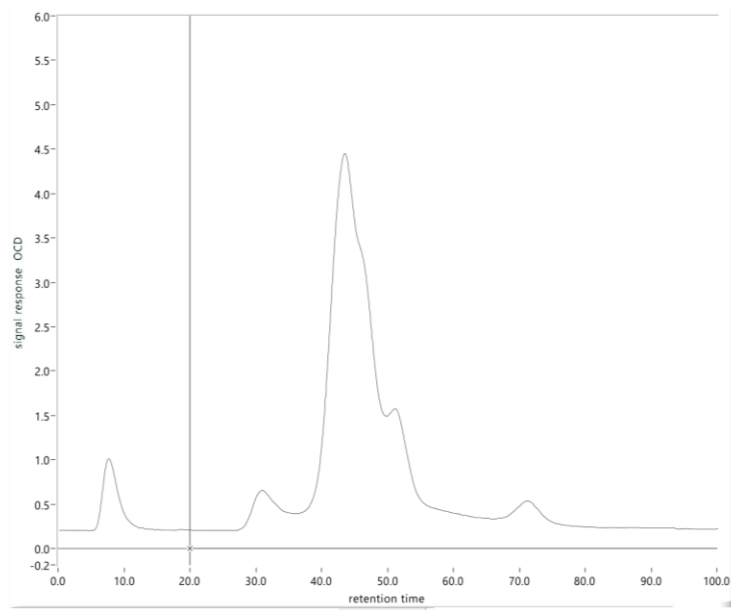


Figure A - 18 LC-OCD Data Jul 18th – F2 PE

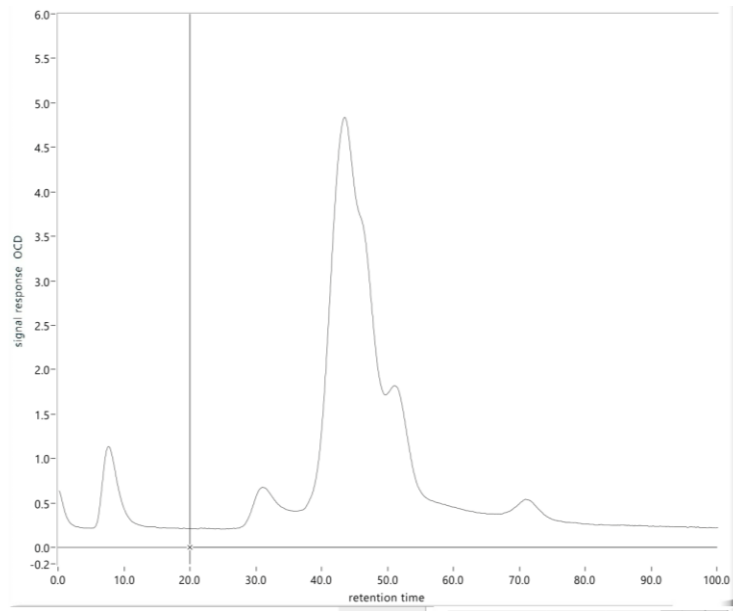


Figure A - 19 LC-OCD Data Jul 18th – F3 PE

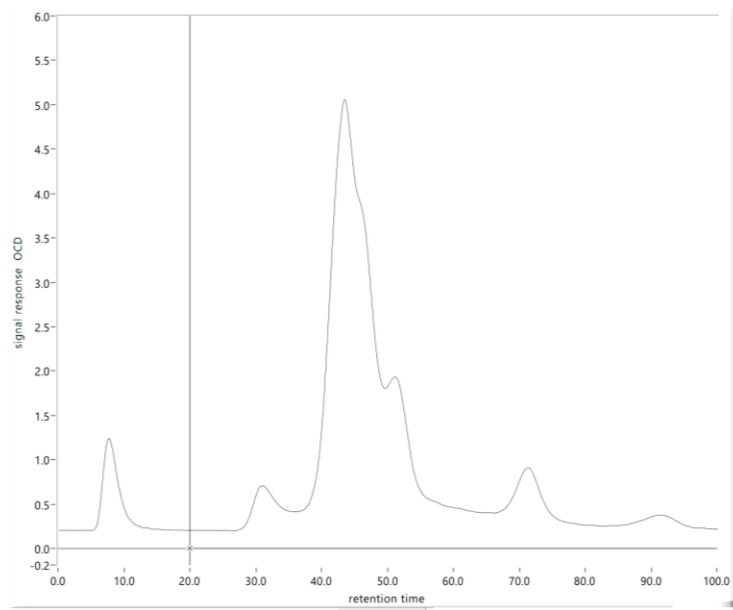


Figure A - 20 LC-OCD Data Jul 18th – F4 PE

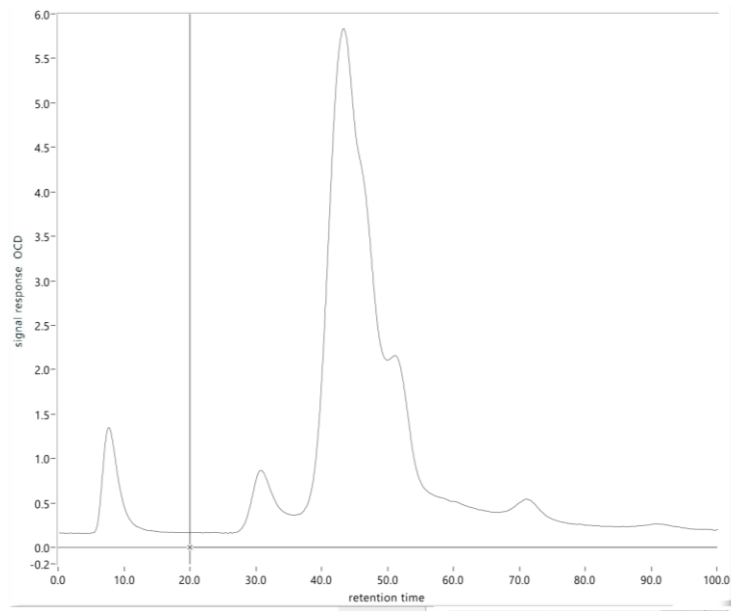


Figure A - 21 LC-OCD Data Jul 20th – INF

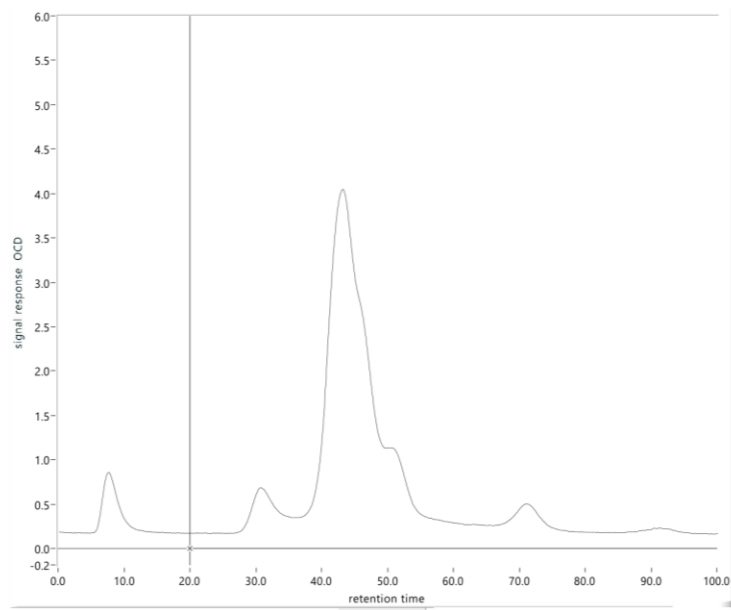


Figure A - 22 LC-OCD Data Jul 20th – F1 PE

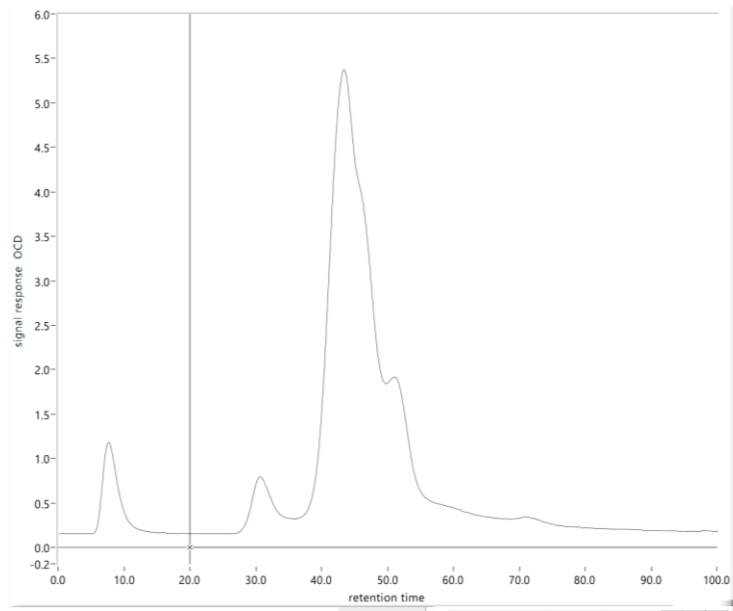


Figure A - 23 LC-OCD Data Jul 20th – F2 PE-2

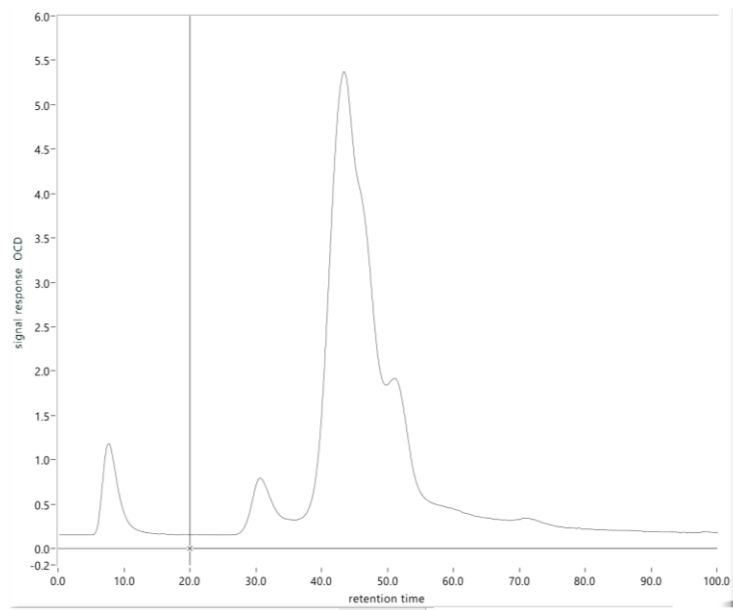


Figure A - 24 LC-OCD Data Jul 20th – F3 PE

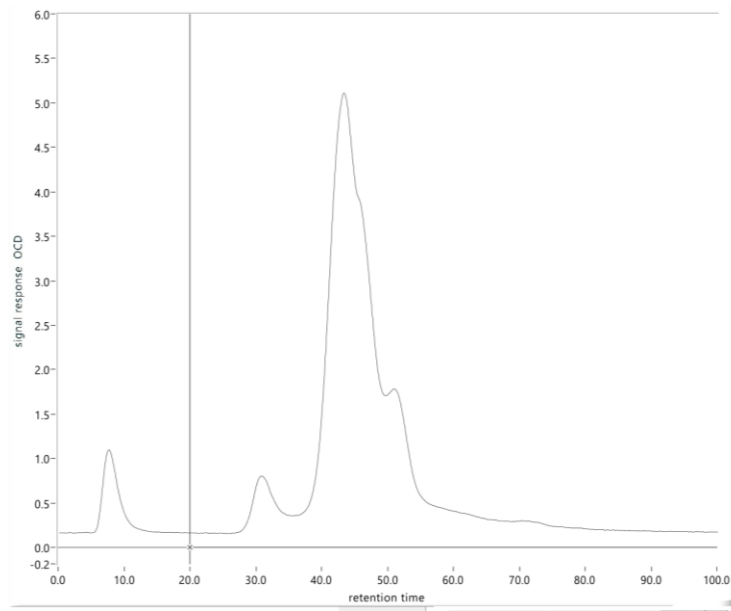


Figure A - 25 LC-OCD Data Jul 20th – F3 PE Degradation Day 20

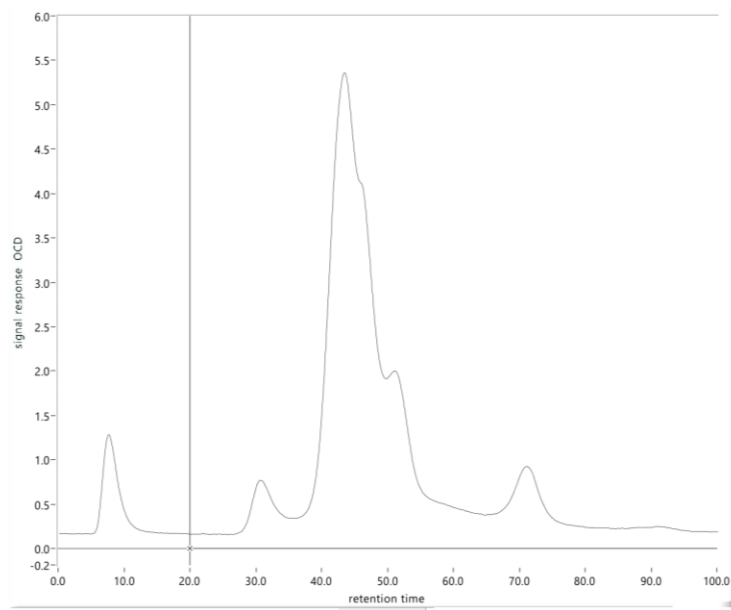


Figure A - 26 LC-OCD Data Jul 20th – F4 PE

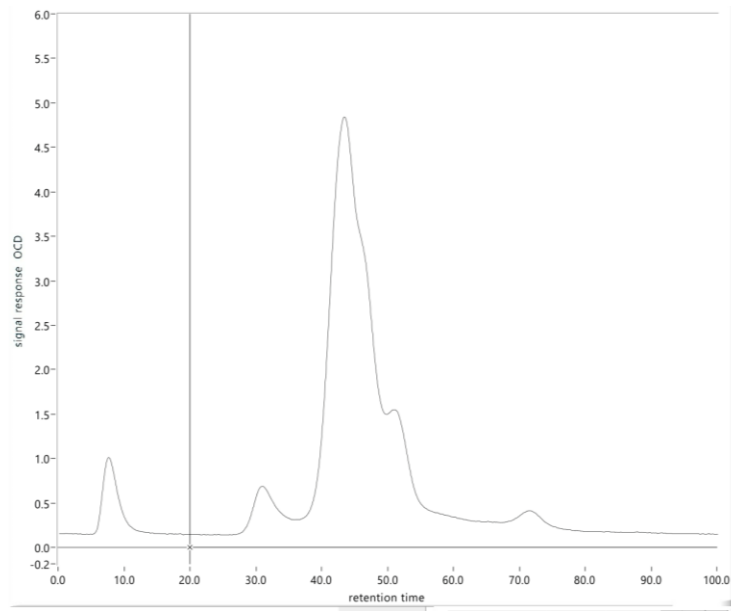


Figure A - 27 LC-OCD Data Jul 20th – F2 PE-2

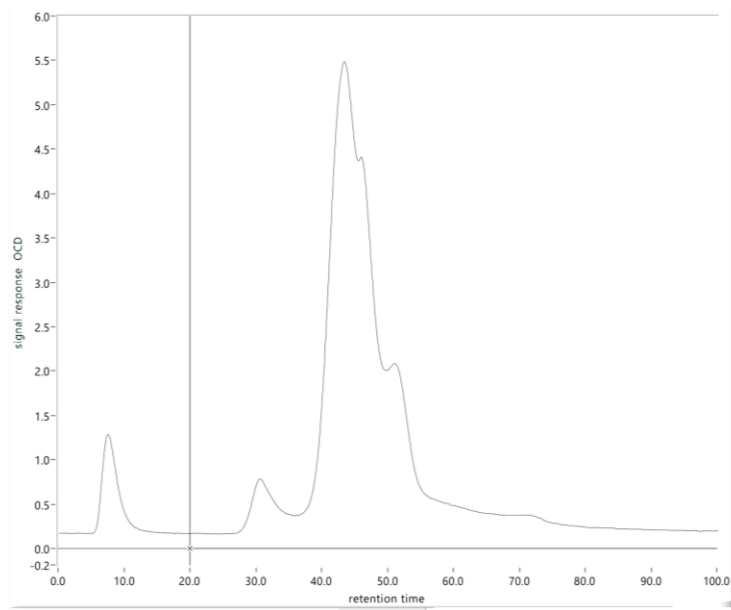


Figure A - 28 LC-OCD Data Jul 27th – INF

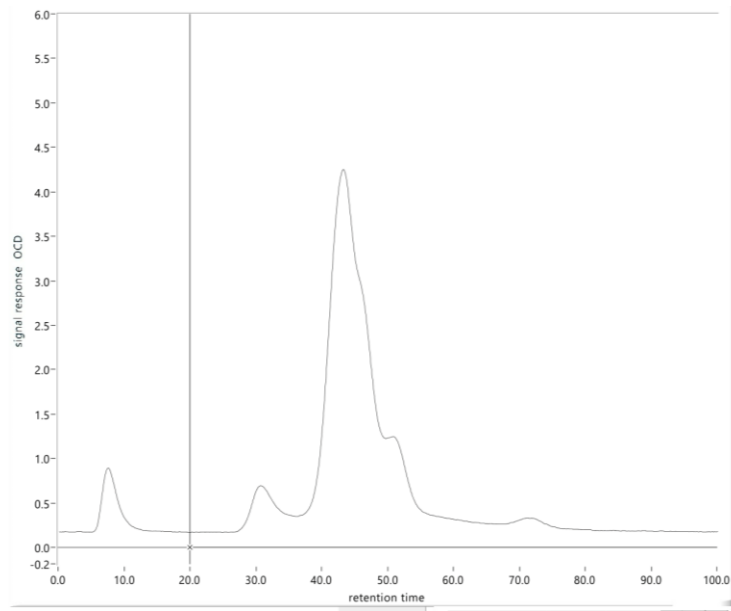


Figure A - 29 LC-OCD Data Jul 27th – F1 PE

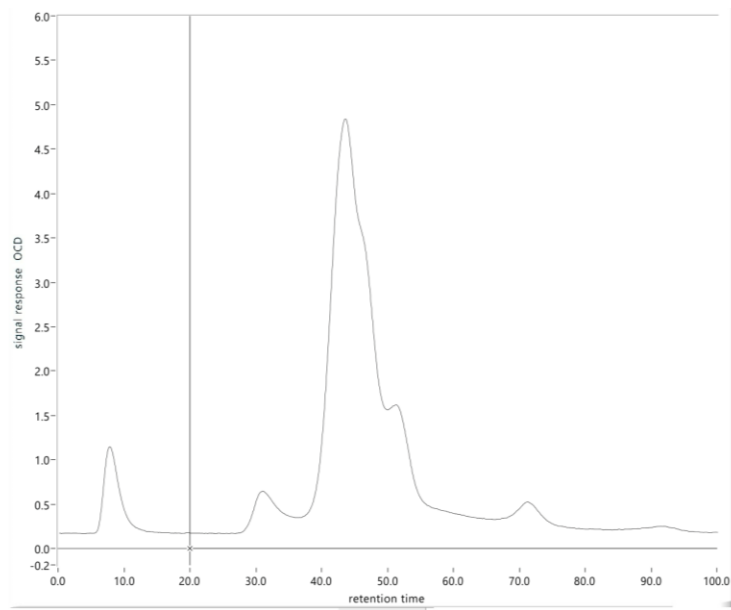


Figure A - 30 LC-OCD Data Jul 27th – F2 PE

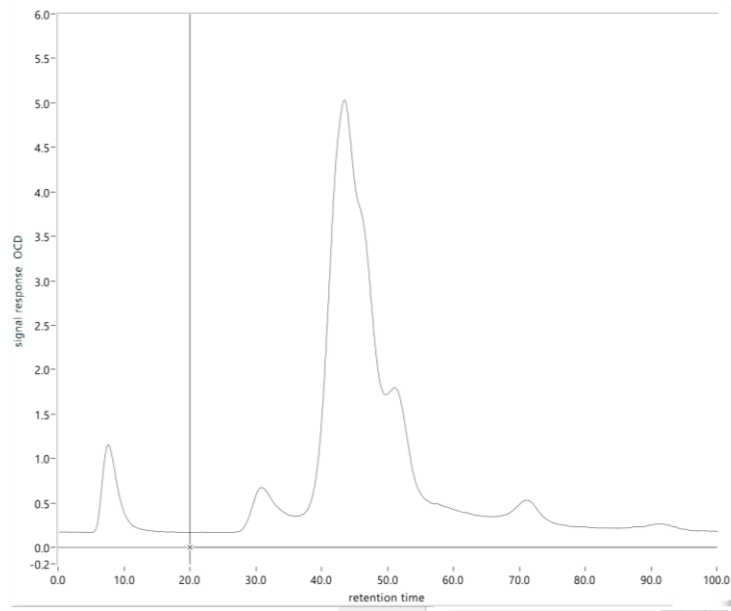


Figure A - 31 LC-OCD Data Jul 27th – F3 PE

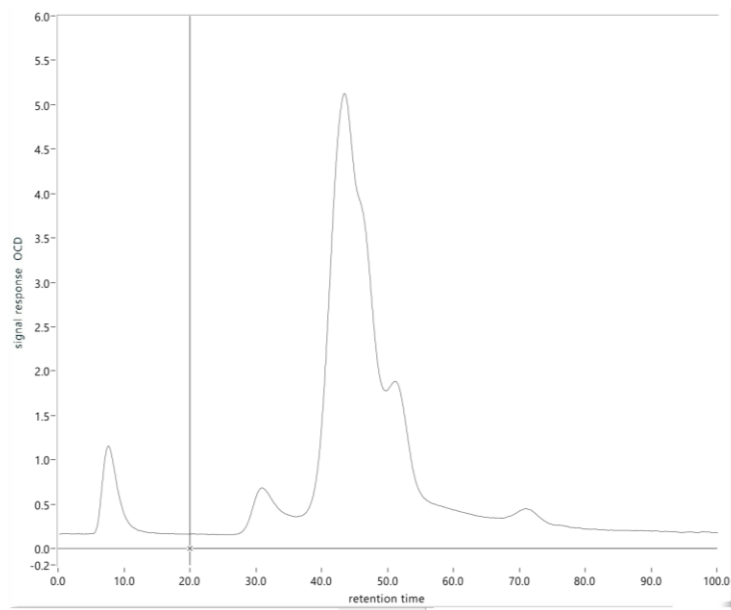


Figure A - 32 LC-OCD Data Jul 27th – F4 PE

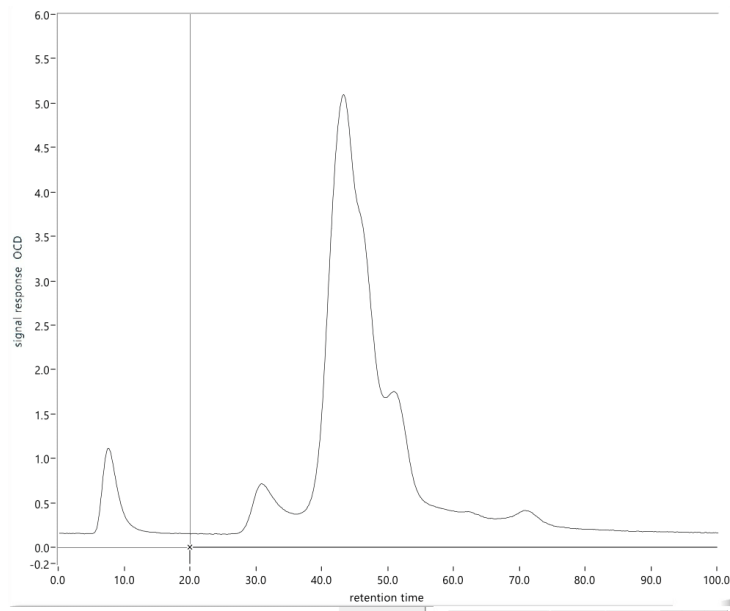


Figure A - 33 LC-OCD Data Jul 27th – F3 PE Degradation Day 25

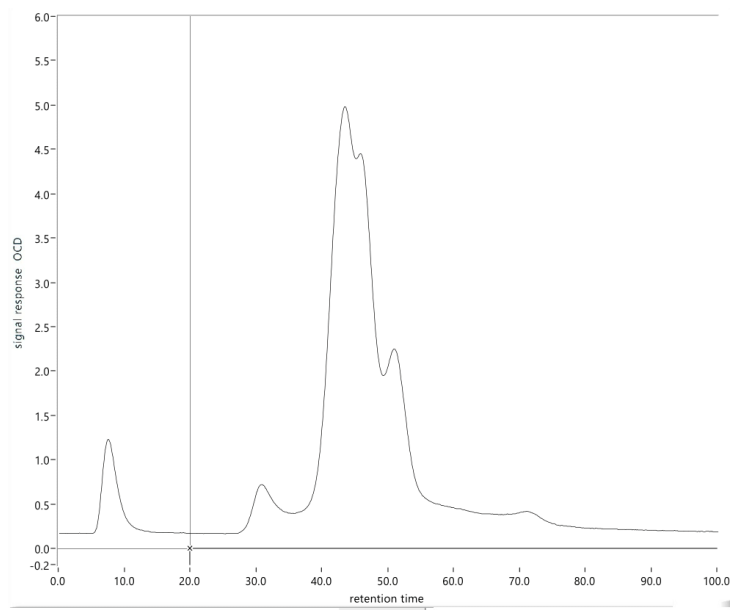


Figure A - 34 LC-OCD Data Aug 2nd – INF

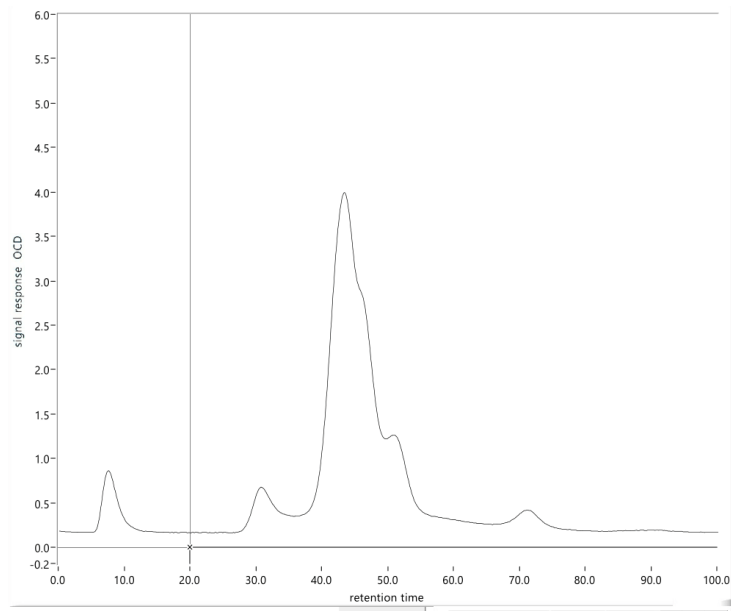


Figure A - 35 LC-OCD Data Aug 2nd – F1 PE

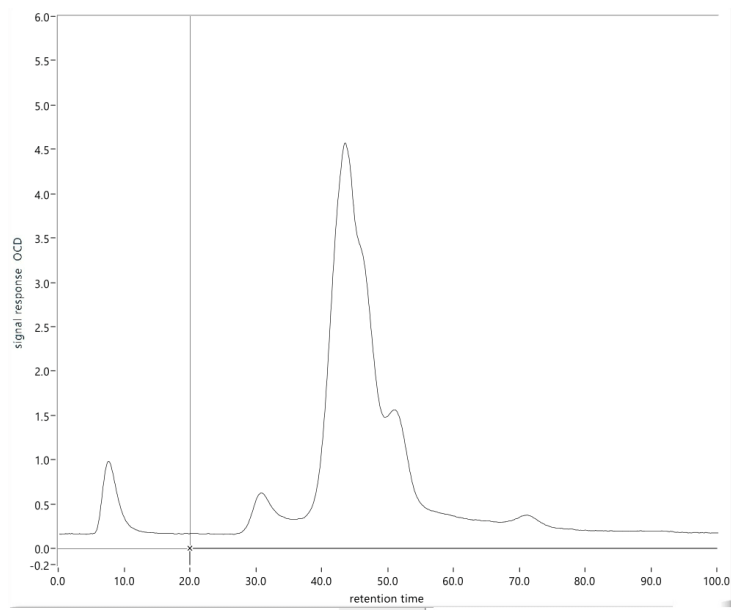


Figure A - 36 LC-OCD Data Aug 2nd – F2 PE

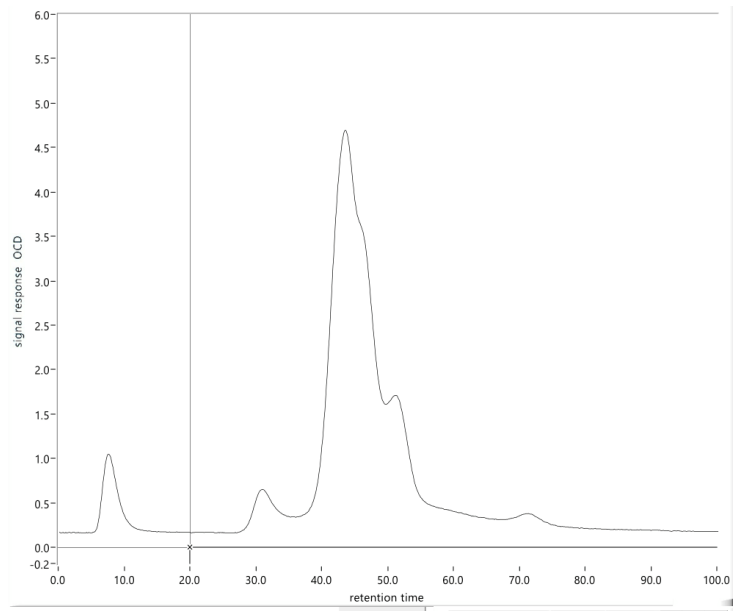


Figure A - 37 LC-OCD Data Aug 2nd – F3 PE

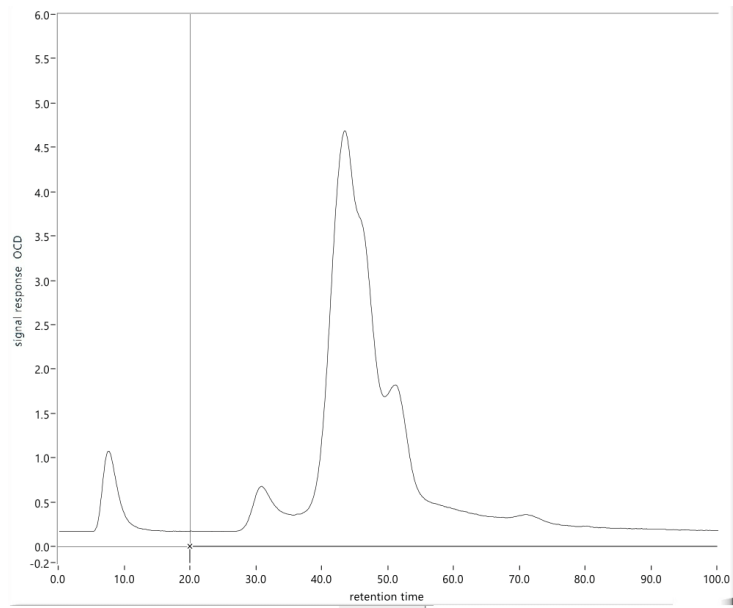


Figure A - 38 LC-OCD Data Aug 2nd – F4 PE

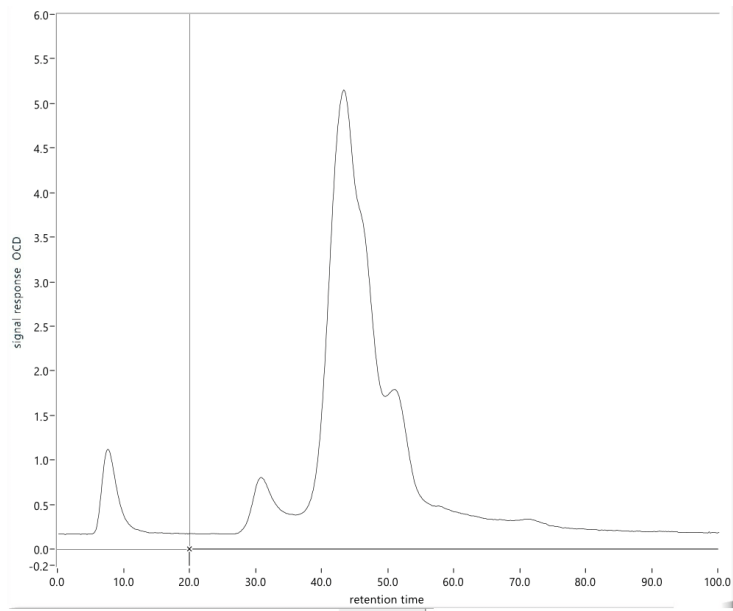


Figure A - 39 LC-OCD Data Aug 2nd – F3 PE Degradation Day 31

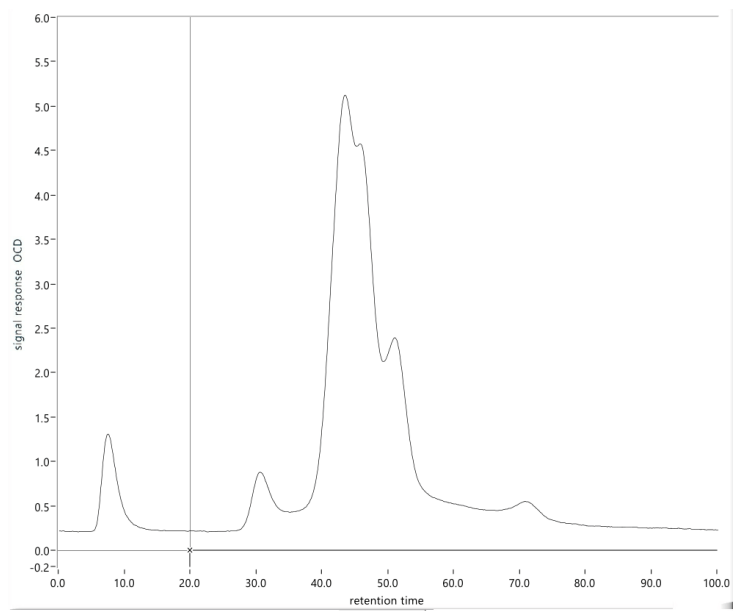


Figure A - 40 LC-OCD Data Aug 14th – INF

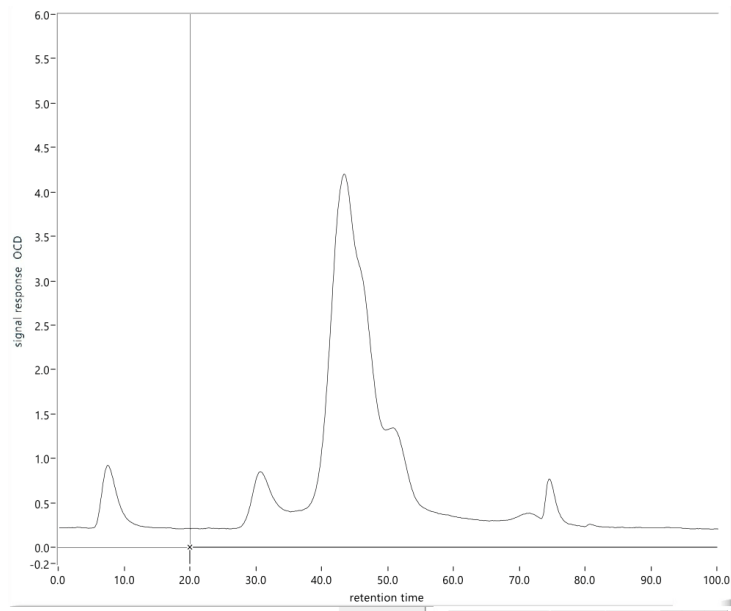


Figure A - 41 LC-OCD Data Aug 14th – F1 PE

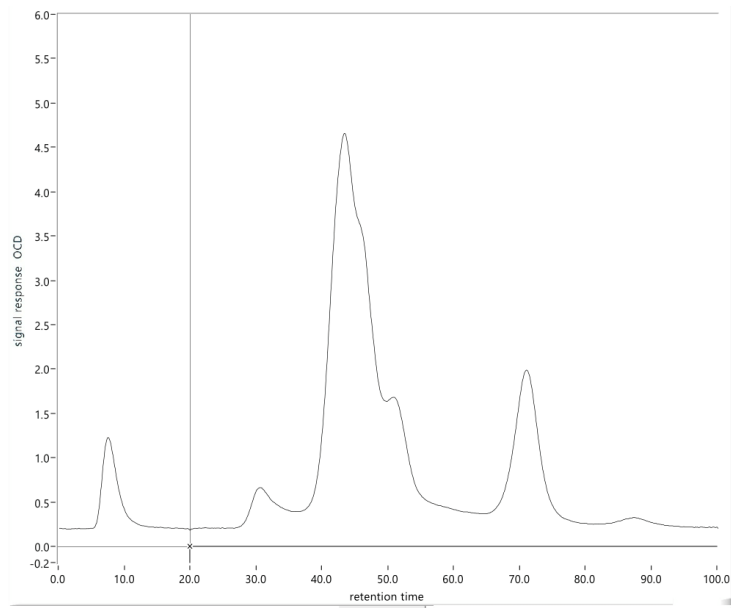


Figure A - 42 LC-OCD Data Aug 14th – F2 PE

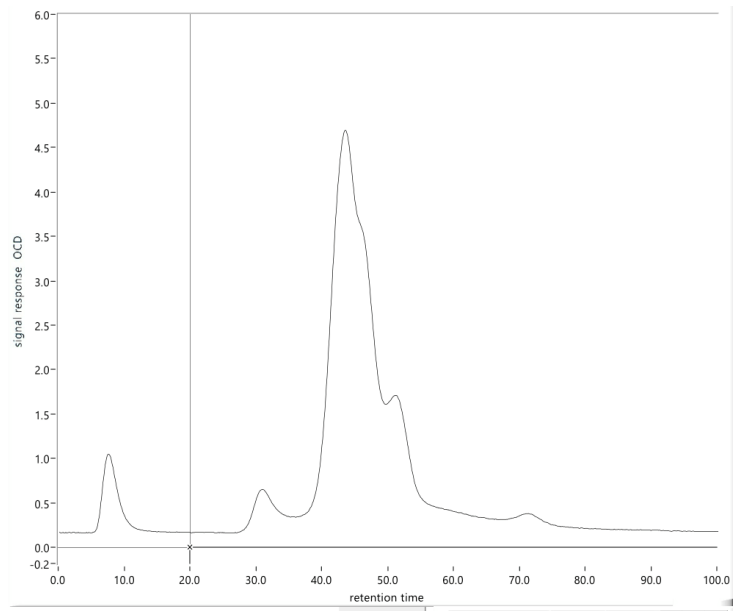


Figure A - 43 LC-OCD Data Aug 14th – F3 PE

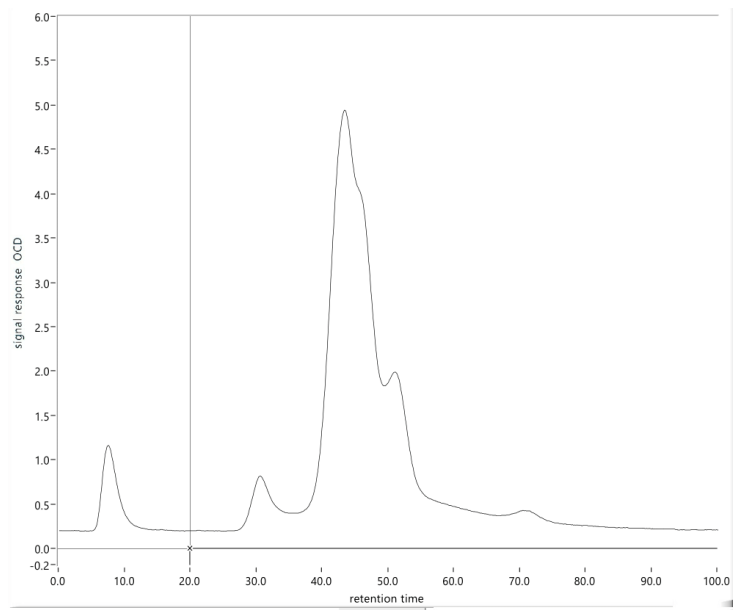


Figure A - 44 LC-OCD Data Aug 14th – F4 PE

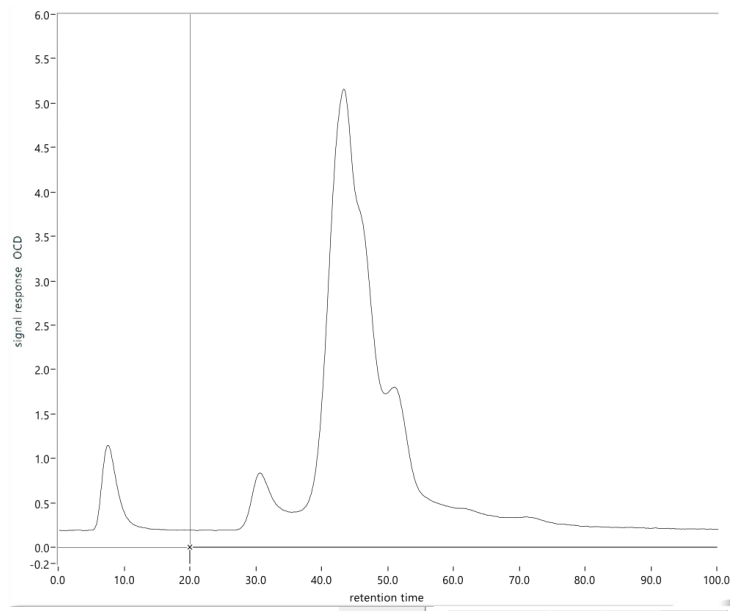


Figure A - 45 LC-OCD Data Aug 14th – F3 PE Degradation Day 44

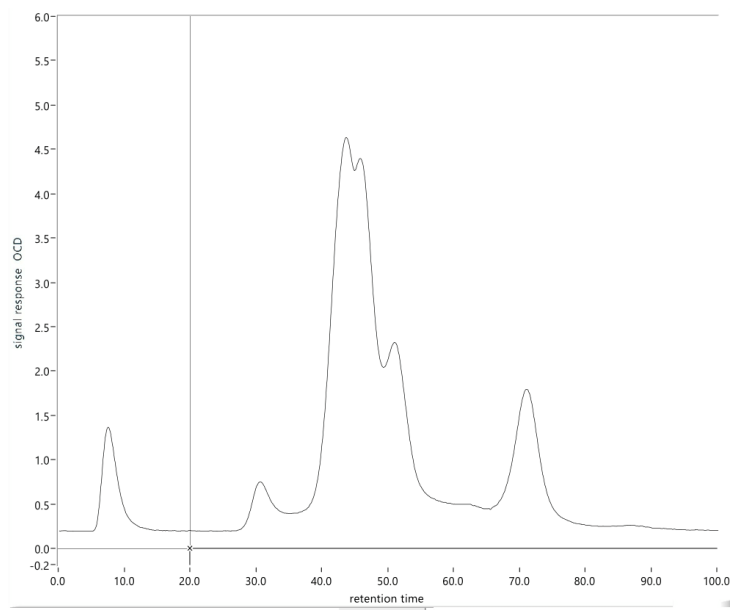


Figure A - 46 LC-OCD Data Aug 21st – INF

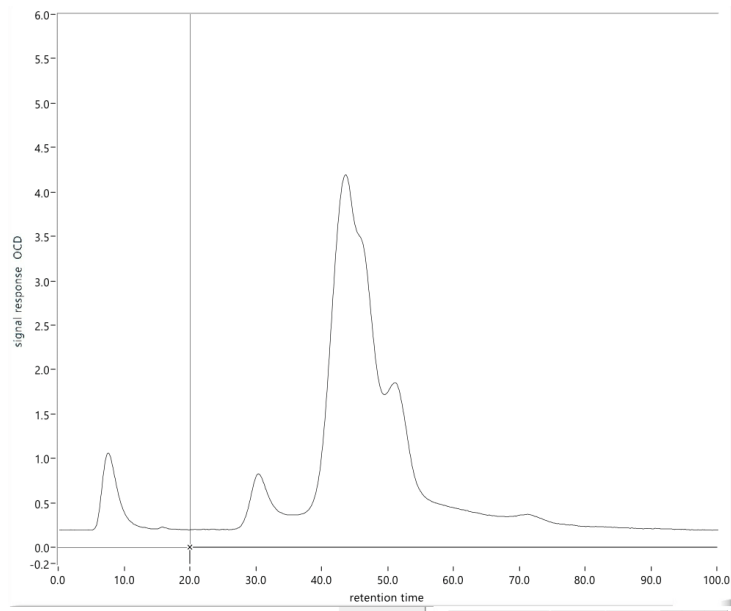


Figure A - 47 LC-OCD Data Aug 21st – F1 PE

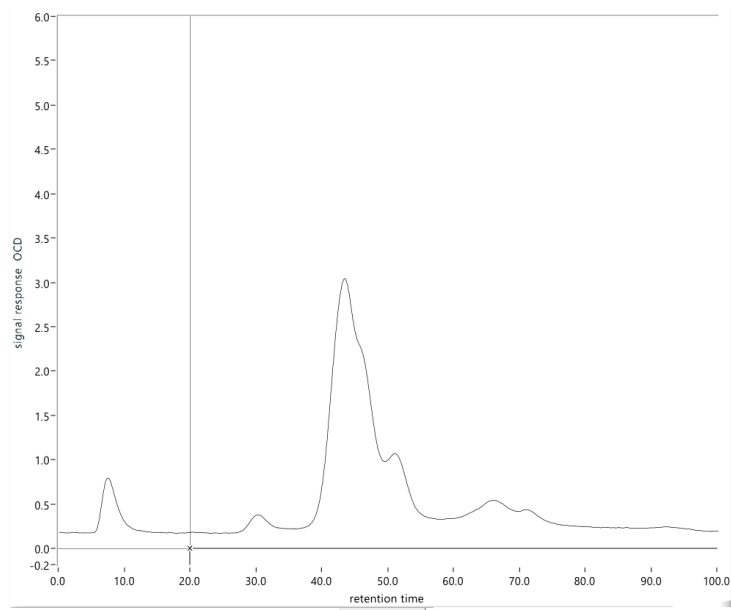


Figure A - 48 LC-OCD Data Aug 21st – F2 PE

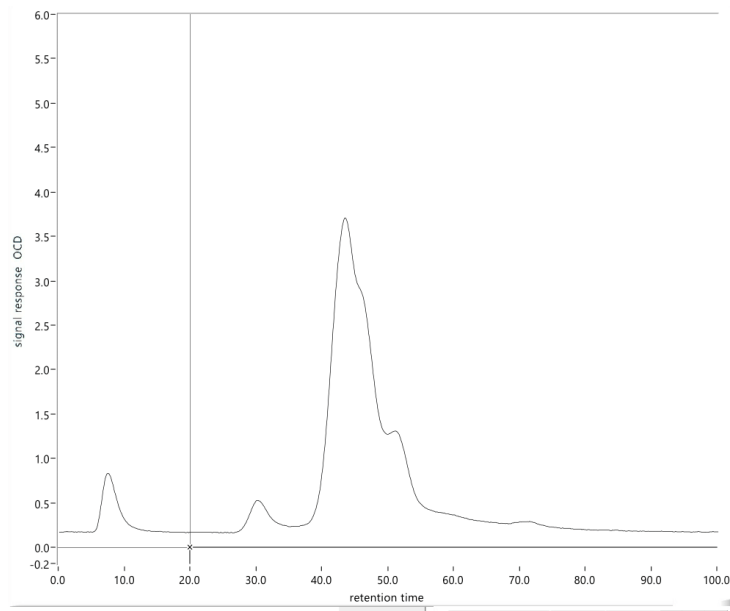


Figure A - 49 LC-OCD Data Aug 21st – F3 PE

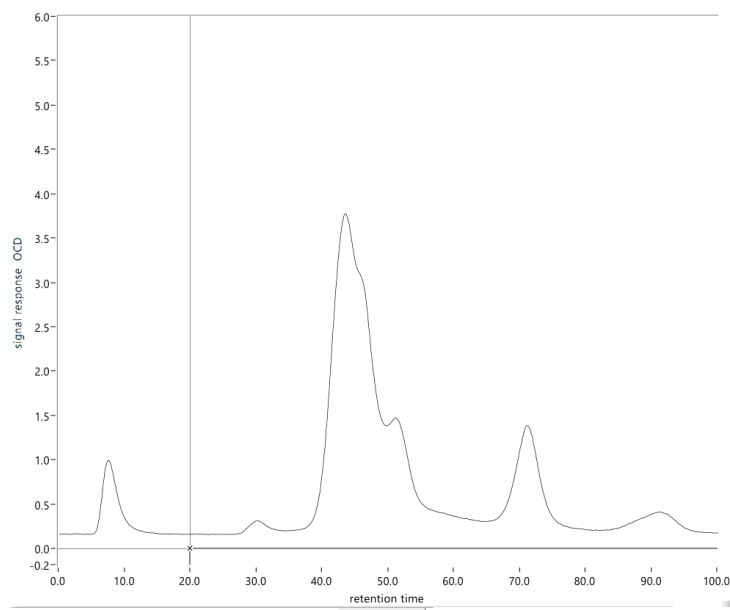


Figure A - 50 LC-OCD Data Aug 21st – F4 PE

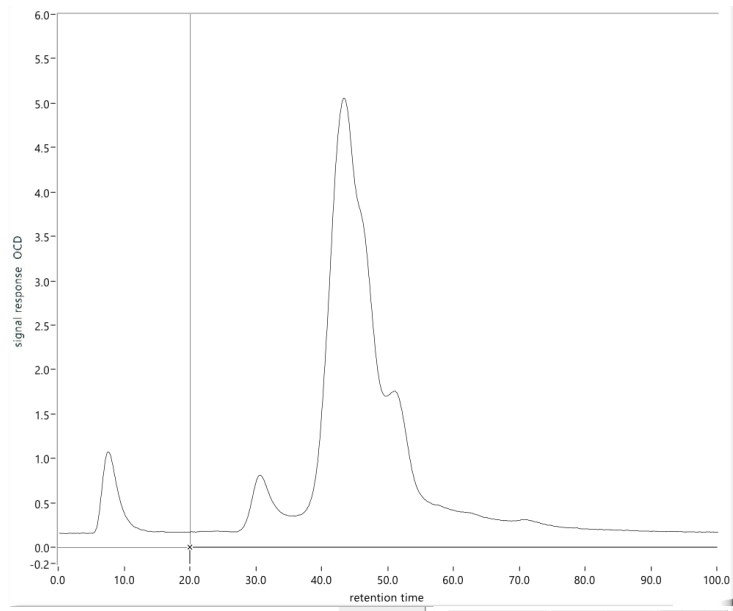


Figure A - 51 LC-OCD Data Aug 21st – F3 PE Degradation Day 52

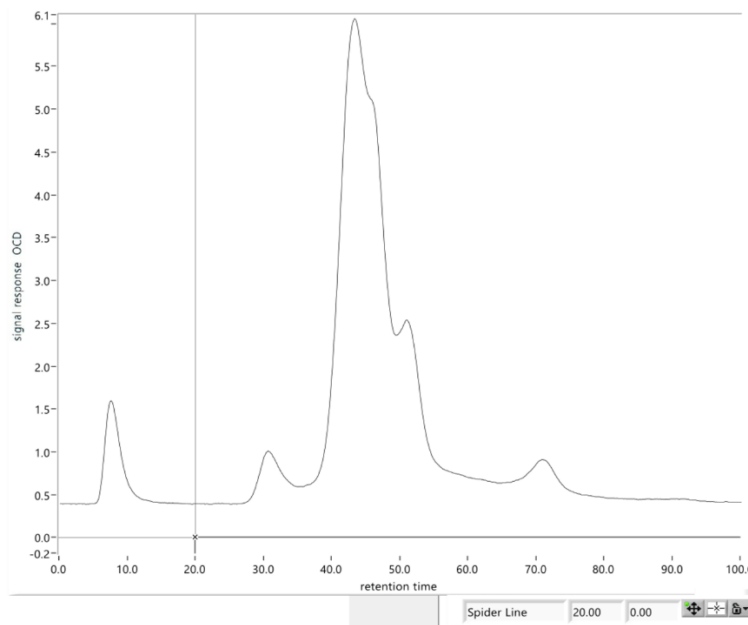


Figure A - 52 LC-OCD Data Sept 2nd – INF

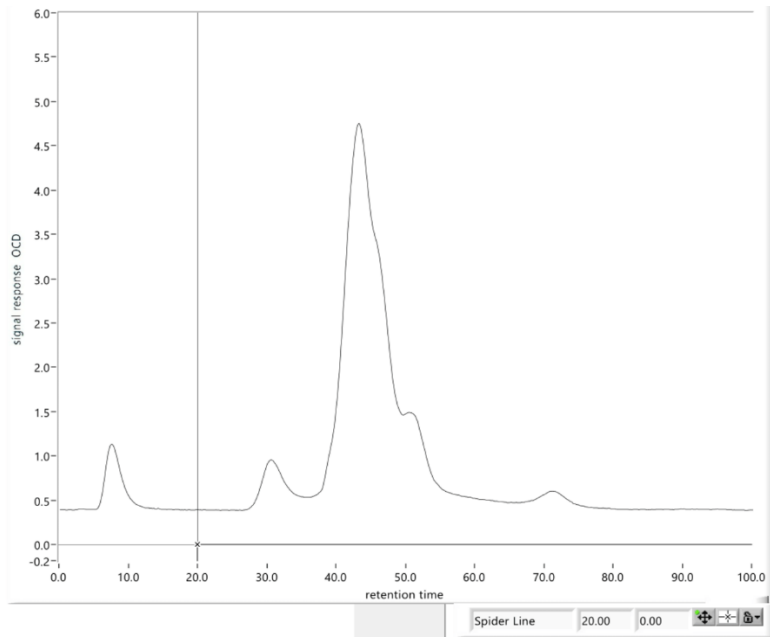


Figure A - 53 LC-OCD Data Sept 2nd – F1 PE

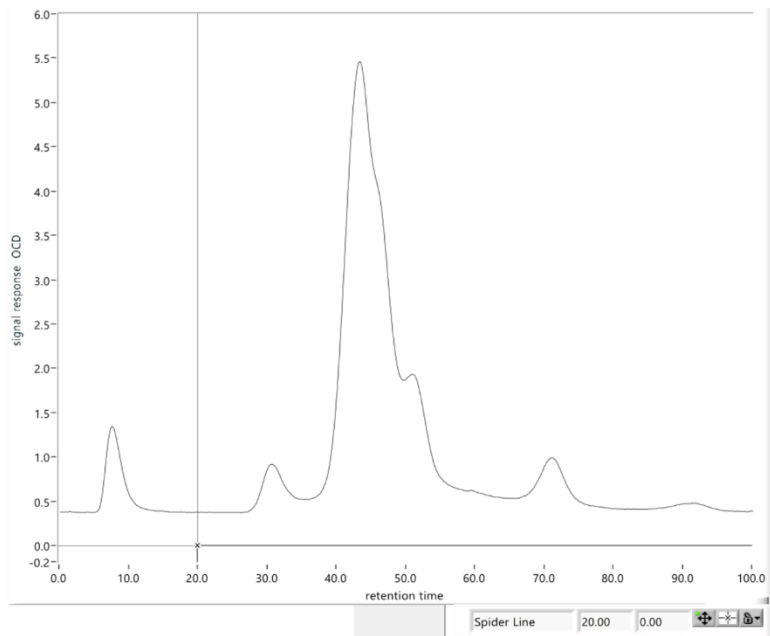


Figure A - 54 LC-OCD Data Sept 2nd – F2 PE

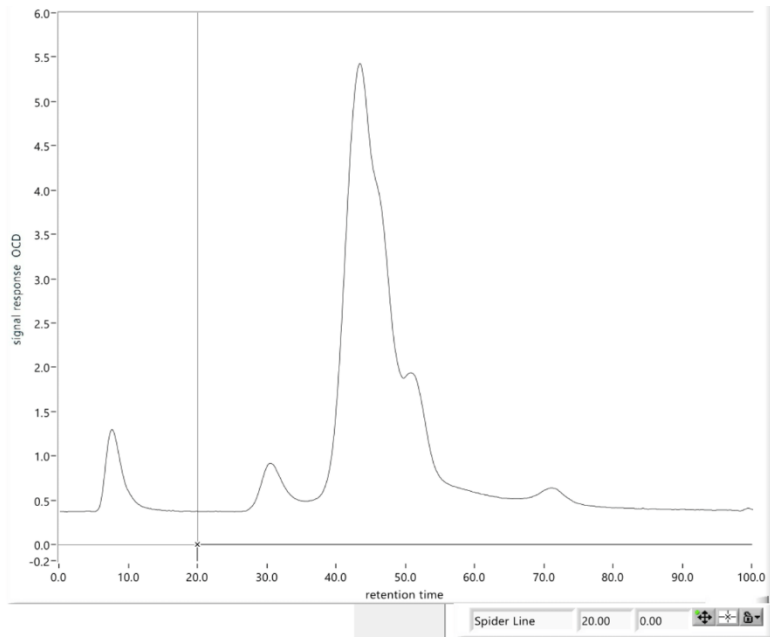


Figure A - 55 LC-OCD Data Sept 2nd – F3 PE

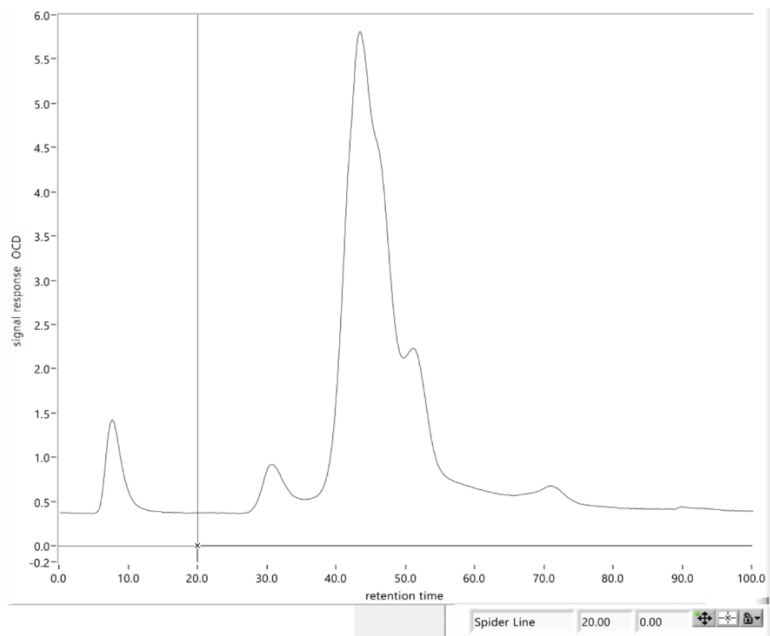


Figure A - 56 LC-OCD Data Sept 2nd – F4 PE

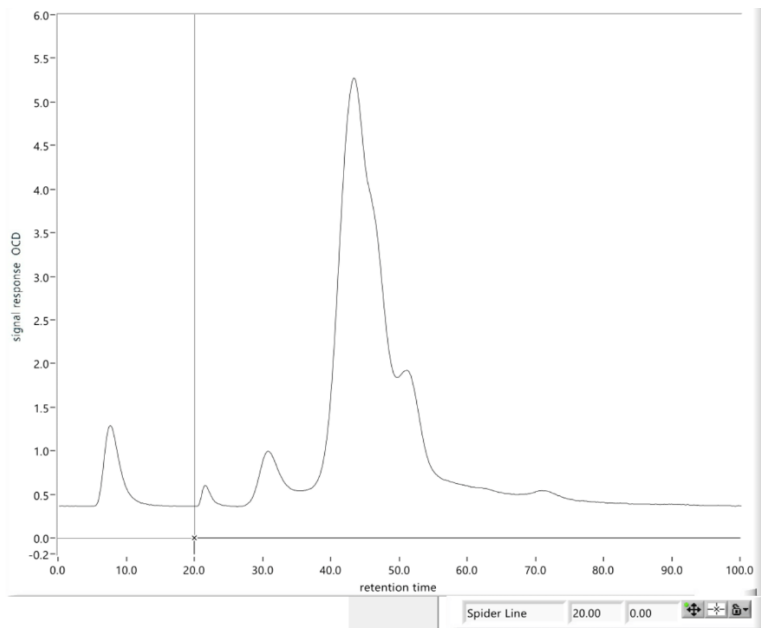


Figure A - 57 LC-OCD Data Sept 2nd – F3 PE Degradation Day 78

Microbiological Data – ATP Concentration

Table A - 19: ng ATP per g of dry media for Filter 1

DATE	PORT 2	PORT 3	PORT 4	PORT 5
04-JUN-18	4	0	0	0
11-JUN-18	3	2	2	3
20-JUN-18 ¹	52	51	52	NR
27-JUN-18 ¹	81	76	76	78
06-JUL-18 ¹	47	49	49	49
12-JUL-18	71	58	34	42
23-JUL-18	96	111	85	120
31-JUL-18	131	93	104	106
10-AUG-18	153	124	121	107
26-AUG-18	82	79	88	96
05-SEP-18	108	94	74	74

* Measured in ng atp per gram of dry media

1 - Samples corrected for impact of GAC adsorption (see Appendix B)

NR – Could not collect data

Table A - 20: ATP per media for Filter 2

DATE	PORT 2	PORT 3	PORT 4	PORT 5
04-JUN-18	4	90	62	16
11-JUN-18	95	72	82	41
20-JUN-18 ¹	114	104	96	86
27-JUN-18 ¹	121	120	126	116
06-JUL-18 ¹	69	70	71	NR
12-JUL-18	83	76	81	67
23-JUL-18	208	174	153	137
31-JUL-18	230	126	183	128
10-AUG-18	192	170	164	129
26-AUG-18	157	146	157	119
05-SEP-18	166	162	146	NR

* MEASURED IN NG ATP PER GRAM OF DRY MEDIA

1 - samples corrected for impact of GAC adsorption (see Appendix B)

NR – Could not collect data

Table A - 21: ATP per media for Filter 3

DATE	PORT 2	PORT 3	PORT 4	PORT 5
04-JUN-18	153	172	214	150
11-JUN-18	142	163	162	75
20-JUN-18 ¹	142	137	133	125
27-JUN-18 ¹	138	135	132	127
06-JUL-18 ¹	71	71	72	71
12-JUL-18	142	116	101	102
23-JUL-18	201	135	83	67
31-JUL-18	220	210	172	136
10-AUG-18	202	181	211	153
26-AUG-18	189	145	173	150
05-SEP-18	186	179	146	173

* Measured in ng ATP per gram of dry media
 1. Samples corrected for impact of GAC adsorption (see Appendix B)
 NR – Could not collect data

Table A - 22: ATP per media for Filter 4

DATE	PORT 2	PORT 3	PORT 4	PORT 5
04-JUN-18	112	7	1	NR
11-JUN-18	83	45	26	21
20-JUN-18 ¹	80	68	54	62
27-JUN-18 ¹	157	122	100	98
06-JUL-18 ¹	50	17	NR	NR
12-JUL-18	154	NR	73	60
23-JUL-18	201	135	83	67
31-JUL-18	166	104	73	50
10-AUG-18	182	125	133	111
26-AUG-18	180	121	112	79
05-SEP-18	191	138	139	116

* Measured in ng ATP per gram of dry media
 1. Samples corrected for impact of GAC adsorption (see Appendix B)
 NR – Could not collect data

Appendix B – Calculations and Error Determination

Backwashing – Estimating Sub-fluidization Velocity

Extensive backwash studies (Amirtharajah et al., 1991) have been conducted to optimize collapsed-air pulse washing for biological filters. This includes altering the hydraulic loading rate to varying fractions of the media's minimal fluidization velocity (V_{mf}). It has been found that, even with different air flowrates, a fraction of 40% (V/V_{mf}) was the most optimal in terms of turbidity remaining at the end of the backwash (Figure A - 58).

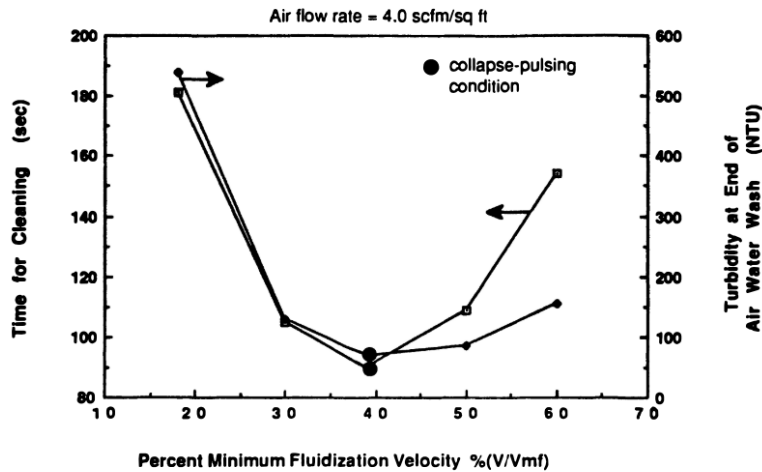


Figure A - 58: Time of backwashing versus fluidization velocity (Amirtharajah, 1993)

For the experiments conducted herein V_{mf} was calculated for each filter media depth, and then reduced to 40% of that value for the hydraulic loading rate. The following equations show how V_{mf} was obtained from the media properties.

$$(1) \quad V_{mf}(\text{for Filters 1, 2, 3 and 5}) = V_{mf-sand} \left[\frac{V_{mf-GAC}}{V_{mf-sand}} \right]^{X_{GAC} 1.69}$$

$$(2) \quad V_{mf}(\text{for Filter 4}) = V_{mf-sand} \left[\frac{V_{mf-Anthracite}}{V_{mf-sand}} \right]^{X_{Anthracite} 1.69}$$

$$(3) \quad X_{GAC} = \frac{\text{Mass of GAC in Filter}}{\text{Total mass of Filter Media}}$$

$$(4) \quad X_{Anthracite} = \frac{\text{Mass of Anthracite in Filter}}{\text{Total mass of Filter Media}}$$

$$(5) \quad V_{mf} = \frac{R_{mf} \mu}{d_{90} \rho}$$

$$(6) \quad R_{mf} = \sqrt{33.7^2 + 0.0408Ga} - 33.7$$

$$(7) \quad Ga = \frac{d_{90}^3 \rho_w (\rho_s - \rho_w) g}{\mu^2}$$

Table A - 23: Physical Media Properties

<u>Assumed Values</u>	<u>Units</u>	<u>Value</u>
Particle density for all types of GAC	kg/m ³	1350
Particle density for anthracite	kg/m ³	1600
Particle density for sand	kg/m ³	2650
Uniformity Coefficient for all media	-	1.4
Porosity for GAC and Anthracite	-	0.5
Porosity for Sand	-	0.42
d10 for GAC	mm	1.4
d10 for Anthracite	mm	1.4
d10 for Sand	mm	0.48
Water Density	kg/m ³	998.2
Dynamic Viscosity	kg/m.s	0.001002

From equations 1 to 7, the following backwash values were calculated:

Table A - 24: Hydraulic loading rates during low-rate wash (calculated)

	Filter 1	Filter 2	Filter 3	Filter 4
Hydraulic Loading Rate (m/h)	11.0	11.0	11.0	13.0

These were eventually amended to the values in Table A - 25, as the values in Table A - 24 did not adequately mix the media.

Table A - 25: Hydraulic loading rates for air-scour during low-rate wash (from operating filters)

	Filter 1	Filter 2	Filter 3	Filter 4
Hydraulic Loading Rate (m/h)	12.4	12.4	12.4	14.3

Data – Error Evaluation

ATP – Necessary Laboratory Adjustment

The ATP concentration per GAC samples collected on June 20th, June 27th, and July 6th, 2018 were prone to systematic error due to the GAC's adsorptive properties. The ATP concentrations were analysed as instructed by the LuminUltra Deposit & Surface Analysis Kit (LuminUltra Technologies Ltd., Fredericton, New Brunswick, Canada), where one gram of media was submerged in an UltraLyse solution that lyses the cells attached to the media and releases the ATP. This lyse solution is extracted, diluted, and analysed in subsequent steps.

For a typical non-adsorptive solid media sample such as anthracite or sand, it is acceptable to leave the sample in the UltraLyse solution at 4°C for up to one week before proceeding with the next steps, as the ATP concentration is stable at this stage in the analysis. However, solid media samples that are adsorptive are problematic. It was observed that the ATP was adsorbed back onto the solid surface of the sample while the lyse is being stored, effectively lowering the concentration of ATP in the supernatant part of the UltraLyse tube, skewing the results.

On June 20th, June 27th, and July 6th, 2018, samples were left in lyse solution for 1 to 3 days. To recover lost data for those three sampling rounds, an ATP degradation curve was re-created (Figure A - 59). First, media samples were extracted from Port 3 of all the filters. Then the samples were each divided into 6 portions, placed in 6 separate lyse tubes, submerged, and shaken as per the manufacturer instructions. The different lyse tubes were then analysed for their ATP concentration after being stored at varying time intervals – 15 minutes, 45 minutes, 120 minutes, 12 hours, 36 hours, and 72 hours. By plotting the ATP concentration against the time that the Lyse tubes were stored, it was possible to re-create the effect of GAC adsorption on the final ATP results.

A control was made by submerging GAC into a lyse tube, then, immediately after the ATP would have been released, the lyse solution was removed from the GAC. This lyse was then measured at varying time intervals, while it was stored in a way so that GAC did not influence the results.

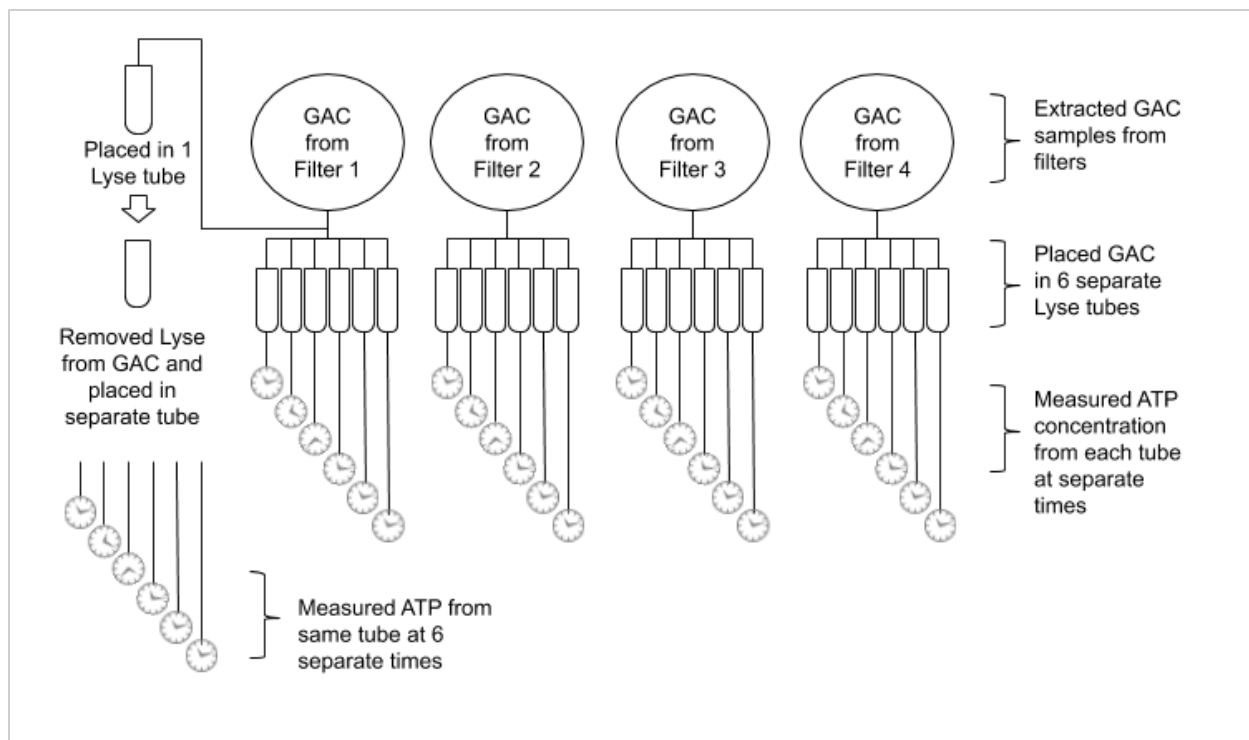


Figure A - 59: Flow chart of steps for experiment that re-creates ATP adsorption in lyse tubes

The ATP concentrations declined at a rate that agrees with an adsorption degradation curve. This was the case for Filters 1, 2 and 3. The overall ATP degradation curve for Filter 4 was most difficult to interpret, as the media from Port 3 is likely to be a combination of GAC and anthracite. It is assumed that the ATP concentration declines at a linear rate for this filter.

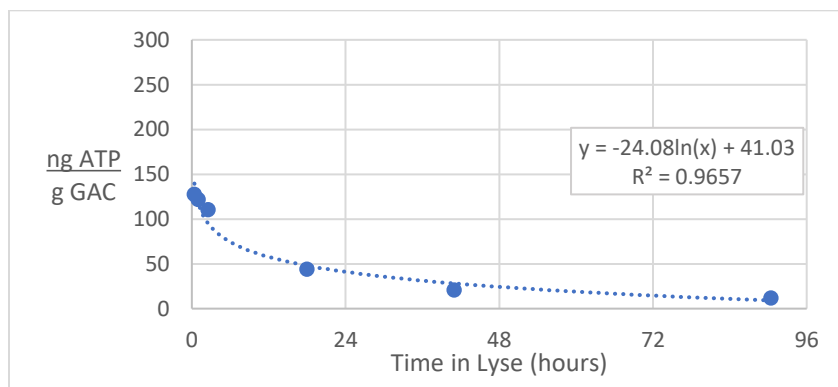


Figure A - 60 ATP Degradation curve in lyse for F1 sample

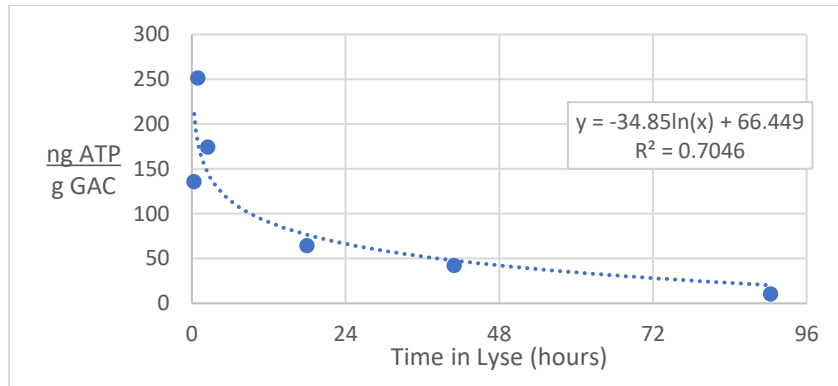


Figure A - 61 ATP Degradation curve in lyse for F2 sample

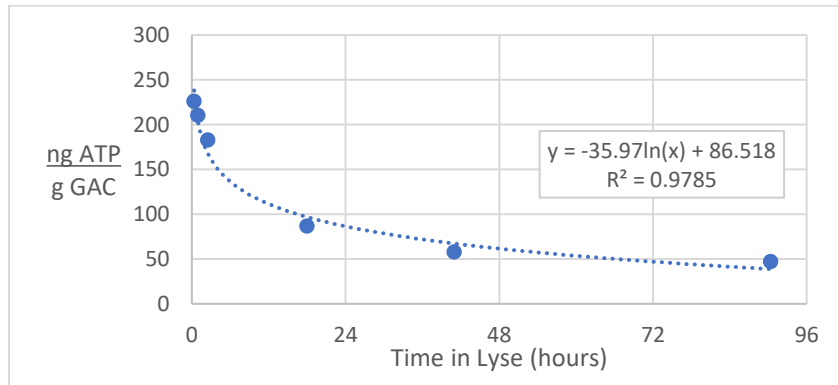


Figure A - 62 ATP Degradation curve in lyse for F3 sample

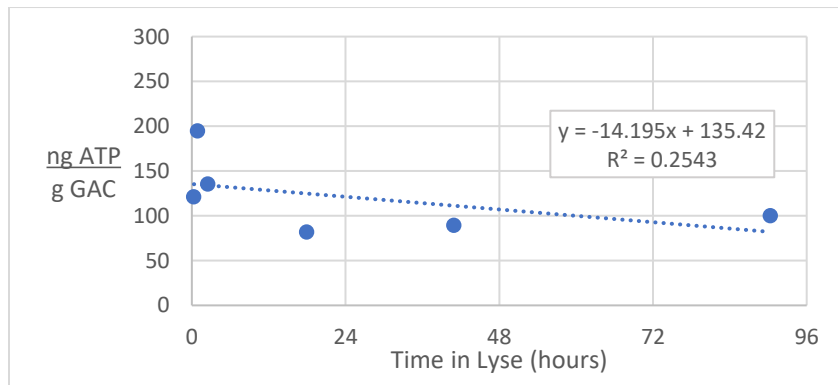


Figure A - 63 ATP Degradation curve in lyse for F4 sample

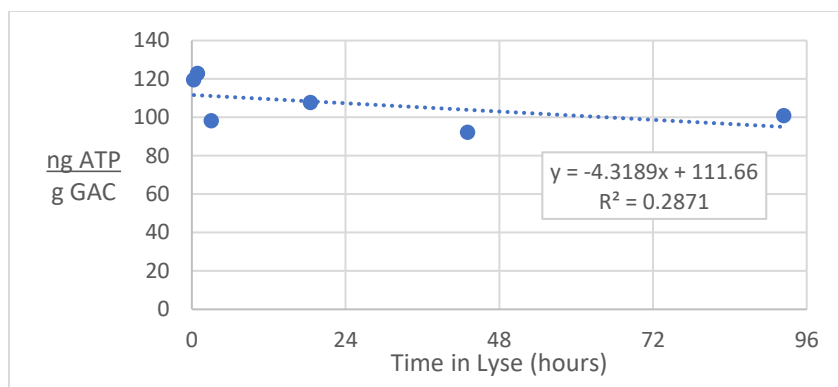


Figure A - 64 ATP Degradation curve in lyse for Control (F1) sample

The model equations from each of these curves were used to adjust the ATP concentrations of the samples affected by the laboratory mishap. The calculations are as follows:

Modeled Eq'n for F4

$$y = m(x) + C$$

Modeled Eq'ns for F1, F2 and F3

$$y = m \ln(x) + C$$

Moving forward, the known values from samples June 20th, June 27th, and July 6th is the ATP concentration (y_1), and the number of hours this media sample had spent in the lyse (x_1). Further calculations also assume that the degradation rate ($m(x)$, or $m \ln(x)$) does not change between sampling dates, but C will change.

The calculations are therefore as follows:

Eq'n for F4

$$C = -m(x_1) + y_1$$

$$y_2 = m(x_2) + C$$

Eq'n for F1, F2 and F3

$$C = -m \ln(x_1) + y_1$$

$$y_2 = m \ln(x_2) + C$$

Where y_2 is the ATP, had the lyse for the media sample been extracted within a proper time frame (x_2).

UV Absorbance – Error caused by storage

Water samples collected for UV absorbance must be analysed within 48 hours, as stated in SMWW 5910 (American Water Works Association et al., 2012). Due to pragmatic reasons, the UV absorbance was instead analysed within 10 days of collection.

Some samples were analysed twice in order to address the potential impact of storage times longer than 48 hours. 9 samples, collected on June 14th, 2019, were measured after 1 day of storage and again after 11 days of storage, and 10 samples, collected on July 31st, 2019, were measured after 8 days and again after 20 days of storage. The rate of change in UV absorbance was approximated from these points and plotted to check for the influence of the quantity of the starting UV absorbance (Figure A - 65). Overall, the rates of change in UV absorbance were evenly distributed.

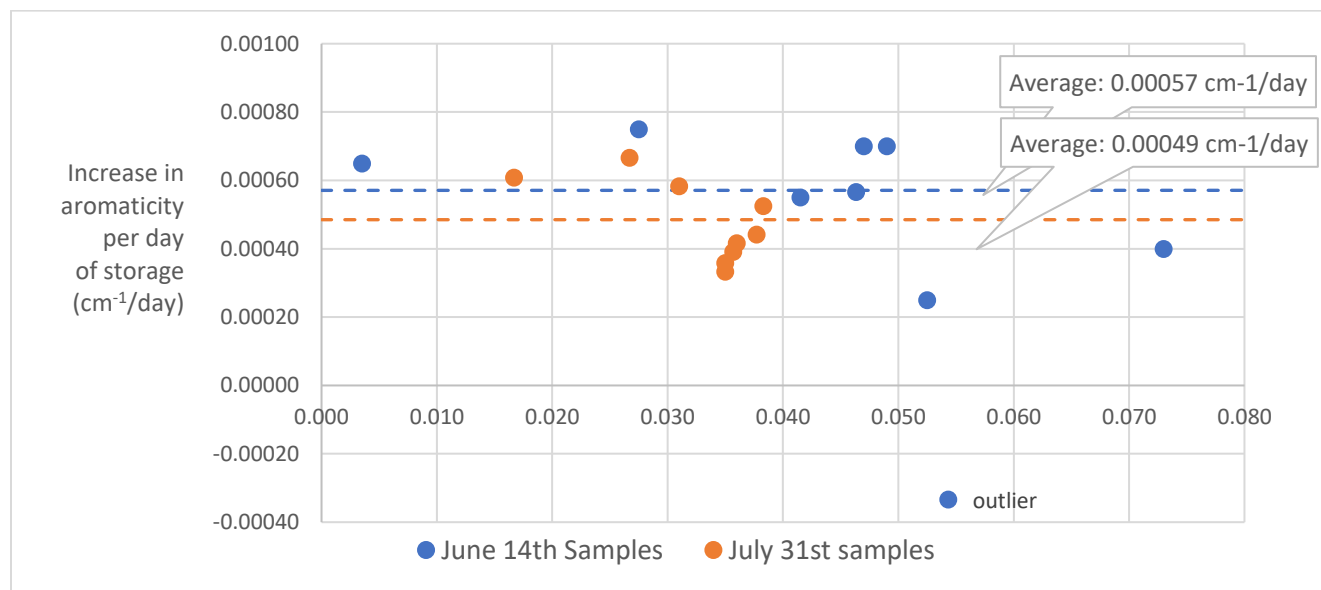


Figure A - 65: Approximations of rate of change in UV absorbance over days that the sample is stored – plotted against the starting UV absorbance of that sample

A true measurement of the change of UV absorbance over storage time should involve taking several readings of the same sample, instead of just two, as was done in this experiment. However, this is just an approximation and is not meant to definitively establish the rate at which UV absorbance changes.

The approximation of change in UV absorbance was calculated to as 0.00053 cm⁻¹/day (the UV absorbance can only be measured with a precision of 0.000 cm⁻¹, the additional decimal points are construed). This potential change in UV storage was deemed to not significantly affect the final UV readings (Figure A - 66 to A-69.).

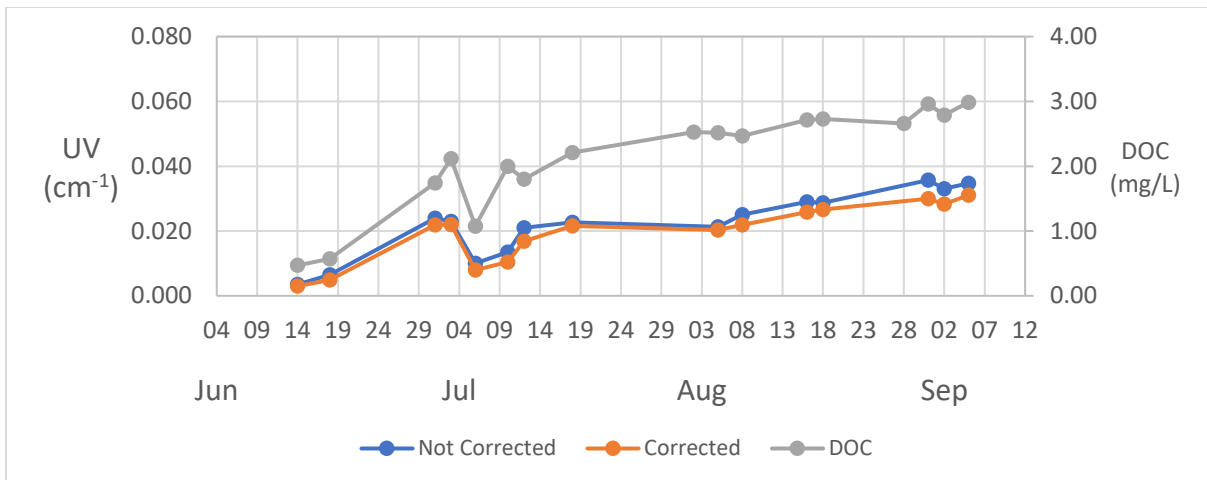


Figure A - 66: UV absorbance in F1 Effluent and correction for the impact of sample storage

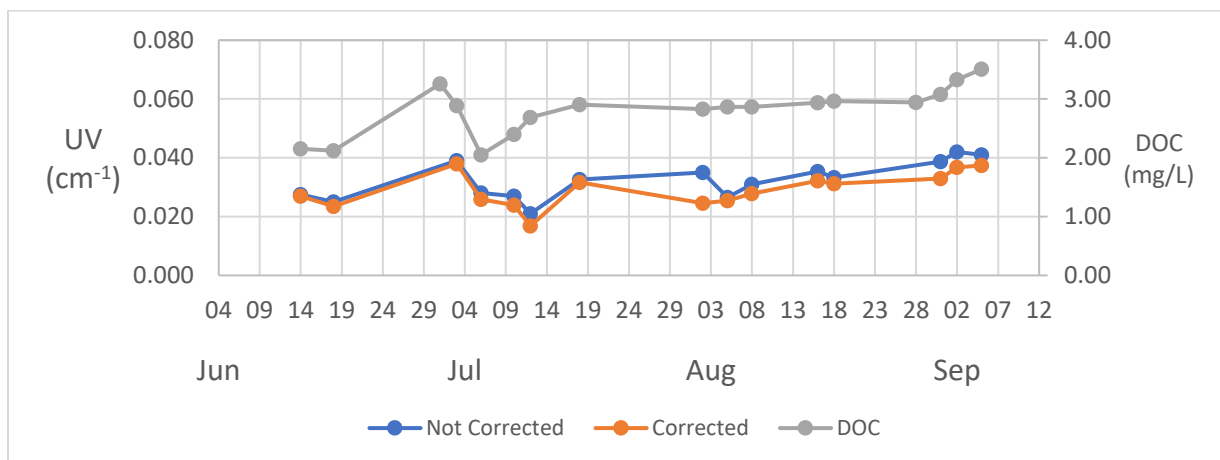


Figure A - 67: UV absorbance in F2 Effluent and correction for the impact of sample storage

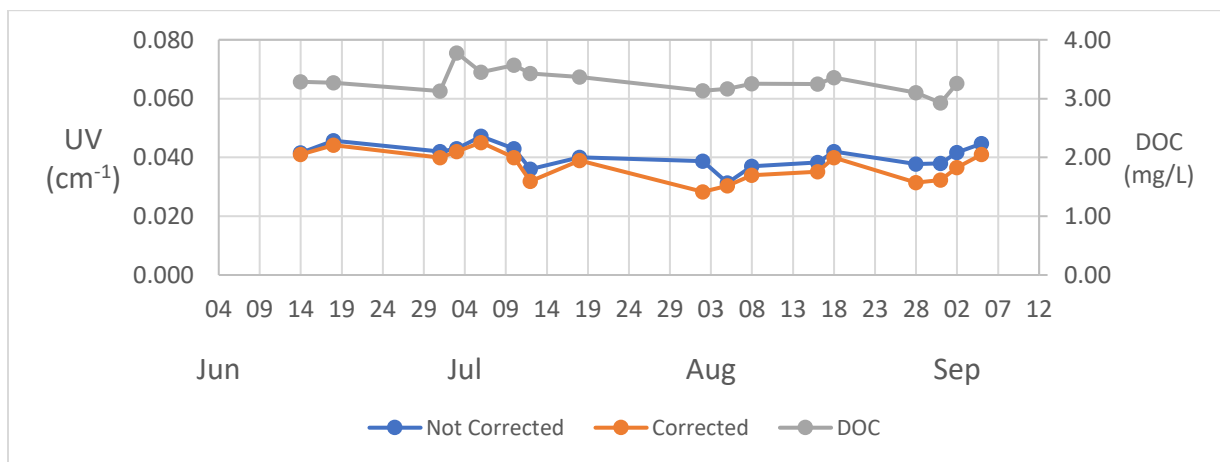


Figure A - 68: UV absorbance in F3 Effluent and correction for the impact of sample storage

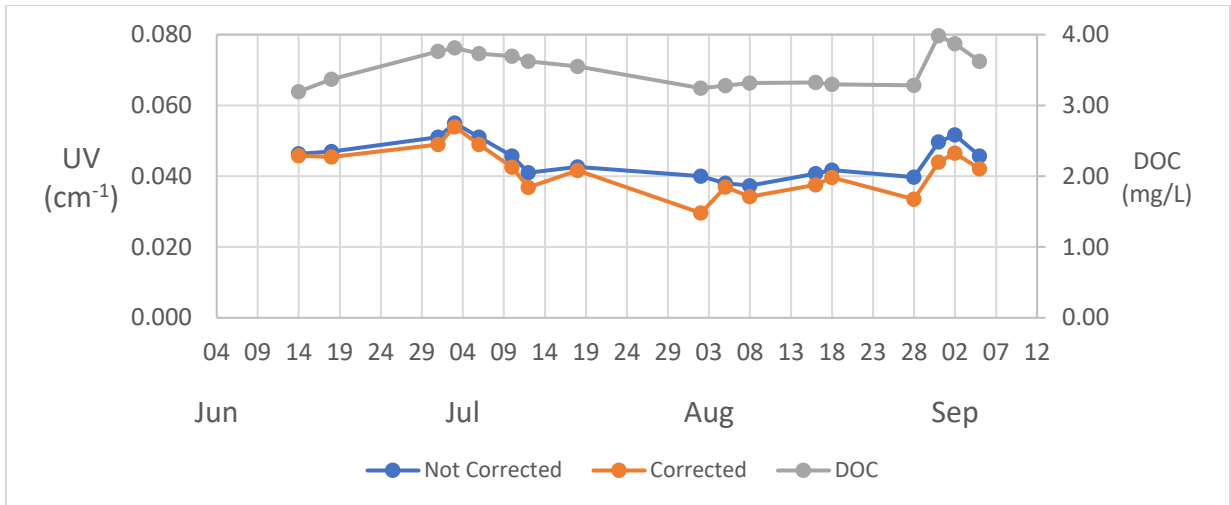


Figure A - 69: UV absorbance in F4 Effluent and correction for the impact of sample storage

LC-OCD – Error caused by storage

As with UV absorbance, the LC-OCD measurements were subject to change while in storage prior to analysis. The impact of this storage was estimated by leaving one filtered sample (Filter 3 effluent, collected on July 10th, 2019) in storage at 4°C, and repeatedly measuring it.

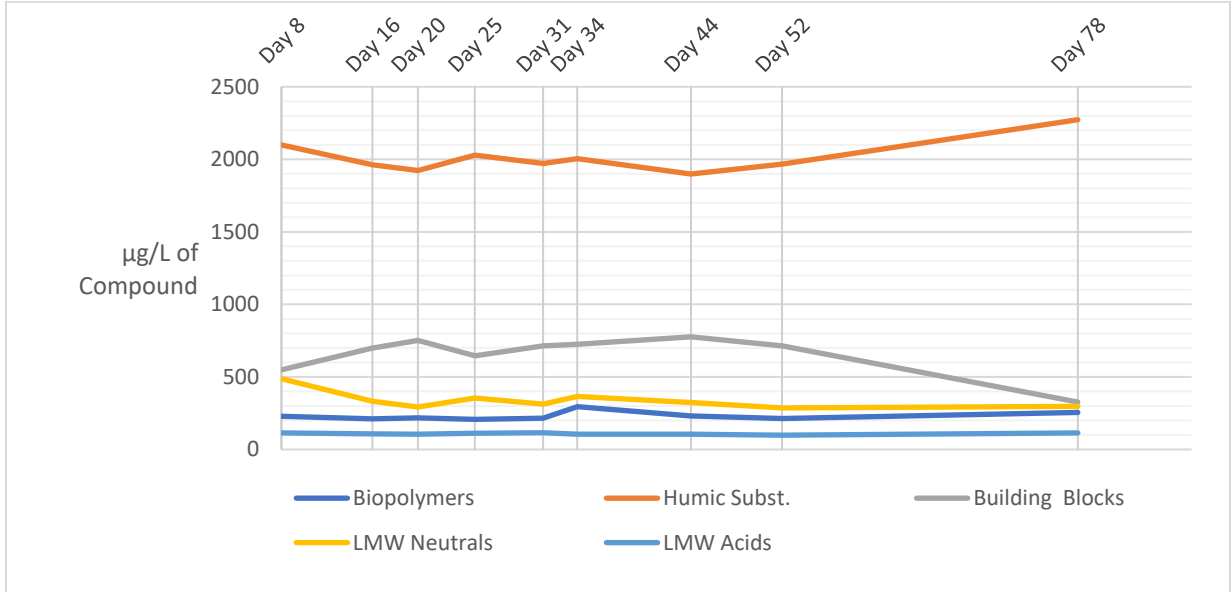


Figure A - 70: Repeated LC-OCD readings over storage of same sample

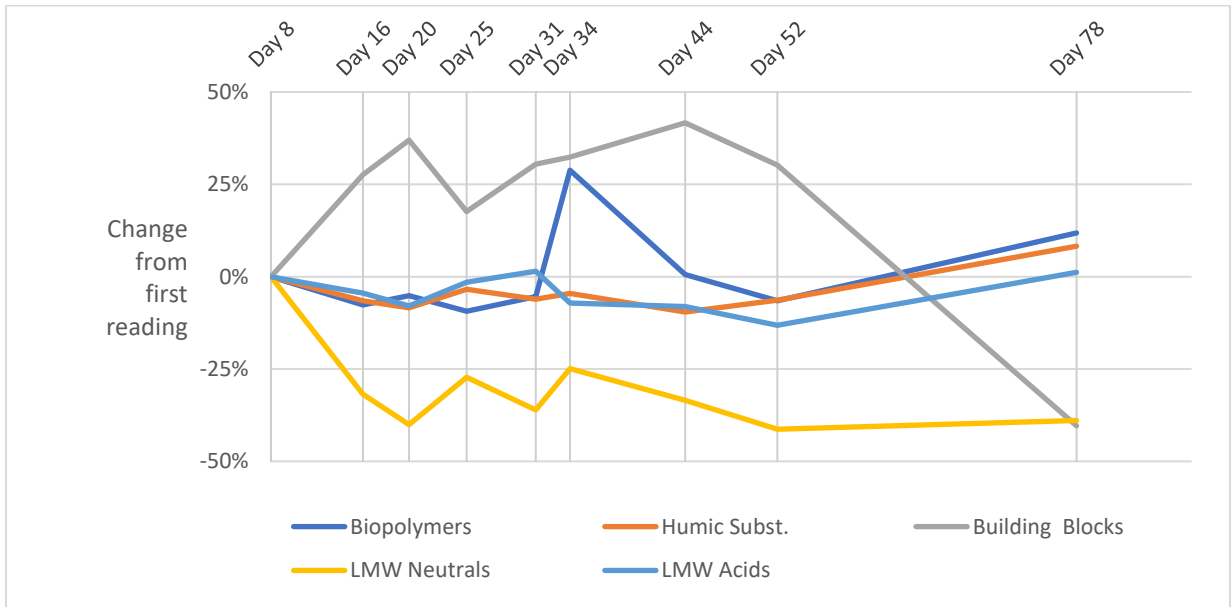


Figure A - 71: Change in LC-OCD concentrations in same sample over its storage

The LC-OCD samples collected throughout the biological filtration experiment were measured within approximately 2 weeks. It appears that the LMW neutrals and the Building Blocks fraction of LC-OCD would be prone to change if stored for that long, but the biopolymers and humic substances must have remained relatively unaffected (Figure A - 70 and Figure A - 71). On day 34, there is an unexpectedly high biopolymer concentration – this is an outlier as it deviates from the overall pattern and there is no explanation for it.

Aside from its relevance to the biological filtration experiment, the long-term pattern of LC-OCD fractions has some interesting implications. For one, there is a decrease in the amphiphilic and hydrophilic, smaller-sized LMW neutrals, and there is an increase in the larger, more humic-like Building Blocks. This is a potential explanation for the tendency of UV absorbance to increase during storage. It is also interesting that the largest changes in the LC-OCD samples occur from storage day 8 to 16 and from day 52 to 78. One theory to explain this is that these changes are somehow caused by microorganisms. For example, when an environmental sample is isolated, the cell growth within the sample enters 4 phases; 1) lag, where the cells are adjusting to the new environment, or the individual cells grow larger in size, but don't multiply, 2) the cells multiply at an exponential rate 3) substrate supply begins to be depleted and cell growth reaches a stationary phase, and 4) substrate is completely depleted and cell death causes the cell population to decline (Bitton et al., 2002). This familiar growth pattern could be associated with the pattern of change in building blocks and LMW neutrals, however, this association would take thorough experimentation to show.

Recommendations for further research in this area are to take more frequent LC-OCD measurements during the first 14 days of storage, and to measure cell growth all throughout the LC-OCD storage.

Appendix C - Statistical Analysis

Equations

Linear Regression Equations

In a linear regression analysis, a series of paired observations (independent, X_i and dependent, Y_i) are fitted into model that minimizes the residual sum of squares.

Fitted linear regression model:

$$Y_i = \beta_0 + \beta_1 X_i + \varepsilon_i$$

Residual sum of squares:

$$RSS = \sum_{i=1}^n (Y_i - \hat{Y}_i)^2$$

A linear regression model is appropriate if the data meets the following assumptions 1) that a linear model is correct (as opposed to a non-linear model), 2) that each X_i variable is measured without error, 3) the errors associated with Y are normally distributed and 4) the variance is roughly equal along the regression line.

To test these assumptions, the residuals of the models were plotted and visually observed for non-normal distributions, non-linear patterns, or heteroscedasticity. Data that presented any of these issues were log-transformed (base 10 and e) or square-root transformed, and analysed again, as recommended by (Gotelli and Ellison, 2013).

Paired t-test

The paired t-test is a popular robust method of determining if two sets of data are statistically different. The calculated P-value is usually presented as the result of the t-test. If the P-value is sufficiently large, then there is no reason to reject the null hypothesis – in other words, randomness is the primary reason between the differences in the set of data. And if the P-value is sufficiently low, it is concluded that something more than random variation is contributing to the difference in results. The P-value depends on the sample-size of the data sets, the difference between the means of the samples, and the level of variation among them (Gotelli and Ellison, 2013).

Testing Assumptions – Normality and Equal Variance

Paired t-Tests Histograms – Influent Results

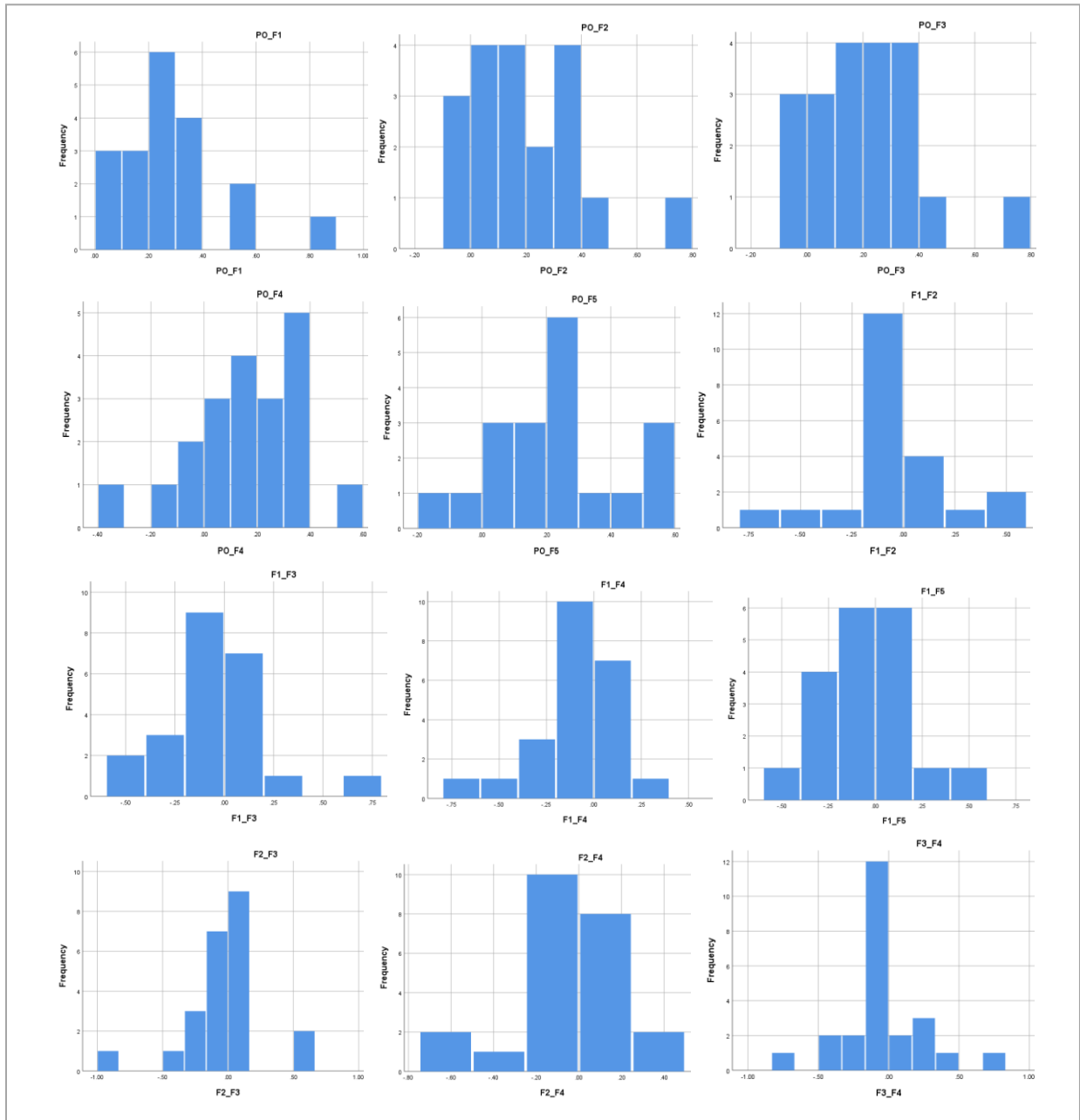


Figure A - 72 Histograms for paired t-tests among DOC influent (Post-ozonated influent, and Port 1 from Filter 1, Filter 2, Filter 3 and Filter 4)

Paired t-Test Histograms – Filter 1

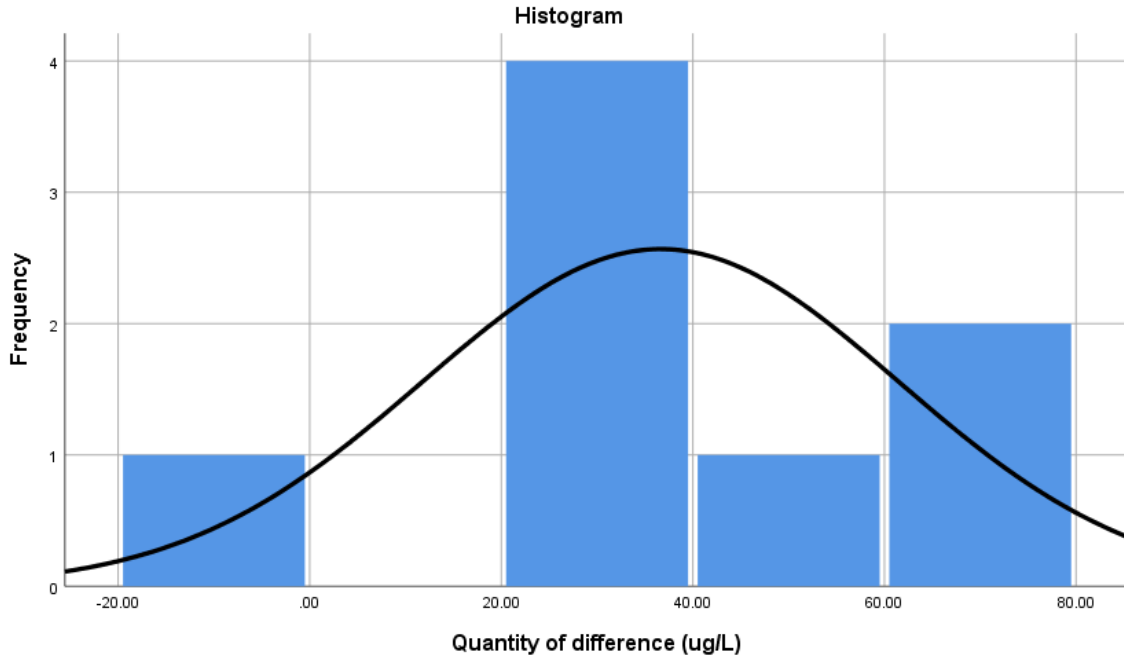


Figure A - 73: Frequency diagram of differences between pairs for influent biopolymer concentration and Filter 1 effluent biopolymer concentration

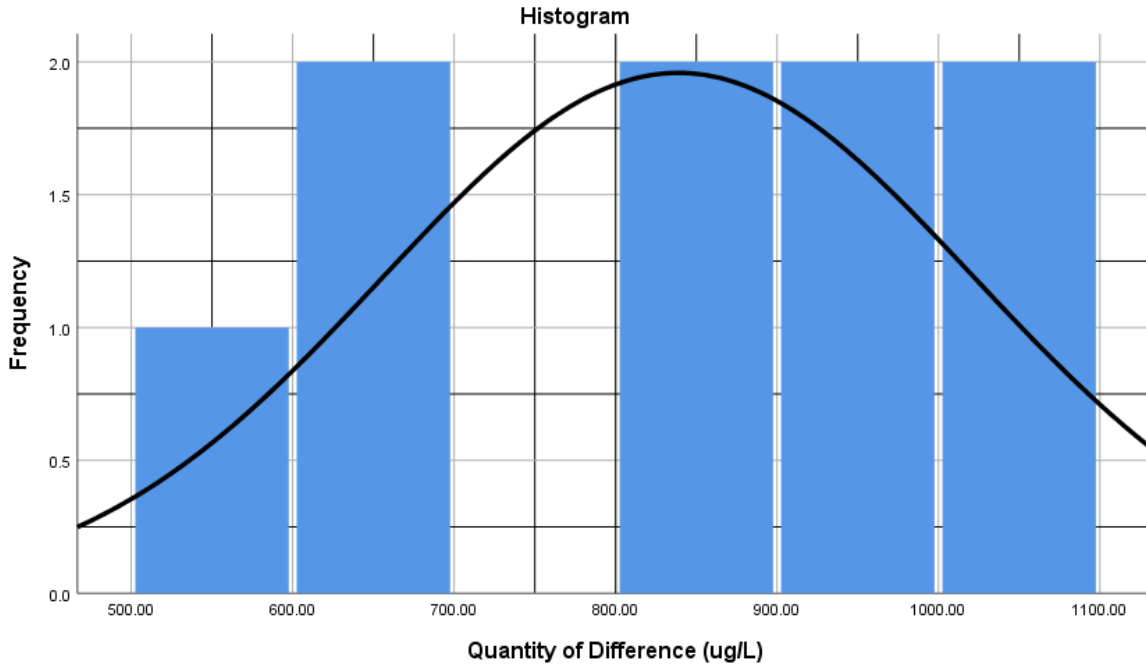


Figure A - 74: Frequency diagram of differences between pairs for influent humic substance concentration and Filter 1 effluent humic substance concentration

Paired t-Test Histograms – Filter 2 Results

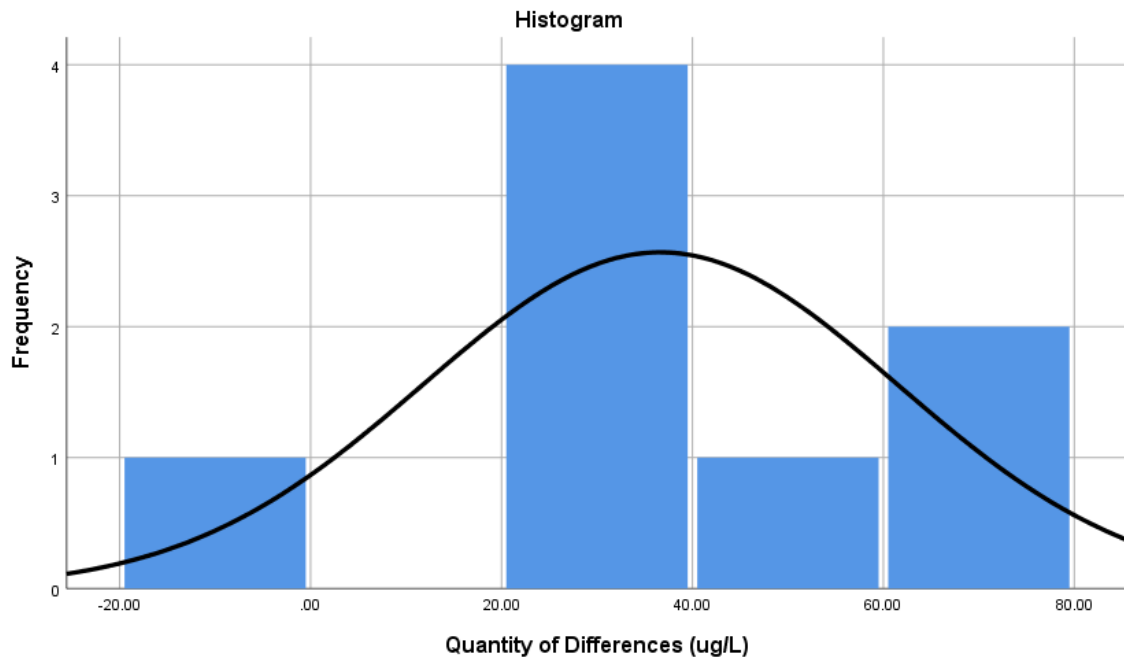


Figure A - 75: Frequency diagram of differences between pairs for influent biopolymer concentration and Filter 2 effluent biopolymer concentration

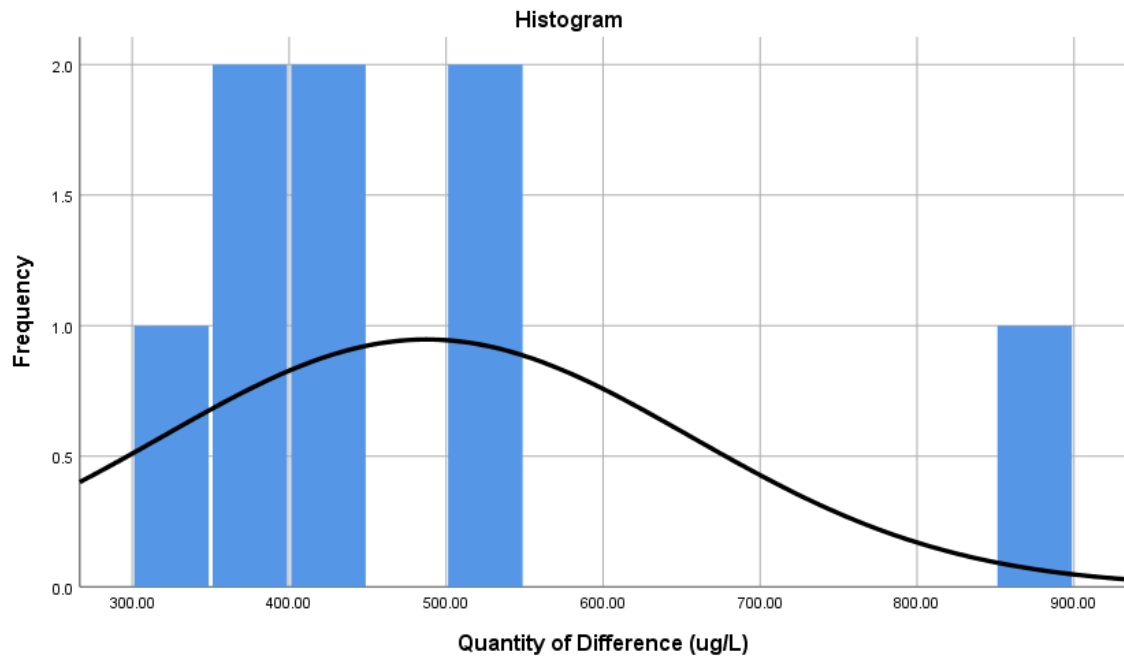


Figure A - 76: Frequency diagram of differences between pairs for influent humic substance concentration and Filter 2 effluent humic substance concentration

Paired t-test Histograms – Filter 3 Results

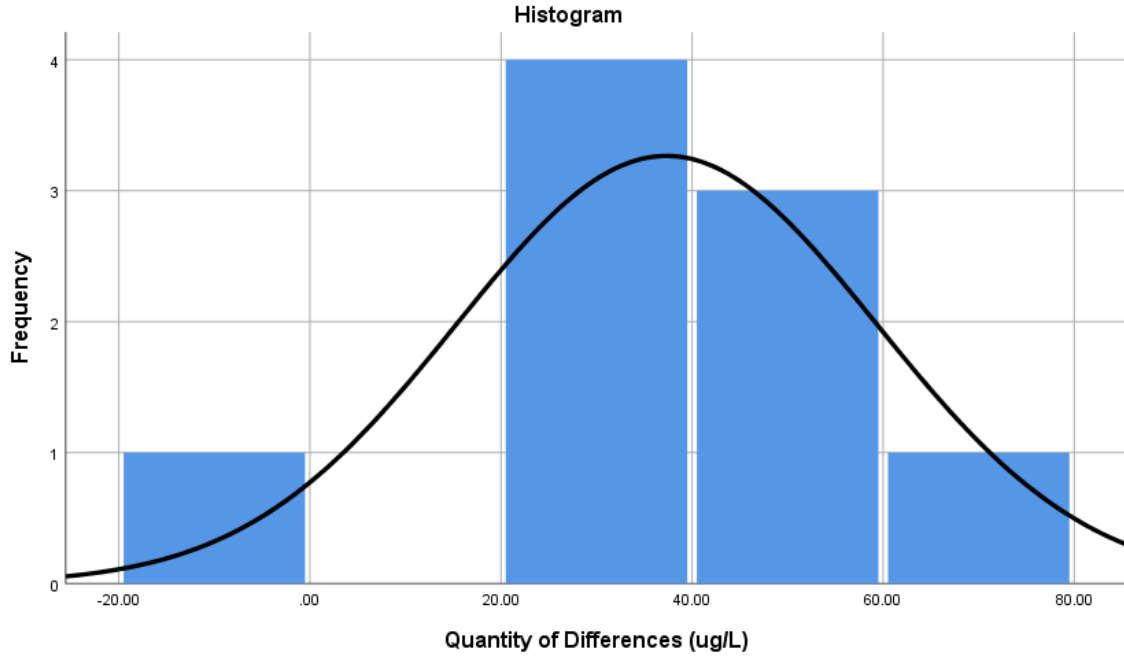


Figure A - 77: Frequency diagram of differences between pairs for influent biopolymer concentration and Filter 3 effluent biopolymer concentration

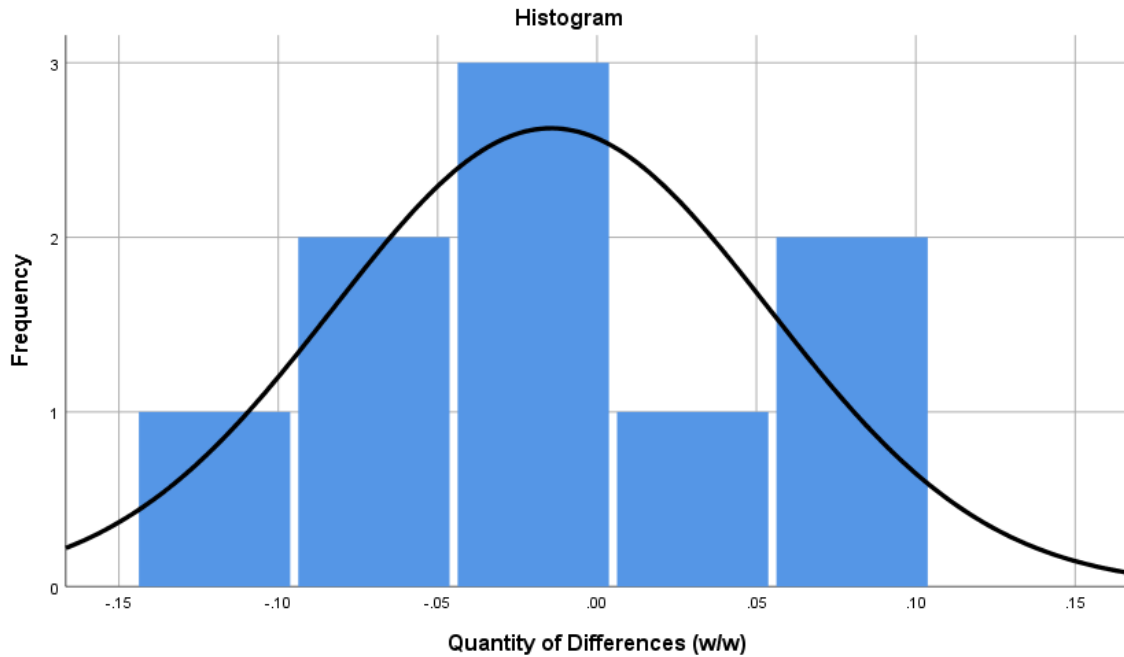


Figure A - 78: Frequency diagram of differences between pairs for the removal of biopolymers in Filter 1 and the removal of biopolymers in Filter 3

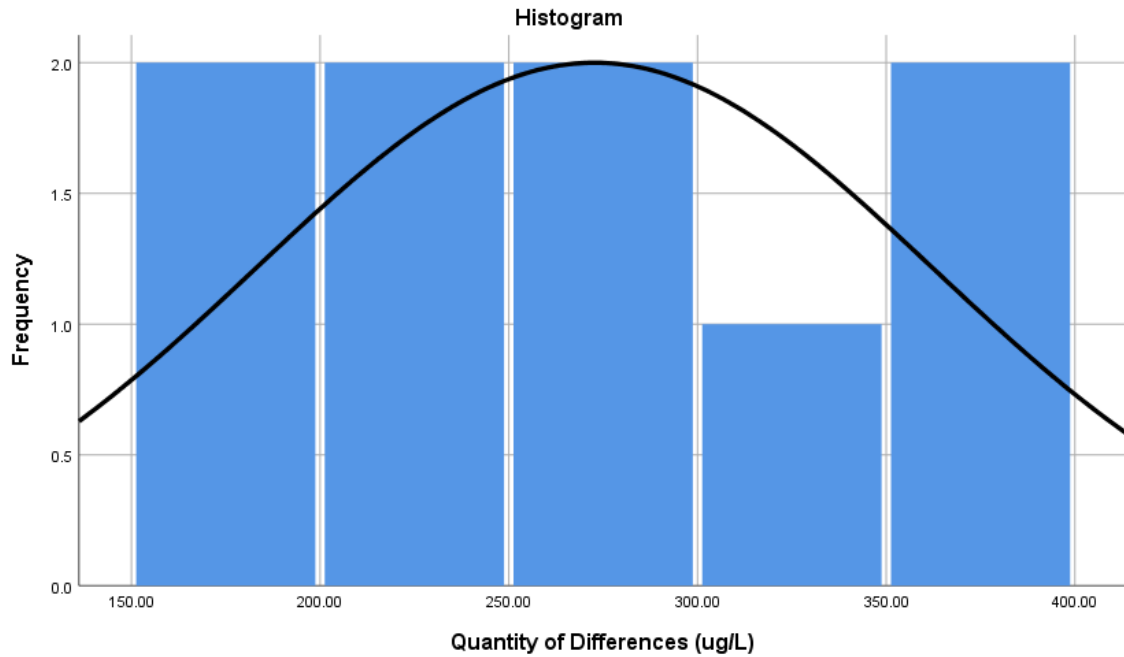


Figure A - 79: Frequency diagram of differences between pairs for influent humic substances concentration and Filter 3 effluent humic substances concentration

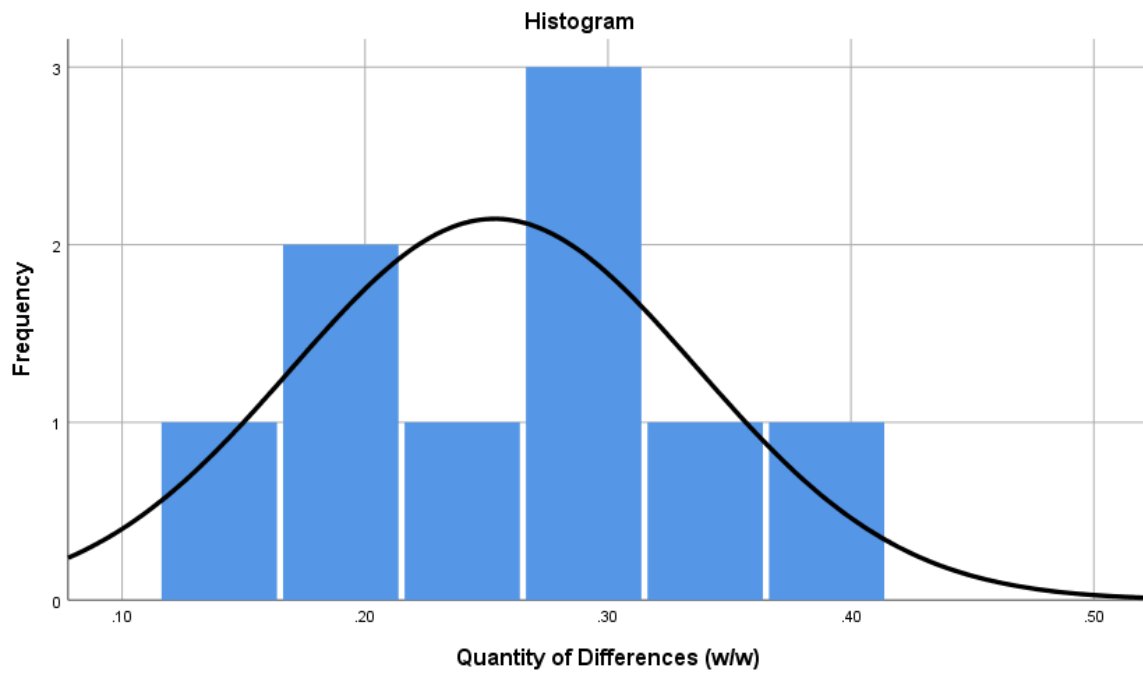


Figure A - 80: Frequency diagram of differences between pairs for the removal of humic substances in Filter 1 and the removal of humic substances in Filter 3

Paired t-Test Histograms – Filter 4 Results

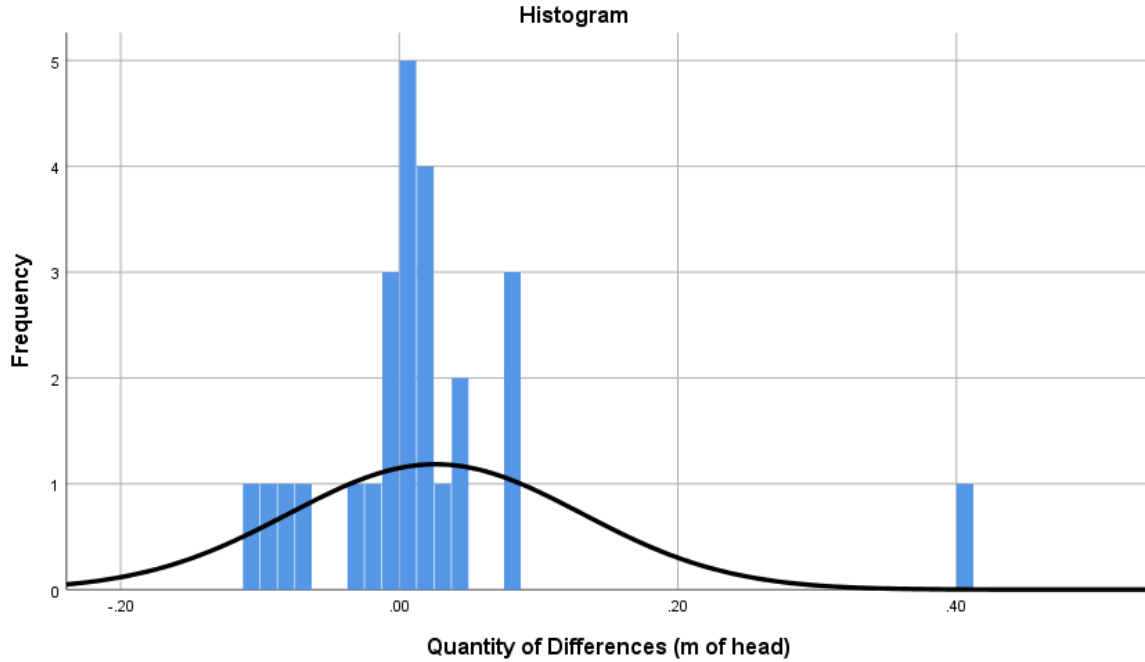


Figure A - 81: Frequency diagrams of differences between pairs for headloss accumulation in Filter 3 and the headloss accumulation in Filter 4

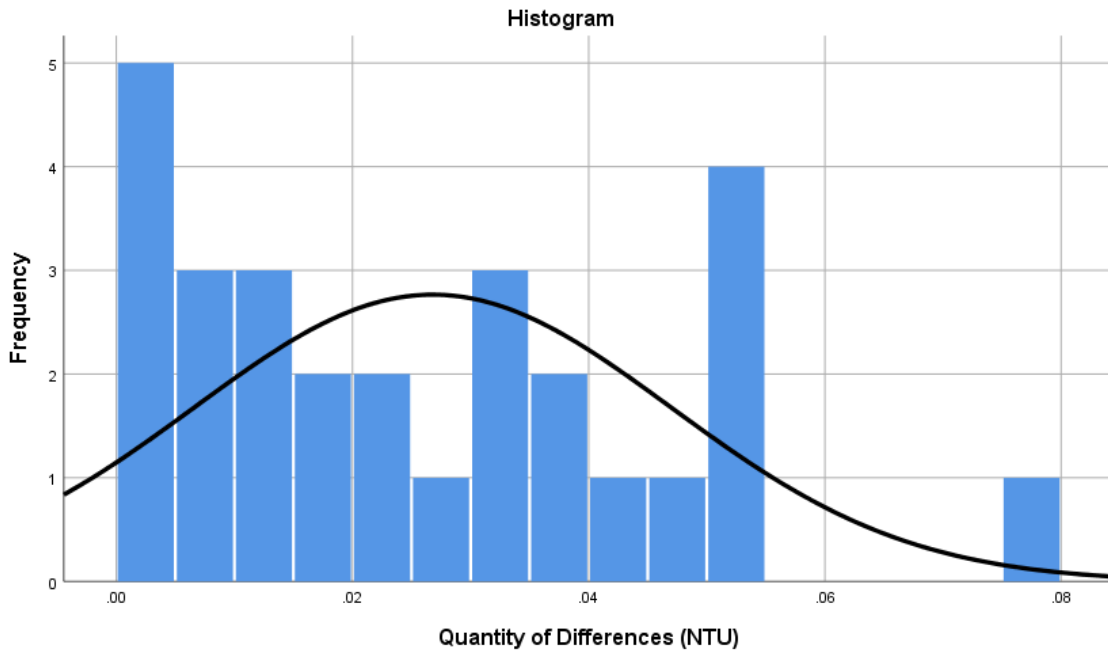


Figure A - 82: Frequency diagrams of differences between pairs for the effluent turbidity in Filter 3 and the effluent turbidity in Filter 4

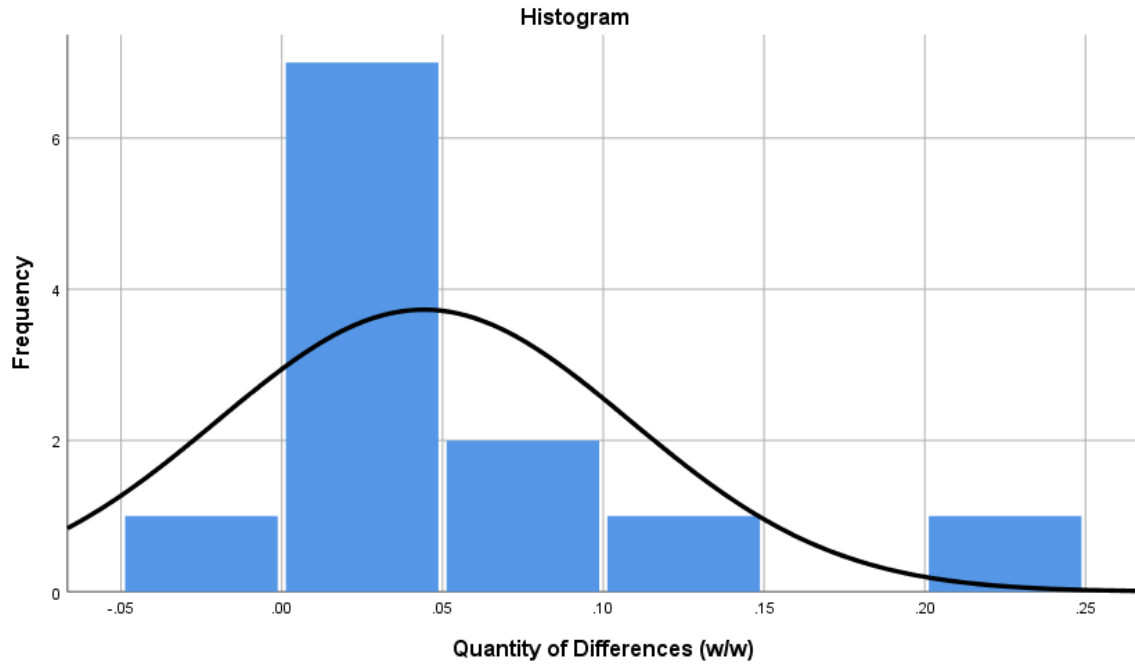


Figure A - 83: Frequency diagram of differences between pairs for F3 impact on the SUVA of the water and the F4 impact of the SUVA

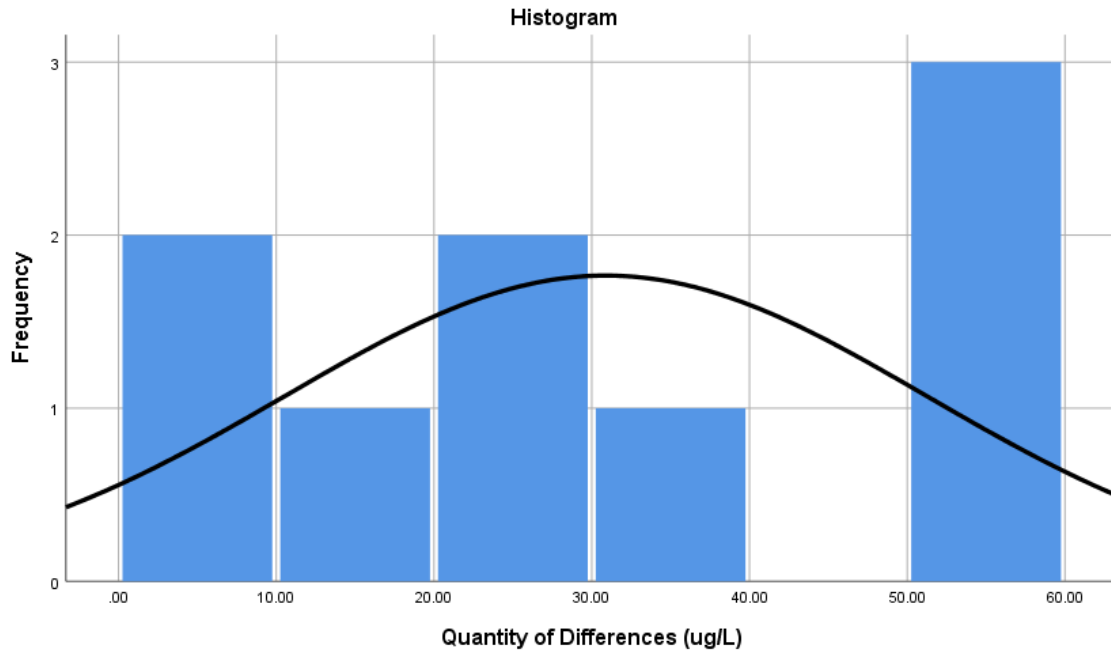


Figure A - 84: Frequency diagram of differences between pairs for influent biopolymer concentration and Filter 4 effluent biopolymer concentration

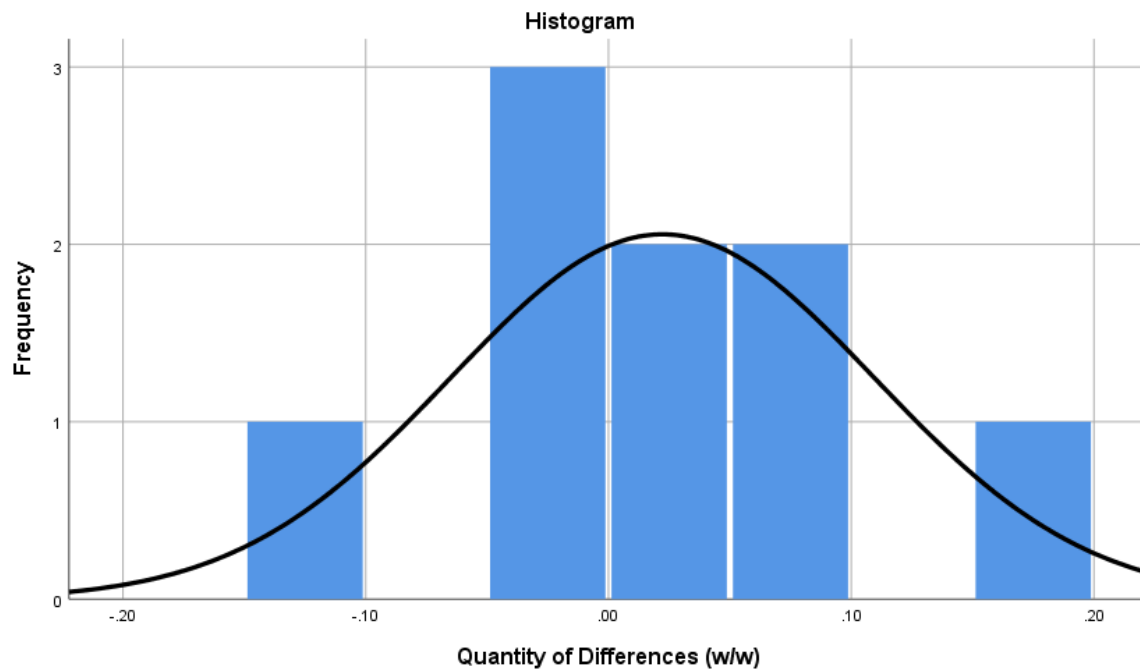


Figure A - 85: Frequency diagram of differences between pairs for the removal of biopolymers in Filter 3 and the removal of biopolymers in Filter 4

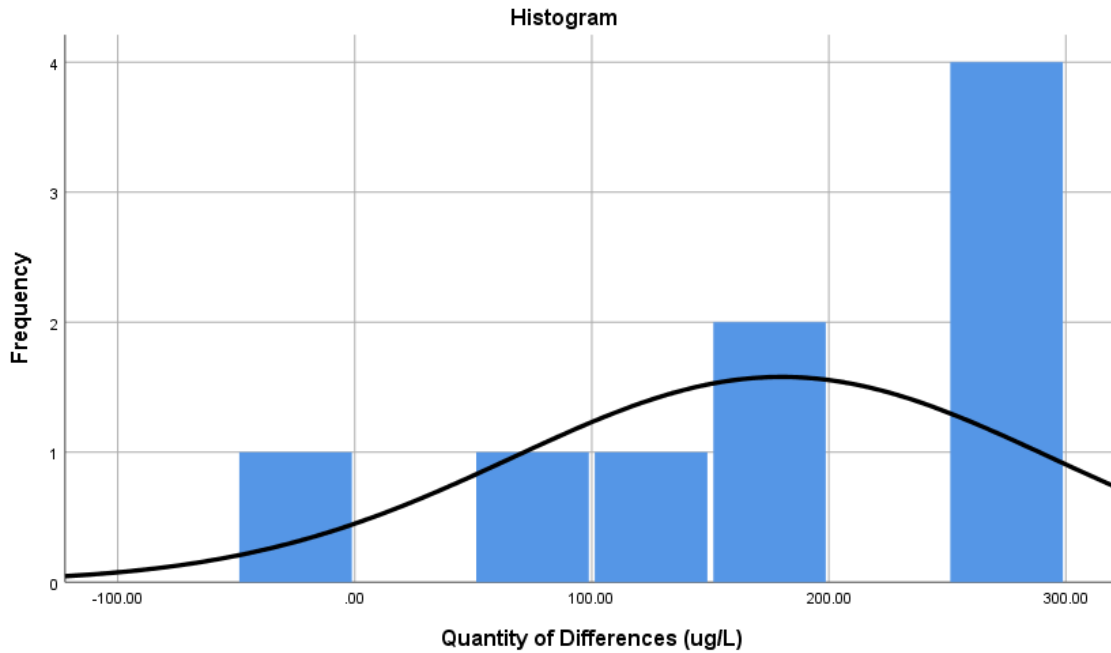


Figure A - 86: Frequency diagram of differences between pairs for influent humic substances concentration and Filter 4 effluent humic substances concentration

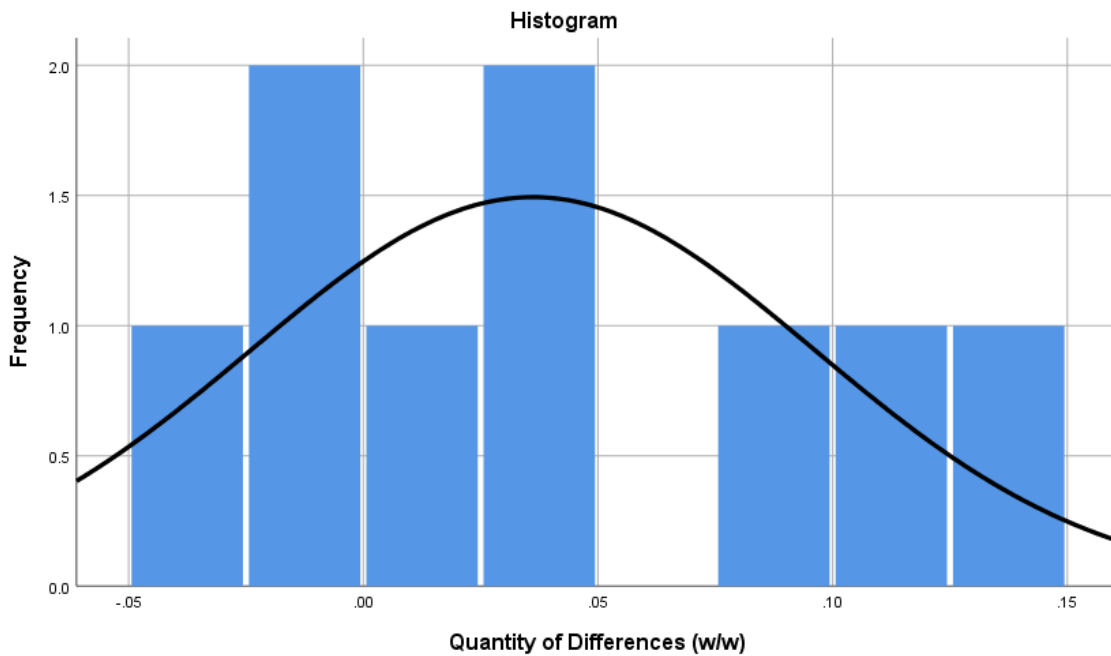


Figure A - 87: Frequency diagram of differences between pairs for the removal of humic substances in Filter 3 and the removal of humic substances in Filter 4

Linear Regression Residuals – Filter 1 DOC Removal over Experimental Period

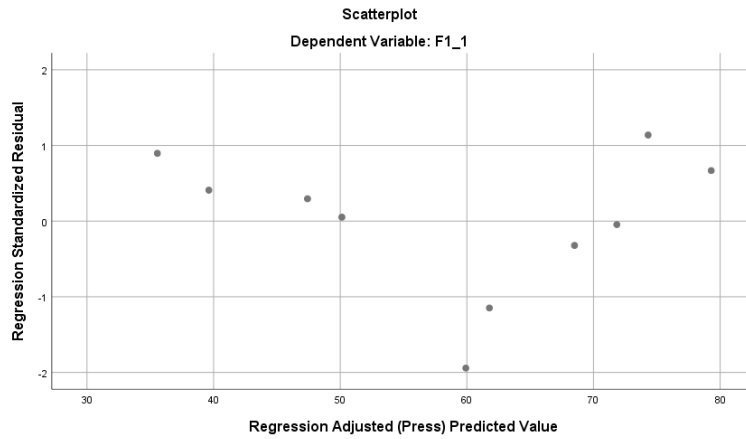


Figure A - 88: Linear regression residuals for DOC removal in Filter 1 – Iteration 1

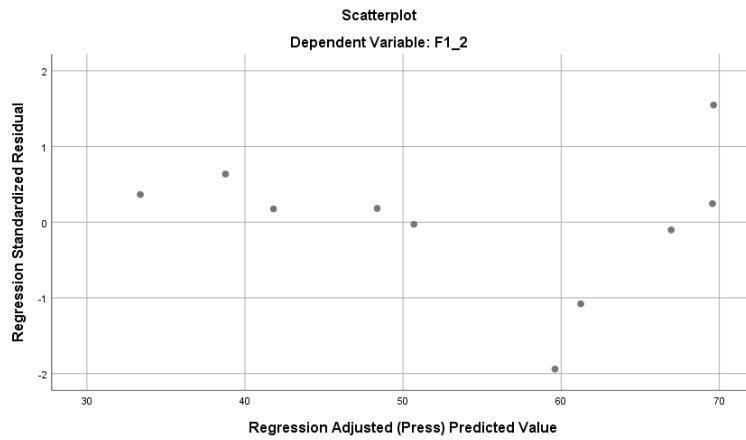


Figure A - 89: Linear regression residuals for DOC removal in Filter 1 – Iteration 2

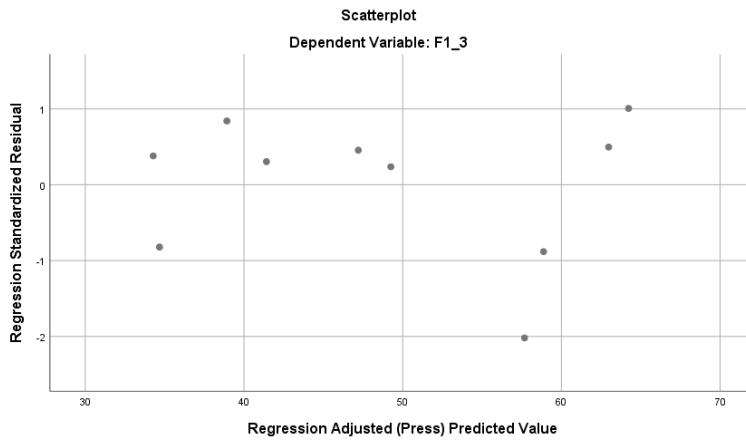


Figure A - 90: Linear regression residuals for DOC removal in Filter 1 – Iteration 3

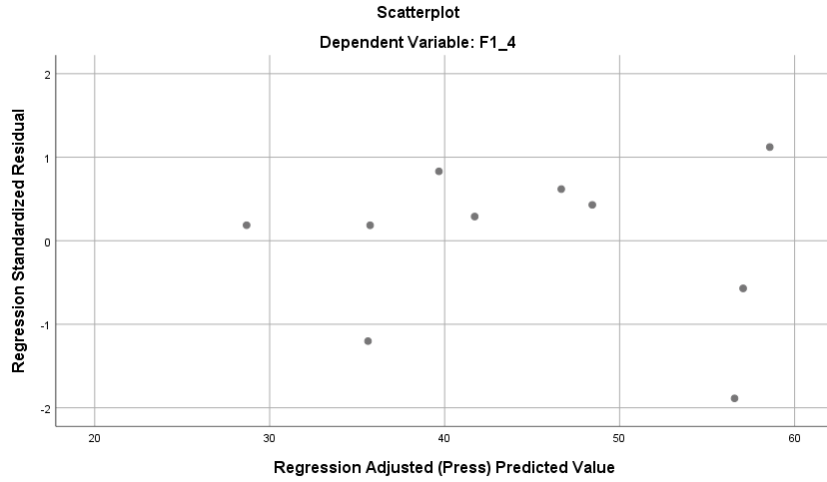


Figure A - 91: Linear regression residuals for DOC removal in Filter 1 – Iteration 4

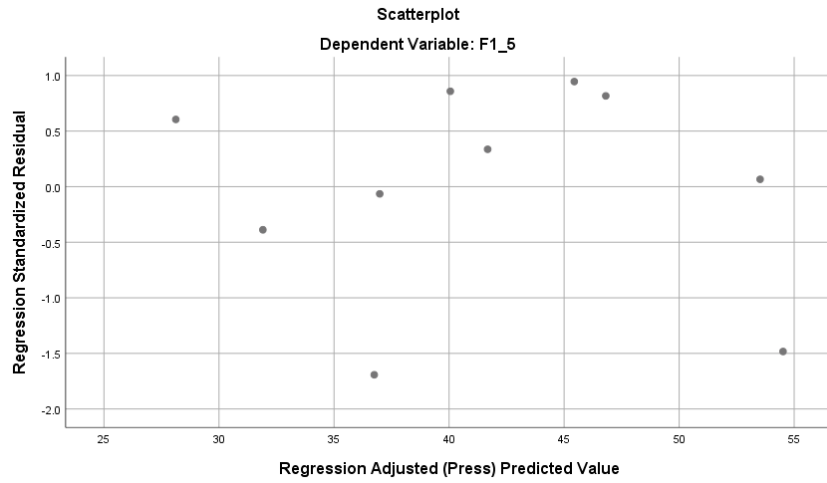


Figure A - 92: Linear regression residuals for DOC removal in Filter 1 – Iteration 5

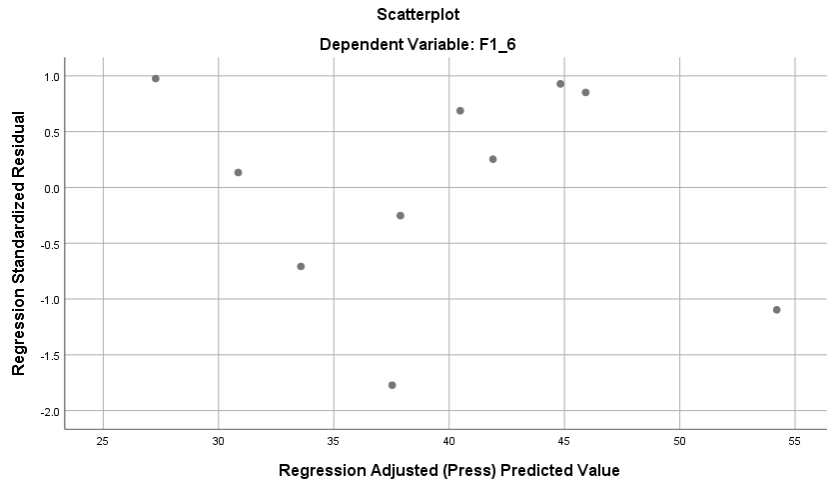


Figure A - 93: Linear regression residuals for DOC removal in Filter 1 – Iteration 6

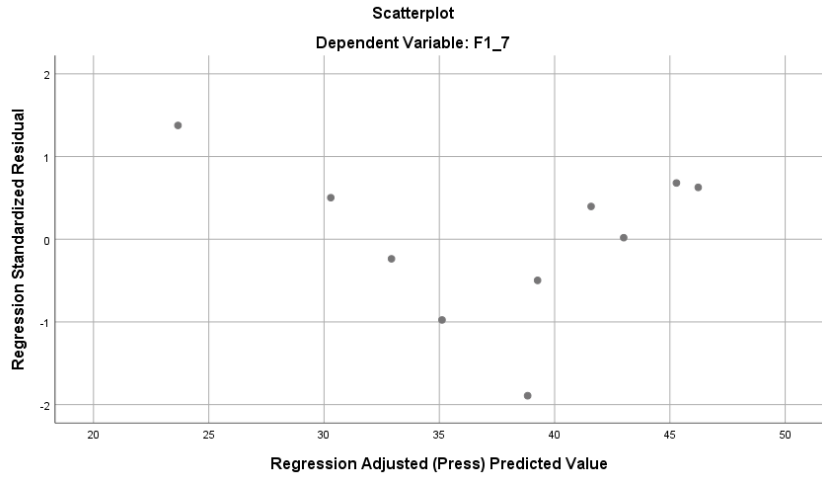


Figure A - 94: Linear regression residuals for DOC removal in Filter 1 – Iteration 7

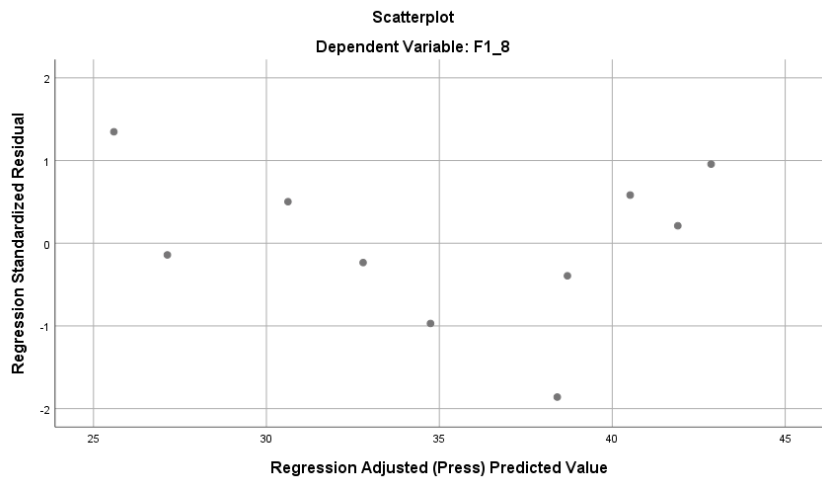


Figure A - 95: Linear regression residuals for DOC removal in Filter 1 – Iteration 8

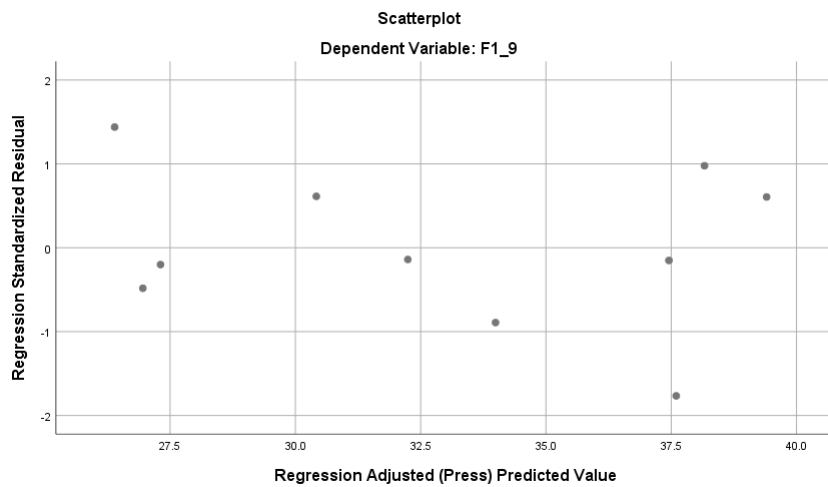


Figure A - 96: Linear regression residuals for DOC removal in Filter 1 – Iteration 9

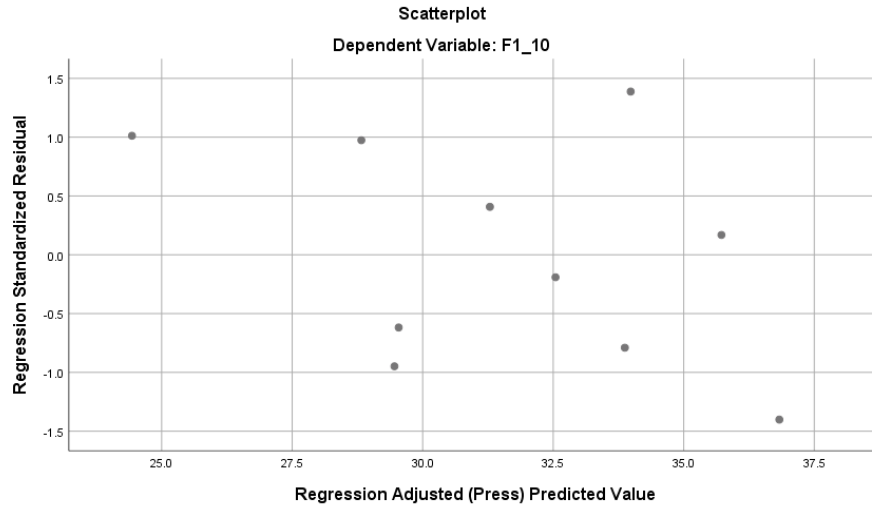


Figure A - 97: Linear regression residuals for DOC removal in Filter 1 – Iteration 10

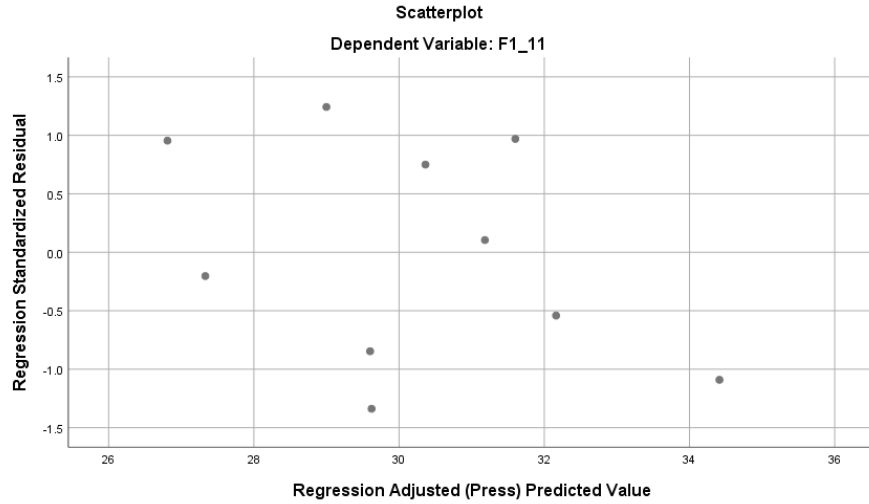


Figure A - 98: Linear regression residuals for DOC removal in Filter 1 – Iteration 11

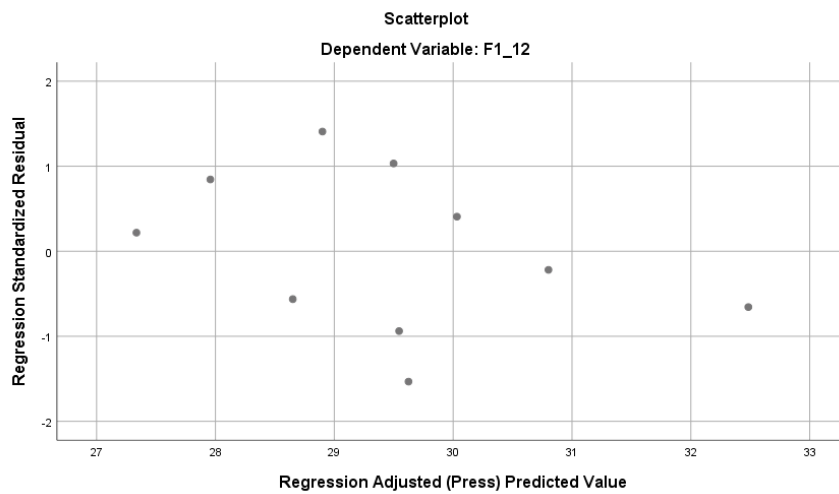


Figure A - 99: Linear regression residuals for DOC removal in Filter 1 – Iteration 12

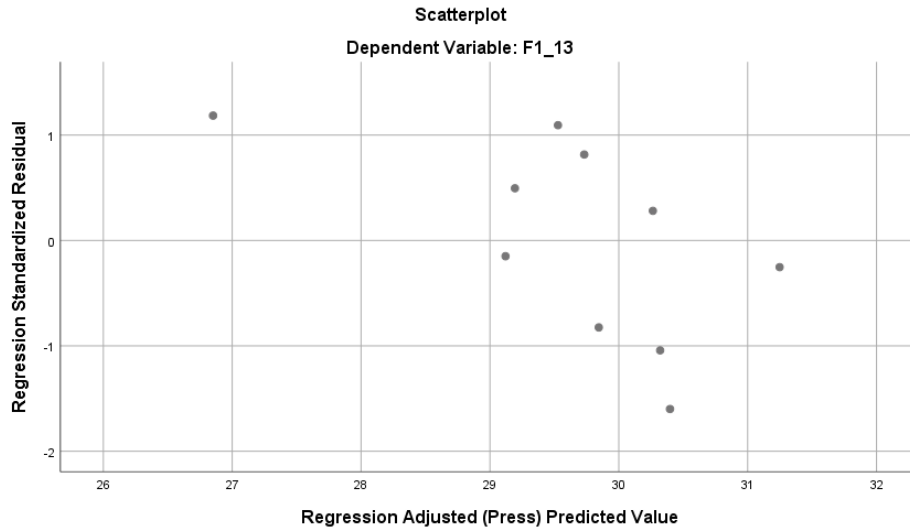


Figure A - 100: Linear regression residuals for DOC removal in Filter 1 – Iteration 13

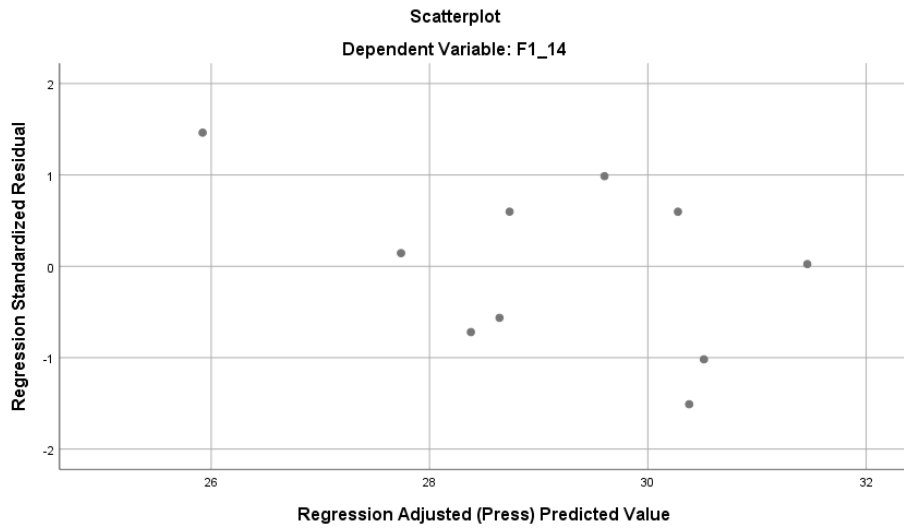


Figure A - 101: Linear regression residuals for DOC removal in Filter 1 – Iteration 14

Linear Regression Residuals – Filter 1 Fractions of DOC Removal over Experimental Period

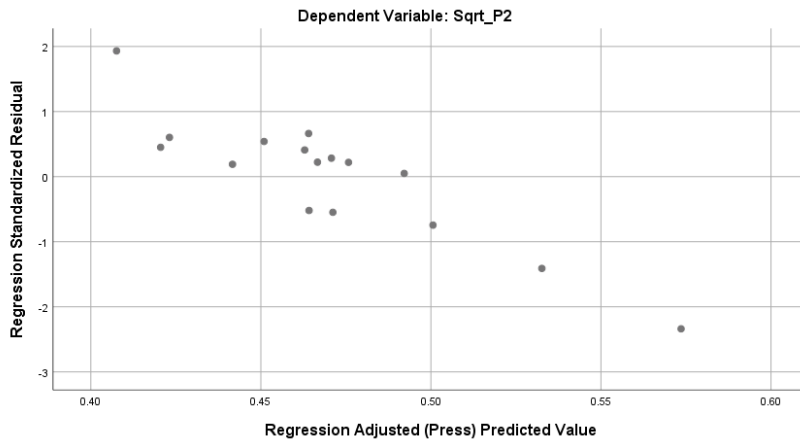


Figure A - 102: Linear regression residuals for fraction of DOC removed between the top to Port 2 in Filter 1– over experimental period

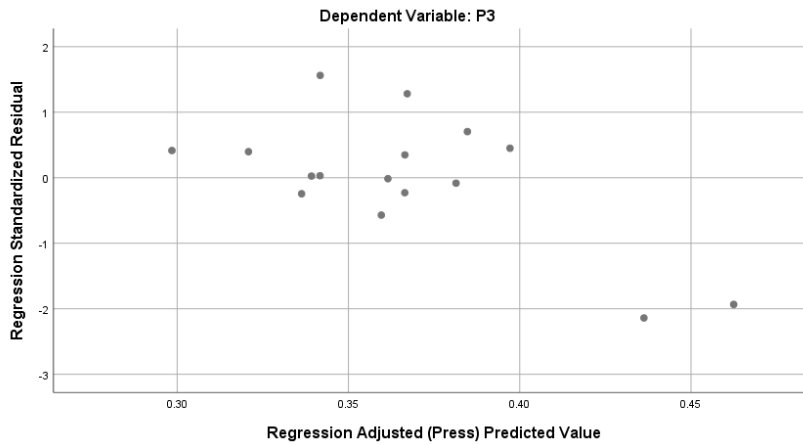


Figure A - 103: Linear regression residuals for fraction of DOC removed between Port 2 and Port 3 in Filter 1– over experimental period

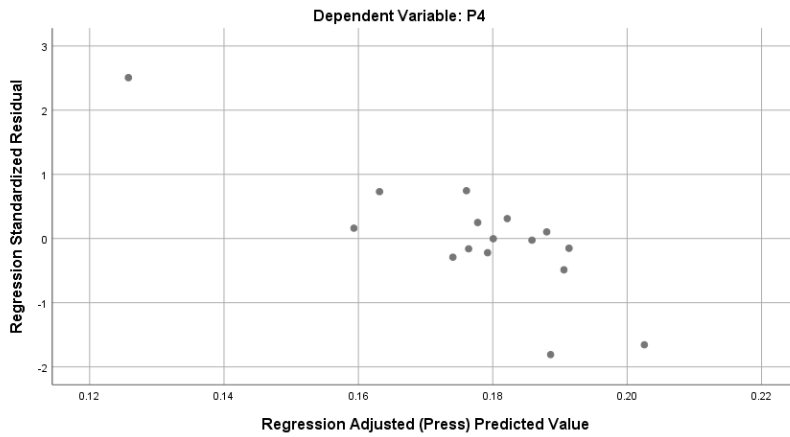


Figure A - 104: Linear regression residuals for fraction of DOC removed between Port 3 and Port 4 in Filter 1– over experimental period

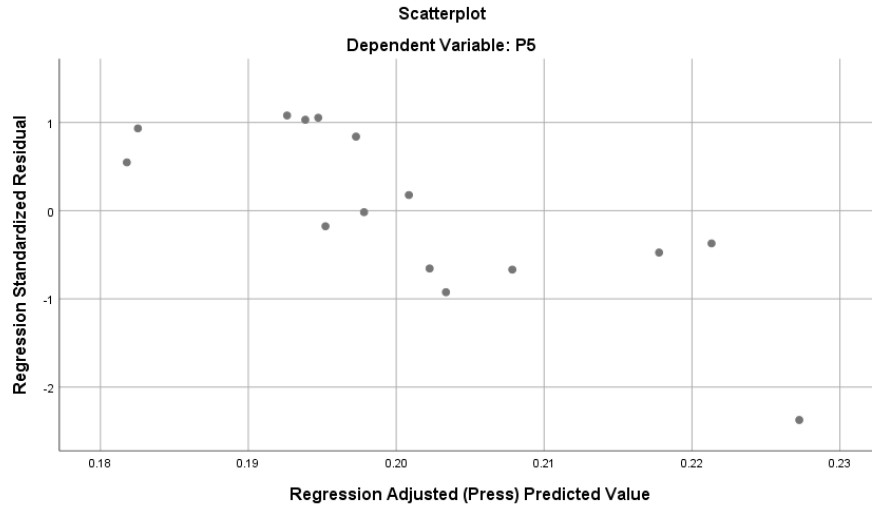


Figure A - 105: Linear regression residuals for fraction of DOC removed between Port 4 and Port 5 in Filter 1– over experimental period

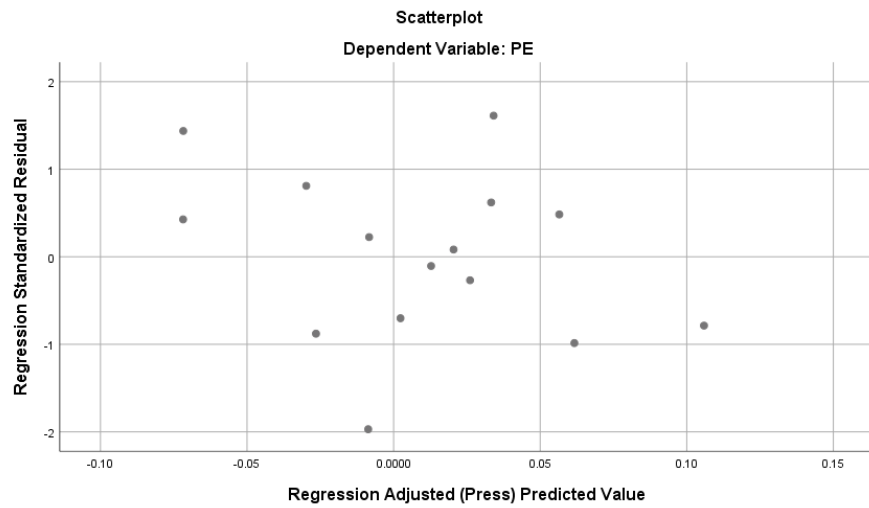


Figure A - 106: Linear regression residuals for fraction of DOC removed between Port 5 and Effluent Port in Filter 1– over experimental period

Linear Regression Residuals – Filter 2 DOC Removal Over Experimental Period

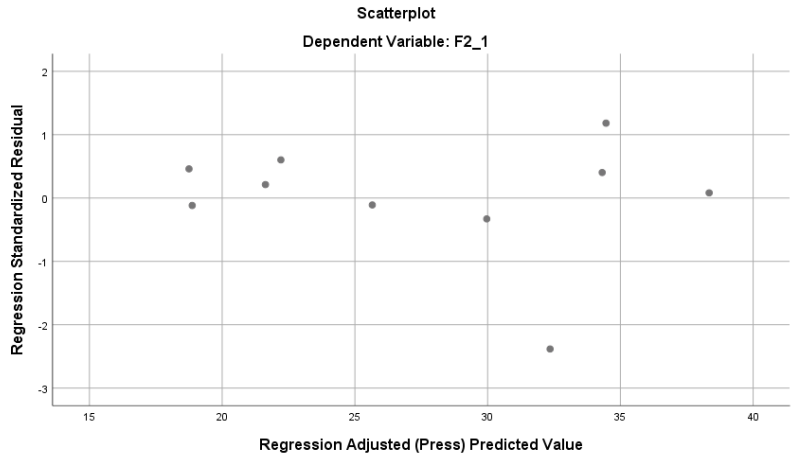


Figure A - 107: Linear regression residuals for DOC removal in Filter 2 – Iteration 1

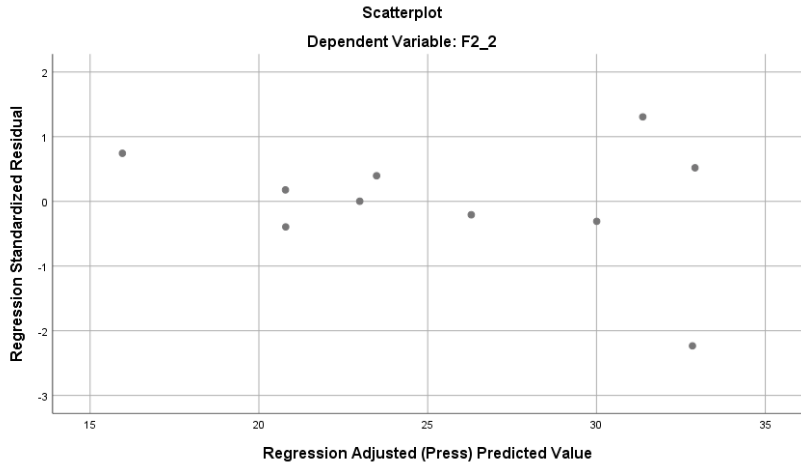


Figure A - 108: Linear regression residuals for DOC removal in Filter 2 – Iteration 2

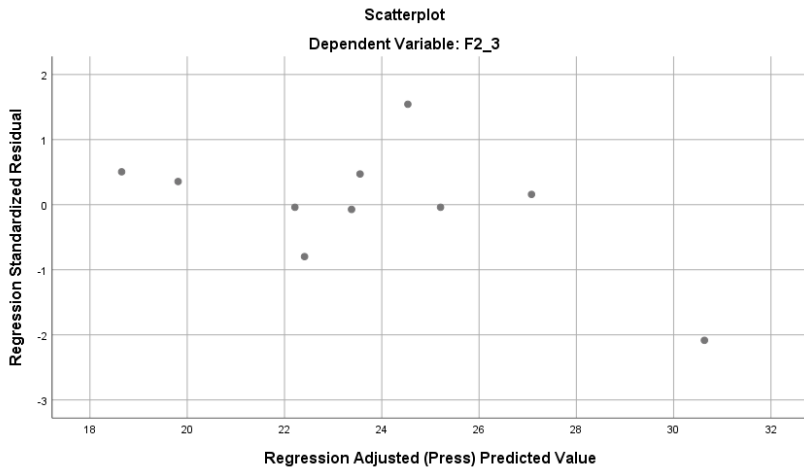


Figure A - 109: Linear regression residuals for DOC removal in Filter 2 – Iteration 3

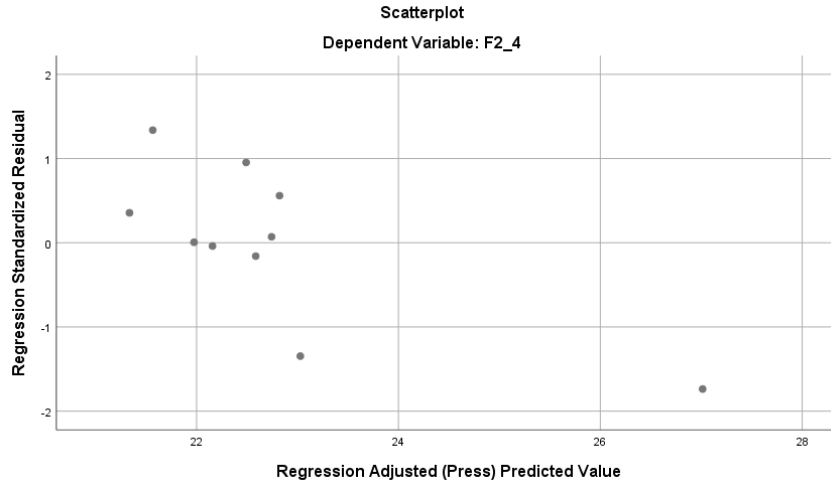


Figure A - 110: Linear regression residuals for DOC removal in Filter 2 – Iteration 4

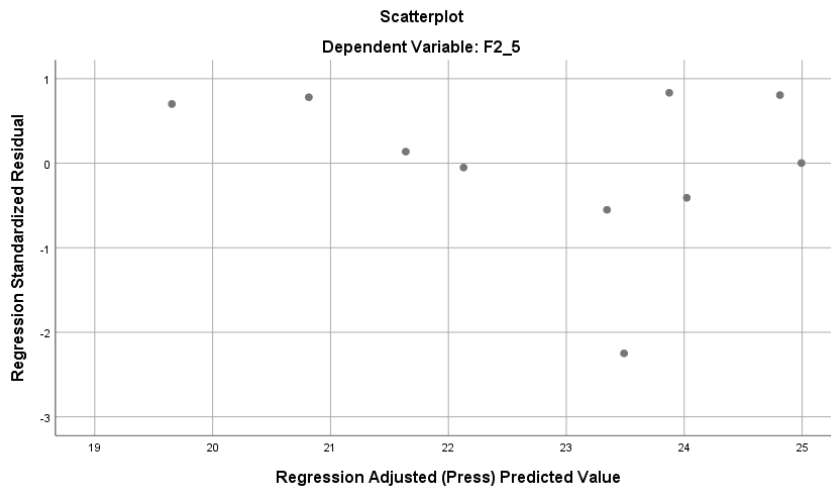


Figure A - 111: Linear regression residuals for DOC removal in Filter 2 – Iteration 5

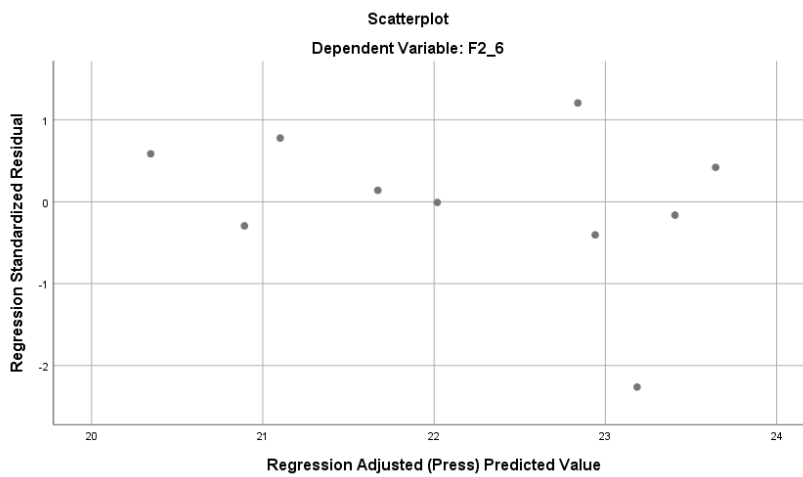


Figure A - 112: Linear regression residuals for DOC removal in Filter 2 – Iteration 6

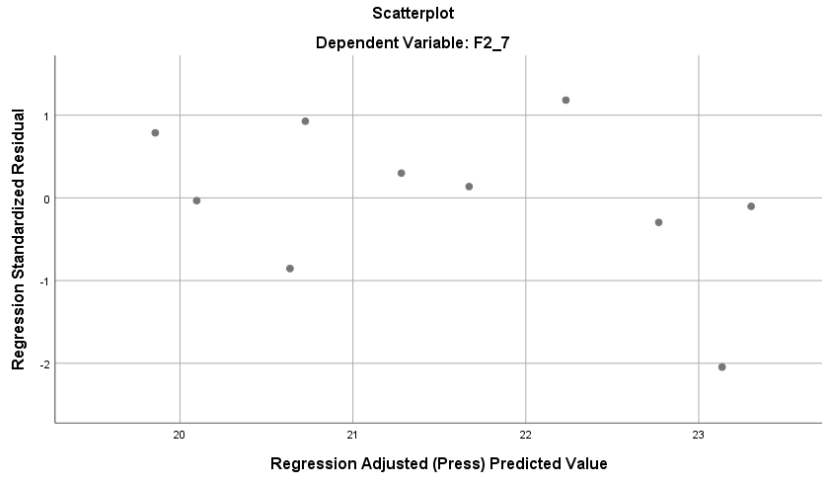


Figure A - 113: Linear regression residuals for DOC removal in Filter 2 – Iteration 7

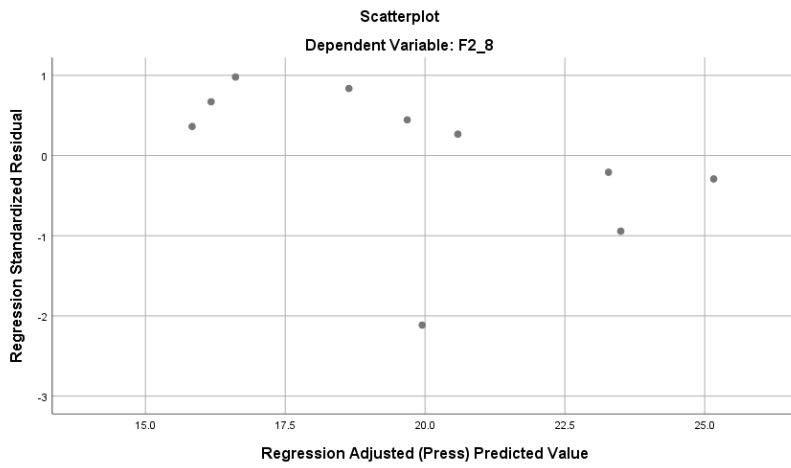


Figure A - 114: Linear regression residuals for DOC removal in Filter 2 – Iteration 7

Linear Regression Residuals – Filter 3 DOC Removal Over Experimental Period

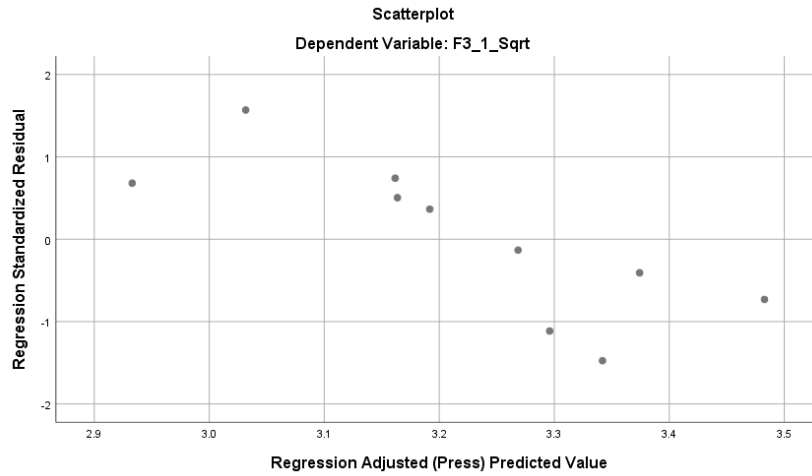


Figure A - 115: Linear regression residuals for DOC removal in Filter 3 – Iteration 1

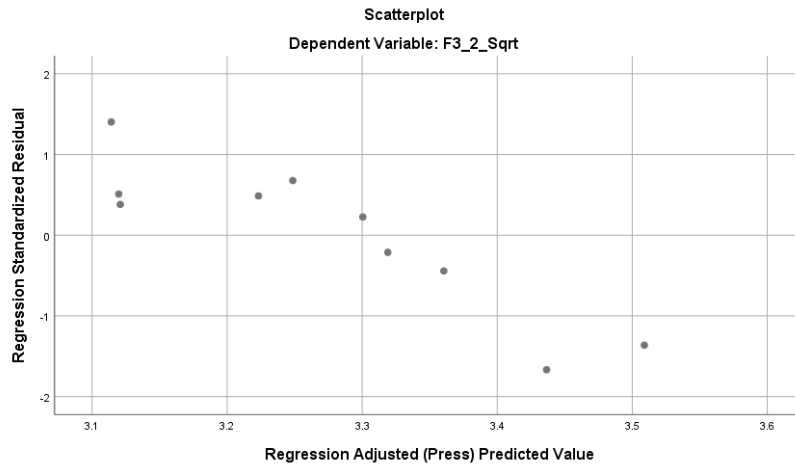


Figure A - 116: Linear regression residuals for DOC removal in Filter 3 – Iteration 2

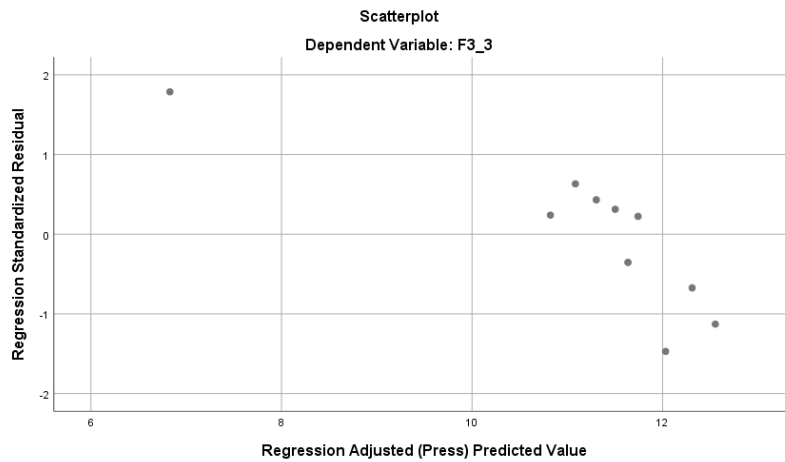


Figure A - 117: Linear regression residuals for DOC removal in Filter 3 – Iteration 3

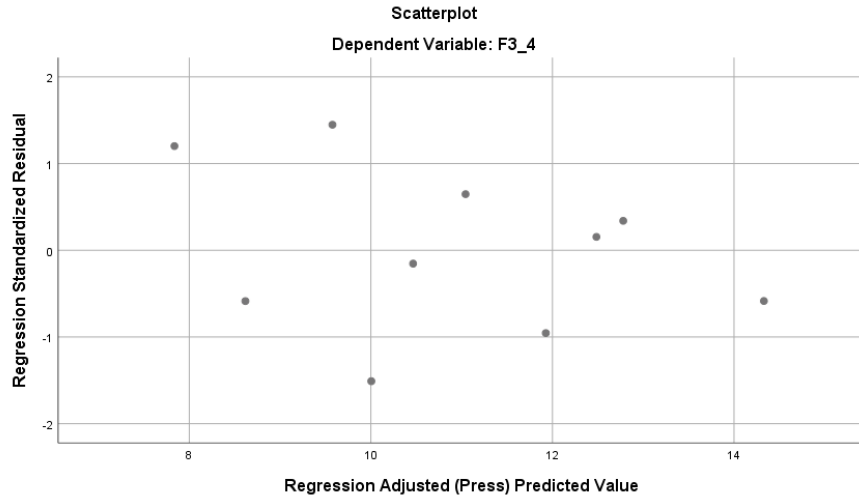


Figure A - 118: Linear regression residuals for DOC removal in Filter 3 – Iteration 4

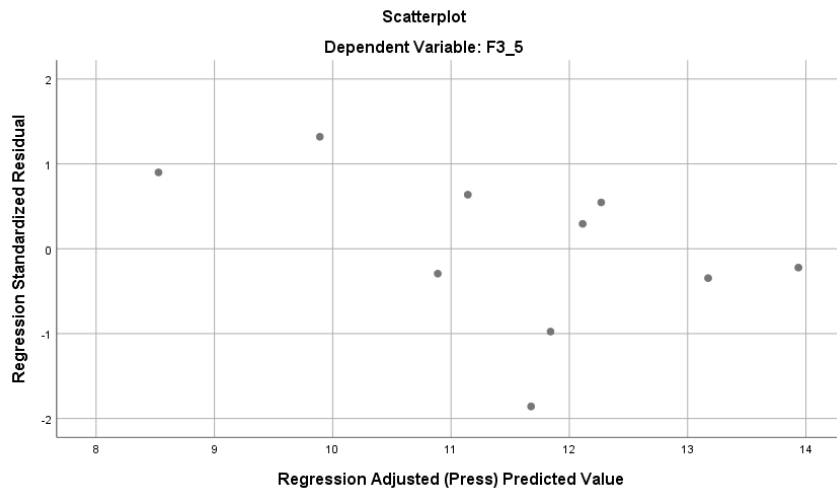


Figure A - 119: Linear regression residuals for DOC removal in Filter 3 – Iteration 5

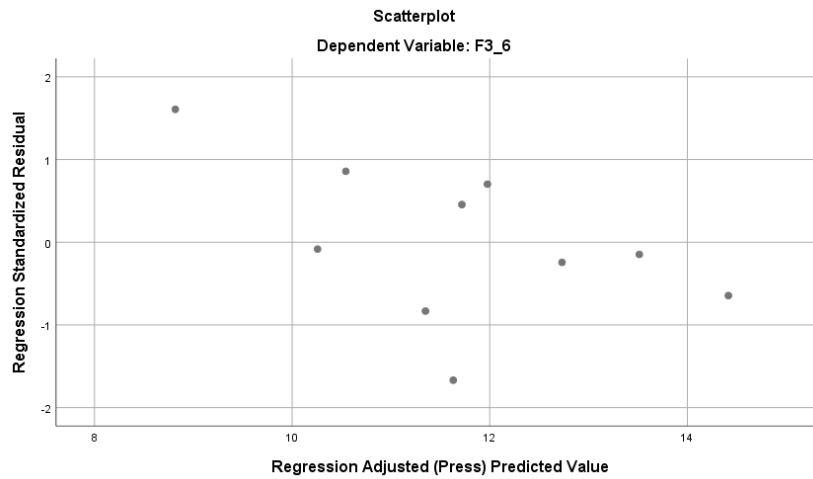


Figure A - 120: Linear regression residuals for DOC removal in Filter 3 – Iteration 6

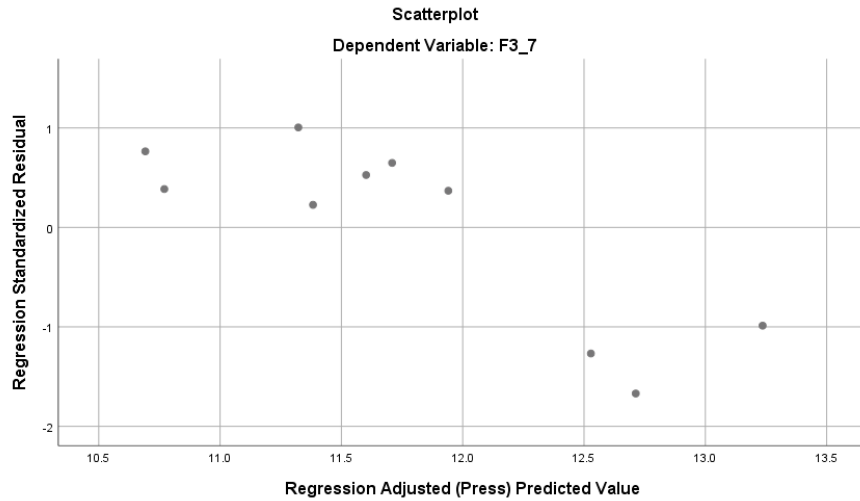


Figure A - 121: Linear regression residuals for DOC removal in Filter 3 – Iteration 7

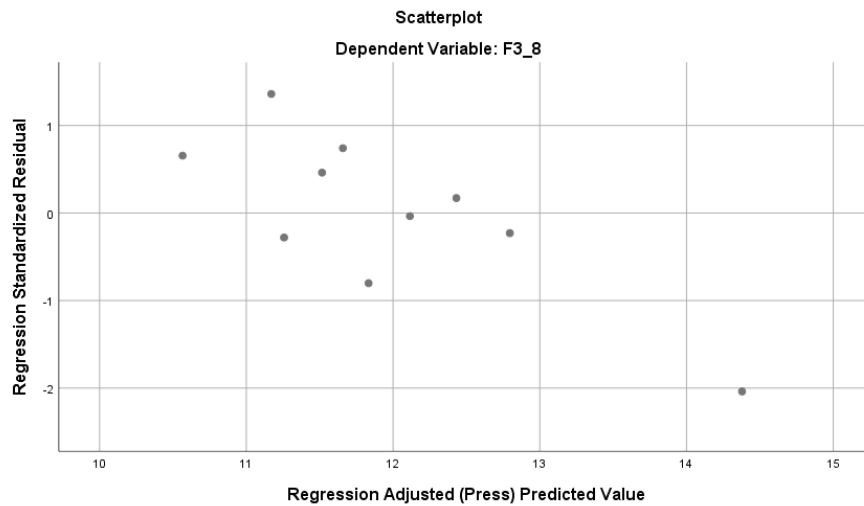


Figure A - 122: Linear regression residuals for DOC removal in Filter 3 – Iteration 8

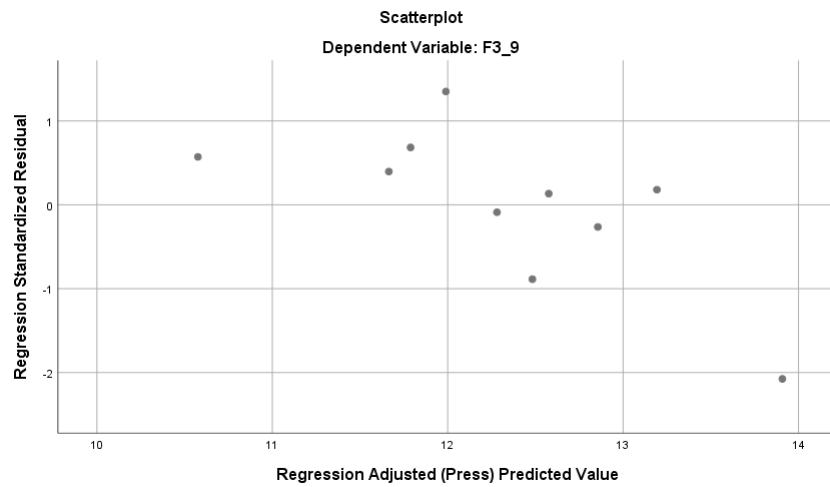


Figure A - 123: Linear regression residuals for DOC removal in Filter 3 – Iteration 9

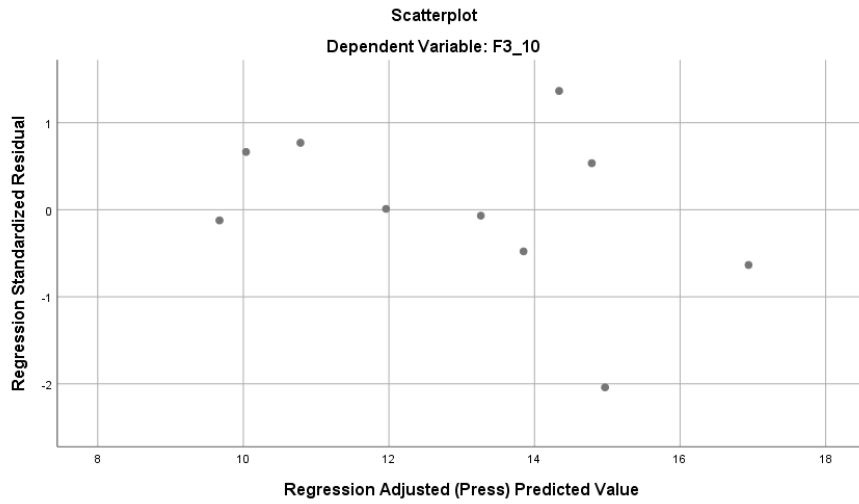


Figure A - 124: Linear regression residuals for DOC removal in Filter 3 – Iteration 10

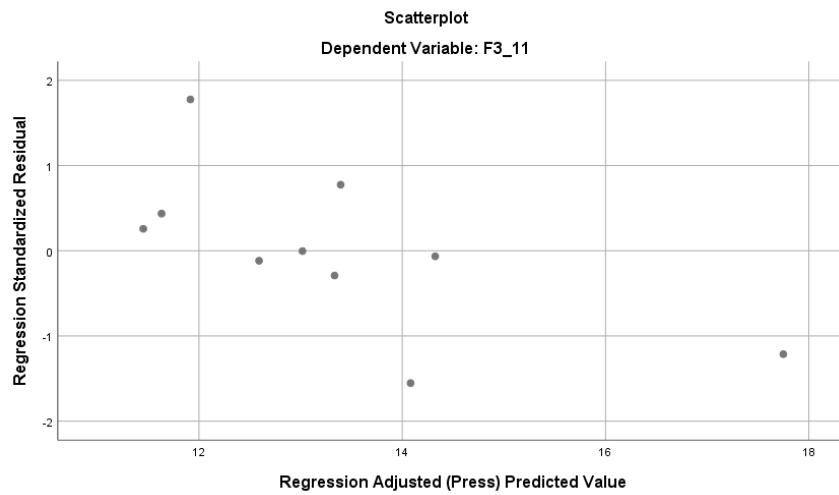


Figure A - 125: Linear regression residuals for DOC removal in Filter 3 – Iteration 11

Linear Regression Residuals – Filter 3 Fractions of DOC Removal over Experimental Period

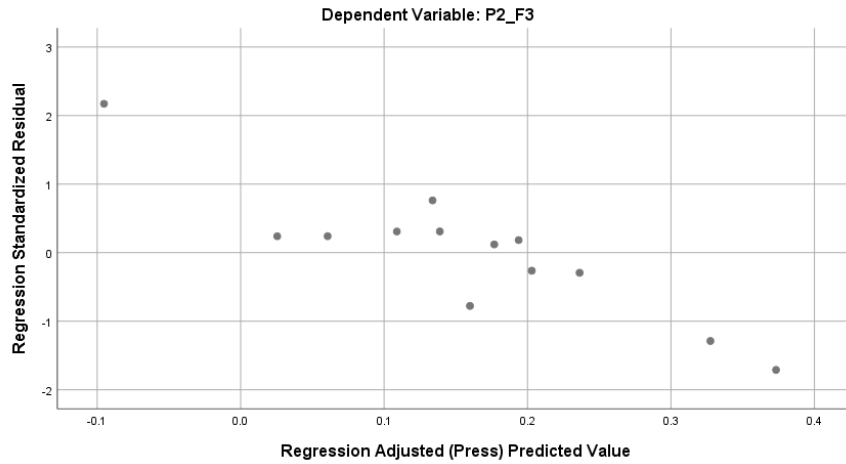


Figure A - 126: Linear regression residuals for fraction of DOC removed between the top to Port 2 in Filter 3– over experimental period

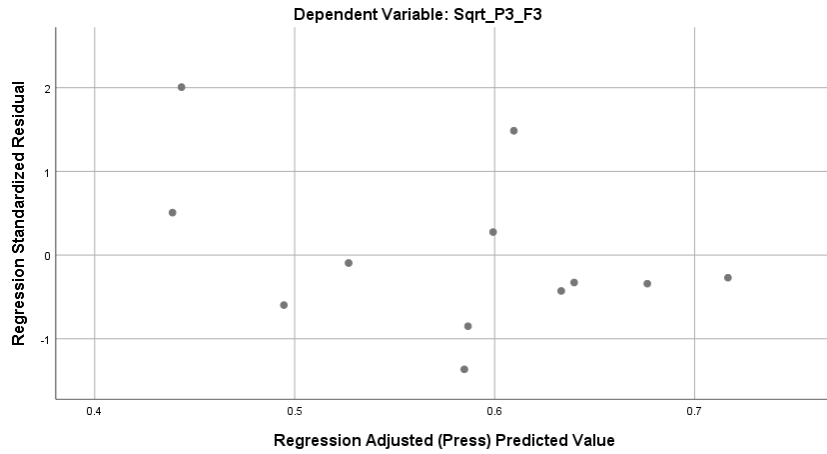


Figure A - 127: Linear regression residuals for fraction of DOC removed between Port 2 and Port 3 in Filter 3– over experimental period

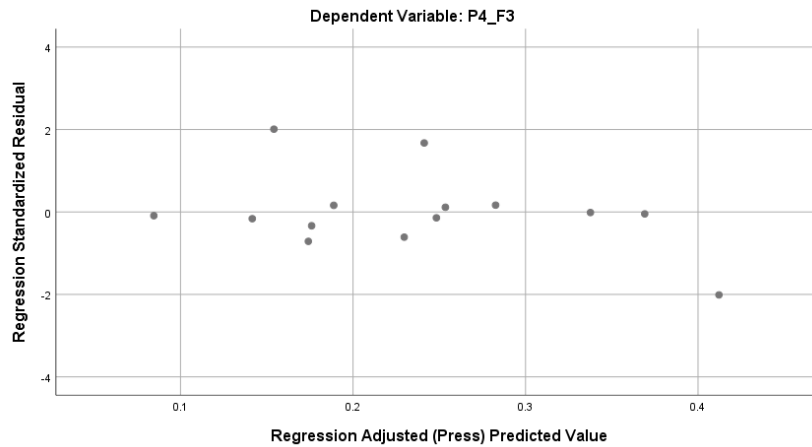


Figure A - 128: Linear regression residuals for fraction of DOC removed between Port 3 and Port 4 in Filter 3– over experimental period

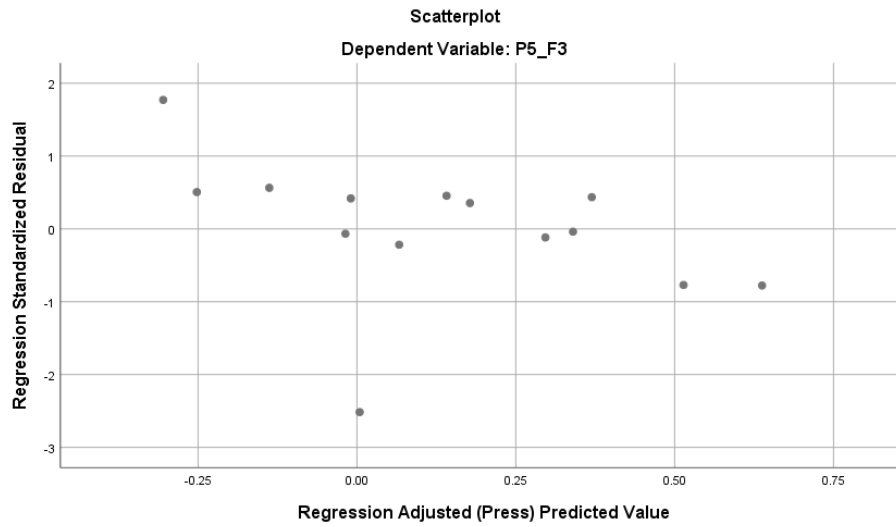


Figure A - 129: Linear regression residuals for fraction of DOC removed between Port 4 and Port 5 in Filter 3– over experimental period

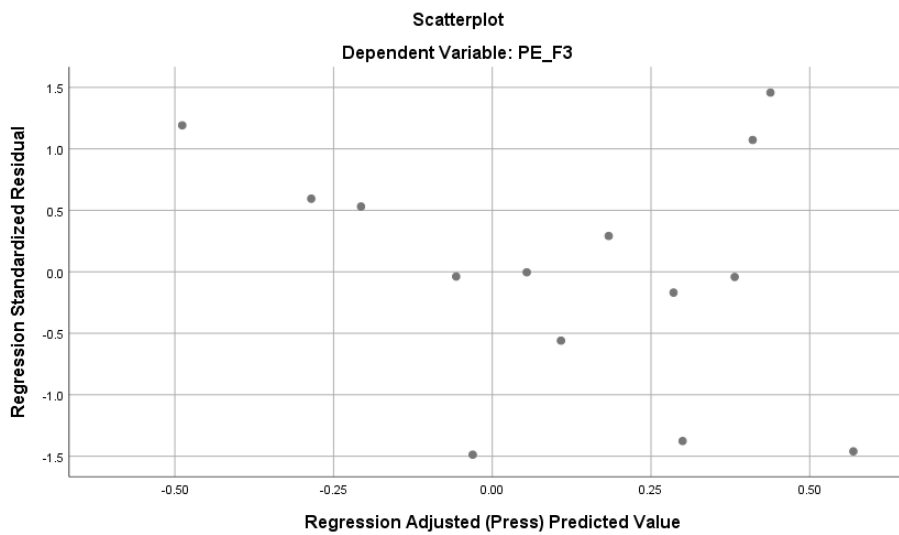


Figure A - 130: Linear regression residuals for fraction of DOC removed between Port 5 and Effluent Port in Filter 3– over experimental period

Linear Regression Residuals – Filter 4 DOC Removal Over Experimental Period

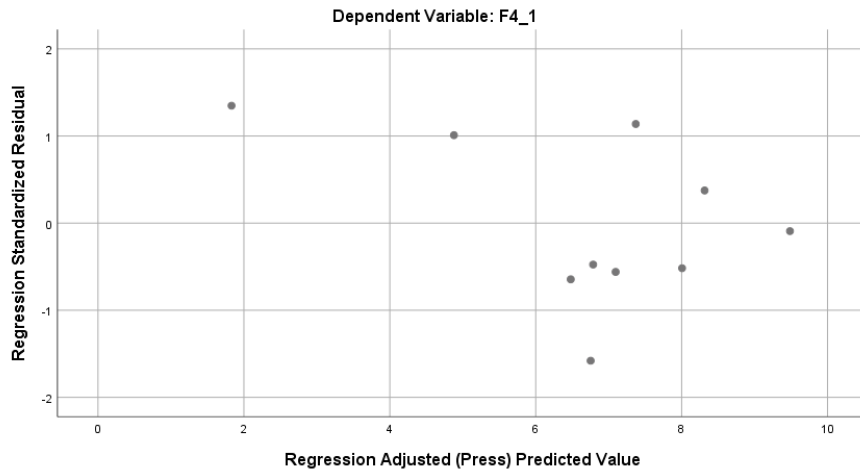


Figure A - 131: Linear regression residuals for DOC removal in Filter 4 – Iteration 1

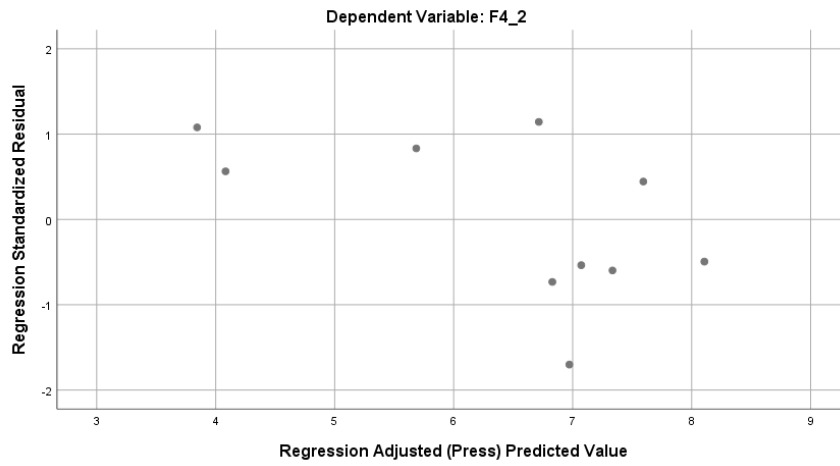


Figure A - 132: Linear regression residuals for DOC removal in Filter 4 – Iteration 2

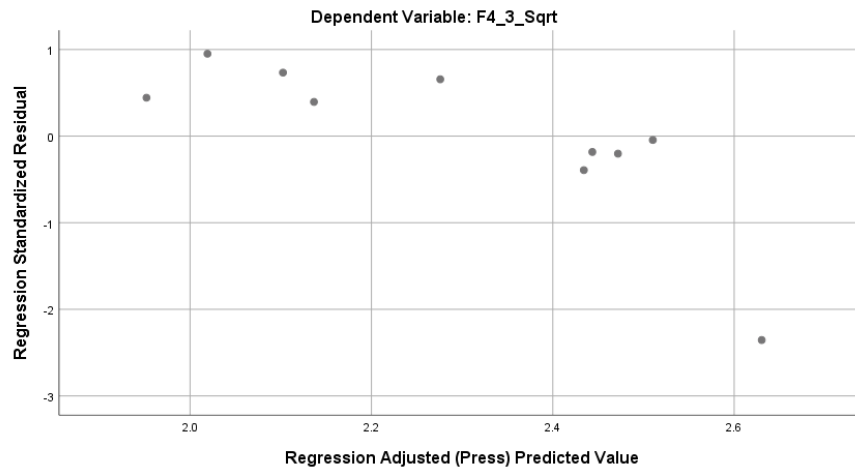


Figure A - 133: Linear regression residuals for DOC removal in Filter 4 – Iteration 3

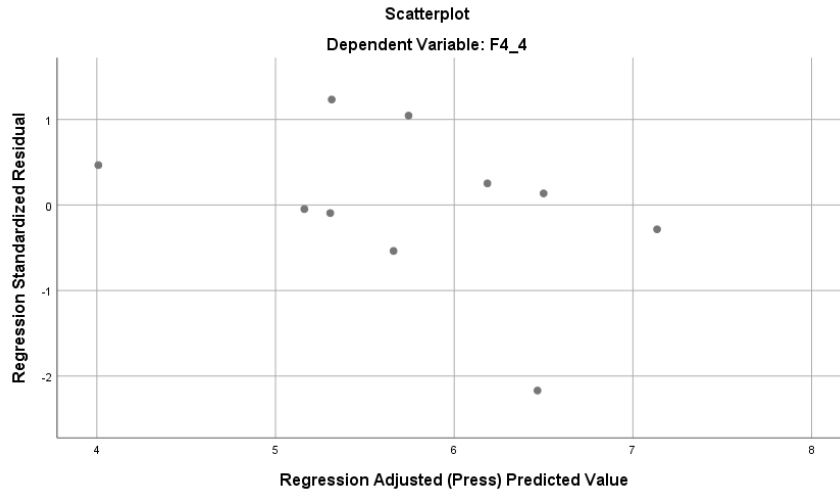


Figure A - 134: Linear regression residuals for DOC removal in Filter 4 – Iteration 4

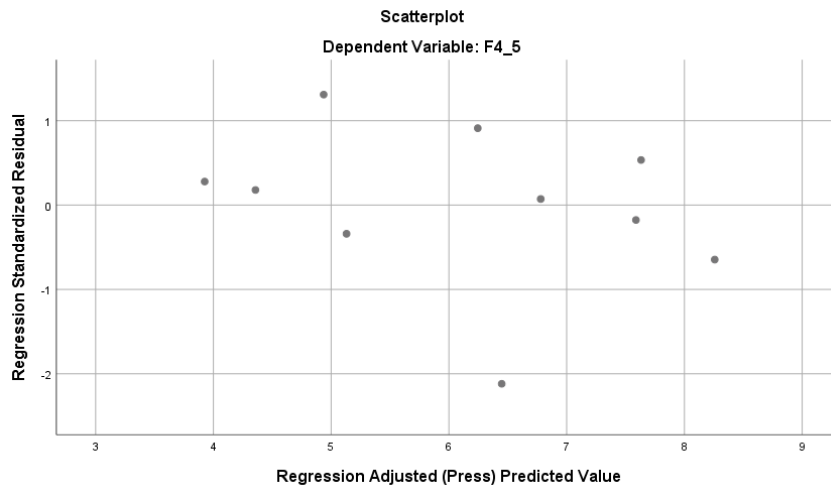


Figure A - 135: Linear regression residuals for DOC removal in Filter 4 – Iteration 5

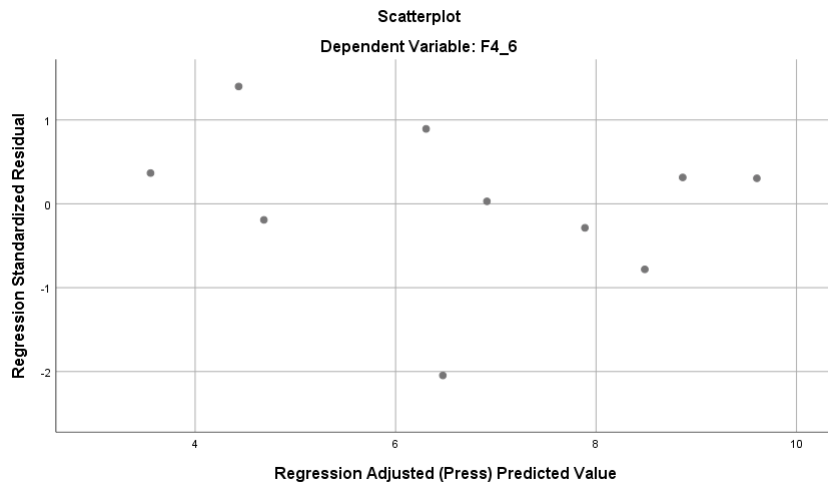


Figure A - 136: Linear regression residuals for DOC removal in Filter 4 – Iteration 6

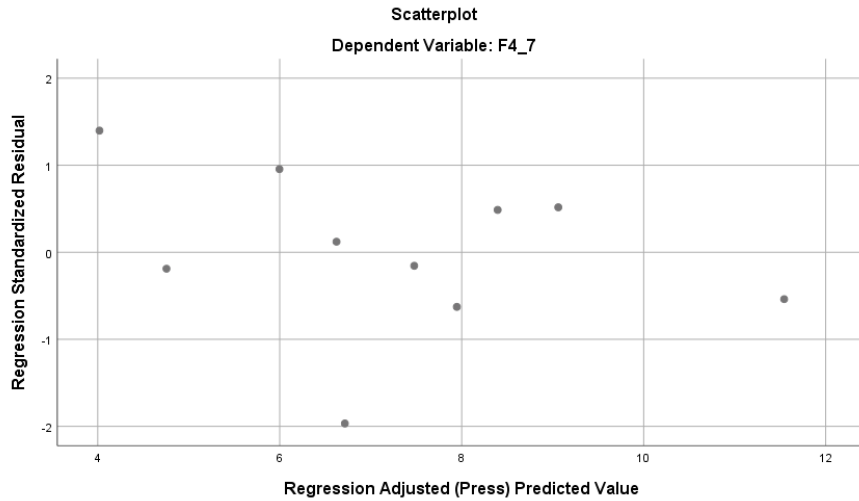


Figure A - 137: Linear regression residuals for DOC removal in Filter 4 – Iteration 7

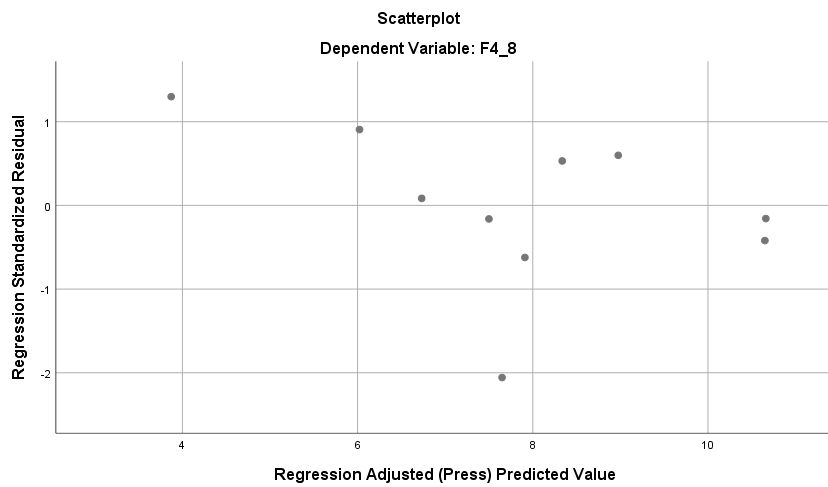


Figure A - 138: Linear regression residuals for DOC removal in Filter 4 – Iteration 8

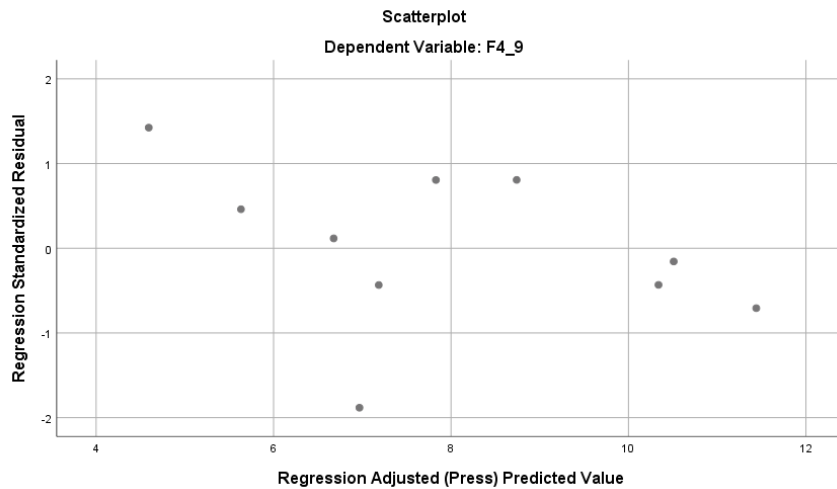


Figure A - 139: Linear regression residuals for DOC removal in Filter 4 – Iteration 9

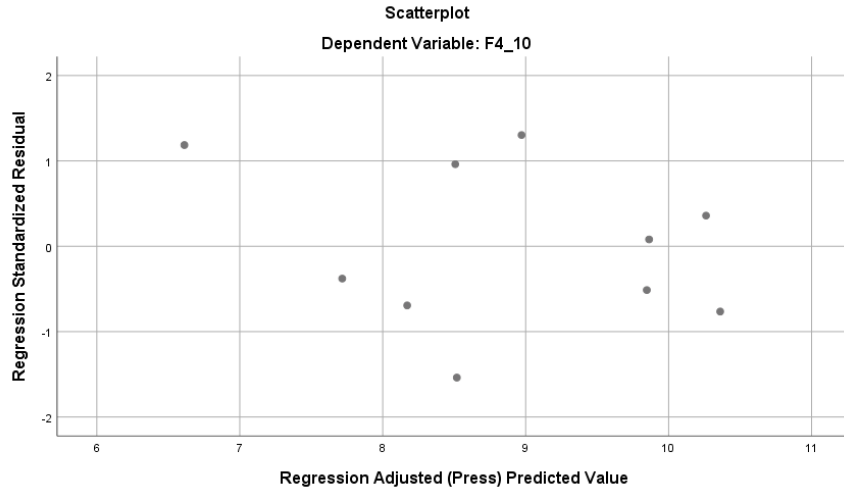


Figure A - 140: Linear regression residuals for DOC removal in Filter 4 – Iteration 10

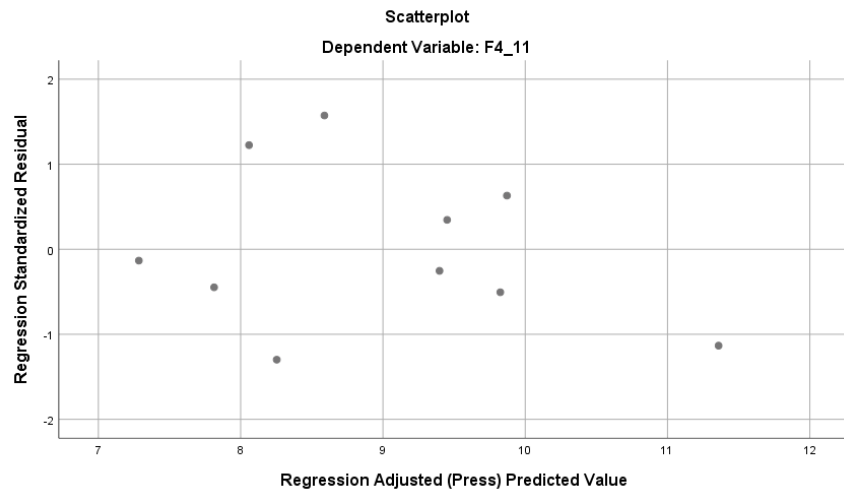


Figure A - 141: Linear regression residuals for DOC removal in Filter 4 – Iteration 11

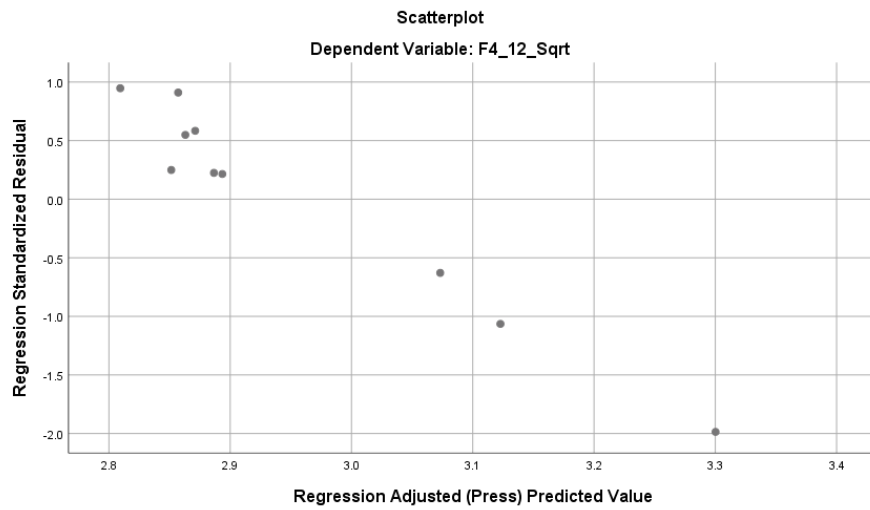


Figure A - 142: Linear regression residuals for DOC removal in Filter 4 – Iteration 12

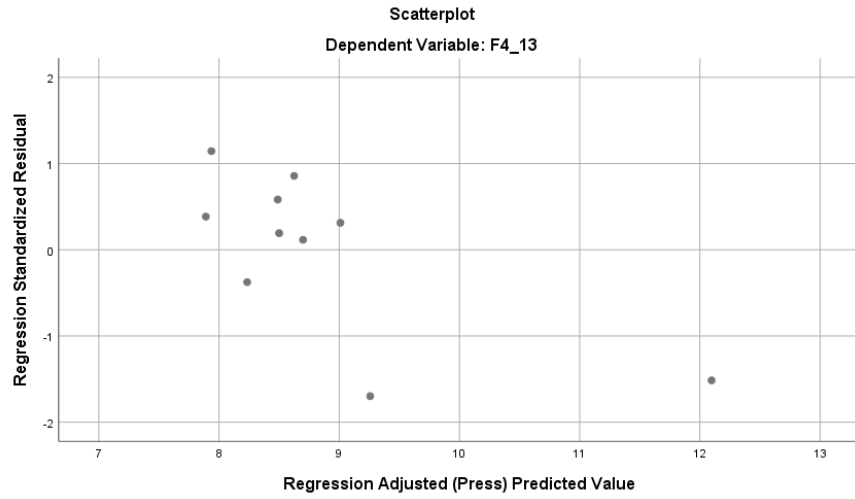


Figure A - 143: Linear regression residuals for DOC removal in Filter 4 – Iteration 13

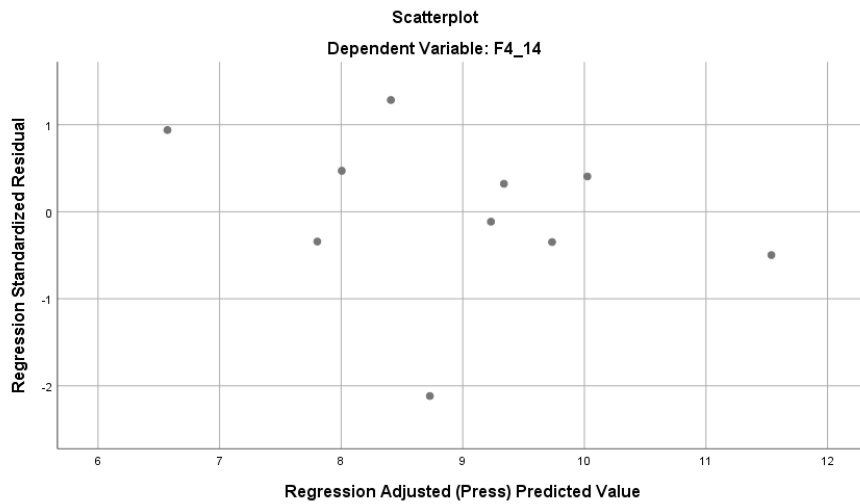


Figure A - 144: Linear regression residuals for DOC removal in Filter 4 – Iteration 14

Appendix D – Filtration Media Specs

Sieve Analysis

In order to confirm that the grain size distributions of the filters were sufficiently similar, all the filter media was sieved as recommended by AWWA and ANSI (2002).

Table A - 26: Sieve analysis results

Sample	D10 (mm)	Uniformity Coefficient (mm)
Mannheim GAC	1.37	1.30
New GAC	1.29	1.59
Anthracite	1.43	1.43
Sand Trial	0.44	1.53

The media was air-dried prior to measuring. The grain size of GAC is lower than the anthracite, this may be explained by the presence of fines. Overall, the grain size distribution is as expected.

Wet-Dry Conversion

For the ATP analysis, it was necessary to determine how much more the filter media weighs when it is wet versus when it is dry.

Table A - 27: Wet-dry conversion results

	Mannheim GAC	New GAC	Anthracite (Trial 1)	Anthracite (Trial 2)
Wet (g)	1222.2	1133.6	153.1	150.8
Dry (g)	743.1	677.6	97.7	95.2
Ratio	1.64	1.67	1.57	1.58

This was approximated to 1.7 for GAC, and 1.6 for anthracite.

Filtration Media Specification Sheets



Anthrafilter Media & Coal Ltd.
 20 SHARP ROAD, R.R. #6, BRANTFORD, ONTARIO N3T 6L8 TEL: (519) 751-1080 FAX: (519) 751-0617



Contract ; Anthrafilter Filter Media
 PO# 85843
 Specifications ; E.S. 1.40-1.50 ; U.C. < 1.50
 Sample ID ; 1540 Blend / Lot #1
 # of C.F. 13 C.F. Skids @ 2500 / 16.25 Tons

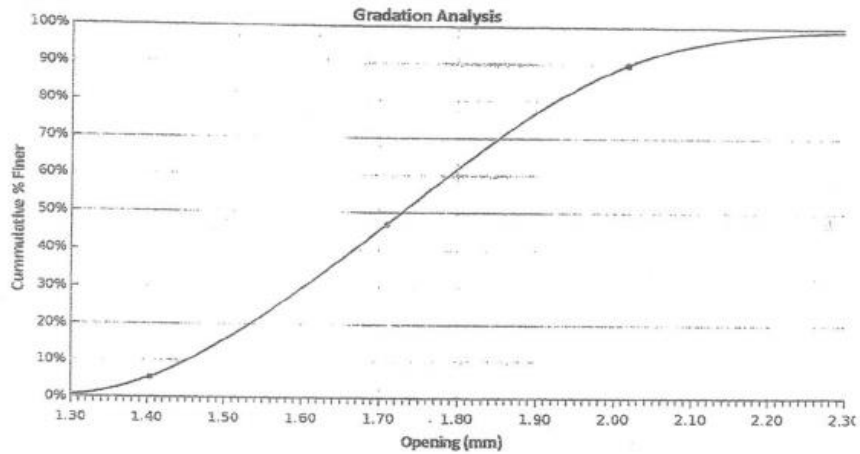
ES	1.45
UC	1.24

D ₁₀	1.449
D ₆₀	1.797
D ₉₀	2.018

Date
06/20/17

Starting Wt.
155.6

Sieve Opening						
IN	MM	US	Wt	% Ret.	% Finer	Opening (mm)
0.1110	2.86567	NO# 7	0.00	0.0%	100.0%	2.86567
0.0937	2.36086	NO# 8	0.80	0.5%	99.5%	2.36086
0.0787	2.01820	NO# 10	15.00	9.6%	89.8%	2.01820
0.0661	1.71009	NO# 12	66.90	43.0%	46.9%	1.71009
0.0555	1.40381	NO# 14	64.50	41.5%	5.4%	1.40381
0.0469	1.18246	NO# 16	5.90	3.8%	1.6%	1.18246
0.0394	1.00735	NO# 18	0.80	0.5%	1.1%	1.00735
0.0331	0.84843	NO# 20	0.40	0.3%	0.8%	0.84843
0.0278	0.70994	NO# 25	0.30	0.2%	0.6%	0.70994
0.0234	0.59977	NO# 30	0.00	0.0%	0.6%	0.59977
0.0197	0.50224	NO# 35	0.00	0.0%	0.6%	0.50224
Pan			0.70	0.4%	0.193%	
Total			155.30			



FILTRASORB® 816

Granular Activated Carbon

Applications



FILTRASORB 816 activated carbon can be used in a variety of liquid phase applications for the removal of dissolved organic compounds. FILTRASORB 816 has been successfully applied for over 40 years in applications such as drinking and process water purification, wastewater treatment, and food, pharmaceutical, and industrial purification.

Description

FILTRASORB 816 is a granular activated carbon developed by Calgon Carbon Corporation for the removal of dissolved organic compounds from water and wastewater as well as industrial and food processing streams. These contaminants include taste and odor compounds, organic color, total organic carbon (TOC), and industrial organic compounds such as TCE and PCE. This activated carbon is made from select grades of bituminous coal through a process known as reagglomeration to produce a high activity, durable, granular product capable of withstanding the abrasion associated with repeated backwashing, hydraulic transport, and reactivation for reuse. Activation is carefully controlled to produce a significant volume of both low and high energy pores for effective adsorption of a broad range of high and low molecular weight organic contaminants. FILTRASORB 816 is also formulated to comply with all the applicable provisions of the AWWA Standard for Granular Activated Carbon (B604), the stringent extractable metals requirements of ANSI/NSF Standard 61, and the Food Chemicals Codex.

Features / Benefits

- Calgon Carbon's reagglomerated coal-based granular activated carbons have several properties which provide superior performance in a wide range of applications
- Produced from a pulverized blend of high quality bituminous coals resulting in a consistent, high quality product
- The activated carbon granules are uniformly activated through the whole granule, not just the outside. This results in excellent adsorption properties and constant adsorption kinetics in a wide range of applications
- The reagglomerated structure ensures proper wetting while also eliminating floating material
- High mechanical strength relative to other raw materials, thereby reducing the generation of fines during backwashing and hydraulic transport
- Carbon bed segregation is retained after repeated backwashing, ensuring the adsorption profile remains unchanged and therefore maximizing the bed life
- Reagglomerated with a high abrasion resistance, which provides excellent reactivation performance
- High density carbon resulting in a greater adsorption capacity per unit volume

Specifications¹

	FILTRASORB 816
Iodine Number, mg/g	900 (min)
Moisture by Weight	2% (max)
Effective Size	1.3–1.5 mm
Uniformity Coefficient	1.4 (max)
Abrasion Number	75 (min)
Screen Size by Weight, US Sieve Series	
On 8 mesh	15% (max)
Through 16 mesh	5% (max)

¹Calgon Carbon test method

Typical Properties*

	FILTRASORB 816
Apparent Density (tamped)	0.50 g/cc
Water Extractables	<1%
Non-Wettable	<1%

*For general information only, not to be used as purchase specifications.

Safety Message

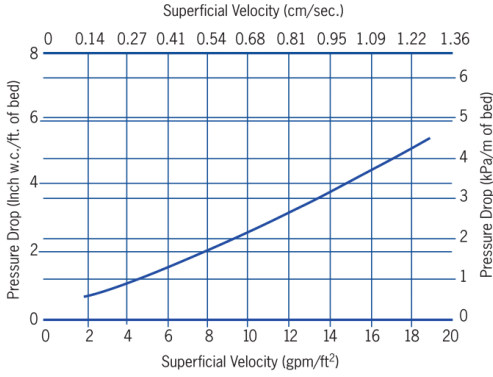
Wet activated carbon can deplete oxygen from air in enclosed spaces. If use in an enclosed space is required, procedures for work in an oxygen deficient environment should be followed.

1.800.4CARBON calgoncarbon.com

© Copyright 2015 Calgon Carbon Corporation, All Rights Reserved
DS-FILTRA816-EIN-E1

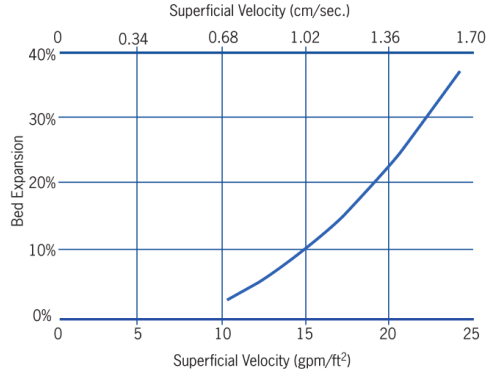
Typical Pressure Drop

Down Flow Pressure Drop at 13C/55°F
Based on a backwashed and segregated bed



Typical Bed Expansion During Backwash

Bed Expansion During Backwash at 13C/55°F
Based on a backwashed and segregated bed



Design Considerations

FILTRASORB 816 activated carbon is typically applied in down-flow packed-bed operations using either pressure or gravity systems. Design considerations for a treatment system is based on the user's operating conditions, the treatment objectives desired, and the chemical nature of the compound(s) being adsorbed.

Safety Message

Wet activated carbon can deplete oxygen from air in enclosed spaces. If use in an enclosed space is required, procedures for work in an oxygen deficient environment should be followed.

1.800.4CARBON calgoncarbon.com

© Copyright 2015 Calgon Carbon Corporation, All Rights Reserved
DS-FILTRA81616-EIN-E1